Capturing the Dynamics of Cell Division and Fate Specification during Arabidopsis Leaf Development

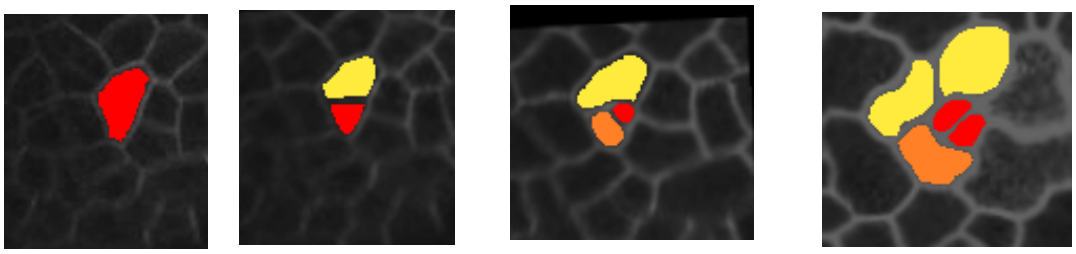

Sarah Robinson

A thesis submitted for the
Degree of Doctor of Philosophy

2010

University of East Anglia
John Innes Centre

Statement of originality

Unless otherwise mentioned in the text, the work presented in this thesis is that of the author.

Abstract

Asymmetric cell divisions provide a universal means of generating different cell fates in the development of multi-cellular organisms. However, their role in patterning growing tissues is not well understood. Asymmetric cell divisions require tight regulation of their orientation and timing. The process is particularly important in plants where growth is symplastic. In this system the orientation of divisions determines neighbourhoods of cells, and the timing determines their area. Little is known about how growth, cell division and differentiation are integrated. Formation of stomata within the Arabidopsis leaf epidermis provides a physically accessible system to study cell divisions into a developing tissue. As development is a dynamic multi-scale process, we tracked plant growth at the tissue, cell and protein level by using time-lapse microscopy. The data captured was used to produce a descriptive model of the growing and dividing cells of the leaf. Descriptive rules were then replaced by mechanistic ones in a stepwise manner, recapitulating *in vivo* behaviour. The resulting model of asymmetric cell divisions made testable predictions, validated by further experiments. As a result, this thesis provides a plausible model of how patterning of the stomata might be achieved by asymmetric cell divisions and how this pattern can be integrated into the developing tissue.

Acknowledgements

I would like to thank my two supervisors Enrico Coen, and Przemyslaw Prusinkiewicz for assistance, advice, opportunities, good times, praise and criticism; all of which I appreciate very much.

For their direct contribution to the work in this thesis I would like to thank Pierre Barbier de Reuille who developed the modelling environment used as well as all of the other tools. I would also like to thank Pierre for teaching me to program and for advice on all things computational and mathematical. Grant Calder who designed the time-lapse chamber used in this thesis and who helped me with all of my imaging worries. Samantha Fox, Jordi Chan, Jérôme Avondo and Erika Kuchen for teaching me biological and computational techniques. I would also like to thank all of the Prusinkiewicz lab who helped me greatly in learning to model, particularly Adam Runions, Jeyaprakash Chelladurai, Wojtek Pałubicki and former member Richard Smith.

I would like to thank our collaborator Dominqiue Bergmann for useful conversations, feedback and plant material.

Finally I would like to thank the rest of the Coen lab, my fellow students at the JIC and my friends and family for making my PhD a wonderful experience.

Table of Figures

Commonly used Abbreviations

BASL	BREAKING OF ASYMMETRY IN THE STOMATAL LINEAGE protein
basl	BREAKING OF ASYMMETRY IN THE STOMATAL LINEAGE mutant
DAS	Days after stratification
Epi/LRC	epidermal/lateral root cap
GaMC	ganglion mother cell
GMC	guard mother cell
GMC	Guard Mother Cell
GSC	germline stem cells
MMC	meristemoid mother cell
NB	neuroblast
NC	neighbour cells
PPB	pre-prophase band
QC	quiescent centre
SMC	subsidiary mother cells
SOP	sensory organ precursors
spch	*speechless* mutant
SPCH	SPEECHLESS PROTEIN
tmm	*too many mouths*
VVe	Vertex-Vertex extended (modelling environment)

Introduction

1.1 Asymmetric cell division

When a cell divides the progeny can be the same or different. Divisions which produce cells of different fates are termed asymmetric divisions, (Horvitz and Herskowitz, 1992). Asymmetric cell divisions provide a universal means of generating different cell fates in the development of multi-cellular organisms. There are some key issues that apply to all asymmetric divisions: 1) whether the cells fate is determined intrinsically or extrinsically, (i.e. whether the daughters are produced differently directly following the division or whether they are produced the same but receive external signals to determine their fate (Horvitz and Herskowitz, 1992)) 2) in what orientation the division should occur, 3) whether the division is physically asymmetric, and 4) whether there is an associated asymmetry in the potential of the daughter to divide. We can consider these issues a little further and then look at them in the context of some examples.

1) Intrinsic versus extrinsic

The hypothesis that a cell division could produce two daughter cells that are different straight from the division was proposed in 1878 by Whitman and supported by studies in 1905 (Conklin) (cited with in (Horvitz and Herskowitz, 1992)). Both observed the differential segregation of cytoplasmic components into the two daughter cells and

hence observed an intrinsic mechanism of specifying daughter cell fate. Extrinsic mechanisms also exist, whereby daughter cells that are initially the same acquire different fates due to external signals (ten Hove and Heidstra, 2008). These two mechanisms of generating different daughter cells are not always mutually exclusive.

2) The orientation of the division

Cell division orientation determines the position and neighbourhood of the cells. Its relative importance in plants and animals may vary.

3) Physical asymmetry

Cell divisions are classed as asymmetric if the daughters acquire different fates regardless of whether or not the cells have different sizes (Horvitz and Herskowitz, 1992). However, as we will see in some cases the division has an associated physical asymmetry while in others there is only a fate asymmetry.

4) Stem cell versus non-stem cell

Asymmetric cell divisions can be classified based on whether one or both daughters are different from the mother cell. If one daughter retains the fate of the mother then this is classed as a stem cell type division. In stem cell type divisions the regenerated cell maintains the ability to divide. Differentiated daughters usually have only limited ability to divide.

The four issues outlined are general to all asymmetrically dividing organisms. However I would like to consider an issue which is specific to multi-cellular animals. That is how the asymmetric divisions generate patterns in developing tissues. Can we understand how a pattern is generated by considering these four key issues? I will consider examples of multi-cellular plants and animals. Both kingdoms must find solutions to the problems encountered in generating asymmetric divisions under different constraints.

1.1.1 Asymmetric Division in Animals

The Drosophila sensory organ precursors (SOPs)

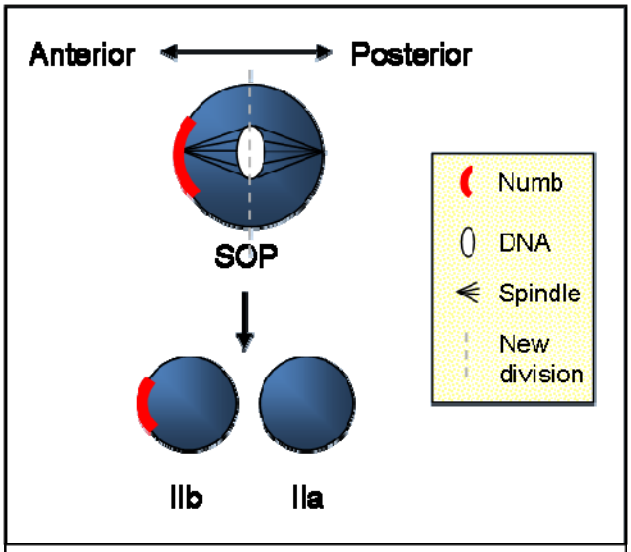

Figure 1.1 Asymmetric division of SOP cells. SOP cells divide to produce IIa and IIb cells. Numb is localised to a cresent on the anterior side and is inherited by only one cell. The divisions are oriented with the tissue polarity, which requires FRIZZELED.

The sensory organ precursor (SOP) cell divides to produce four cells in the production of the peripheral nervous system of *Drosophila* (reviewed by (Jan and Jan, 1998; Wu et al., 2008)). The first division in this process is asymmetric. It produces two cells of different fates referred to as the IIa and the IIb cell (Figure 1.1). It is therefore a non-stem cell type division. The daughter cell fate is controlled intrinsically by the distribution of a membrane associated protein Numb. Numb becomes localised to a crescent at one of the spindle poles prior to division. It is segregated to one daughter cell and conveys IIb cell fate. Mutation or over-expression studies cause both cells to adopt the IIa or IIb fate respectably. Numb is also thought to influence the fate of the daughters by altering their cell-cell interactions. This modification takes the form of a down regulation of Notch. Removing *Notch* function results in two IIb cells (Bultje et al., 2009; Guo et al., 1996). SOPs thus provide an example of how intrinsic and extrinsic signals might be integrated.

The orientation of the division is coupled to the fate determinants to ensure one daughter receives one fate. The localisation of Numb requires another protein Inscuteable which is localised to the opposite side of the cell. Inscuteable also has a role in orienting the mitotic spindle. Mutations in Inscuteable cause the division to be oriented randomly while miss-expression can induce inappropriate divisions in other

cells. Inscuteable is likely to be responsible for coupling the orientation of the division to the fate determinants (Jan and Jan, 1998).

The division of the SOP cells is also oriented relative to the anterior posterior axis of the fly. This orientation requires the Frizzled receptor which plays a role in orienting the Numb crescent and the spindle (Gho and Schweisguth, 1998) via Baz and the Dlg/Pins. complex (Bellaiche et al., 2001). Frizzled coordinates cell polarity in the fly.

The *Drosophila* neuroblast

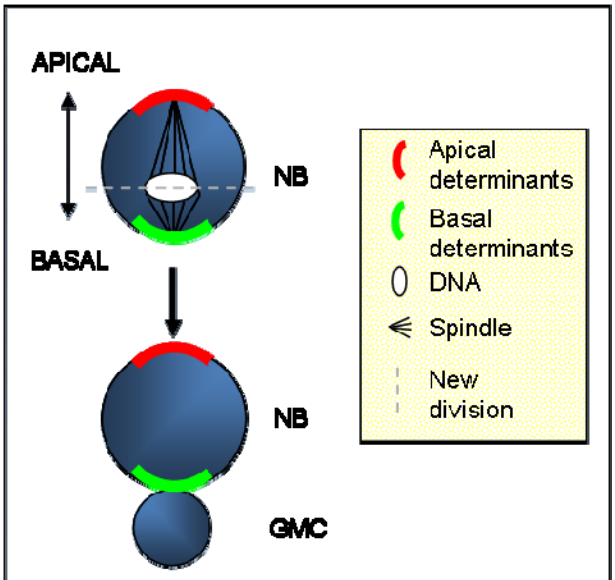

Figure 1.2 Asymmetric division of NB cells. NB undergo stem cell division to produce another large apical NB and a small basal GMC.

Neuroblast (NB) cells under go stem cell type divisions as they produce a large cell which maintains NB identity and a small ganglion mother cell (GaMC) which contributes to the *Drosophila* central nervous system (Figure 1.2). All of the NB cells divide to place the GaMC on the basal side of the cell (reviewed by (Wu et al., 2008) (Knoblich, 2001) and (Yu et al., 2006)). A primary feature is the establishment of apical-basal polarity of fate determinants in the NB cells. The polarity is established intrinsically by localising a complex of proteins known as the Par complex to the apical pole of the cell. The Par complex co-localises in an apical crescent with Inscuteable (Insc). This complex directs the localisation of the cell fate determinants, Prospero (Pros), Numb, Miranda (Mira) and Partner of Numb (Pon). The fate determinants are localised via the action of two cortically localised tumour suppressors Dlg and Lgl. Lgl is phosphorylated by a member of the Par complex aPKC resulting in

its inactivation. The active form of Lgl at the basal cortex recruits the cell fate determinants. Lgl also interacts with myosin II and the vesicle transport machinery to direct the determinants. After division Pros is released by Miranda and moves to the nucleus to initiate differentiation of the GaMC. Numb also plays a role in the larval NB via Notch signalling in the GaMC.

In animal cells the determinants are aligned with the orientation of the spindle to ensure the determinants are inherited by one daughter cell. In the NB the apical Insc/Par complex recruits a protein complex including Partners of Inscuteable (Pins) and the G protein sub-unit Gαi (Pins/Gαi). The Pins/Gαi complex is responsible for orienting the spindle, it does so via the microtubule-associated adaptor protein, Mushroom body defect (Mud). In mud mutants the spindle orientation no longer aligns with the apical crescent. There is also a microtubule dependent pathway (the Dlg/Khc-73/microtubule pathway) that localises the Pins/Gαi complex. This pathway can act independently of the Insc/Par complex to localise the Pins/Gαi complex. Khc-73 associates with the plus end of the astral microtubules (Siegrist and Doe, 2005) and with Dlg which has been shown to bind Pins and thus recruit the Pins/ Gαi complex (Bellaiche et al., 2001). In the absence of a functioning Insc/Par complex the Pins/Gαi complex is coordinated with the centrosome, however, it is not in the apical side of the cell. Similarly without the Dlg/Khc-73/microtubule pathway the Pins/Gαi complex is apically localised but is not aligned with the spindle (Yu et al., 2006) (Siegrist and Doe, 2005).

In the neuroblast the polarity of the cell is also aligned with the tissue. NB cells are created by symmetric division of neuroectodermal cells which divide in the plane of the epithelium. NB cells rotate their mitotic spindle so it is perpendicular to the epithelial plane and divide asymmetrically. The apical side of all the neighbouring cells is on the same side. Exactly how the polarity of the cells is coordinated is unknown (Wu et al., 2008). However, studies of isolated NB cells show that rather than being an intrinsic property it requires the cell to be in contact with neighbours. Isolated NB will divide but the spindle orientation is random and GaMCs are produced from different places. These observations suggest a role for cell-to-cell communication in establishing the spindle orientation although no receptors have yet been identified (Siegrist and Doe, 2006).

The division of the NB cells is physically asymmetric. The NB cells have a diameter of 10-12 µm compared to 4-6 µm for the GaMCs. The difference in size between the NB and GaMC is thought to be produced by an apically biased spindle (Yu et al., 2006). The mitotic spindle is initially symmetric but the apical aster enlarges and the basal aster shrinks ((Wu et al., 2008)) moving the division plane towards the basal pole. The mother centrosome is always retained in the NB and is likely to play a part in this asymmetry (Yu et al., 2006).

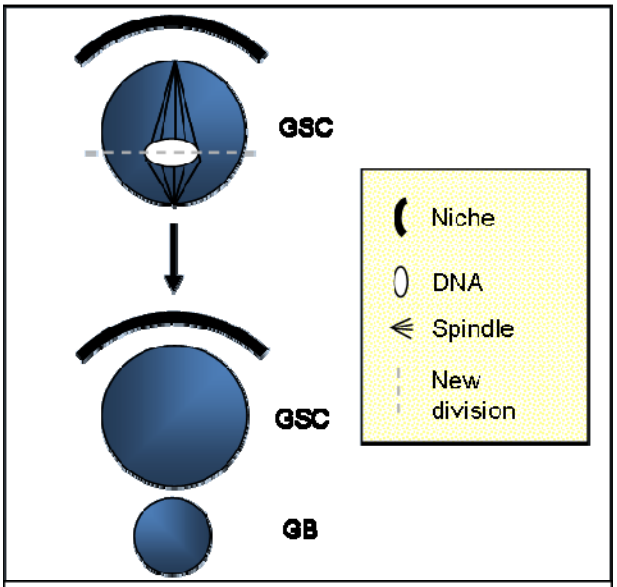

Figure 1.3 Asymmetric division of GCS cells. GSC cells are maintained as stem cells by the niche. They divide to produce a GB with differentiates. The larger GSC remains in contact with the niche and remains a stem cell.

The NB division is a stem cell type division. The NB is regenerated and continues to proliferate while, the GaMC is terminally differentiated and divides only once. This suggests an asymmetric segregation of proliferating and differentiation factors to the daughter cells. One such factor identified is aPKC which is inherited to the NB and is sufficient to promote its renewal. Mutations in aPKC reduce the number of NBs while over expression results in ectopic NB divisions. Pros and Brain Tumour (Brat) are thought to be responsible for the differentiation of the GaMC. Both Pros and Brat are localised to the basal cortex via their interaction with Mira. After division they are released and move to the nucleus. In *brat* mutants the GaMCs do not terminally differentiate but can be rescued by Pros. Brat acts to inhibit the translation of dMyc a regulator of cell cycle progression and growth which is usually only found in the NB.

Drosophila germline stem cells

The asymmetric division of Drosophila germline stem cells (GSC) is an example of stem cell fate in a niche environment. The niche cells for the male germline are called hub cells while the niche cells for the female germline are called cup cells. Both hub and cup cells produce short range signals that maintain stem cell identity. The male hub cells produce a self renewal factor Unpaired (Upd). Upd activates stem cell maintenance pathways (Toledano, 2009). The GSC divides to produce two daughters (Figure 1.3). One remains in contact with the niche and retrains GSC fate. The other daughter moves out of the range of the signal and differentiates into a gonialblast (GB) (Fuller and Spradling, 2007). When the male germline stem cell GSC divides asymmetrically the mother centrosome is retained by the GSC while the daughter centrosome is inherited by the differentiated cell (Wu et al., 2008). The difference in their actions is thought to be responsible for the physical asymmetry in the division.

1.1.2 Asymmetric Division in Plants

The three examples of asymmetric divisions in animals showed some ways in which animals solve the problems of creating asymmetric divisions. Some of the mechanisms are likely to be animal cell specific. The mitotic spindle played a role in making the divisions physically asymmetric, in orienting the divisions relative to extrinsic cues and coupling the division plane to the segregation of determinants. In plants the division plane is defined by pre-prophase band (PPB) formation before the mitotic spindle is assembled (Pickett-Heaps.Jd and Northcot.Dh, 1966). Feedback between the localisation of determinants and the spindle is therefore not available as a mechanism. The GSC provided an example of stem cell fate being maintained by a niche. The differentiated daughters moved away from the signal and lost stem cell identity. Plant cells can not move so this method is also not available to them. Plants need to have different solutions to the production of asymmetric divisions that do not depend upon

the spindle or the ability of cells to move. We will now consider a few plant examples to compare the methods used to create the asymmetric division.

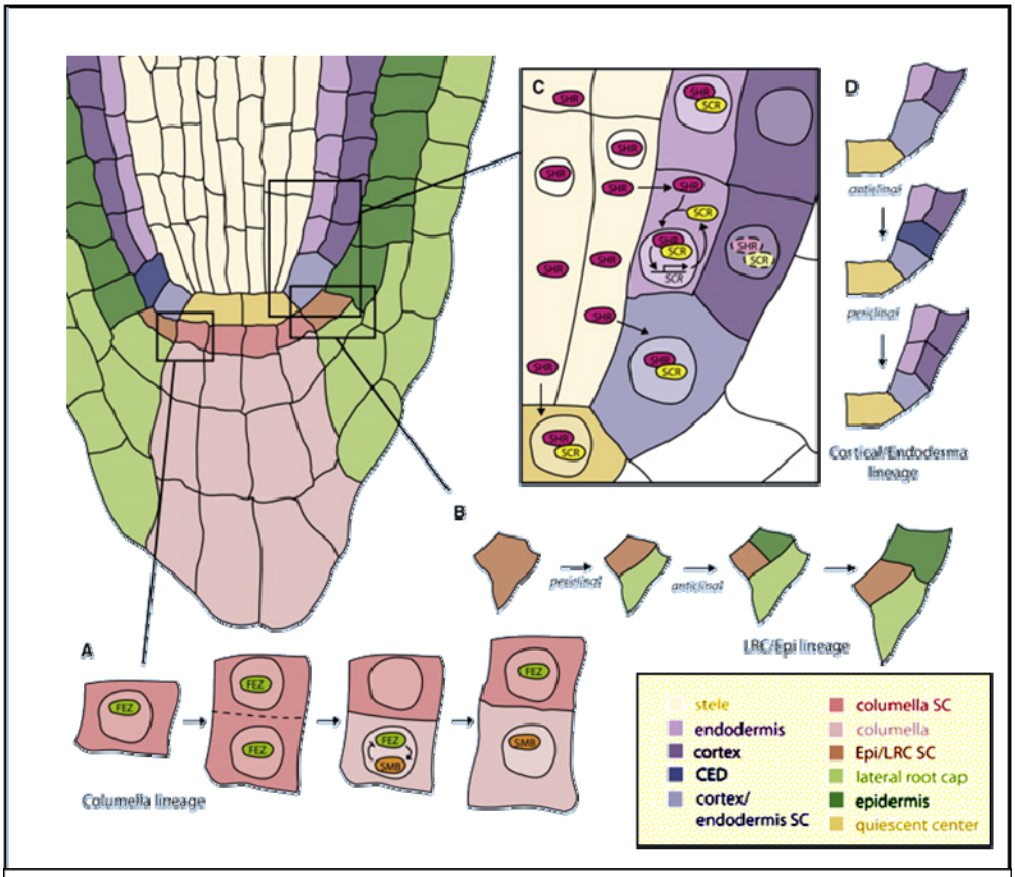

Figure 1.4 The root apical meristem (taken from (Abrash and Bergmann, 2009)).The root meristem has a QC which maintains the stem cell fate of the initials. (a) The Columella stem cells divide to produce the Columella A feedback loop between FEZ and SMB determines cell fate. (b) The Epi/LRC cell divides in two orientations to produce two different differentiated cells. (d) The ground tissue requires the movement of SHR to divide the CEI and (c) pattern the epidermis.

The Arabidopsis root meristem

The root meristem consists of a quiescent centre (QC) where cells rarely divide. Neighbouring the QCs are initials which have stem cell fate. The division of initials

generates differentiated cells and another initial which remain in contact with the QC (Fig 1.4 (Abrash and Bergmann, 2009)). Laser ablation studies show that the QC maintains the stem cell fate of the initials via short range signals (Vandenberg et al., 1995). This is similar to the maintenance of the stem cells in the GSC except the daughters in the GSC move away from the signal coming from the niche. Plant cells are not mobile. Instead the division orientation places the daughter away from the niche and out of range of the signal. The daughter cell is then moved away from the niche by the growth of the tissue.

Stem cell division in the Arabidopsis root meristem

The division of the Columella and epidermal/lateral root cap (Epi/LRC) stem cells were found to be regulated by the same pair of NAC domain transcription factors FEZ and SOMBRERO (SMB) (Willemsen et al., 2008). The columella stem cells divide to increase the number of columella layers (Figure 1.4a). The Epi/LRC stem cells divide anticlinally to produce epidermis and periclinally to produce lateral root cap (Figure 1.4b). The division of the columella stem cell and the periclinal division of the Epi/LRC stem cells is controlled by FEZ. Its specific role in only the periclinal division of the Epi/LRC stem cell suggests a role for FEZ in orienting the division plane. FEZ also seems to promote stem cell identity as it is usually present in the stem cell. The differentiation of the daughter cell is controlled by SMB (Willemsen et al., 2008). In the division of the columella cell the process seems to be controlled by a negative feedback loop where SMB inhibits FEZ. This system shows that like in animals the division orientation is important and the possible dual role of FEZ in orienting the division and conferring stem cell identity provides a mean by which the two could be coupled. The precise mechanisms however are not clear ((Willemsen et al., 2008) and reviewed by (Abrash and Bergmann, 2009)).

Patterning of the ground tissue in the *Arabidopsis* root

SHORT-ROOT (*SHR*) and *SCARECROW* (*SCR*) are required for Asymmetric division of cortical/ endodermal stem cell to produce the cortical/ endodermal initial and its

division to create the two ground tissue layers in the root of Arabidopsis (Figure 1.4d). Mutations in either SHR or SCR results in a single ground tissue layer (Benfey et al., 1993; DiLaurenzio et al., 1996; Scheres et al., 1995). In the *scr* mutant the layer has both enodermal and cortex characteristics while in the *shr* mutant it has only cortex characteristics. SHR functions in a non-cell autonomous manner (Helariutta et al., 2000). Its mRNA is produced in the vasculature but the protein can be detected in the CEID and the endodermal cell layer. The SHR protein can be seen to move from the vasculature where it is present in the cytoplasm and nuclei to the nuclei of the endodermal layers which neighbour the vasculature (Nakajima et al., 2001) (Figure 1.4c). The interaction of SHR and SCR in the same cells induces the division of the CEID and maintain endodermal fate (Cui et al., 2007; Levesque et al., 2006; Nakajima et al., 2001; Nakielski, 2008). The division is therefore controlled extrinsically by the movement of a signal that can diffuse by only one cell.

Stomata subsidiary cell division in Maize

Stomata in Maize form by the asymmetric division of cells within specific cell lineage to forms a guard mother cell (GMC) (Figure 1.5 (Sack and Chen, 2009)).The neighbour cells to the GMCs are subsidiary mother cells (SMCs). The SMCs divide asymmetrically to produce subsidiary cells which neighbours the GMC. Finally, the GMC divides longitudinally to produce a pair of guard cells (Smith, 2001).

Before the SMC undergoes an asymmetric division it is polarised. The nucleus is displaced towards the GMC via a process that depends upon an actin patch proximal to the GMC. PANGLOSS1 (PAN1), PANGLOSS2 and Brick (Brk1) are required for orienting the asymmetric division of stomata subsidiary cells in maize (Cartwright et al., 2009; Gallagher and Smith, 2000). PAN1 co-localises with actin and the nucleus is displaced towards it. After division PAN1 is then inherited by the smaller cell which becomes a subsidiary cell. The *pan1* mutation results in defects in the polarisation of the

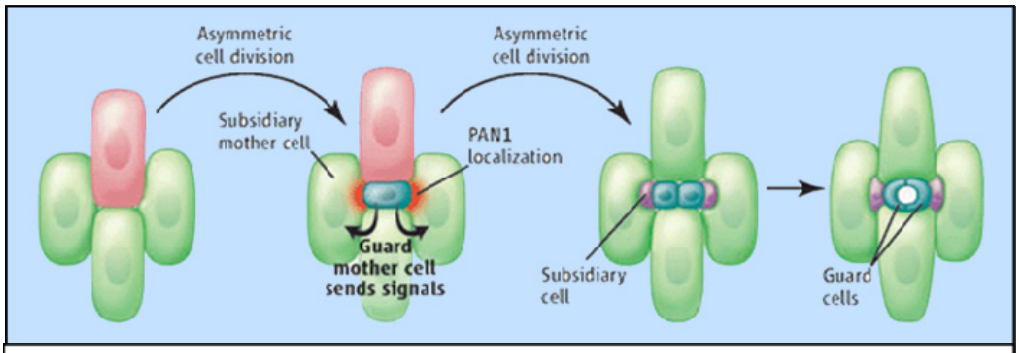

Figure 1.5 Maize stomata development (taken from Sack and Chen, 2009). maize stomata are formed by the asymmetric division of the GMC. The subsidiary cell forms by the asymmetric division of the SMC that neighbour the GMC. This process required PAN1.

SMC and abnormal subsidiary cells. The initial signal from the GMC to localise PAN1 demonstrates an extrinsic influence. Following the localisation of PAN1 the system proceeds intrinsically and is therefore more similar to the SOP and NB examples than the niche examples of the GSC and root meristem.

1.1.3 Summary of asymmetric divisions in animals versus plants

We can return to the key issues of asymmetric division identified originally and consider them in the context of plant and animal divisions. By comparing animals and plants in this way we can see the gaps in our knowledge.

1) Intrinsic versus extrinsic

In animal cells positioning the fate determinants at the poles of the spindle provides an elegant solution to ensuring one cell inherits one fate. Whether such a mechanism could work in plants is not clear. Although plants are traditionally thought to rely more on positional information (Scheres, 2001) both plants and animals use extrinsic factors to control the asymmetric division. There are examples from both plants and animals of using niches to maintain populations of stem cells. However, there are also examples of non-niche stem cell populations. Whether there are common mechanisms to maintain these populations is less clear.

2) Orientating the division

The examples showed that in both plants and animals asymmetric divisions can be oriented within the tissue. For the examples where stem cell populations had a niche, or asymmetric divisions received external cues the orientation of the division was relative to this. We also saw examples where the orientation of the division was controlled by tissue polarity. In animals the orientation can be controlled by re-orienting the spindle. How mechanistically the division orientation is controlled in plants it is not clear.

3) Physical asymmetry

Both plants and animals are capable of producing physically asymmetric divisions. Animal cells and budding yeast produce physically asymmetric divisions via the spindle (McCarthy and Goldstein, 2006). In plants the nucleus may play a role in the deposition of the cortical microtubules and therefore the PPB. Experiments in *Allium* cotyledon cells and *Adiantum* protonemata showed that if the nucleus is moved by centrifugation then a new PPB forms *((Mineyuki et al., 1991)* and (Murata and Wada, 1991) cited in (Scheres and Benfey, 1999)). In fission yeast the position of the nucleus dictates where the new division wall is placed. Moving the nucleus prior to division using optical tweezers can move the division plane of the yeast cell (Tolic-Norrelykke et al., 2005). In the case of the Maize subsidiary cell the nucleus moves towards PAN1. The relationship between the nucleus and the orientation of the division has not been thoroughly investigated.

4) Stem cell divisions

Both animals and plants produce cells which have a stem cell fate and continue to proliferate. In the case of stem cell niches this is controlled by external signals. In non-niche stem cell populations there must be inheritance of proliferating factors by one cell. There must also be factors to ensure the differentiated cells do not keep proliferating. In plants such intrinsically separated factors have not been identified.

1.1.4 Asymmetric cell divisions in the context of tissue patterning

Although we have addressed the major issues of asymmetric division we still know very little about how the asymmetric division can produce tissue level patterning. If the cells are differentiating near a niche or external signal then the interplay between patterning and position is obvious. But, what about stem cells that are not dividing next to a niche, how are they controlled and what can they tell us about patterning a tissue? The aim of this thesis is to integrate asymmetric stem cell divisions with tissue growth and patterning where there is no obvious stem cell niche. The formation of stomata on the Arabidopsis leaf epidermis provides an excellent system in which to do this.

1.1.5 Stomata formation in Arabidopsis

Stomata are an example of a differentiated structure that forms by a series of asymmetric division during plant development. Stomata are specialized epidermal structures found in the leaves of all higher plants. They consist of two guard cells and a central pore and act as valves to regulate water loss and gas exchange. Stomata obey a strict one cell spacing rule (Sachs, 1991). In wild-type *Arabidopsis* stomata never form adjacent to one another. Only 0.4% of stomata form in contact compared to the 45% predicated if distributions were random (Geisler et al., 2000).

Studies in animals have served to highlight the gaps in our current knowledge regarding the asymmetric division of plants and the interplay between asymmetric divisions and tissue patterning generally. Stomata provide a physically accessible system in which to study stem cell divisions in plants. The stomata do not form next to a niche like in the

root meristem so it is unclear what regulates their stem cell fate. Stomata form within the context of the growing and dividing epidermis and thus allow the interplay between these elements to be studied. A huge amount of work has identified the genetic components regulating the stomatal development and patterning. However, almost nothing is known about how stomata lineage cells actually undergo asymmetric divisions.

Stomata development

I will first introduce the development of stomata and key genes known to be responsible before considering these genes along with others in the context of forming an asymmetric cell division.

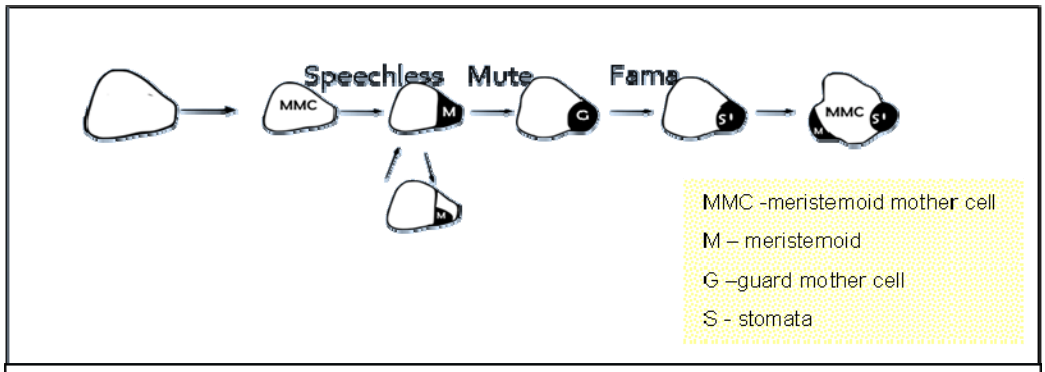

Figure 1.6 Stomata formation in Arabidopsis. Stomata are formed through a series of asymmetric cell divisions. The MMC divides to form a meristemoid. This process requires SPCH. The meristemoid can divide upto 3 times before becoming a GMC, in a process that requires MUTE. The GMC divides to form the 2 guard cells of the stomata. The neighbouring cells may divide again to form secondary meristemoids.

The first asymmetric division in the stomata lineage is that of the meristemoid mother cell (MMC) which divides to produce a smaller meristemoid (Figure 1.6). The meristemoid has limited stem-cell fate: it can differentiate immediately into a Guard Mother Cell (GMC) or can continue to divide up to three times. Each subsequent division produces another meristemoid and another sister cell (Geisler et al., 2000). Once the meristemoid has stopped dividing it progresses to form a GMC which undergoes one symmetric division to form the two guard cells of the mature stomata.

The remaining cells that surround the stomata have a number of possible fates: mature to form pavement cells, divide asymmetrically to form another meristemoid, or divide symmetrically to produce two cells that again have all these fates.

1.1.6 Asymmetric cell division in the stomatal lineage

In the beginning of the introduction four key issues regarding the formation of asymmetric divisions were identified. I will discuss what is known about stomata in the context of addressing these issues.

1) Intrinsic versus extrinsic fate determinants

The stomata do not have a niche to regulate their stem cell and no factors which are inherited by only one daughter have been identified. So what conveys stem cell fate to the meristemoids? Whether stomata are controlled by extrinsic or intrinsic signals has been long debated and relates to how the observed pattern of stomata could be created ((Sachs, 1994) (Croxdale, 2000; Larkin et al., 1997; Sylvester et al., 1996)). There are three main theories as to how stomata could be patterned: i) Pre patterning of MMCs. ii) Lineage mechanism whereby stomata are surrounded by clonally related cells. iii) cell-to-cell interactions to prevent neighbours of stomata becoming stomata. The idea of long range inhibitory signals that come from stomata to inhibit new stomata was proposed in 1956 by Bűnning. Patterning via long range inhibitors and pre-patterning have been ruled out due to the formation of secondary meristemoids next to stomata (Geisler et al., 2000). Cell-to-cell communication has been shown through the orientation of secondary meristemoids (Geisler et al., 2000; Geisler et al., 2003). Dental resin impressions (Berger and Altmann, 2000) and clonal analysis (Serna et al., 2002) studies suggest a role of cell lineage in spacing. The overall spacing is likely to be a combination of lineage and context sensitive rules (Sachs, 1994). Many genes have been identified, by mutant screens, that regulate stomata formation but whether they act intrinsically or extrinsically is not always clear.

Stomata promoting factors

Positive regulators of stomata fate have been identified that when mutated eliminate stomata; these are all candidates for conferring stem cell fate. All of the key developmental genes fall into this category. The pathway from MMC to stomata requires three bHLH transcription factors SPEECHLESS (SPCH), MUTE and FAMA (Figure 1.6). SPCH has been identified as being required for the first asymmetric division of the MMC a cell that until it divides is indistinguishable from the other cells of the epidermis (MacAlister et al., 2007). The *spch* mutant *spch-1* produced no stomata while the weak mutant *spch-2* produced fewer stomata than wild-type. The spch-1 mutant did not produce any physically asymmetric divisions (MacAlister et al., 2007). However, over expressing SPCH does not result in all cells acquiring stomata cell fate. SPCH is regulated post-transcriptionally (MacAlister et al., 2007) by YODA phosphorylating which inactivates the SPCH protein (Lampard et al., 2008). Removal of the key phosphorylation sites results in many more asymmetric divisions and more stomata. SPCH is a possible candidate but it is not known whether all cells which express SPCH become stomata. SPCH expression is reported to be in more cell than can acquire stomata fate (Abrash and Bergmann, 2009).

MUTE is required for the arrest of meristemoid divisions and the formation of GMCs (Pillitteri et al., 2008). The *mute* mutants produce spirals of meristemoids that undergo 3-6 rounds of division rather than the 1-3 reported for wild-type meristemoids. These cells do not have the appearance of GMCs and do not express GMC specific genes. MUTE is therefore required to limit the replication potential of the meristemoids to enable GMC formation. Overexpression of MUTE under the 35S promoter results in all cells becoming stomata (Pillitteri et al., 2008).

FAMA is required for the final division of the GMC to produce a pair of guard cells (Ohashi-Ito and Bergmann, 2006). FAMA is sufficient to make any epidermal become a guard cell if overexpressed using the estrogen inducible system (Ohashi-Ito and Bergmann, 2006). MYB88 and FOUR LIPS also play a role in the production of guard cells from the GMC.

SCREAM (SCRM), also called INDUCER OF CBF EXPRESSION (ICE) due to its role in freeze tolerance, and SCREAM2 (SCRM2) interact with and direct the action of SPCH, MUTE and FAMA (Kanaoka et al., 2008). They act redundantly in stomatal

lineage initiation. The double *scrm scrm2* mutant like the *spch* mutant does not have any stomata.

There are positive regulators of stomata formation that target higher order complex formation (AGL-16, and GPA1) by promoting secondary meristemoid divisions (Serna, 2009) (see next section). GPA1 is a G protein α subunit which binds the β subunit AGB1. GPA1 promotes secondary complex formation while AGB1 reduces it. Both subunits are therefore likely to have a role in signalling to regulate stomata formation (Zhang et al., 2008). ALG-16 is a MADS box protein which also promotes formation of secondary meristemoids. It is regulated by micro RNA miR824 (Claudia Kutter, 2007).

There are also positive regulators that act more generally. Stomagen acts promotes stomata production and is produced in the mesophyll (Sugano et al., 2010).

There is difficulty in distinguishing between genes that regulate the density of stomata, i.e. the number of MMCs, and genes that are required for the stem cell fate of the meristemoids. To show that a factor is acting as a fate determinant it would be necessary to see it maintained by only one daughter as in the animal examples or to see them move into and convey a particular fate by the activation of differentiation genes. To visualise either alternative requires a more dynamic view of the developing system.

Factors restricting stomata formation

Fate determination does not just require factors that promote stomata lineage fate, there must also be factors to eliminate this fate. The role of YODA in regulating SPCH has already been discussed. There are other mitogen-activated protein kinases thought to act down stream of YODA: MKK4/MKK5 and MPK3 and MPK6. However, their expression is too general to be a segregated determinant. They are more likely to respond to stimuli to silence the stomata development via other intermediates. Expression of YODA in GMCs seems to promote guard cell formation suggesting a positive role depending on the timing of expression (Lampard et al., 2009).

A number of other factors also increase stomata number when mutated but they also disrupt spacing and are therefore thought to be required for orienting the divisions and will be discussed in the next section.

EPF2 is a small secretory protein expressed by MMCs, meristemoids, sisters of meristemoids and GMCs . Overexpresssion of EPF2 results in decreased stomatal density and a reduction in the number of small cells. The *epf2* mutant has increased stomata but they do not form clusters, there is also an increase in the density of pavement cells. EPF2 may regulate entry to the stomata lineage versus pavement cell differentiation. EPF2 inhibits its own expression and may therefore act as a diffusible inhibitor of stomatal entry. EPF2 is not expressed in the *spch* mutant. EPF2 seems to require TMM, the ER family and YODA (Hara et al., 2009; Hunt and Gray, 2009). EPF2 and BASL act independently with the double mutant showing an increase in both symmetric and asymmetric divisions (Hunt, 2010).

2) Orienting the asymmetric division

Meristemoids have been sub-divided into primary meristemoids which form by the division of isolated MMCs and secondary meristemoids which are formed by the divisions of MMCs which are adjacent to stomata or stomata precursors (Geisler et al., 2000). In the case of secondary meristemoids the division is known to be oriented so that the new meristemoid forms distal to the stomata or stomata precursor (Sachs, 1994). This is thought to be a component of the extrinsic control mechanism. The orientation of asymmetric divisions is critical in the patterning of plant cells as plant cells can not move. Division orientation therefore dictates the neighbours of a cell and makes a large contribution to the spacing pattern of stomata. How the divisions are oriented is not clear. One mechanism could be by altering the location of the nucleus. The location of the nucleus in cells neighbouring stomata (neighbour cells (NC)) was found to be distal to the stomata. NC with distal nuclei were more likely to divide than ones without, however, not all NC with distal nuclei divided (Geisler et al., 2003). The orientation of the subsequent secondary meristemoid divisions and the division of primary meristemoids remains cryptic. Dental resin impression have been used to trace

stomata lineages and led to the conclusion that the orientation of primary meristemoids was random (Geisler et al., 2000).

A number of patterning mutants have been identified which disrupt the division orientation of the secondary meristemoids. The *too many mouths (tmm)* mutant was one of the first characterised, it increases stomata numbers but also disrupts spacing with clusters of stomata forming across the surface of the leaf (Yang and Sack, 1995). Following lineages via dental resin impressions found that the orientation of division which gave rise to secondary meristemoids in *tmm* were not statistically different from random (Geisler et al., 2000). *TMM* encodes a leucine-rich-repeat (LRR)-containing receptor like protein but lacks a cytplasmic kinase domain (Nadeau, 2002). Structurally it is similar to CLV2 which regulates differentiation in the meristem. TMM is expressed in cells surrounding stomata and is thought to play a role in communicating the location of stomata. TMM also seems to play a role in promoting amplifying divisions of the meristemoids. Some cells in the *tmm* mutant produce meristemoids and GMCs without dividing (Geisler et al., 2000). How TMM could mechanistically orient the divisions is not clear as it has a uniform distribution throughout the cells. The position of the nuclei was not disrupted in the *tmm* mutant suggesting that it is not responsible for moving the nucleus (Geisler et al., 2003). Stomata are also regulated by environmental factors e.g. CO2. In low CO2 more stomata form. In an extreme example plants were grown in sealed containers with no gas exchange. These conditions resulted in plants with clustered stomata similar to those seen in the *tmm* mutant (Serna and Fenoll, 1997).

A number of other genes identified have been suggested to work with TMM. STOMATAL DENSITY and DISTRIBUTION (SDD) is a subtilisin-like serine protease. Mutations in SDD result in an increase in stomata density and some clustering (Berger and Altmann, 2000). It is thought to act as a signalling molecule (von Groll et al., 2002) and to require TMM. There are suggestions that SDD and TMM work in a signalling pathway with TMM acting as the receptor. However, TMM has functions that do not depend on SDD (Nadeau, 2003; Serna, 2002). ER, ERL1, and ERL2 are LRR receptor kinases (LRR kinases) (Shpak et al., 2005) and have been suggested to function with TMM to receive positional signals from stomata and stomata precursors such as EPF1 which is expressed in stomata precursors. Over expression of EPF1 results in

reduced stomatal number while mutations result in increased stomatal density and clustering (Hara et al., 2007).

3) Physical asymmetry

The asymmetric division of the MMC and meristemoids are reported to be physically asymmetric. Prior to division the nucleus and organelles can be seen to be asymmetrically located (Zhao and Sack, 1999). Earlier we saw that moving the nucleus might provide a plant specific alternative to the spindle in creating a physically asymmetric division. What controls this is not known though the recent identification of the novel protein BREAKING OF ASYMMETRY IN THE STOMATAL LINEAGE (BASL) might shed some light on the issue (Dong et al., 2009). The *basl* mutant *basl-1* has excessive numbers of small epidermal cells and their stomata are clustered. The *basl-2* mutant showed a reduction of cells that were physically asymmetric from 68% to 12%, based on whether the small cell was less than 35% of the mother cell. Difficulties in identifying MMCs mean it is not clear what range of physical asymmetry is exhibited by the non-stomatal lineage cells. BASL might also have a role in the fate asymmetry of the cells based on MUTE expression and the observation that one, both or neither daughter acquired guard cell fate in the mutants (Dong et al., 2009).

BASL expression can be seen in nucleus of meristemoid cells and correlates with the expression of TMM and SPCH. BASL is also seen as a crescent in the cell periphery of meristemoids, identified by their characteristic triangular shape. The crescent is usually distal to the nucleus and if the cell neighbours another stomata, proximal to it. BASL is always distal to the new meristemoid even in and *epf1* mutants where meristemoids form in contact with stomata. In *epf1* mutants the BASL crescent does not form next to the existing stomata. In cells where BASL is in the nucleus and the periphery the cells undergo an asymmetric division. Cells with BASL in the nucleus tended to form GMCs and while cells with BASL at the periphery formed pavement cells. Localising BASL to the periphery was sufficient to rescue the mutant phenotype. Overexpressing BASL under the 35S promoter results in ectopic out growths.

4) Stem cell

The meristemoids have limited stem cell fate. They divide 1-3 times before differentiating. As the meristemoids do not divide near a niche it would be expected that one cell must inherit a proliferating factor to maintain it in a stem cell state. The fate of the sister cell is also variable, they have one of three fates: mature to form pavement cells, divide asymmetrically to form another meristemoid, or divide symmetrically to produce two cells that again have all these fates. The ability of the sister cells to divide as secondary meristemoids suggests that the separation of daughter fates might not be as clear as in some other systems and does not make the task of identifying fate determinants any easier.

Summary

The interplay between the patterning of stomata and the asymmetric divisions makes it difficult to understand what is going on. Which factors are required for the asymmetric divisions and are they intrinsic or extrinsic?

1.2 Putting the stomata into a tissue context

Considering the meristemoids in the context of the other asymmetric divisions has highlighted some of the issues and some of the gaps in our knowledge. It is unclear how the cells make an asymmetric division and how the numerous patterning factors are integrated. To understand how the patterning of stomata might occur and the role of the asymmetric divisions in this we need to consider the tissue itself.

Plant development is a dynamic process where cells grow, divide and differentiate, in a symplastically growing space (Priestley, 1930). The Arabidopsis leaf epidermis is a tissue consisting of a single layer of cells of various: sizes, shapes, and functions. To understand how to integrate stomata patterning into the epidermis we first must consider how it is growing and dividing.

1.2.1 Cell division timing and orientation

In asymmetric cell divisions the timing and orientation of the division is tightly controlled. But what about the division of the other cells, how is this regulated?

1.2.2 Cell division orientation

There are a range of theories as to how cells might position their new walls. Hofmeister observed in 1863 that new cell walls are perpendicular to the axis of growth (Hofmeister, 1863). Sachs claimed that new cell walls meet the old walls at 90° (Sachs, 1878). Errera proposed that cells behave as soap bubbles and new cell walls follow the shortest path across the cell that will halve its volume (Errera, 1888). Studies in which cells in suspension were compressed showed that cells oriented their division perpendicular to the stress, however, this was also the shortest path across the cell (Lynch and Lintilhac, 1997).

In 1936, Sinnott showed that the root cells he observed tended to divide transverse to the axis of the root. The new walls avoided forming four way junctions and most new wall met old walls in their centre unless, this created daughters of unequal volume (Sinnott, 1936). He proposed that the new wall was positioned as a compromise between avoiding existing junctions and dividing the mother cell in half. More recent studies of cell division in the root concluded that the new wall was positioned based on the growth directions of the cells. (Nakielski, 2008). The model predicted the orientation of the division wall by computing the principle direction of growth of the cells and dividing them either along this axis, or perpendicular to it, depending on which gave the shortest new wall. The model did not always divide cells through the centre but, with some distribution around it.

Two further division models were proposed in order to explain cell division in the fern gametophyte (*Thelypteris palustris*): the longest wall and the closest point (Korn, 1993). The longest wall algorithm involved dividing the longest wall of the cell and accounted for 182/200 division seen in the fern gametophyte. The closest point divided the cell

using the closest point to the centre and a point on the opposite wall that would be reached by a wall joining the centre to the first point which explained 192/200 divisions.

There have also been many studies into cell division in the meristem. Sahlin used a mass spring model to assess the ability of different division rules to recreate the observed cell divisions (Sahlin, 2010). The models output was assessed in terms of final cell geometry and topology. Placing the division wall so it passed through the centre of mass was preferable to placing it randomly. The shortest path across the cell was found to be a better approximation than dividing the cell orthogonal to the parental division plane; although they often produced a similar result. For isotropically growing cells, the principle direction of stress is ambiguous and dividing perpendicular to it is similar to dividing randomly. Dividing cells along the shortest path across the cell, going through the centre of mass, created two daughters of roughly equal size, similar to what is seen in the meristem (Sahlin, 2010). However, studies of the stresses in the meristem suggest that the central region has isotropic stresses while, in the peripheral region the stresses are orientated and the microtubules are aligned with this direction (Grandjean et al., 2004; Hamant et al., 2008).

It is unclear which mechanism might be responsible for symmetric cell division in the leaf and how this might be altered to produce asymmetric divisions.

1.2.3 Cell division timing

Cells in multicellular tissues are subjected to symplastic growth (Priestley, 1930). Therefore, the differences in cell area between neighbours must be due to differences in division rate (Ivanov et al., 2002). Cell division timing is therefore an important generator of tissue level pattern. When cells divide can be thought of in two different time scales, in the short term it is linked to entry into the mitotic phase of the cell cycle. In the longer term cells have a limited competence to divide; this is traditionally thought of as cell arrest.

The cell cycle

"The cell cycle of a growing cell is the period between the formation of the cell by the division of its mother cell and the time when the cell itself divides to form two daughters" (Mitchison, 1971). The cell cycle is divided into several phases: named G1, S, G2 and M in the 1953 by Howard and Pelc (Mitchison, 1981). In G1 the cell grows and synthesises proteins. S phase sees the replication of the DNA. In G2 the cell grows and synthesises proteins before the cells divide in M phase. The mechanisms that control progression through the cell cycle are conserved between all higher eukaryotes (Dewitte and Murray, 2003). The rate of progression is primarily controlled just before S phase or just before M phase. The progression through these control points is controlled by the action of cyclin-dependent kinases CDKs. The first CDK cdc2 was identified in Schizosaccharomyces pombe (L. De Veylder, 1998).

In yeast cell size is tightly controlled. Yeast cells divide symmetrically at the threshold area ~14µm and produce two daughters of ~7µm. These cells grow to double their size then divide again (Martin and Berthelot-Grosjean, 2009). Any deviation in cell size resulting from an unequal division is corrected within one cell cycle (Fantes, 1981b). Two alternative models have been suggested for regulating the size of division. 1) Release of a constant amount of inhibitor once each cell cycle. Once the level is half the amount released the cell can divide. 2) Positive factors accumulate throughout the cell cycle and are counted. At a certain level they trigger cell division. To control size the rate of production must relate to the size of the cell (P.Nurse, 1981). Studies in fission yeast (Schizosaccharomyces pombe) have identified components that use the first method and relate progression through the cell cycle to the size of the cells (Moseley et al., 2009). Pom1 forms gradients with the highest concentration at the cell ends. POM1 inhibits cell division by inhibiting Cdk1. As the cell enlarges the concentration of POM1 in the centre of the cell decreases and inhibition is reduced. Levels of POM1 thus convey the size of the cell to the cell division machinery and ensure all cells divide at the same size (Martin and Berthelot-Grosjean, 2009; Moseley et al., 2009).

Many cell cycle regulators have been identified in Arabidopsis; the CDKs have been classified into 5 types (A-E) based on sequence homology (Dewitte and Murray, 2003). Although much work has been done to elucidate components of the cell cycle little is

known about how the timing of cell division is controlled in the developing leaf. In plants many signals feed into the cell cycle. The expression of D-type cyclins correlates with the presence of hormones or other extracellular signals. For example the expression of D-type cyclin CYCD3;1 can be induced by cytokinins and brassinosteriods. Overexpression of CYCD3;1 induces growth of Arabidopsis leaf calli; providing evidence of hormonal control of cell cycle genes and organ growth.

Differentiation also impacts on the cell cycle. Endoreduplication is associated with differentiation in many plant tissues including production of pavement cells or trichomes (Melaragno et al., 1993). Endoreduplication correlates with a reduction in expression of cell cycle regulators particular ones with roles in M phase (e.g.CYCB1;2 expression in trichomes induces divisions) (Dewitte and Murray, 2003). Giant cells in the sepal also form through endoreduplication and it is possible to model their formation through stochastic endoreduplication events which inhibit cell division (Roeder et al., 2010). The model was supported by the identification of cell cycle inhibitors that regulated the number of giant cells (e.g. overexpression of the cell cycle inhibitor KIP RELATED PROTEIN increased the number of giant cells).

Cell cycle genes which target the stomata have also been identified. CDKB1;1 is required for cell division in stomata lineage but not for stomatal differentiation(Boudolf et al., 2004). Over expressing a dominant negative version of CDKB;1.N161 showed reduced size, cell number and stomata number in both the leaf and the cotyledon. They also observed a lack of secondary meristemoids suggesting that CDKB1 is necessary for meristemoid divisions. The meristemoids in the mutant are blocked in the G2 phase and do not divide however they do still differentiate into guard cells. (Kono et al., 2007).

E2F family of transcription factors heterodimerise with dimeristation protein DP and also interact with Retinoblastoma proteins (Rb). Over expression of one E2F found in Arabidopsis EF2a with DPa leads to ectopic divisions or endoreduplication of cells in the leaf. Which occurred depended on whether the cells were competent to divide (De Veylder et al., 2002). Usually E2F-DP is inhibited by Rb which are thought to act to promote differentiation. In maize Rb gradients correlated with cell differentiation (De Veylder, 1998).

Cell arrest

In addition to endoreduplication all cells have a limited competence to divide and eventually arrest division. The traditional view of cell arrest in a leaf is that it occurs progressively from the tip. This idea was introduced by (Donnelly et al., 1999). They used cyclAt::GUS reporter to mark cell proliferation in wild-type (Columbia) Arabidopsis leaves. They found that initially (4DAS) GUS activity was high over most of the leaf except for the base of the mid-vein and the petiole. By 8DAS they saw a proximal distal gradient in GUS activity. All cells in the proximal half of the leaf were labelled but only the meristemoids were labelled in the distal regions. By 12DAS the gradient in GUS activity is evident but restricted to the distal third. The authors report a sharp reduction in labelling at 16DAS with GUS only visible in the petiole and adaxial meristemoids. They therefore conclude a basiplastic gradient of cell cycling with the exception of secondary merisemoids which remain competent to divide some time after the surrounding cells have arrested. White proposed that stomata and vascular precursors cells (dispersed meristematic cells (DMC))arrest later than the other cell types of the leaf (White, 2006). A gene PEAPOD was identified as being responsible for the arrest of DMCs. Mutants have increased stomata and an increase in leaf area but no increase in leaf perimeter which results in a curved phenotpye. CYCB1;1::GUS expression analysis showed that meristemoids arrested cell cycling at 12DAG while the mutant meristemoids had still not arrested after 20DAG.

Recently, it was proposed that the competence to divide might come from the base rather than the traditional distal-proximal wave of cell arrest (Kazama et al., 2010). Proliferating cells were identified in dead leaves aged 3-8DAS using pCYCB;1::CYCB;1::GUS. The arrest front was defined as the position where the expression level value was half the maximum expression seen. This allowed the proliferation of stomata lineage cells to be ignored. Based on these results they showed that the arrest front was a fixed distance of 100 µm. They also consider the final arrest of the base of the leaf a phenomenon observed as a sharp reduction in cell proliferation at 16DAS (Donnelly et al., 1999). Kazama *et al* propose a mechanism based on the expression of KLU which they propose is responsible for promoting cell division. The evidence for this is limited to the expression of KLU which is initially expressed

throughout the leaf and is then restricted to the base. None-the-less they are able to create a model for cell cycle arrest which is plausible. They produce a mathematical model where the leaf is represented as a 1D growing system. The growth rates are matched to the growth of the leaf length but vary only in time and not space, i.e. they assume growth is uniform along the leaf. Their model is calibrated with the expression level of KLU which they observe to have a bell shaped expression over time. They also assume production at the base and a decay term to generate an exponential profile. Their profile changes with time as the levels of KLU are not constant. The final drop in KLU expression is responsible for the final arrest of the leaf base.

How stomata arrest is unclear. Individual lineages arrest when MUTE is expressed. MUTE expression restrict meristemoids to 1-3 divisions. Although given the difficultly in identifying MMCs it is not obvious when to begin counting. Stomata arrest also requires no new MMCs to be recruited but how this occurs is also unknown.

1.2.4 Growth

The cell divisions both symmetric and asymmetric are occurring in the growing surface of the leaf epidermis. Studies have suggested a link between cell division orientation and growth in the root and the meristem (Hamant et al., 2008; Nakielski, 2008; Sahlin, 2010). To asses whether such a relationship exists in the leaf and whether it impacts on the patterning of the tissue it is necessary to know the growth across the leaf.

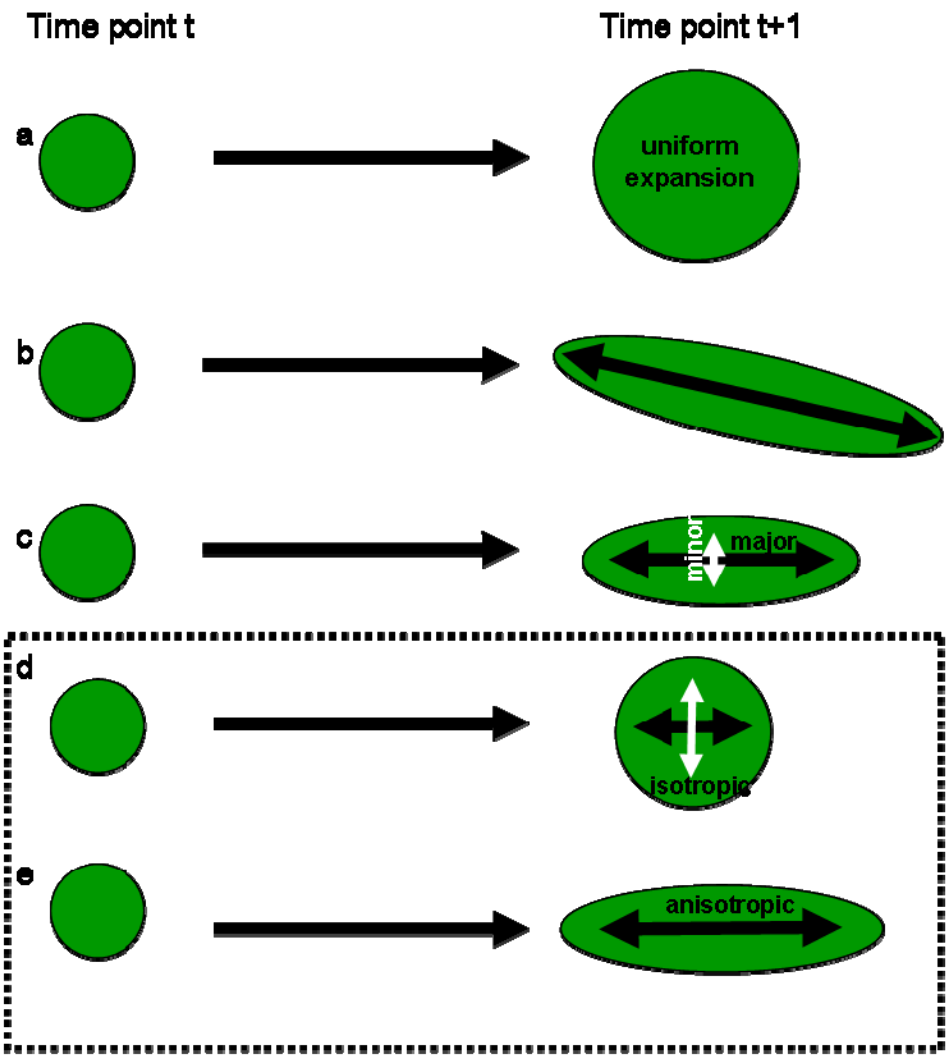

Figure 1.7 Growth Parameters. a) A circle can enlarge uniformly with an areal growth rate. b) If the circle grows non-uniformly then there is a principal direction of growth. The orthogonal direction is the minor growth direction. c) The rates of growth in these directions are the major and minor growth rates. d) The ratio of the minor to major growth rate is the anisotropy, if it is 1 then Kmajor is equal to Kminor i.e. the growth is equal in both directions. e) If the ratio is 0 then growth is in only one direction the Kmajor direction and thus growth is perfectly anisotropic.

D'Arcy Thompson in the early 20th century introduced the idea of calculating growth using grids drawn onto growing organisms (Thompson, 1917). In 1933 Avery drew grids onto tobacco leaves and observed the distortion of the grid through time in order to study the leaves growth (Avery, 1932). The grid data generated by Avery was used by Richards and Kavanagh to quantify growth by calculating a field of velocity vectors

(Richards and Kavanagh, 1945). It is easy to think about growth in terms of a velocity field as we can imagine the points moving away from each other and calculating the rate at which they are moving. However, it is more useful to consider the different elements of the growth. Growth of an infinitesimally small region can be accounted for by four parameters (Coen et al., 2004; Hejnowicz and Romberger, 1984) (Figure 1.7): the growth rate- which tells us the increase in length, area or volume (a), the major axis of growth – which tells us the direction in which the most growth is occurring (b), the anisotropy – which tell us the degree to which growth occurs preferentially in the direction of the major axis (d-e), and the rotation – which tells us how much the regions are turning relative to each other. The velocity is thought to be a result of the growth so is not usually considered (Coen et al., 2004). Calculation of the growth tensor allows full characterisation of the growth (Hejnowicz and Romberger, 1984). The growth tensor can be calculated from the velocity field as growth is most simply considered as the change in velocity over the change in position. (For more details on calculating growth rates refer to methods)

1.2.5 Imaging methods to allow growth and cell division to be compared

Although marking a grid onto a leaf can be used to compute growth rates it does not provide information on the cell divisions necessary for a direct comparison between growth rate and cell division. It is also limited to large specimens. Other techniques permit both to be considered.

Clonal analysis

Clonal analysis provides an alternative to drawing grids. It involves marking a cell early in development in a way that will be inherited by its progeny. After the tissue has grown the progeny of the cell can be identified. One such method is the use of ionizing radiation to induce chromosomal rearrangements that result in a visible phenotype which is passed on to the daughters when it divides. This method was used to study the growth and cell division rates across cotton leaves (Dolan and Poethig, 1998). The size of the clone can provide information on the growth of the cell (Rolland-Lagan et al.,

2005). Assuming the events that mark the cells are rare, each clone is derived from a single cell, the size of the clones reflects cell division rate and the shape can give an idea about cell division orientation. However, the resolution is low and the precise order, timing and orientation of divisions can not be seen.

As plant cells do not slide past each other the cell vertices are conserved and can be used as landmarks from which to calculate growth. Therefore, imaging methods that can capture successive images of the leaf with a cellular resolution can be used for both the study of growth and the study of cell division. The benefit of using tracking data to study cell division was recognised in 1936 (Sinnott, 1936). However, using direct tracking to study growth and cell division has only recently become feasible enough to be popular, and a lot of work has been done on the meristem ((Dumais and Kwiatkowska, 2002; Kwiatkowska, 2006; Reddy et al., 2004) and the root (Nakielski, 2008)). This work is based on two different methods of direct tracking: sequential replicas and time-lapse confocal imaging.

Sequential replicas

The use of sequential replicas was first introduced by Williams and Green in 1988 and has since been used to study of cell division and growth of the meristem ((Dumais and Kwiatkowska, 2002), Kwiatkowska D, 2006). It involves making a mould of the specimen which is used to produce the replica. The replicas are then viewed using SEM. This technique is non-invasive so the same specimen can be viewed repeatedly. This permits individual cells lineages to be followed and growth rates to be calculated on a cellular basis. This technique allows the monitoring of cell division and growth simultaneously. The technique, does, however rely on physical changes in the surface of the epidermis so can not be extended to the lower layers and in some cases induces a delay between the new wall forming and the event being captured. There is also a complex process of reconstructing and aligning the images to identify corresponding cells.

Time-lapse confocal imaging

Time-lapse confocal imaging, like the use of replicas, is non-invasive and allows continuous monitoring of the same specimen (Shaw, 2006). In contrast to the use of replicas, confocal imaging permits the use of GFP labelled proteins. Short term time-lapse can be used to study sub-cellular dynamics (Chan et al., 2007; Dong et al., 2009). The technique is also being extended to allow monitoring of organ growth. The specimen can either be kept in a chamber under the microscope or can be put under the microscope at regular intervals. Time-lapse confocal imaging is used extensively in animal research to study cell division (Olivier et al., 2010) and cell movements. In plants time-lapse imaging has been optimised for studies of meristem development (Reddy et al., 2004). The use of fluorescent probes enables brighter images of the cell walls to be collected giving a more accurate timing for when the wall appears. The enhanced contrast makes the output easier to analyse using image processing techniques (Fernandez et al., 2010). There is however problems with ensuring the specimen are kept alive and healthy while at the same time capturing useable images (Shaw, 2006). So far no studies have been conducted in to the patterns of cell division and growth across the Arabidopsis leaf using time-lapse confocal imaging.

1.3 Aims and approaches of the thesis

The aim of this thesis is to integrate asymmetric stem cell divisions with tissue growth and patterning where there is no obvious stem cell niche. Time-lapse confocal imaging provides a means of capturing the cell division, and growth of a live specimen. However integrating growth, cell division and patterning is a challenge. I will therefore use computational models to help formalise the ideas and generate testable hypothesis.

1.3.1 Using modelling to study development

Causality is the relationship between an event (the *cause*) and a second event (the *effect*), where the second event is a consequence of the first. Aristotle provides the example of a builder building a house. In this case the builder building is the cause and

the house being built the effect. In development there is no builder. Organisms build themselves and hence cause and effect can become confused. Modelling can provide a means by which to formalise our hypothesis regarding cause and effect and providing we have a suitable framework can often allow us to distinguish between competing hypothesis. Computational modelling which has gained popularity within the field of biology has the advantage over traditional conceptual models and schematics in that they can generate quantitative predictions which can be tested (review by (Chickarmane et al., 2010)).

Modelling development poses additional problems to the field of modelling. Biological systems are dynamic so there maybe changes in the state of the system (e.g. the concentration of molecules). Biological systems also have a structure made of discrete parts and the state of the model can be viewed as the sum of the state of all of the separate parts (e.g. the concentration gradient can be calculated on a per cell basis). Finally as an organism grows the number of elements that make up the structure may increase (e.g. the number of cells might increase due to cell division). Biological systems are, therefore, described as being dynamic systems with dynamic structures (DS^2) (J-L. Giavitto, 2002).

There are different modelling approaches and they have different purposes. In some cases the aim is to produce as realistic a model as possible. This can involve inputting a lot of data. For example a descriptive model of the development of an Arabidopsis plant was created using precise biological measurements (Mundermann et al., 2005).The construction of this model helped identify what features were essential in characterising the growth of a plant. It highlighted many issues regarding the integration of biological data into a model such as the need to interpolate between data points to produce a smooth growing structure. The model also provides a framework in which to integrate more mechanistic elements. Other modelling approaches can involve producing the simplest model possible, to determine the minimum number of elements need to capture the essence of a system. For example an array of tree forms can be generated using only a few parameters (Palubicki et al., 2009). Both types of models can produce testable hypothesis, highlight missing data and inspire new experiments. Combining experimental results and modelling is becoming popular and has led to many important breakthroughs in understanding particularly in the meristem. The role of auxin in

phylotaxis and vein formation was elucidated through model driven experiments (Smith et al., 2006a) (Smith and Bayer, 2009), along with a mechanism of generating and maintaining the auxin gradients in the root (Grieneisen et al., 2007).

1.3.2 Combining modelling with time-lapse imaging

Combining the use of modelling and time-lapse imaging techniques has been used previously to study cell division and growth in the meristem (Sahlin, 2010) and to study the orientation of stresses in the meristem (Grandjean et al., 2004; Hamant et al., 2008). The cell shapes are more complex in the leaf than in the meristem so they may grow differently. The complex cell shapes may also make it easier to distinguish between the different division algorithms.

1.3.3 Approach of the thesis

The aim of this thesis is to integrate asymmetric stem cell divisions with tissue growth and patterning where there is no obvious stem cell niche. This will be done using a combination of time-lapse imaging and computational modelling techniques. The thesis will first consider the development of the epidermis then the formation of stomata. A problem of understanding the relationship between the tissue and the asymmetric divisions is that they are integrated. In this thesis normal cell divisions will be studied using the *spch* mutant which does not produce any stomata. A descriptive model of the leaf will be produced and used as the framework for studying the cell divisions. The asymmetric cell divisions will then be considered and related to the tissues development. Live imaging of stomata formation will provide a better understanding of their formation and enable the expression of key factors within the stomata lineage to be followed.

2 Methods

During the course of my PhD I helped to develop a work flow to take the user from raw images to a descriptive model. Raw images where acquired using time-lapse confocal microscopy. These images where then processed, filtered and projected to produce an image sequence. The images were then digitised using the point tracker. The point tracker output was read into matlab for data analysis and into VVe to drive the descriptive model of cell growth and division.

2.1 Data acquisition

Growth media (MS) used for growing plants on plates (1 litre)

Murashige and Skoog (macro and micro elements) 4.4g
Glucose 10g
MES 3ml
pH to 5.7 with KOH
0.9% agar 9g

Liquid Growth media used to perfuse growth chamber (1 litre)
(Diluted to quarter strength)
Murashige and Skoog medium
micro and macro elements including vitamins1.1g
Sucrose 7.5g
Adjust pH to 5.8 with 1M NaOH
The sucrose/glucose in both media is essential for the growth of the SPCH mutant which does not have stomata. To avoid bias I used the same media for the wild-type experiments. All media was supplied by the John Innes Media kitchen.

Plant lines

Lt16b line (Cutler et al PNAS (2000) 3718-3723) in Columbia background was used to visualise the wild-type cell outlines. Marks the plasma membrane and was identified in a screen for markers.
SPCH::SPCH-GFP kindly provided by Dominique Bergmann (MacAlister et al., 2007)crossed to PIN3 line from was used to visualise the SPEECHLESS protein, PIN3-GPF (Zadnikova et al., 2010) provide the membrane outline as it is brighter than Lt16b. Additionally PIN3 membrane expression is brighter around the GMCs so helps in their identification.
BASL::GFP BASL; plasma membrane mCherry kindly provided by Dominique Bergmann (Dong et al., 2009) was used to image BASL protein.
spch-2; Q8 (MacAlister et al., 2007) was used to study cell division in the speechless mutant. Q8 marks the cell membrane. This line was kindly provided by Dominique Bergmann

Plant growth conditions

Plants were grown on plates, about 20 per plate. The plates contained 15ml of GM media. They were placed upright in a growth chamber to make the plants easier to

remove and to prepare them for growing in the chamber (see later). The conditions in the growth room were 20^0C, with 16hr light per day.

2.1.1 Time-lapse image acquisition

To capture the dynamics of growth and cell division living seedlings were imaged for up to 6 days under the confocal microscope. The seedlings were transferred from the growth room to a specially chamber where they remained for the course of the experiment. The chamber was custom made by JIC workshops (Norwich, UK). The chamber allows liquids to perfuse through it. The plants received liquid growth media at a rate of $1\mu l^{-s}$. Inside the imaging chamber the tissue is supported on a stainless steel mesh to position it within the working distance of the objective and separate the sample from the flow of the incoming liquid which could move or damage the tissue. The 20 micron pores in the mesh allows the exchange of incoming liquid by passive diffusion. Samples are imaged through the glass top (Agar Scientific 24x32mm Number 1.5 for high resolution imaging). The chamber was designed by Grant Calder (Sauret-Güeto et al paper in progress) and the information is from this paper. The chamber was built thanks to Chris Hindle and John Humble from the workshop at JIC.

Time-lapse confocal imaging presents a trade-off between image quality and specimen health. The plant is in the chamber under the microscope for the duration of the experiment. It is therefore necessary to ensure the conditions in the microscope room are as close as possible to the growth chamber in terms of temperature and light regime. The laser obviously has an effect on the health of the specimen so its use must be kept to a minimum.

The leaves were imaged using a Zeiss LSM 5 EXCITER. The GFP probes were excited using the 488-nm line of an argon ion laser and emitted light filtered through a 500-550-nm band-pass filter. The mCherry probe was excited using the 543-nm line of a Green helium-neon laser and the emitted light was filtered through a 575-615-nm band pass filter. To ensure a cellular resolution a x20/0.8 objective was used. The plants were never imaged more than every two hours. In most cases the time interval was larger (4-10 hours). The precise interval varied and depended upon the size of the leaf. If the leaf

was larger than the field of view and thus required multiple tiles it could take up to 4 hours to image the whole leaf per channel. Imagine every 4-10 hours ensured that cells rarely divided twice between. The laser power was kept as low as possible 3-5% for the argon laser and 20% for the helium-neon laser. The scan speed was kept as fast as possible to still ensure a good image. The precise settings varied between leaves and for different ages of the same leaf. The leaf typically grew towards the top of the chamber with time and therefore a faster scan speed was used. Scan speeds varied between 23 seconds and 2min 15 seconds per z slice of size 1024 x 1024.

2.2 Image Processing

2.2.1 Processing the raw image files

Time-lapse imagining generates up to a 100GB of data per experiment. A range of tools have been developed to facilitate storing and using this data. The raw data is exported from the microscope as an LSM file which is specific to Zeiss and must be converted to a form that can be used by other software – bioformats convertor (http://cmpdartsvr1.cmp.uea.ac.uk/wiki/BanghamLab/index.php/BioformatsConverter) was used to create pngs. The microscope settings are based on keeping the plant alive rather than optimising the image quality so some post processing must occur to improve the images. Image quality was improved as much as possible to ensure the vertices could be identified. Most images were subjected to a median filter with a 2 pixel threshold. The worst images were also subjected to a rolling ball background subtraction to reduce the background noise. Image processing was done using ImageJ (Abramoff, 2004.). Once the necessary post-processing was established it was performed automatically on the entire data stack for which the processing was appropriate using macros created within ImageJ. This macro also stored the name and path of the images as well as a few other parameters. This text file automated the passage of the data to the next step in the processing with only minimal user input. Although these processes are very simple the repetition of them on thousands of images is time consuming and error prone, so the use of macros is highly beneficial. Images of

BASL expression and SPCH expression were processed separately to remove noise and enhance the signal to noise ratio to give a clear image of the localisation.

For the purpose of this thesis the leaf was considered as a 2D surface. The leaf is not perfectly flat. However, the leaves imaged were young, and the edges of epidermis were not included in the study so there was relatively little curvature. 2D projections can be made using software like ImageJ, However, projections such as Max projections project the brightest information from the stack and typically have a lot of noise from the lower layers. Instead I used Merryproj which was developed to make a surface projections of the meristem from the z- stacks(Barbier de Reuille et al., 2005). It works by building the image from the bottom up and replacing the image with the stack above if there is a cell like structure in it. Thus cell walls from the lower layers are removed and replaced by the open spaces of the cells above. The text file generated from the ImageJ macro can be input into Merryproj to enable automatic loading, projecting, and saving of the large datasets. The automation of these processes means the images can be processed at night when the network speed is faster, the computers are otherwise idle and the users do not need to keep track of all the image names and parameters which reduce errors.

If the leaf was too large to be imaged in a single window then the projections of the different tiles were stitched together using the photo merge tool in Photoshop. This step has to be carried out manually. In some cases because the leaf grew it is not possible to stitch the tiles together exactly. In these cases the cells on the border were ignored in the analysis and there position was estimated by interpolation to create the descriptive model.

2.2.2 Manual identification of cell lineages

To study cell division, dividing cells must be identified from the data. As plant cells do not slide past each other vertices can be used as landmarks to follow in successive images. Figure 5 shows a small patch of cells. The vertex between the yellow, green and purple cell can be identified in all images. This is a point of correspondence. By

following the initial vertices we can identify cell lineages and produce a fate map. We can now observe when and how the cells divided.

2.2.3 Tracking cells with the point tracker

The point tracker developed by P. Barbier de Reuille provided the first step in the data extraction. It enables the user to load the projected images and mark corresponding vertices in successive images. The software provides the user with a graphical user interface that allows movement or deletion of marked points. It also allows the user to group the points belonging to the same cell and to define cell division events. Hence it is possible to store everything you need to analyse growth and cell division.

2.3 Data analysis

This information stored in the point tracker is in a comma separated file that can be opened by excel or read by a range of programs including matlab which was used for data analysis. Although the process is manual, the points are stored in a clear data structure and can be queried many times using the data analysis tools and used in the modelling environment. This data was used to: measure the growth of the leaf, analyse the cell divisions and to generate a descriptive model of the leaf.

2.3.1 Growth

What is growth and how can we use the information stored about the cells and their vertices to calculate it?

Growth of 1D shapes

The simplest growing shape is a line defined by two points p1 and p2. We can follow these points through time and record their coordinates (Figure 2.1). Given the coordinates of the points and the times they were recorded we can compute the velocity of the points.

a

No Growth	t1	t2	t3
Time	0	10	20
Position p1 on x-axis	0	1	3
Position p2 on x-axis	1	2	4

b

Growth	t1	t2	t3
Time	0	10	20
Position p1 on x-axis	0	1	3
Position p2 on x-axis	1	3	6

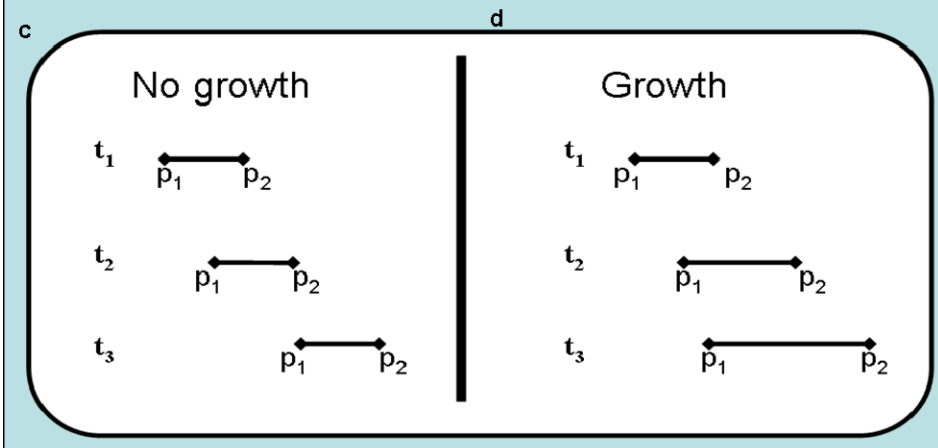

Figure 2.1 Considering growth in 1D. We can define a line (p1p2) which joints two points p1 and p2. The length of this line can be fixed (a,c) or vary in time (b,d). We can follow this line through time and take the coordinates of the points at successive intervals (a-b).

Velocity = change in position/change in time.

We can plot the velocity of the points against time. For a line of fixed length (Figure 2.2a) both points have the same velocity so the lines are on top of each other. The gradient of the line is the acceleration. It can be calculated:

$$\textit{Acceleration} = \textit{change in velocity/ change in time} = \frac{dV}{dt}$$

Acceleration tells us how the velocity changes with respect to time.

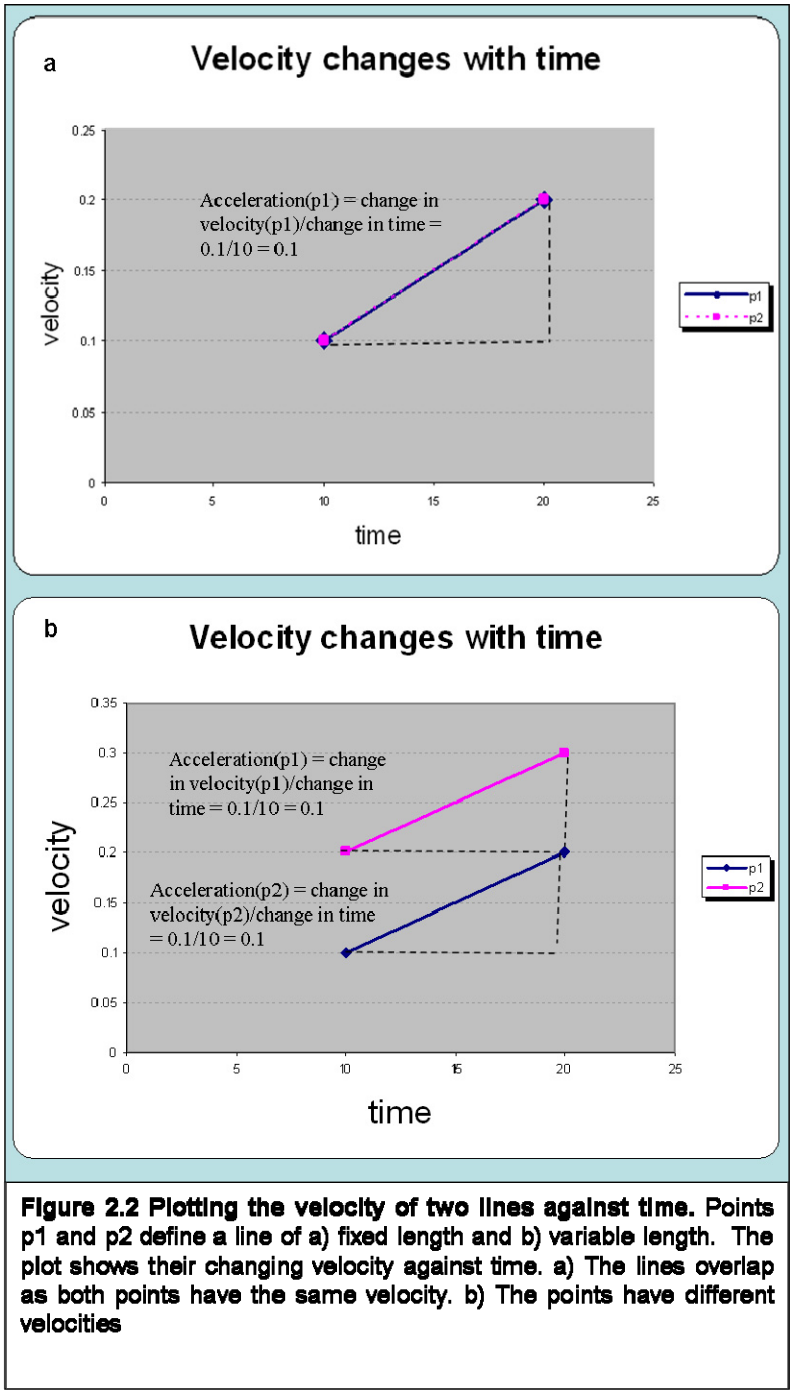

Figure 2.2 Plotting the velocity of two lines against time. Points p1 and p2 define a line of a) fixed length and b) variable length. The plot shows their changing velocity against time. a) The lines overlap as both points have the same velocity. b) The points have different velocities

If we look at a line of variable length (Figure 2.2b) and calculate the velocities of the two points over time we notice that the two points have different velocities. We can compute the acceleration as before.

How does velocity changes with position along the line? Just as we plotted velocity over time we can plot the velocity of the points against their (original) position (Figure 2.3). The first plot (Figure 2.3a) shows the line of constant length there is a constant velocity, i.e. the velocity is independent of the position on the line where the measurement is taken. This is the idea that we are most familiar with, if you

measure the speed of a car it does not matter whether you measure the speed of the front or the back of the car; the result is the same. However, in the second (Figure 2.3b) plot we see that the velocity does change with position this is because the length of this line can change, i.e. the line can grow. The gradient of this plot is the growth rate of the line. Note the similarity to acceleration.

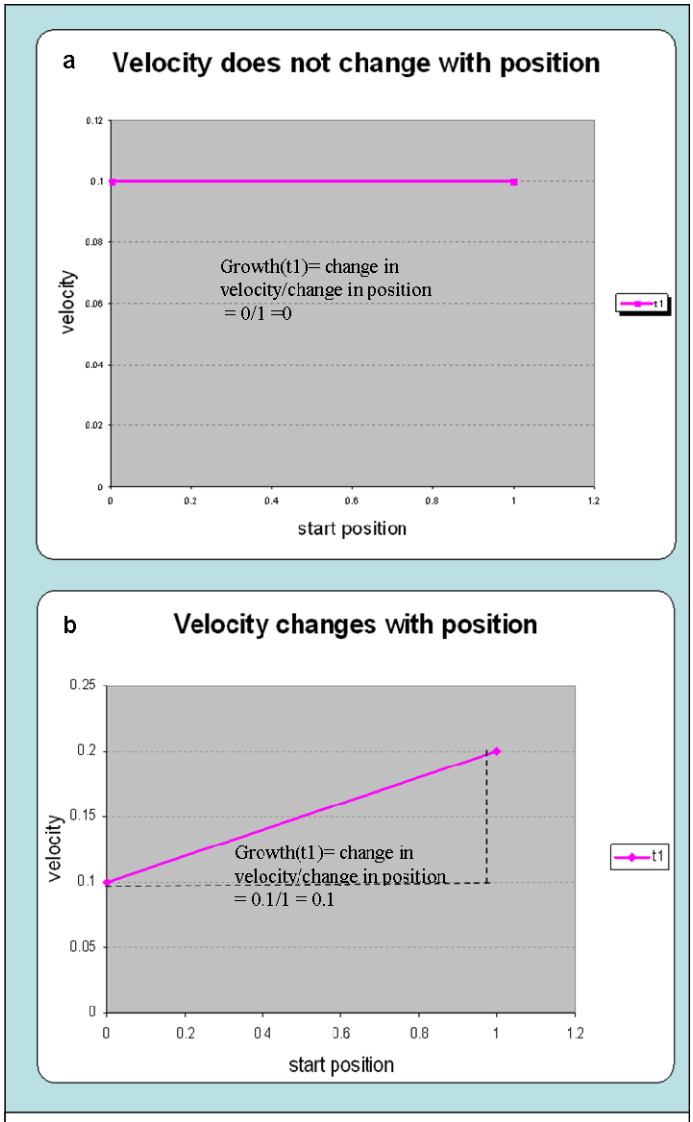

Figure 2.3 Plotting the velocity of the points plotted against their start positions. a) shows a line of fixed length the velocity does not change with position. b) for the line of variable length the velocity changes with the initial position on the line.

Growth = change in velocity/change in position

$$= \frac{dV}{dx}$$

The steeper the gradient is the faster the growth rate. For the graph of the line that has a constant length we see the gradient is zero, so this line is not growing.

Extending the growth calculation to a 2D object

Just as we calculated the growth of a line we can calculate the growth of, a small triangle, the simplest 2D shape. Comparing the position of the triangles points in successive time points allows us to compute their velocities and generate a velocity field. The velocity field is a little more complicated than in the line example as the points can move in more than one direction so the

velocity field must define the direction the points are moving as well as the rate of movement. At every point there is a component of velocity in the *x* direction *Vx* and a component in the y direction *Vy*. We can still calculate acceleration in terms of velocity changes over time and the growth in terms of velocity changes over position. To calculate the changes in velocity over position we must consider the changes in all directions so in addition to considering the change in velocity in the x direction with respect to the x directions $\frac{\partial Vx}{\partial x} = Vxx$ as we did for the line we must also consider: changes in the velocity in the x direction with respect to the y direction $\frac{\partial Vx}{\partial y} = Vxy$, changes in the velocity in the y direction with respect to the x direction $\frac{\partial Vy}{\partial x} = Vyx$, and changes in the velocity in the y direction with respect to the y direction $\frac{\partial Vy}{\partial y} = Vyy$. Calculating the change relative to the axis is enough to give us the information for all the directions in the case of a triangle. The output is therefore not a single number but a 2x2 matrix called a growth tensor.

$$T\left(\frac{x}{y}\right) = \begin{bmatrix} \frac{\partial Vx}{\partial x} & \frac{\partial Vy}{\partial x} \\ \frac{\partial Vx}{\partial y} & \frac{\partial Vy}{\partial y} \end{bmatrix} = \begin{bmatrix} Vxx & Vyx \\ Vxy & Vyy \end{bmatrix} = Growth$$

In the single line example the output was a single growth rate. In two dimensions a single number is not sufficient to explain growth. The growth tensor can be approximated by a single linear transformation as long as the shape and the time-step are infinitesimally small.

How to estimate the changing velocities from the displacement of a point cloud

If we look at the triangle p1, p2, p3 again we know how to calculate the velocity of the points as change in position over change in time. We can display this as the change in x

position over time and the change in y position over time. Imagine the triangle $\begin{pmatrix} p1_{t1} = & (0, & 0) \\ p2_{t1} = & (1, & 1) \\ p3_{t1} = & (2, & 0) \end{pmatrix}$ (where pi_{tj} is the position of point i at time j), after growth the triangle has points $\begin{pmatrix} p1_{t2} = & (0, & 0) \\ p2_{t2} = & (2, & 2) \\ p3_{t2} = & (5, & 0) \end{pmatrix}$. We compute the velocities in terms of x as $\begin{pmatrix} \frac{\Delta P1x}{\Delta t} = V_{p1x} = & 0 \\ \frac{\Delta P2x}{\Delta t} = V_{p2x} = & 1 \\ \frac{\Delta P2x}{\Delta t} = V_{p3x} = & 3 \end{pmatrix}$ (where V_{pix} is the velocity of point i along the x axis, or the change in the position of P1 in the x direction) and in terms of y $\begin{pmatrix} \frac{\Delta P1y}{\Delta t} = V_{p1y} = & 0 \\ \frac{\Delta P2y}{\Delta t} = V_{p2y} = & 1 \\ \frac{\Delta P3y}{\Delta t} = V_{p3y} = & 0 \end{pmatrix}$.

The velocities can be considered as sample points of a velocity field. Vx therefore gives the x component of the velocity of every point in space, and Vy the y component. $V(x_{ij}, y_{ij})$ therefore gives the velocities of any point i at time t_j. Assuming the velocity field is linear, we can describe it using two equations that define a plane: $\begin{cases} Vx = a_x x + b_x y + c_x \\ Vy = a_y x + b_y y + c_y \end{cases}$. We need to solve these general equations to get the growth tensor. Taking the spatial derivatives of V_x and V_y we find:

$$\frac{\partial V_X}{\partial x} = a_x = V_{xx} \quad \frac{\partial V_X}{\partial y} = b_x = V_{xy}$$
$$\frac{\partial V_y}{\partial x} = a_y = V_{yx} \quad \frac{\partial V_y}{\partial y} = b_y = V_{yy}$$

We can write these equations in terms of the velocities calculated above.

$\begin{pmatrix} V_{xp1} = V_{xx} x_{p1t1} + V_{xy} y_{p1t1} + cx = 0 \\ V_{xp2} = V_{xx} x_{p2t1} + V_{xy} y_{p2t1} + cx = 1 \\ V_{xp3} = V_{xx} x_{p3t1} + V_{xy} y_{p3t1} + cx = 3 \end{pmatrix}$ and the same in terms of y or more generally

$\begin{cases} V_X = V_{XX}x + V_{xy}y + c_x \\ V_Y = V_{YX}x + V_{yy}y + c_y \end{cases}$. We want to solve this for V_{xx}, V_{Xy}, V_{yx} and V_{yy} therefore we write this equation as a matrix multiplication so we can isolate them.

$$\begin{bmatrix} V_{xp1} \\ V_{xp2} \\ V_{xp3} \end{bmatrix} = \begin{bmatrix} x_{p1t1} & y_{p1t1} & 1 \\ x_{p2t1} & y_{p2t1} & 1 \\ x_{p3t1} & y_{p3t1} & 1 \end{bmatrix} \begin{bmatrix} V_{xx} \\ V_{xy} \\ cx \end{bmatrix}$$ So, $V_X = MX$ and $V_y = MY$

V M X

We can rearrange the equation to find X and Y as $X = M^{-1}V_X$ and $Y = M^{-1}V_y$. Where M^{-1} is the inverse of matrix M. $M^{-1} = \begin{bmatrix} -0.5 & 0 & 0.5 \\ -0.5 & 1 & -0.5 \\ 1 & 0 & 0 \end{bmatrix}$ For this example there is an exact solution as there are three unknowns and three equations.

Using the example we can see that:

$$\begin{bmatrix} V_{xp1} = 0 \\ V_{xp2} = 1 \\ V_{xp3} = 3 \end{bmatrix} = \begin{bmatrix} x_{p1t1} = 0 & y_{p1t1} = 0 & 1 \\ x_{p2t1} = 1 & y_{p2t1} = 1 & 1 \\ x_{p3t1} = 2 & y_{p3t1} = 0 & 1 \end{bmatrix} \begin{bmatrix} V_{xx} \\ V_{xy} \\ cx \end{bmatrix} \quad X = M^{-1}Vx$$

$$X = \begin{bmatrix} -0.5 & 0 & 0.5 \\ -0.5 & 1 & -0.5 \\ 1 & 0 & 0 \end{bmatrix} * \begin{pmatrix} 0 \\ 1 \\ 3 \end{pmatrix} = \begin{pmatrix} 1.5 \\ -0.5 \\ 0 \end{pmatrix}$$ So, $V_{xx} = 1.5$, $V_{xy} = -0.5$

$$\begin{bmatrix} V_{yp1} = 0 \\ V_{yp2} = 1 \\ V_{yp3} = 0 \end{bmatrix} = \begin{bmatrix} x_{p1t1} = 0 & y_{p1t1} = 0 & 1 \\ x_{p2t1} = 1 & y_{p2t1} = 1 & 1 \\ x_{p3t1} = 2 & y_{p3t1} = 0 & 1 \end{bmatrix} \begin{bmatrix} V_{yx} \\ V_{yy} \\ cy \end{bmatrix}$$

$$Y = M^{-1}Vy \; Y = \begin{bmatrix} -0.5 & 0 & 0.5 \\ -0.5 & 1 & -0.5 \\ 1 & 0 & 0 \end{bmatrix} * \begin{pmatrix} 0 \\ 1 \\ 0 \end{pmatrix} = \begin{pmatrix} 0 \\ 1 \\ 0 \end{pmatrix}$$

So, $V_{yy} = 0$, $V_{yx} = 1$.

Therefore, for this example the growth tensor is $T = \begin{bmatrix} V_{xx} & V_{yx} \\ V_{xy} & V_{yy} \end{bmatrix} = \begin{bmatrix} 1.5 & 1 \\ -0.5 & 1 \end{bmatrix}$.

Growth of biological tissues

The point tracker stores the coordinates of the cell's vertices at different time points (Figure 2.4). To calculate growth the coordinates at two time points t_1 and t_2 are needed. At each images new points are added due to divisions. However, the growth is calculated using only points present at both time t_1 and t_2. Cells have more than three vertices and so the point cloud will be larger.

A point cloud with more than three points: $\begin{bmatrix} V_{xp1} \\ V_{xp2} \\ V_{xp3} \\ \vdots \\ V_{xpn} \\ \\ \end{bmatrix} = \begin{bmatrix} x_{p1t1} & y_{p1t1} & 1 \\ x_{p2t1} & y_{p2t1} & 1 \\ x_{p3t1} & y_{p3t1} & 1 \\ & \vdots & \\ x_{pnt1} & y_{pnt1} & 1 \\ & & \end{bmatrix} \begin{bmatrix} V_{yy} \\ V_{xy} \\ cx \end{bmatrix}$ In this case

we can not find the exact solution however we can use the matlab function \ and find $X = M \setminus V_X$ by minimizing the errors to calculate $V_{xx,}$ V_{Xy}. We can repeat this process for the velocities in the y direction to get V_{yx} and $V_{yy.}$ This gives us the growth matrix $T = \begin{bmatrix} Vxx & Vyx \\ Vxy & Vyy \end{bmatrix}$ as before.

We have calculated the growth tensor that will minimize the difference between the observed position of the points and the position of the points obtained if we grow the points by the tensor. The accuracy depends on the size of the object and the time step.

Extracting growth parameters from the tensor

As we saw in the introduction the growth tensor matrix contains all the components necessary to define growth in 2D, growth rate, direction of growth, anisotropy and vorticity. The growth is usually referred to as the strain tensor and is found by removing the vorticity part from the original matrix. Vorticity tells us how much the points are rotating and is usually a consequence of the different growth rates, therefore, it is of less interest to us here.

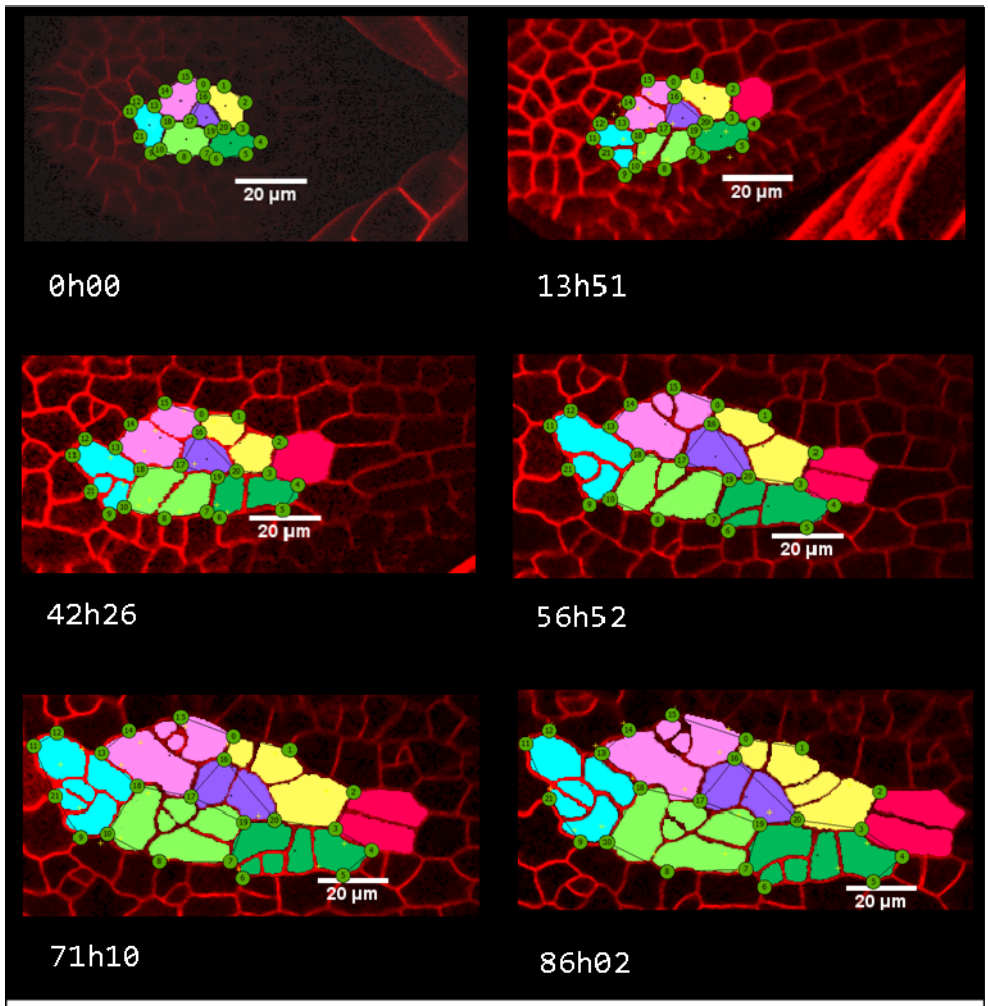

Figure 2.4 A patch of wild-type cells followed through time. Cell lineages were manually identified using the point tracker (see methods section). Corresponding vertices that can be identified in all images are marked and have an identifying number in the circle, e.g. the vertices shared by the purple, pink and yellow cell is number 16. This junction can be identified in all images.

1). Calculating the strain matrix by removing the vorticity matrix

Because we have a square matrix we can break it down into a symmetric and non-symmetric part. Symmetric matrices have the form: $M=\begin{bmatrix} a & b \\ b & d \end{bmatrix}$ while anti symmetric have the form: $M=\begin{bmatrix} 0 & b \\ -b & 0 \end{bmatrix}$. This can be written more formally as: a symmetric matrix is the same as its transpose (^tM) so $M={}^tM$ while an anti symmetric matrix is the negative of its transpose $M=-{}^tM$ where ^tM is the transpose of the matrix M.

We can re-write M as $M=\frac{M+{}^tM}{2}+\frac{M-{}^tM}{2}$, this is useful as $M=\frac{M+{}^tM}{2}$ is symmetric and $M=\frac{M-{}^tM}{2}$ is anti-symmetric. We can verify this if we compute their transpose. If we find the transpose of $\frac{M+{}^tM}{2}$ and re-arrange it: $^t\left(\frac{M+{}^tM}{2}\right)=\frac{{}^tM+{}^t\left({}^tM\right)}{2}=\frac{{}^tM+M}{2}$ we can see that it is the same as the original matrix M so this part is symmetric. While the transpose of $\frac{M-{}^tM}{2}$; $^t\left(\frac{M-{}^tM}{2}\right)=\frac{{}^tM-{}^t\left({}^tM\right)}{2}=\frac{{}^tM-M}{2}=-\left(\frac{M-{}^tM}{2}\right)$ is minus the original M and therefore this is the anti-symmetric part. The anti symmetric part represents the vorticity. We can use a simple example (Figure 2.5) to demonstrate that applying such a matrix can rotate a shape. If we take a triangle (o) with coordinates (0,0), (0,2) and (1,1) and a simple anti-symmetric matrix $\Omega=\begin{bmatrix} 0 & 1 \\ -1 & 0 \end{bmatrix}$ we can compute the new position (n) of the triangle after it is rotated by Ω as we get $\begin{pmatrix} 0, & 0 \\ 2, & 0 \\ 1 & -1 \end{pmatrix}$ which we can see is a rotation of the original triangle of the same size (Figure 2.5a). This is a basic geometric computation in the case of growth it is referred to as a vorticity matrix rather than a rotation matrix and represents a rate of rotation applied over very small time-steps to the original small shape. We compute the position of the triangle and successive time steps as the old coordinates plus the rotation matrix multiplied by a time interval

(*dt*). This can also be written as $n = = (\Omega * dt + I)o$; where ***I*** is the identity matrix; $I = \begin{bmatrix} 1 & 0 \\ 0 & 1 \end{bmatrix}$.

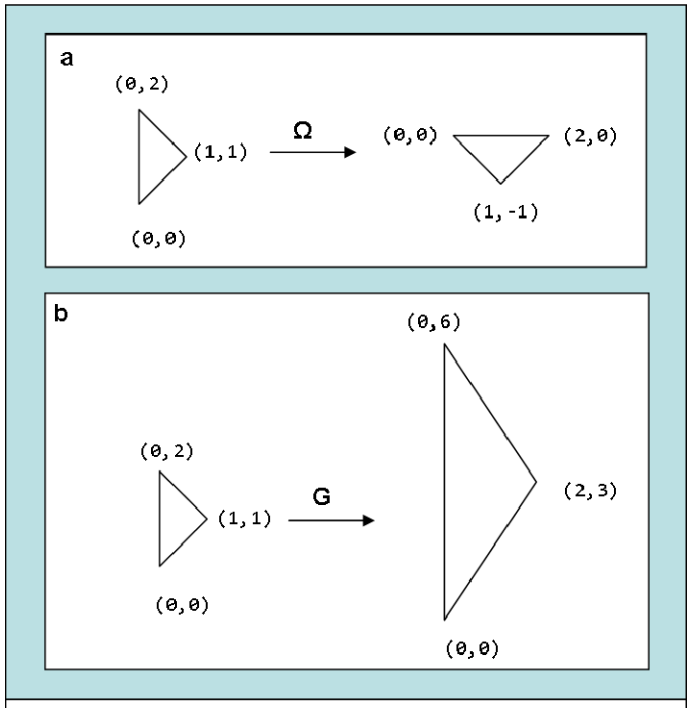

Figure 2.5 Basic operations on a triangle. a) applying a rotation matrix Ω rotates the triangle. b) applying a simple growth tensor G enlarges the shape. (see text)

2). Extracting growth parameters from the strain matrix

We have calculated the growth matrix for a shape and extracted the vorticity to leave behind the strain tensor; the symmetric part of the original matrix. The strain tensor contains the features we typically use to define growth; growth rate, direction and anisotropy. We now need to extract these parameters from the symmetric strain matrix which has the form $\begin{bmatrix} a & b \\ b & d \end{bmatrix}$. If b is 0 then the growth in the x direction is **a** and growth in the y direction is **d**, e.g.: we can take the triangle from before $\begin{pmatrix} (0,0) \\ (1,1) \\ (0,2) \end{pmatrix}$ and show that if we applied such a matrix $G = \begin{bmatrix} 2 & 0 \\ 0 & 3 \end{bmatrix}$ it would enlarge to give the coordinates $\begin{pmatrix} (0,0) \\ (2,3) \\ (0,6) \end{pmatrix}$ the same triangle but twice as big in the x direction and 3 times as big in the y direction (Figure 2.5b). Again to use the matrix as a strain tensor then it must be applied to the original coordinates in a small time dependent manner. However, if the numbers in the **b** positions are not 0 then the object that is growing is not aligned with the x and y axis (Figure 2.6) and growth in the x direction is no longer equal to a it is instead ax+by, and

growth in the y direction is cx+dy due to the rules of matrix multiplication:

$$\begin{pmatrix} x_1 & y_1 \\ x_2 & y_2 \\ x_3 & y_3 \end{pmatrix} \begin{bmatrix} a & b \\ b & c \end{bmatrix} = \begin{matrix} ax_1 + by_1 & bx_1 + cy_1 \\ ax_2 + by_2 & bx_2 + cy_2 \\ ax_3 + by_3 & bx_3 + cy_3 \end{matrix} .$$

In Figure 2.6a and b the triangle grew by the same amount but the growth in b is in a different direction. Rotating the axis of **b** so that it looks like **a,** allows us to know the growth rate. The amount we had to rotate the axis gives us the direction of growth.

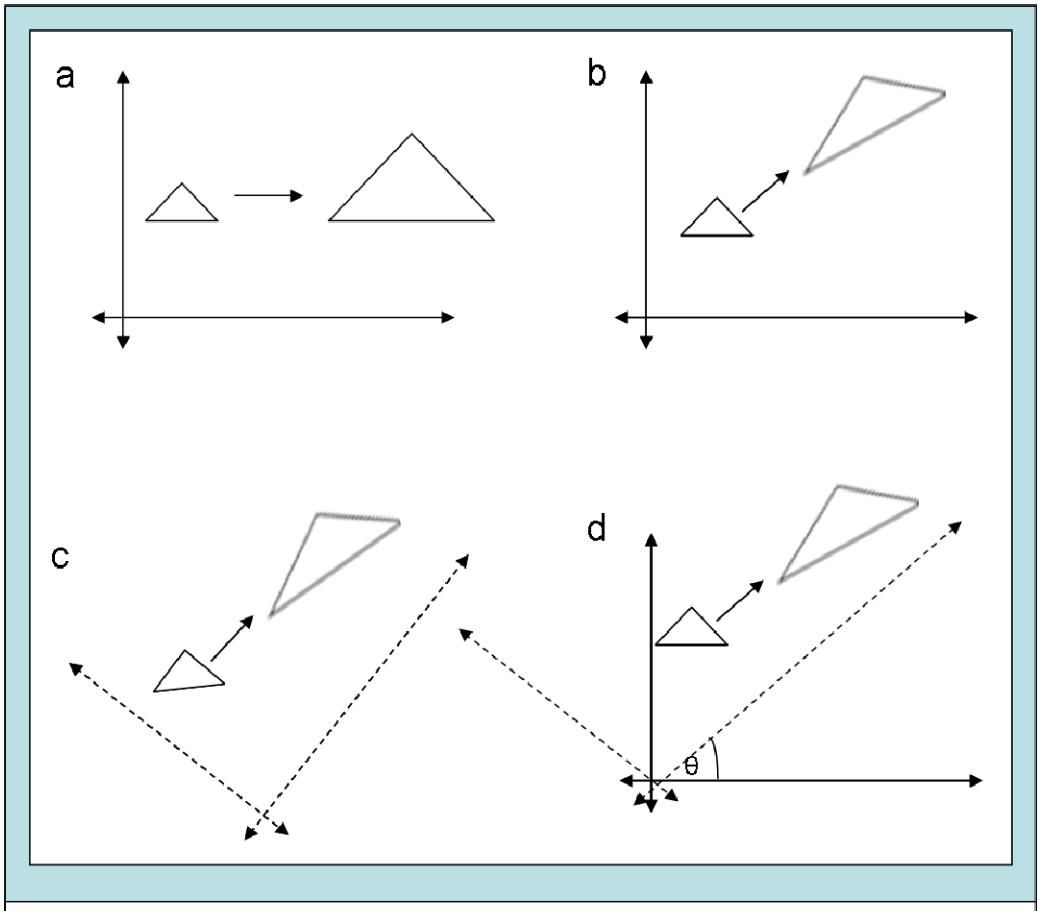

Figure 2.6 Aligning growth with the axis. Triangle (a) and (b) grew by the same amount however the growth of triangle (b) is not aligned with the axis. If we rotate the axis (c) we can get the growth rate. The angle of rotation θ is the major axis of growth (d).

Calculating the growth

I computed growth using the method outline above in the VVe environment which will be introduced later. However, these calculations can be made in any maths package. There are a number of options available in terms of the scale in time and space at which the growth calculations can be made. At the broadest scale we can consider the patch of cells as a whole and compute one growth tensor for the whole patch. We can also use only the position of the points in the first and last time point. To do this it is necessary to identify the vertices on the edge of the graph in the first time-step and identify the coordinates of the same vertices at the later time point. These two sets of coordinates are the two point clouds required by the methods discussed earlier. This method produces one growth tensor for the entire patch over the entire time period. As discussed earlier the larger the patch and the larger the time change the less uniform the growth and hence the less accurate the calculation. At the other extreme the growth tensor can be calculated for every cell at every time point. This is possible as every new division was stored in the tracking data, therefore, for each pair of images the coordinates of the vertices of each cell in the first can be found in the second and used to compute the growth. If the cell divided in the second image then the growth will be of the clone in this image but the two cells will be considered separately for the next time-step. This in theory should be more accurate as the growth is likely to be more uniform. However, there is a trade off with noise. The points are placed manually on the vertices of the cells and the cell walls can be 1μm wide in some images. For small cells this represents 10% of their length. Although every effort is made to place the points in the centres of the walls if growth rates are low, below 10% then it is more accurate to take large time steps and maximise the growth to noise ratio.

2.3.2 Cell division

Rather than measuring cell features by hand the cell data from the point tracker was input into Matlab and subjected to multiple data analyses. The function to input the data into Matlab was developed as part of the point tracker development by Barbier de Reuille. Once imported the information was stored in a data structure in a way that

could be used by many functions. These functions were concerned with quantifying different aspects of the cell divisions including division orientation, timing of cell division and cell arrest. In all cases data was not included from cells if the vertices could not be clearly identified or if the cells were on the boundary of two tiles.

Division orientation

The cell data not only contained the coordinates of the cells at each time point it also contained the coordinates of the new division walls. The orientation and length of the new walls could therefore be calculated and compared to the length and orientation of division walls produced by different division algorithms (see later) to highlight correlations.

Division timing

To study whether there is a spatial distribution of the timing of cell division I experimented with several plots to look for correlations. For example, to calculate the relationship between the area of a cell at the time of division and its distance from the mid-vein. The time and image in which the cell divided was stored. In the image before division the cell's area and distance from the mid-vein were calculated. The mid-vein was approximated as a straight line which joined two cells that were at either end of the mid-vein. The distance from this line to the cell centre was an approximation of the cells distance from the mid-vein. The area at the time of cell divisions was then plotted against the distance from the mid-vein.

I repeated the process to compare the correlation between cell cycle duration and position on the leaf. This plot only included cells that divided twice during the imaging period. Cells that disappeared from view before dividing or that already existed at the start of imaging had to be excluded.

The same process was used to look at the spatial relationship of other features of cell divisions and in other orientations (results not shown).

This process was also used to investigate the changes in cell division properties over time but plotting the features against the time the cells were observed to divide.

Cell arrest

In addition to information on the timing of cell division I investigated the timing of cell arrest at different positions along the leaf. The arrest of cells is thought to occur from tip to base. At each time-point the leaf was divided into transverse sections and cells with a centroid position inside the section were identified. The cells were defined as arrested if they did not divide again within the course of the experiment. This measure of cell arrest is not a true reflection of the state of the leaf especially towards the end of the experiment.

The percentage of cells which did not divide again was plotted against the distance along the leaf. The leaves were aligned at the tip or the petiole-lamina boundary defined as the base of the mid-vein. The leaves were also scaled so that they had the same length and the percentage of arrested cells plotted against the relative distance.
The results were fitted with trend lines using a curve fitting tool developed by Barbier de Reuille. The base aligned data was best approximated by a logistic curve while the scaled data was better approximated by a combined logistic and exponential function ($y = A/(1 + e^{-k*(x-x0)}) + y0 + Be^{tx}$).

2.4 Creating a model

To study the division algorithms that could account for the orientation and timing of the cell divisions computational modelling was used. Two types of models were

constructed. Simple models were based on geometric shapes with uniform growth. However, to provide a more realistic framework to study the algorithms a descriptive model was also created. This model used all of the data stored from the point tracker to produce a descriptive model of a patch of cells that grew exactly as the observed cells did and divided at the same time. Mechanistic elements were then added to the model and the output was compared directly to the observed cells.

In order to explain the models I will first introduce the modelling environment used.

2.4.1 Introduction to VVe

All of the models in this thesis were made in the modelling framework VVe, an extension of vertex vertex (VV) systems (Smith, 2003). VV systems use graph rotation systems to representing the state of the modelled system (In this case a graph is a connection of vertices). The model of the epidermis contains three graphs which are linked (Figure 2.7). The first graph is the wall graph (black) which links the cell vertices to each other with edges that represent cell walls. The second graph includes additional vertices which represent cell centres (blue) and connects them to the cell vertices. The third graph connects the centres of the cells to their neighbours (green). The structure of the graphs makes it straight forward to use the cell data from the point tracker to build the graphs. All operations are locally defined (e.g. moving along the graph involves going from neighbour to neighbour) making VVe suitable for biological modelling.

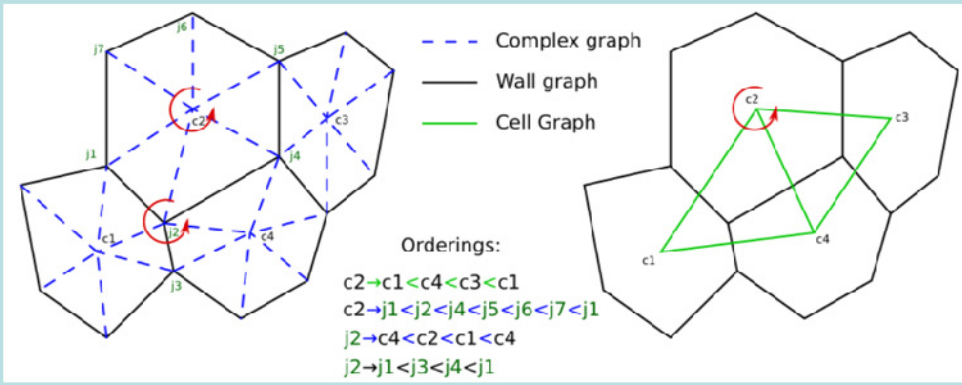

Figure 2.7 VVe tissues are made of three graphs. The wall graph connects the cell vertices with edges that represent cell walls (black). The wall junctions are linked to additional vertices that represent the cell centres (blue). The cell centres are linked to their neighbours by the cell graph(green). (Figure taken from VVE documentation Barbier de Reuille).

The model itself has 5 sections: attribute declaration, initialisation of the model, step function, update from old and drawing.

1) Attribute declaration

In VVe like C++ variables must be defined before they are used. The variables which will be associated with different objects (junctions, cells, walls, etc) are declared before the start of the model. For example position is an attribute of the wall junction vertices, whereas cell type is an attribute of the cell centre.

2) Initialisation of the model

The initial state of the model should be set here. This includes building the graph that will be used. The graph can be as simple as a single square or as complex as reading in all the vertices of the entire leaf. The coordinates of the vertices, and the type of the cell are also set here.

3) Step function

This section is called for each simulation step. This is where the model is evaluated e.g. the position of the vertices are updated to grow the tissue or cells are divided. This section will be examined in detail when we look at the specifics of my model.

4) Update from old

This section is a particular feature of modelling biological tissues. During the modelling the number of elements in the model can change. This poses a problem of how to integrate the new structure into the model. When a cell divides the old cell centres are deleted and replaced by the new centre's of the progeny. This section enables attributes associated with the parent cell to be passed to the daughter cells. It also allows for the production of daughters with new cell types as is the case of asymmetric cell divisions.

5) Drawing

VVe has a viewer and uses Open gl to draw. Therefore the user can use any OpenGL command to draw. I use basic lines and spheres to draw my cells. I colour the cells in the form of a heat map based on different features. In some cases one cell had a value that is outside the range of the other cells. In these cases the scale was capped so that this cell no longer defined the maximum therefore a nicer distribution of colours was produced. The growth tensors were drawn as ellipses with arrows inside to indicate the direction of growth. The colour bar and scale bar are VVe functions which I used.

2.4.2 Using VVe to model cell behaviour

In this thesis I present two types of models, purely mechanistic models and models that combine mechanistic rules into an essentially descriptive model.

A mechanistic model

Cell division can be modelled purely mechanistically. In these cases the cell was represented as a square or triangle. The abstract shape was grown using a growth matrix. A growth matrix is a 2 x 2 matirx which contains the growth tensor introduced

earlier. In these models the growth is principally oriented along the x or y axis. I grow them by applying a diagonal growth matrix. $\begin{bmatrix} K\max & 0 \\ 0 & K\min \end{bmatrix}$. I specify that $K\min = K\max * isotropy$. So if the isotropy value is 1 then the Kmin value is the same as the Kmax value. If the isotropy value is 0 then the growth is only in the Kmax directions and Kmin is zero. At each time step the position of the junctions are computed using a forward Euler scheme Press et al. 1992 . In this case, the new positions are obtained by multiplying their current position by dm where dm = dt*growth_matrix + identity_matrix. This integration scheme requires that dt*smax be relatively small in order to be a good approximation. To specify the growth of a patch of cells the tensor for the patch can be computed and applied to all the cells. The growing cell can then be divided at any specified time using any division rule.

Mechanistic algorithms to divide cells

Here I outline the methods for the different division algorithms tested. I implemented all of the algorithms independently and will discuss my implementation of the methods. However, some of the methods exist as functions of the VVe tissue. Where this is the case I use the built in function in my model as these algorithms have been extensively tested to cope with difficult geometries and unusual situations. However, the built in functions will not be explained as they are more complex and written for multi-dimensional data. Here I will focus on the key ideas of the methods only.

The principle of dividing a cell

There are two stages to dividing cells. The first involves finding the two division points of the cell. When it is time for this cell to divide these points are given to the VVe division algorithm that handles the division of the graphs. The algorithm ensures that all the walls that need to be broken and re-made to divide a cell in this way are carried out.

The assumption of all the division algorithms, unless otherwise stated, is that the new wall passes through the centre of the cell. The first step of all the algorithms is,

therefore, to calculate the centre of the cell. Also, due to this restriction for many of the algorithms it is only necessary to find one division point. The other point is found by calculating where the opposite wall and the new wall passing through this first point and the centre would intersect.

Shortest wall algorithm

This algorithm finds the shortest path across the cell through the centre. In all of the models I discuss the shortest path across a cell is found by approximation. First the cells centre is found. Then the shortest path through the centre is found by iterating over all the walls. For each wall several positions along it are tested (e.g. 100). For each 100th of the distance along the wall a check is made as to whether the line from this point P to the centre of the cell intersects the other walls of the cell. If it does the length of this line is stored and where it intersects the other wall. This is repeated for all locations on all walls. At each iteration if the distance found is shorter than the previously found distance then the coordinates and the distance are the new shortest wall. The coordinates found at the end define the shortest path across the cell. Although I implemented my own shortest wall algorithm I used the built in one from VVe in my model. For example unlike the interpretation presented here the built in algorithm is able to divide cells with non-star shaped geometries.

Longest Wall

This algorithm divides the longest wall of the cell. To find the longest wall of the cell the length of the line between the vertices of each wall is calculated and the longest is stored. The cell is then divided using the mid-point of the longest wall.

Closest Wall

This algorithm divides the cell through the closest point to the cell centre. The closest point to the cell centre is found for each of the cell's walls and the distance is calculated. The point with the shortest distance to the centre is the point of intersection of the wall with the line defined by the centre and the normal to the wall. If these two lines do not

intersect then the shortest distance is to one of the ends of the line and the shortest one can be found.

Closest Midpoint

This algorithm calculates the mid-point of each cell wall. The distance between the mid-point and the cell centre is then calculated and the shortest one is found. The mid-point which is closes to the centre is used to divide the cell.

Shortest path in direction of growth tensor

The major and minor growth directions of each cell are calculated as outlined in the growth section. One axis is selected for the orientation of the division. The length of the wall that would result from dividing the cell through the centre in both orientations is calculated. The orientation that produces the shortest path is selected. It will be parallel or perpendicular to the major growth direction of the cell (Nakielski, 2008).

Fastest growing wall

The rates of growth of all the walls of the cells are calculated. The walls growth rate is: $\frac{newLength - oldLength}{oldLength}$. This assumes that growth is linear which is reasonable for small time steps. Identifying the fastest wall or walls does not define a division point. I therefore use the mid-point of the fastest growing wall.

Two shortest walls

Division wall in the wild-type cells are not always straight across a cell. Sometimes the walls joined adjacent walls or are curved. To capture this, I experimented with allowing the division wall to be curved. Joining the two shortest paths from any walls to the centre can create a division wall that is not straight (Figure 2.8). The points for division are found in the same way as for the closest point algorithm. The closest point and its distance from the centre are stored and the two shortest are selected. Once the shortest distance has been computed the angle between the two lines is calculated. If it is less

than 90º then new points must be found. This algorithm always places new walls at 90º to the old walls as this is the shortest distance between a line and point.

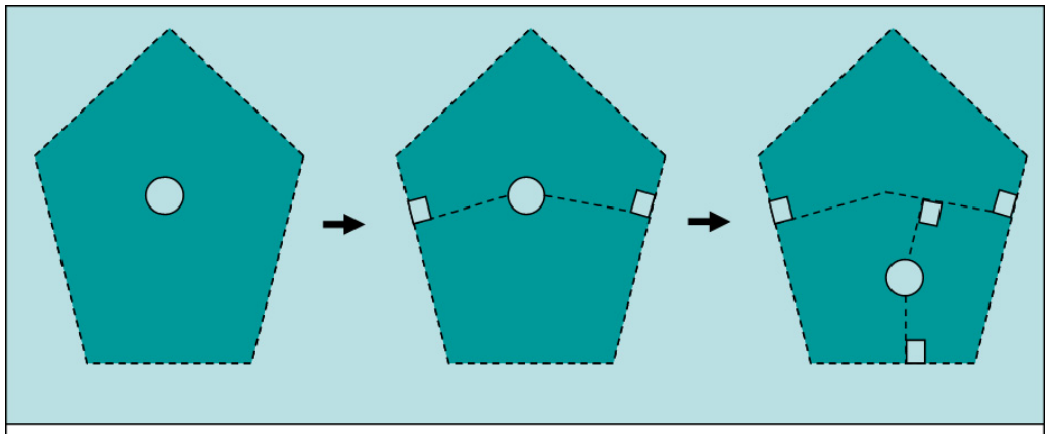

Figure 2.8 Two shortest wall division algorithm. When the first cell divides the two shortest walls to the centre are found. The new wall meet the old walls at 90º. In successive divisions the wall may join and already curved wall.

This algorithm becomes increasingly complicated with successive divisions as the next division may also hit a wall that was curved. Therefore it is necessary to store whether the wall was curved in the parent cell and which side of the centre the new wall is placed as this determines which daughter inherits the curved wall.

Two fastest growing walls

This algorithm joins the mid-points of the two fastest growing walls going through the centre. This algorithm does not always produce straight walls. If the new wall would form an angle at the centre of less then 90° then the mid-point of the third fastest wall is used.

Shifted shortest wall

This algorithm can find the shortest path across a cell through any specified point. It is otherwise the same as the shortest wall algorithm. The specified point represents the nucleus and the fact that it might not always be in the centre of the cell. There are a number of ways to compute the position of the shifted nucleus.

Shifting the nucleus

In the simplest of model the nucleus is moved using a global vector (e.g. in the direction of the x-axis) (Figure 2.9a). In the beginning of the model the nucleus is initialised to the cell centre. For each time step the nucleus is moved a little way along the vector. To ensure the nucleus can not leave the cell the distance (**d**) from the centre to the wall at the point of intersection with the vector is calculated. The nucleus is only moved a fraction of this distance. The amount the nucleus moves depends on a parameter (e.g. 30% of the total distance).

In the later models the nucleus moves along a local vector (Figure 2.9b). This vector is specified by the position of a factor, Factor M (shown in red) and the cell centre. The amount of movement along the vector is still specified by the length available to move in this direction and the parameter.

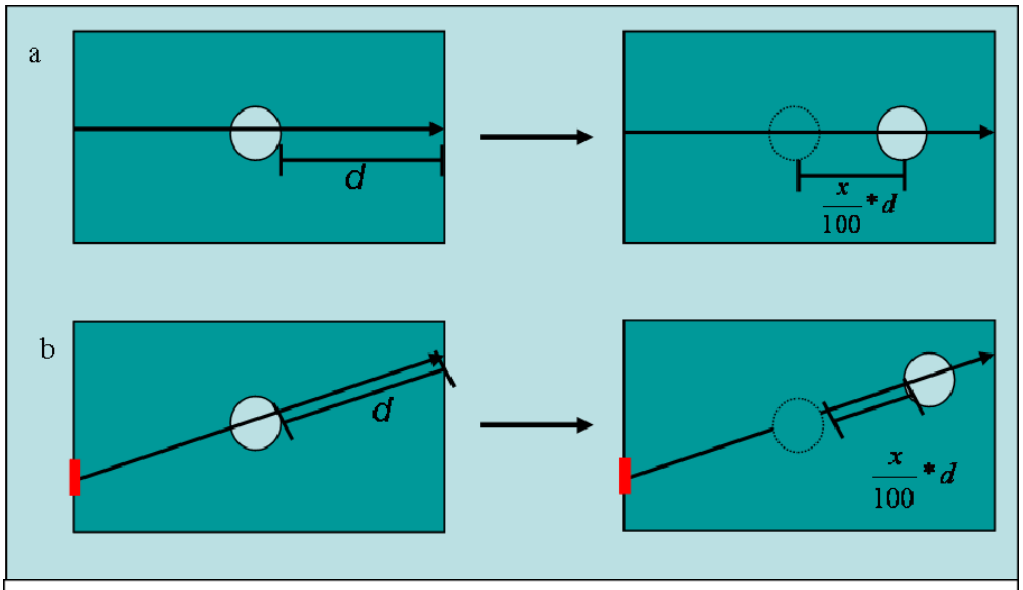

Figure 2.9 Methods of moving the nucleus. a) moving the nucleus using a global vector or (b) by factor M (red). Distance d is the maximum amount the nucleus can move. The percentage of d that the nucleus moves depends on x.

Mechanistic algorithms to determine when to divide the cells

As well as specifying how to divide the cell we must specify when to divide the cell.

Threshold area

This algorithm divides cells when they reach a threshold area. To achieve this, the cells areas are computed at each step and stored as a cell attribute. The division algorithm then iterates over all cells and compares their area to the threshold area input from the parameter file. If the area is larger than the threshold the cell is added to the list of cells to be divided.

Cell cycle duration

This algorithm divides cells every **x** hours, where **x** is a fixed parameter. The cells therefore have an attribute that stores their age in hours. Cells age is initialised to zero at the start of the model because their true age can not be known. After each division cell age is increased and after division it is reset to zero. To select the cells for division their age must be compared to the cell cycle time duration limit **x**, and cells with an age greater than this value are selected to divide.

According to birth size

This algorithm divides cell when they reach a certain proportion of their original size at birth. The birth size is the size they are created when their parent divided. After each division their size is stored. Each cell then has its own area threshold to be compared to which is **x** times its birth size (e.g. for cells maintaining a constant size **x**=2). Some cells are already present at the start of the imaging. Their birth size is approximated as the size they are at the start of the experiment. This will introduce a delay in their division as they are likely to be larger than their birth size.

Depending on cell type

Some division algorithms require cells to divide differently depending upon their type. Any of the division algorithms can be modified to depend on cell type. If a cell is of type A then area threshold is x, if the cell is of type B then the area threshold is $x * y$ where y is a fixed parameter.

Specifying the fate of the daughter cells

Once the cells have divided some information is passed to the daughter cells. If the division is symmetric then the daughters will both inherit the type from the parent cell. However if the division is asymmetric then the fate of the two daughters must be calculated based on their size, neighbours or the presence of a particular factor (e.g. factor M). This is possible in the update from old section of the model. If the fate depends on size then this is calculated and compared. If it depends on the presence of a cell periphery associated factor M then the parent cell location of factor M must be stored. It is then determined which of the two daughters has inherited this part of the parental cell wall. This daughter then acquires one cell fate over the other.

2.4.3 Producing a descriptive model

All features of the model can be specified mechanistically. This is useful to experiment with idea. However, these models make a lot of assumptions and approximations about the shape and growth of the cells. I wanted to be able to compare the model output more directly to the observed data. One way of doing this is to create a purely descriptive model of the growing leaf. The descriptive model was created using the data generated from the point tracker. The initial cell shapes of the model are therefore the initial cell shapes of the observed cells (approximated with straight lines). The cells grow by interpolating the position of the vertices in each image. The cell division information can also be used to divide the cell as it was divided in the observed cells.

Growing of the descriptive model

Growing a patch of cells over a long time period using only a single growth tensor does not maintain their observed growth and resultant cell geometry. To model large patches of cells which have a divergent growth field an interpolation method was used. From the tracking data the position of the cell vertices in all images is stored. The trajectories of these points were assumed to be linear between images so their intermediate positions could be found by interpolation. This produces an expanding set of cell vertices called material points (Figure 2.10a). To add other points to this expanding set of vertices requires us to specify a coordinate system that is local to the leaf, i.e. will be moved with the leaf as it grows. Homogeneous coordinate systems such as the barycentric coordinate system allow the coordinates of a point to be represented using finite coordinates. The barycentric coordinates of any point within a triangle can be calculated in reference to the coordinates of the triangle (Figure 2.10c). However, the cells are not triangles, therefore, the material coordinates were triangulated using a Delauny triangulation (Figure 2.10b). This triangulation method creates triangles which maximise the minimum angles of the triangles so avoiding very thin triangles. The method is well established and present in most libraries. From the triangulated material points the barycentric coordinates of the other points can be found as a weighted average of the triangles vertices.

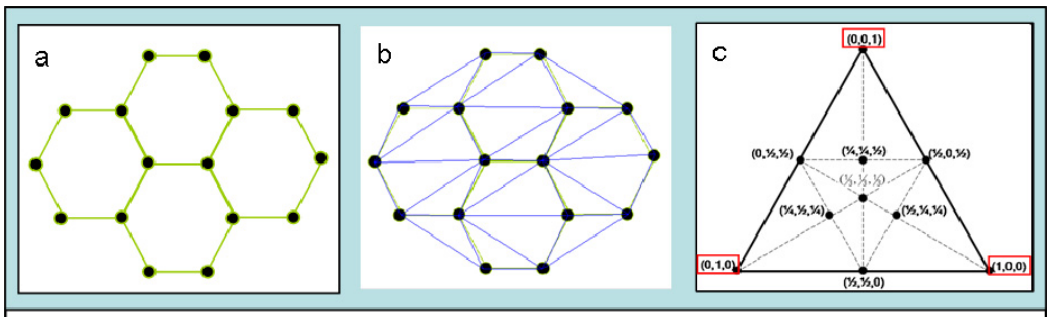

Figure 2.10 Triangulating material coordinates to define a growing surface. (a) material vertices define the cells. (b) Delauny triangulation of the material points (blue lines). (c) The barycentric coordinates of all points inside the triangle are specified based on the weighting of the coordinates of the triangle (highlighted in red). (Images a-b were produced in matlab while c was taken from WWW.CAMBRIDGEFORECAST.ORG.)

The barycentric coordinates of a point p inside a triangle is defined by $p(x,y) = \lambda_1 a + \lambda_2 b + \lambda_3 c$ where a, b and c are the vertices of the triangle and $\lambda_1 + \lambda_2 + \lambda_3 = 1$.

In subsequent time steps the position of the non-material points can be found using their stored barycentric coordinates and the coordinates of the triangle they are in. This method produces a much better approximation of the growth of the tissue than using a single tensor and does not assume uniform growth. However, it is not currently able to include the introduction of new material points during growth.

Dividing a cell in the descriptive model

The coordinates of where the observed cell division met the wall are stored in the tracking file obtained from the time-lapse imaging. They can therefore be used to divide the cell if the time of division is also the same. Note this division might not go through the centre of the cell.

The time that the observed cells divided is known from the tracking data. This can be used to divide the cell in the model by iterating over the cells and assessing if the current time is greater than the cells stored division time. The cells state is then changed to 'divided' so that the same cell can not be called to divide twice as the time will always be bigger than the division time of all the cells that have divided. These cells are then passed to the division algorithms where their division points are computed and they can then be divided. The daughter cells are created with a state of un-divided.

Combining descriptive and mechanistic models

If the mode if grown using the interpolation of cell vertices, and the cells are divided at the observed time and in the observed orientation then the model is fully descriptive. The model output matches the observed cells in terms of number, area, topology and

geometry. However it is also possible to make mixed models that contain some mechanistic elements. The mixed models mean one element of the system can be tested at a time.

The different division algorithms outlined above were applied to the descriptive model cells. The division algorithms were all applied at the time the real cells divided. Separating cell division time and orientation in this way makes the output easier to asses. If the cell was divided at a different time the cell might have a different geometry and divide differently. The different division timing algorithms were also tested on the descriptive model to ensure the cells had an accurate cell area. If the cells were grown using another method the area of the cells might not be accurate.

Problems encountered in making mixed mechanistic and descriptive models

Adding mechanistic elements in a step wise manner to the descriptive model was a very useful method to investigate the division algorithms but it also generated a few problems. To establish the division time of the daughter cells they need to be associated with the observed cells they represent. In the fully descriptive model this is stored in the tracking data. However, if the cells division orientation is selected using a mechanistic model then the daughters in the model and the observed cells might be very different. Which model cell inherits which observed cell identity and hence division time is determined by an algorithm. The daughter cells in the model are compared to the observed cells with both of the possible combinations of fate. The combination that results in the greatest overlap of vertices is used. The daughters are therefore assigned to maximise the number of correct vertices. This means that the topology of the cells should be maintained even if the geometry is not quite right and avoids excessive propagation of errors if an early division is not the same as was observed.

3 Cell division and Growth

3.1 Introduction

To understand the role of the asymmetric divisions in patterning the leaf epidermis we need to understand the tissue itself. In this chapter the cell division and growth of the leaf will be considered.

The growth and cell division patterns of the leaf were studied using time-lapse confocal imaging and modelling. The leaves were imaged, digitised and used to build a descriptive model.

We developed the ability to image living seedlings for up to 6 days by growing them in a specially made chamber that remains under the microscope. This allows the collection of high resolution images that capture the dynamics of the tissue. Time-lapse imaging presents a trade-off between image frequency and specimen health (see methods section). Images were collected every 4-10 hours. To simplify the modelling and data analysis the patches of the leaves studied are assumed to be flat; an approximation that

is reasonable for the age and region of interest. Therefore, all work was carried out on a surface projection of the image stack (using MerryProj).

The cells were digitised using the Point Tracker (see methods) and the coordinates of all the cells, their neighbours and cell division information were all extracted and stored (Figure 3.1). This data was used to generate a descriptive model of the leaf within the VVe modelling environment (see methods). The cells in the descriptive model grow by interpolation of the real data points so their geometry and growth is accurate. They also divide at the time observed and in the same orientation. The cell walls are approximated as straight lines joining the cell vertices. The walls of the observed cells are not always straight. However, wall curvature is associated with the formation of pavement cells which do not divide and are therefore not the focus of this study. The cell vertices were used to study the growth of the leaf as described in the introduction.

The descriptive model produced allows for the gradual replacement of direct data in the descriptive model with hypothetical deterministic rules of cell division. Different division algorithms can, therefore, be tested and verified by comparing the model to the observed data. As the cells in the model correspond exactly to the observed cells, direct comparisons can be made. Adding mechanistic rules one at a time in this way simplifies the process of building and validating the model. The contribution of individual mechanisms can be more easily assessed. As it is possible to separate the different aspects of cell division in the model, I will address them separately in this chapter.

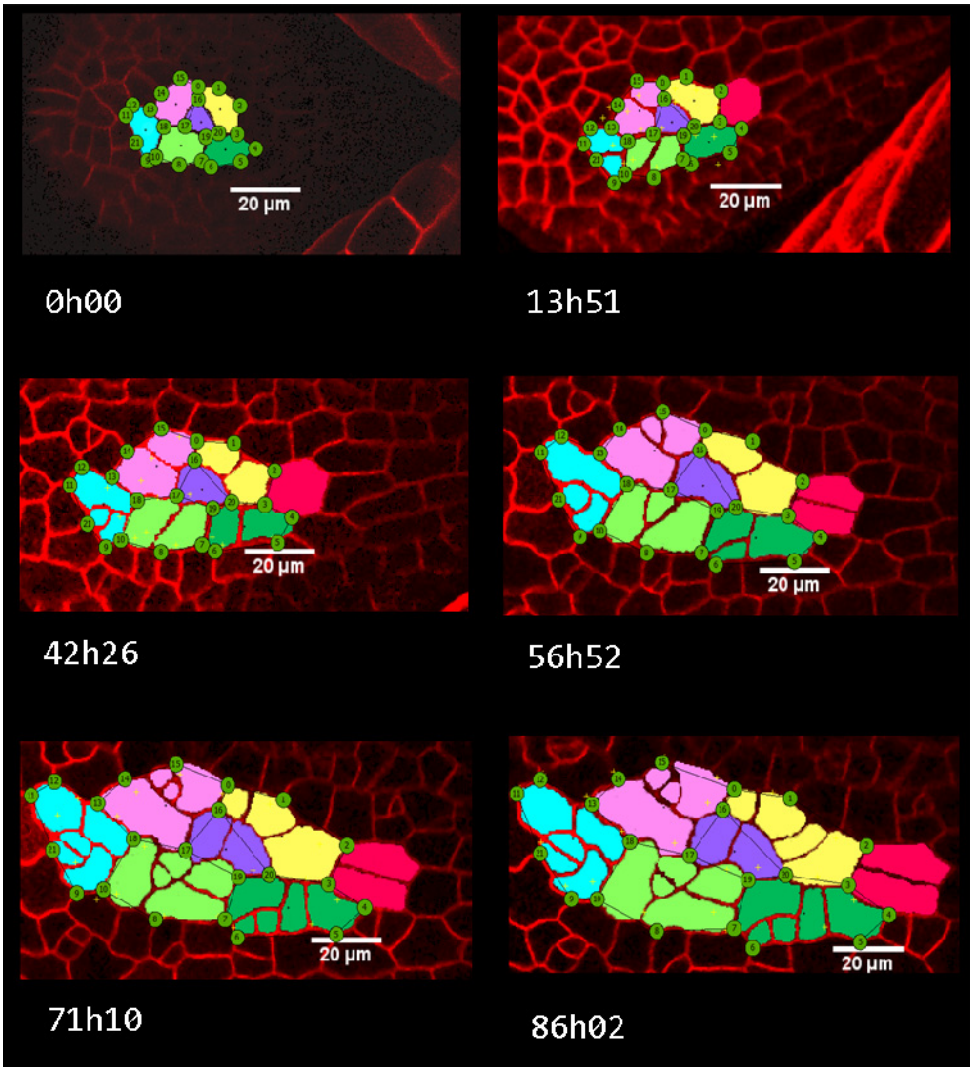

Figure 3. 1 A patch of wild-type cells were followed through time. A sample of the images captured for a small patch of wild-type cells. Cell lineages were manually identified using the point tracker (see methods section). Corresponding vertices that can be identified in all images are marked and have an identifying number in the circle, e.g. the vertices shared by the purple, pink and yellow cell is number 16. This junction can be identified in all images. The time since the imaging started is shown.

3.2 Cell division

There are two main issues regarding cell division. How cells divide and when cells divide. How a cell divides concerns the placement of the new division wall in the cell.

This can be considered in terms of its position and its orientation. When cells divide can be thought of in two different time scales, in the short term it is linked to entry into the mitotic phase of the cell cycle. In the longer term it addresses cells limited competence to divide; traditionally thought of as an arrest wave. In this chapter I will address both how and when cells divide and relate it to the growth of the leaf.

3.2.1 How to orient a division wall

There are a number of ways in which a new cell wall can be placed. However there are some constraints, the position of the wall has to be such that it goes through the nucleus of the cell, and joins two of the original walls. Otherwise, there are a range of theories as to how cells might position their new walls (see introduction). In summary the literature can be broken down into a few main ideas. In terms of the position of the new wall there is a general agreement that it should be at, or close to, the centre of mass of the cell, in both the root and the meristem (Nakielski, 2008; Sahlin, 2010). In terms of the orientation of the wall it is either: the shortest path across the cell (Errera, 1888), close to the cell centre (Korn, 1993), through the longest wall (Korn, 1993), perpendicular to the main axis of growth or strain (Hofmeister, 1863; Lynch and Lintilhac, 1997; Sahlin, 2010), or is positioned to ensure the daughters are of equal size (Errera, 1888; Sinnott, 1936). Additionally it is suggested that the new wall should meet the old wall at 90º (Sachs, 1878; Sinnott, 1936) and avoid existing junctions.

The different division rules are not necessarily mutually exclusive. In some cell types many of the division rules actually produce the same result. This is especially true of the root cells which have a uniform rectangular shape. In these cells the shortest wall is

perpendicular to the main axis of the cell, and perpendicular to the principle direction of growth. The shortest wall will also bisect the longest wall and is likely to contact the closest wall. As the cells are rectangular the new wall will also meet the old wall at 90º. The root and meristem are nice systems to study cell division as; they have areas that are free from cell differentiation so, cell division can be studied more easily. However, the regular shape of the cells means that many different division rules produce the same results. The leaf epidermis provides a more diverse range of cell sizes and shapes in which to study and distinguish the division rules. Studying cell division in the leaf can, therefore, provide additional insight to this old problem.

Modelling division orientation in a patch of wild-type cells

The descriptive model of the growing leaf was used to apply different division rules to the growing cells. Initially a descriptive model was produced based on the observations of a small patch of wild-type cells (Figure 3.1). The division rules were applied to the cells at the observed time of division. This process is, therefore, sensitive to the time interval between images which was typically between 4 and 12 hours (see methods for more details). Although the division times are not perfectly accurate this method means the division rules are being applied to cell geometries similar to those of the observed cells at the time of division. As many of the rules proposed are geometric this is likely to be important.

All the division rules tested were positioned so that they pass through the cell's centre of mass as this seems to be the consensus from studies of other tissues. I then selected the orientation of the new wall based on the division rules.

Initially the shortest wall rule was tested on the small patch of cells (Figure 3.1). This rule finds the shortest straight path across the cell going through the centre. It was computed using an approximate method by iterating over the walls and trying different division paths. As the initial model was descriptive the output from the shortest wall model (Figure 3.2b) can be directly compares to the patch of observed wild-type cells

(Figure 3.2a). The cells grow as they should producing clones of comparable size and shape. What does not match, however, are some of the new division walls. I coloured the walls white that were correct in terms of cell topology and had a reasonable geometry. I was lenient on how accurate the walls had to be to be classified as correct as so few were correct and I did not know how accurately a division wall could ever be placed. Even so, for the shortest wall model only seven of the twenty divisions occurred correctly. If we focus on the bright blue clone on the right we can see that only one wall is in the correct orientation. This results in the cells, of the clone, having the wrong topology and geometry. If we first consider the topology: in the real cells one blue cell neighbours the pink cell, and two blue cells neighbour the green cell. However, in the model two cells neighbour the pink cell and three neighbour the green cell. The cell shapes are also very different between the model and the observed data. Comparing shapes is a difficult process especially when they are so different that correspondence is difficult to find, as is the case here. We will, therefore, use qualitative approaches to judge whether the geometry of the cells is comparable.

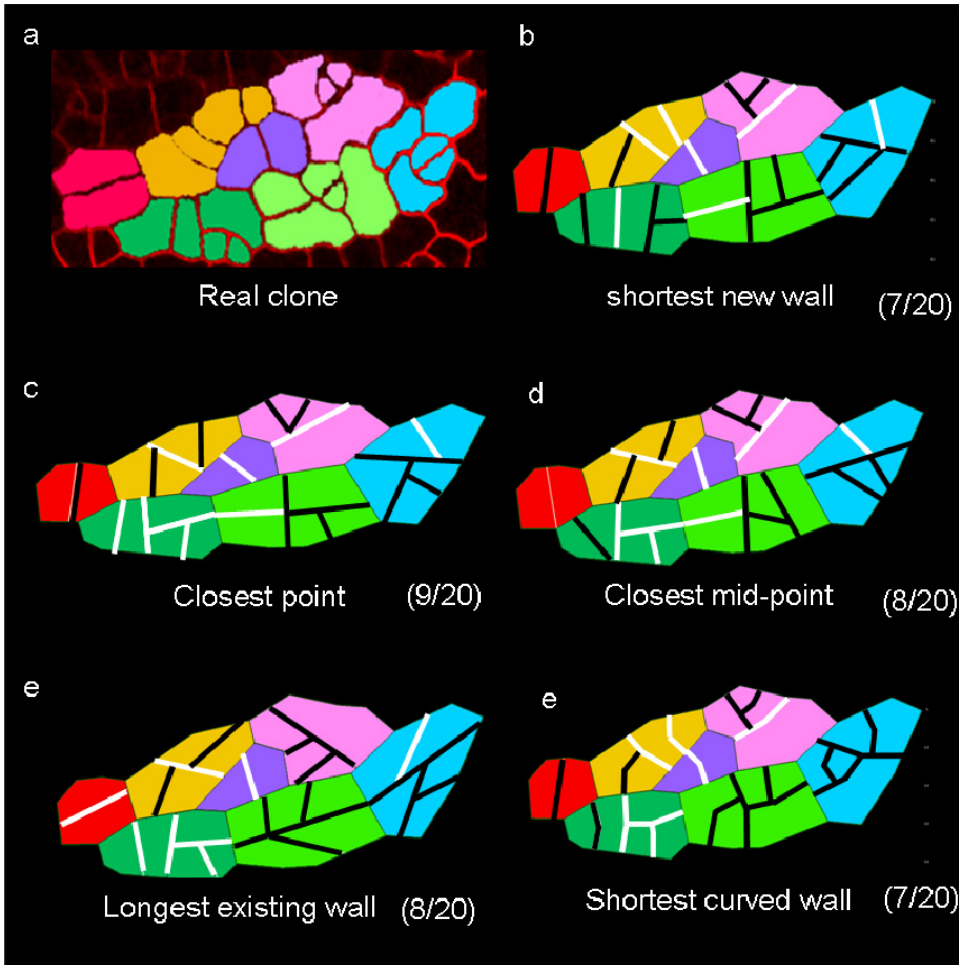

Figure 3. 2 Comparing different geometric division algorithms to the observed cells. a) the observed cells. Clonally related cells are coloured the same colour and Corresponding cells are coloured the same in all images. b-f) the output of the different division algorithms. Cells are divided through the centre by: b) the shortest path across the cell, c) the closest point to the centre, d) the closest mid-point, e) the mid-point of the longest wall or f) the two shortest paths to the centre. Division walls that are white are regarded as correct while black lines are not.

As the shortest wall rule was not able to capture the division orientation of the observed cells, I tried a number of other geometric division algorithms. The division algorithms tested included the longest wall and closest point algorithms (Korn, 1993), (the methods section). The closest point algorithm finds the closest point to the cell centre and joins it to the wall opposite, passing through the centre. The result of the closest point algorithm is very similar to the shortest wall algorithm with nine of the twenty divisions recreated (Figure 3.2c). The dark green clone looks more like the real cells but the cells in the pink and orange clones have incorrect geometry and topology. A variation of this algorithm is to find closest mid-point of a wall the. However, this algorithm also offers no improvement with eight of the twenty divisions marked as correct Figure 3.2d. Positioning the new wall so that it bisects the mid-point of the longest wall (Korn, 1993) produces cells with the least realistic geometry and manages to re-create only seven out of twenty division walls (Figure 3.2e). None of these algorithms can capture the geometry or topology of the cells. I noticed that the new walls were not hitting the old walls at 90° as postulated by Sachs (Sachs, 1878). I attributed this to my model introducing only straight new walls. Even the shortest wall algorithm is not finding the shortest path across the cell. It is finding the shortest straight path across the cell. I tried to improve both factors by finding the two shortest paths from the centre to any wall. I then joined these to better approximate the shortest overall path across the cell, more like the division proposed by Errera (Errera, 1888). This algorithm produces new walls that hit the old walls at 90° as this is always a shorter path. If un-constrained this model can generate new walls that have a very acute angle at the centre and would produce a very small cell. I therefore, did not permit an angle of < 90° at the centre. The cells look a little more like the observed cells in terms of general geometry and size distribution but the details have not been captured (Figure 3.2f).

Another common division algorithm identified in the literature is based on the growth of the cell, initially proposed by Hofmeister (1863) and used in models of the root more recently (Nakielski, 2008). We can calculate the growth of the cells using the method outlined in the introduction and methods. In the previous chapter the principle direction of growth of the small patch of wild-type cells was calculated. The overall growth directions of the clones in the patch (Figure 3.3b) are not isotropic. This means that, at least in parts of the leaf, there is a well defined direction of growth. Algorithms can

therefore be defined based on the growth, unlike in the meristem where there was no overall direction (Sahlin, 2010). I found the shortest path across the cell parallel of perpendicular to the main direction of growth (Nakielski, 2008). However, I still specified that the cell wall should pass through the centre of the cell rather than deviating with a probability. Initially the algorithm was applied using the growth calculated for vertices from successive images (Figure 3.3c). As the data is noisy I also calculated the overall growth tensor for each clone using the position of the vertices in the first and last time-step (Figure 3.3d). Dividing the cells using either growth calculation does not work well. Both algorithms produce similar results that do not match the observed cell divisions. Our model and experimental design does not allow us to investigate whether stresses rather than growth could explain the division patterns.

As the final arrangement of division walls from the algorithms did not match the real data I chose to look at the intermediate time steps. Figure 3.4 shows the output of the shortest wall algorithm and the shortest wall aligned with the growth axis algorithm over time. I concluded that in the early time-steps the orientation of the division wall was comparable in the model and the observed cells, however, as time went on the two diverged. This could be a consequence of accumulating errors. However, the divergence of the model and real cells correlates with the production of small cells. These cells have the appearance of being in the stomata lineage. I therefore concluded that in agreement with the current literature, cells in the stomata lineage divide by a different mechanism to other cells (this will be covered in the next Chapter).

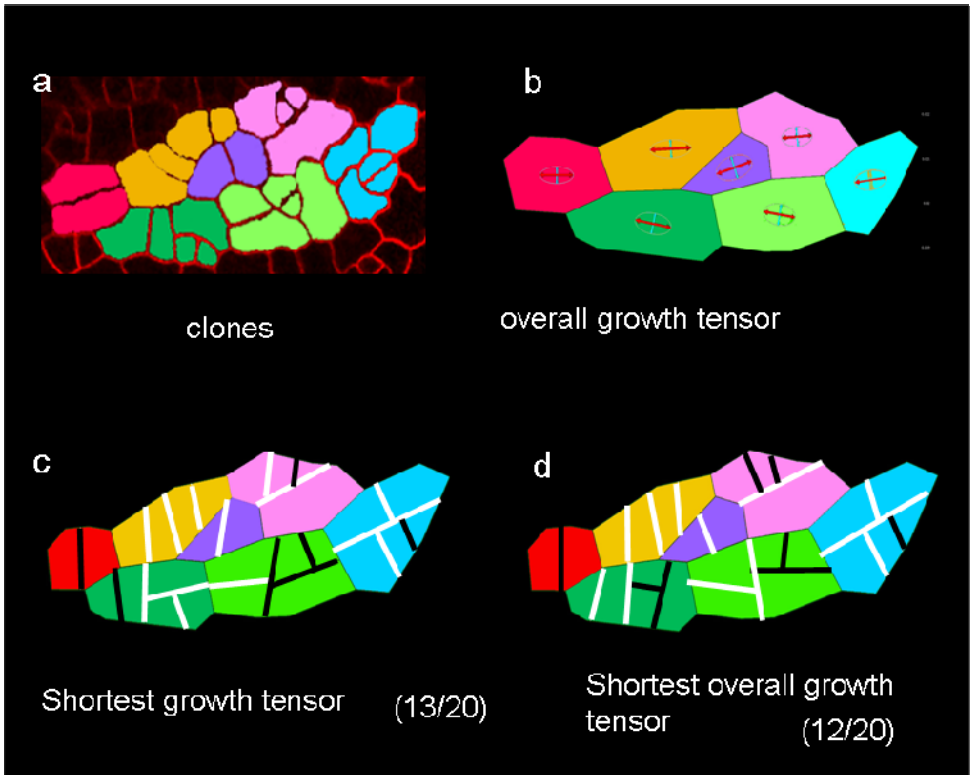

Figure 3. 3 Comparing growth tensor defined division algorithms to the observed cells. a) the clone of cells, b) the overall growth tensor for each clone, calculated from the first and last time-points. The red arrow marks the major growth axis and the blue the minor. The models divide the cells through the centre as in the previous figure. c – d) the output of the models which divide the cells based on the orientation of the growth tensor. The new division wall has the orientation of the growth axis that creates the shortest path across the cell (see methods and text) c) the growth axis is re-calculated every time-step, d) the growth axis are calculated once using only the first and last images as shown in (b).

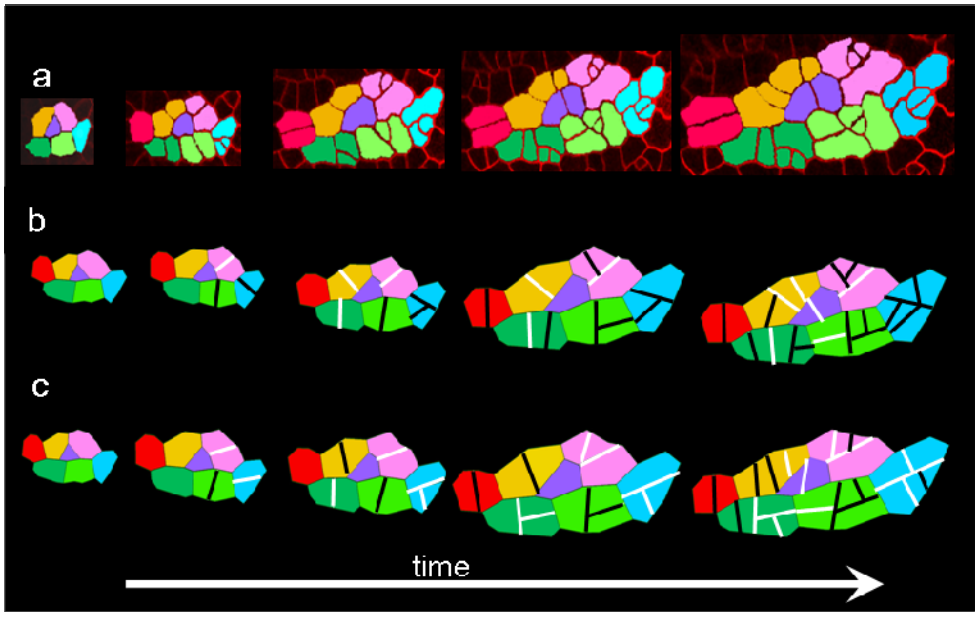

Figure 3. 4 Comparing the model output to the observed cells over time. Rather than only considering the final arrangement of the cells in the clone the divisions can be considered in the order in which they occurred. The observed clone shows the order to cell divisions a), the shortest wall model b) and the shortest growth tensor algorithm c). All algorithms are applied at the observed time of division. This allows us to see more clearly which division algorithms are correct and whether there is a time dependence. Both models are better able to predict the division of the larger cells than the smaller cells.

So far the models have considered different mechanisms for orienting the division wall but the position of the wall is also important. Currently the division walls in all the models passed through the centre of the cells. Nakielski suggested that the division walls might not pass exactly though the centre and allows some fluctuation around the centre (Nakielski, 2008). In the roots this seems to be a valid assumption. I therefore calculated the centre of the cells at the time of division. Figure 3.5 shows the divisions of each clone arranged chronologically with the centres of the cells marked at the time of division. Some cell divisions go through the centre while others do not. In Figure 3.5(i) which represents the first division of the clones all but one division wall goes through the centre. With successive divisions there is more variation. Some divisions are close to the centre but, some are very far away. The distance from the centre seems to be larger for the small stomata precursor cells (Figure 3.5b(ii) and (iv) and e(i) and (ii)) although the division of the stomata cell (b(iv)) does go through the centre. Because, I was able to see a correlation between cell type and the position of the cell wall I wanted to investigate it further rather than trying to account for it by stochastic fluctuations. I therefore looked at the Speechless mutant which does not have stomata to see if the new walls would pass through the centre of the cell.

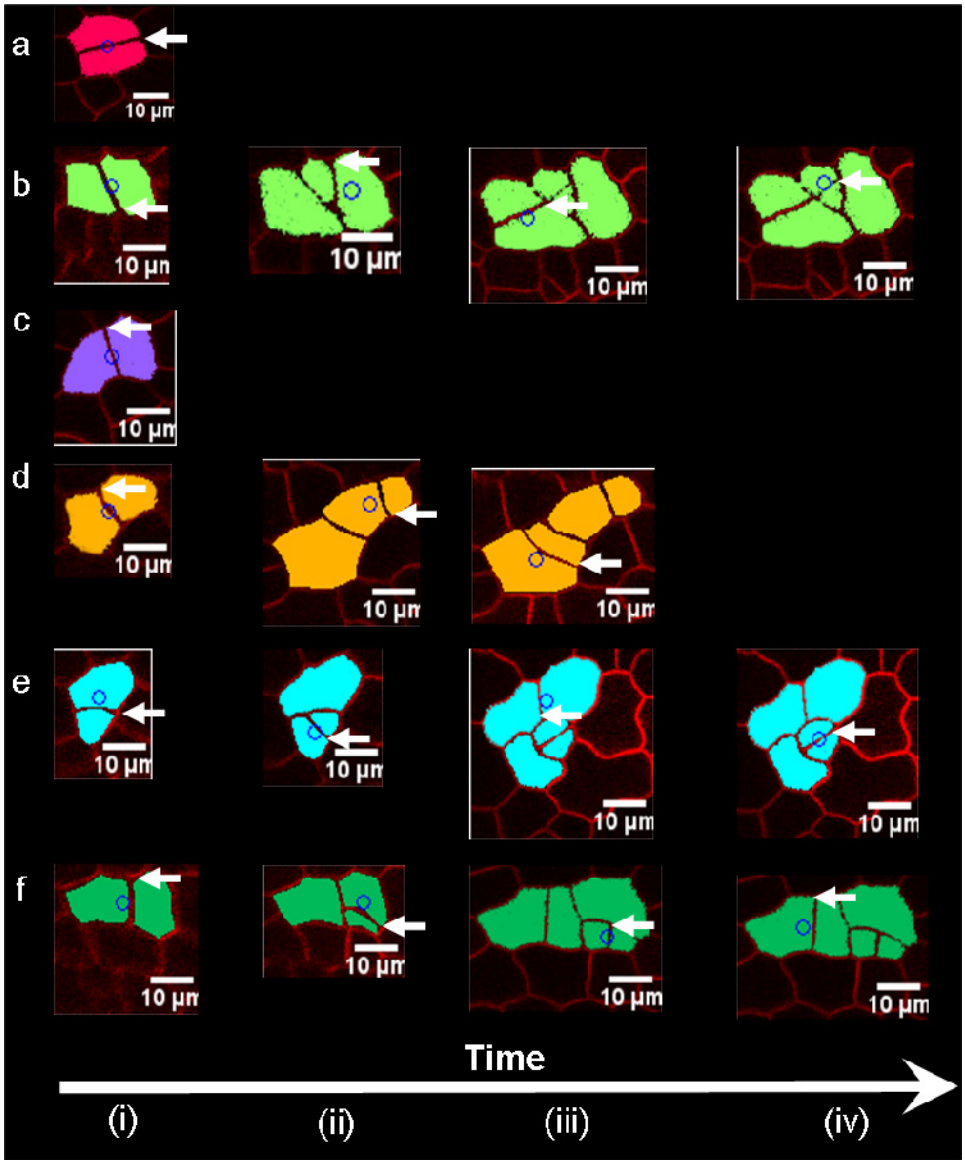

Figure 3. 5 Do new division walls go through the centre of the cell? The centre of mass of each cell has been calculated as close as possible to the time the cell divided and is shown as a blue circle. The new division wall is marked with an arrow. (a-f) shows the different clones from the patch in the previous figures. The images (i-iv) are arranged in order. In (i) the new division walls of cells in clones (a-d) pass through the centre, in f the wall is close to the centre but in e it is clearly shifted away from the centre. In (ii) none of the divisions pass exactly through the centre. In (iii) the division wall of the cell in clone (f) does pass through the centre and the other walls are quite close. In (iv) the division to create the two guard cells in clone (e) goes exactly through the centre but the other divisions are shifted a bit.

Cell division orientation in a small patch of speechless cells

The developing wild-type leaf epidermis contains cells of different types and stages of maturity. Cells divide and differentiate into pavement cells or stomata. Figure 3.6a shows the different options for the cells in epidermis cells, the cells cycle through a number of rounds of division (i), some of these cells stop dividing and become pavement cells (ii) while others divide many times and become stomata (iii). Stomata are a particularly prominent source of complexity as they form throughout leaf development by a series of stereotypical cell divisions. To investigate the mechanisms that might be responsible for regulating stomatal divisions it is important to determine the extent to which the divisions within the stomata lineage differs from the 'normal' cell divisions. How is the orientation of a normal cell division determined? Stomata formation begins with the asymmetric division of a meristemoid mother cell to produce a meristemoid a step which requires a transcription factor Speechless (MacAlister et al., 2007). As speechless is at the beginning of the pathway, knocking it out produces mutants with out any stomata. The speechless mutant, therefore, allows us to study the rules of cell division independently from the division pathway that produces stomata.

I tracked speechless leaves and re-ran the model using this data. Figure 3.7 shows a patch of speechless cells comparable to the size of the previously followed wild-type cells. The speechless mutant is slower to germinate and grow so it is difficult to match the age of the leaves with those of wild-type. However the leaves were imaged at similar sizes to the wild-type and for a similar length of time. I implemented the division rules previously tested on wild-type data on the speechless mutant data. Figure 3.8 shows the model output. The shortest wall algorithm and the closest point algorithms performed best predicting 6/7 divisions correctly.

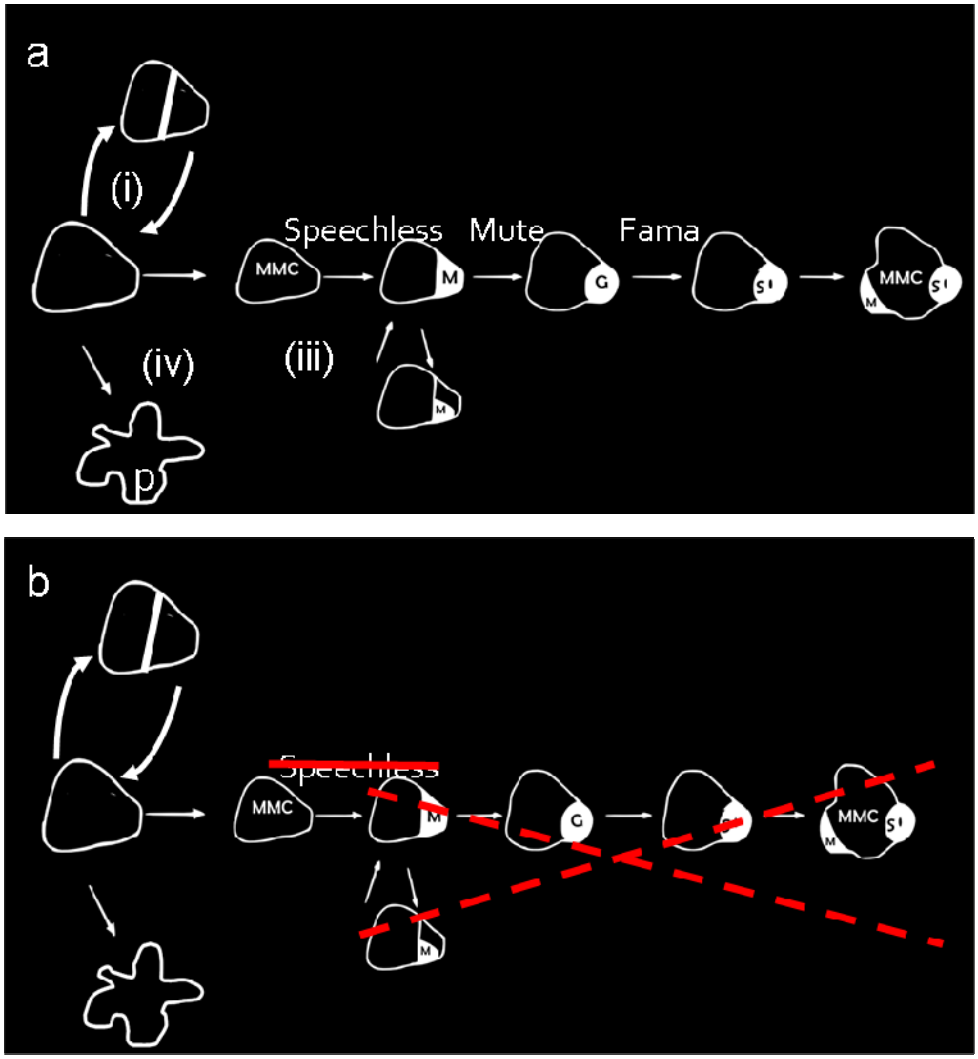

Figure 3. 6 The different pathways for cells in the developing leaf. Within a wild-type (a) developing leaf epidermis cells divide (i), differentiate into pavement cells (ii) or divide to produce stomata (iii). M – meristemoids, G – guard mother cells, and S - stomata. Speechless is involved early in this pathway so the mutants do not produce stomata (b).

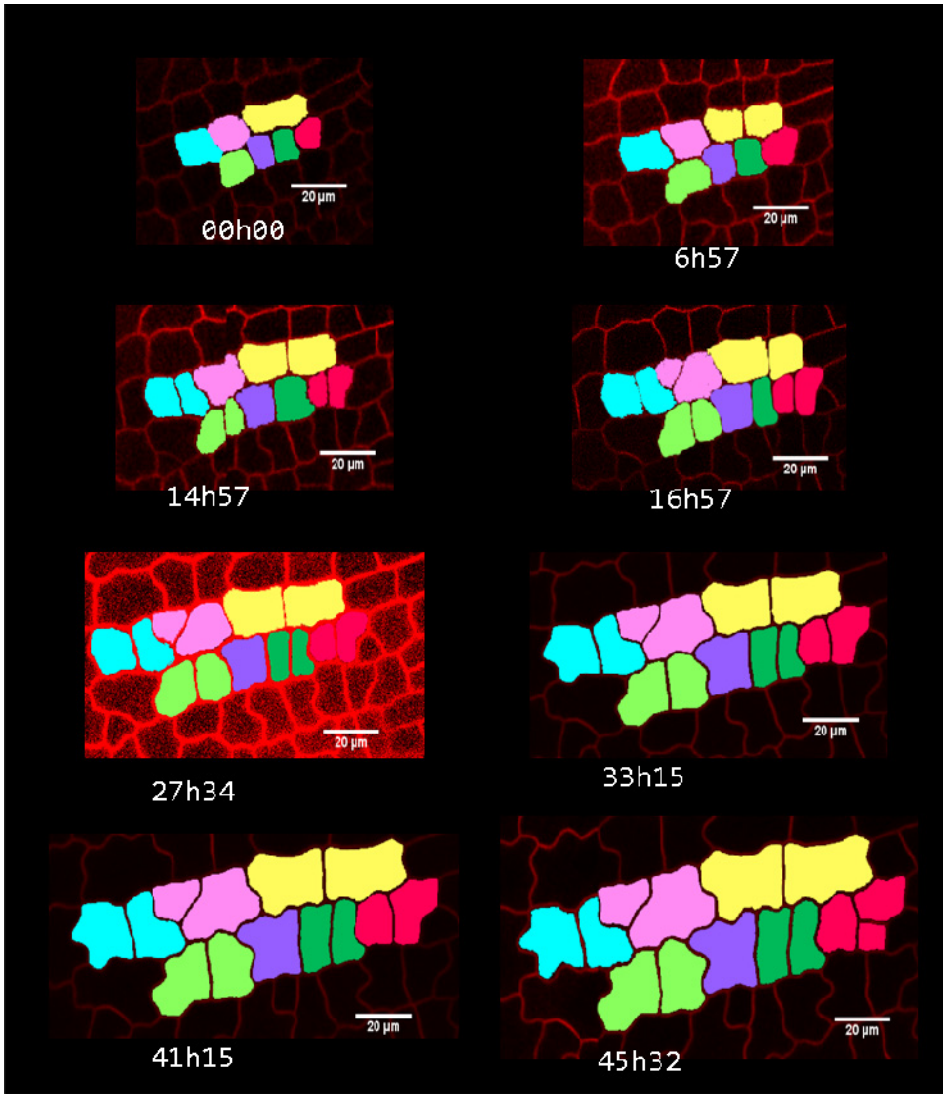

Figure 3. 7 A patch of *spch* cells followed through time. Cell lineages were manually identified and coloured. A sub set of the images are shown. Although this patch was followed for 80 hours no more cell division occurred in this part of the leaf.

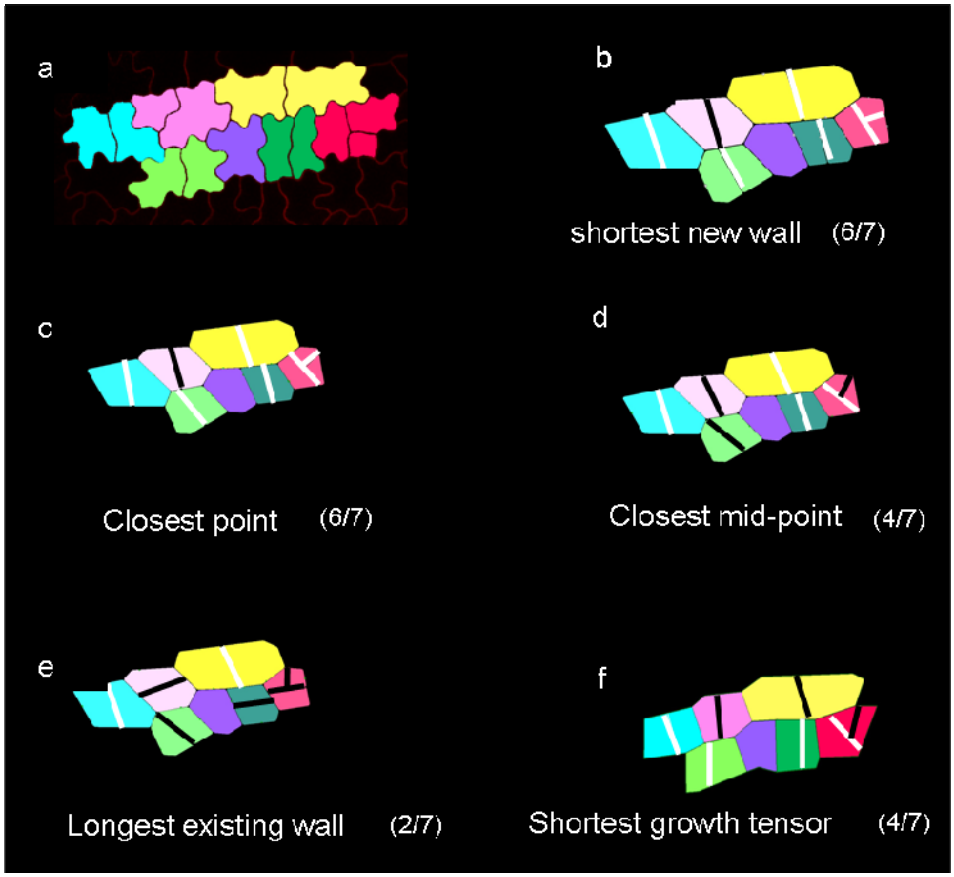

Figure 3. 8 Different division algorithms can be applied to the digitised cells. a) the observed cells. Clonally related cells are coloured the same colour. b-f) the output of different division algorithms applied to the cells in the model. Cells are divided through the centre by: b) the shortest path across the cell, c) the closest point to the centre, and its opposite wall, d) the closest mid-point and the opposite wall, e) the mid-point of the longest wall and the wall opposite, f) the shortest path aligned with a growth tensor. Corresponding cells are coloured the same in all images. White lines show correct division while black lines show incorrectly predicted ones. This is based on topology and geometry. In ambiguous cases the topology is given priority e.g. the division of the yellow cell in f has the correct geometry but the topology is wrong.

Both division rules produce the same output and both fail to predict the asymmetric division of the pale pink cell. The other division rules did not match the observed cell divisions as well. None of them were able to predict the division of the pale pink cell. The worst performing algorithm was the longest wall algorithm that divides the longest existing wall of the cell. Due to the irregular shape of leaf cells, the longest wall of the cell is not perpendicular to the shortest wall so these division algorithms produce different results. Studying the leaf therefore allows us to distinguish between the longest existing wall and the shortest new wall algorithms. The closest mid-point and shortest growth tensor algorithm both match 4 of the observed divisions. The speechless cells undergo fewer divisions during the period they were imaged so only one clone underwent more than one division. This means there is no benefit to looking at the divisions over time. All of the division algorithms produce a better match to the observed cell geometry than they did on the wild-type patch. We can also see that more of the divisions are passing through the centre (Figure 3.9), with the exception of the pink cell and the second division of the red clone. The divisions are not all perfectly aligned with the centre, this could be due to noise in measuring the centre or stochastic fluctuations as suggested by (Nakielski, 2008). However, this data does suggest that as predicted the difference between the model and the observed cells in the wild-type were due to the stomata formation. On such a small patch with so few divisions it is impossible to properly evaluate the division algorithms. I therefore extended the study to a much larger patch covering most of the leaf.

Modelling cell division orientation across the *spch* leaf patch

The time-lapse imaging and point-tracking was repeated on a larger patch of the speechless leaves (Figure 3.10). I was not able to segment the entire leaf as the cotyledons covered part of it in the early stages and the leaf curls in the late stages of development. However, I studied as large a patch as possible.

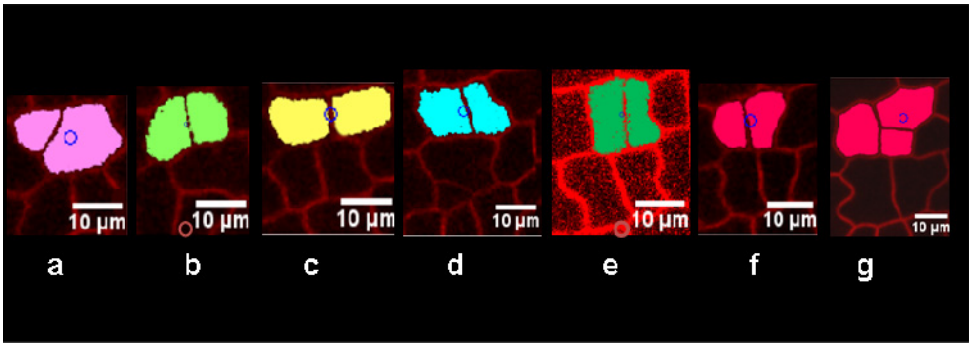

Figure 3. 9 Do new division walls go through the centre of the spch cells? The centre of mass of each cell has been calculated as close as possible to the time it divided and is shown as a blue circle. The division walls of all the cells b-f go through the centre but the pink cell (a) and the second division of the red clone (g) red division do not. The red clone shown in f and g is the only one to have more than one round of division.

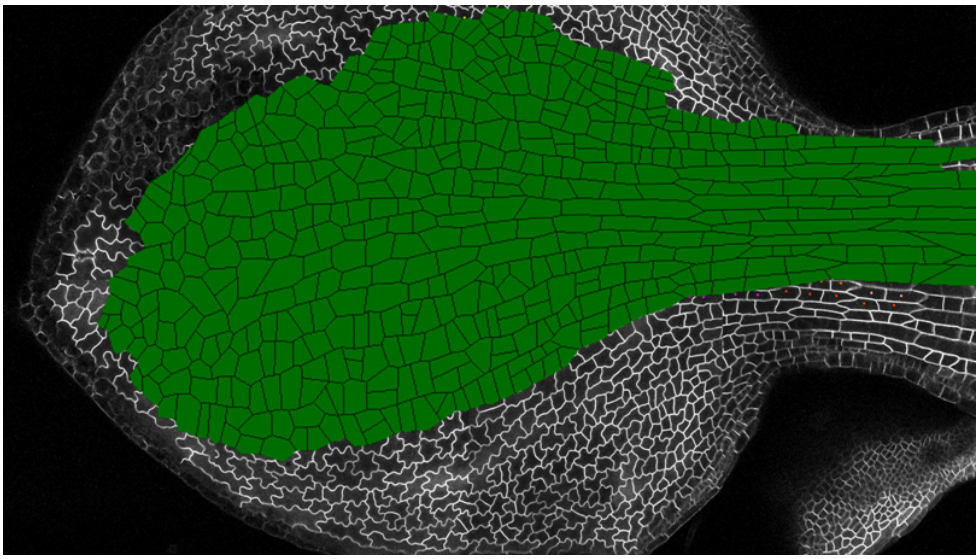

Figure 3. 10 An overlay of the digitised cell on the observed cells. A large patch of the speechless mutant leaf was tracked (shown in green). The cells were digitised by tracking the vertices. Here the final time-point of the image is shown with the digitised cells on top.

A fate map was produced to show the clones produced from single cells across the leaf (Figure 3.11). The clones differ across the leaf in terms of the number and orientation of cell divisions. For now we are only considering their orientation. The fate map shows division walls in the mid-vein and petiole region formed perpendicular to the proximodistal axis of the leaf (Figure 3.11 iii and iv), while divisions in the blade region occurred in other directions as well (i and ii). Therefore, even without stomata, the orientation of cell division is variable across the leaf. We can use the model to test whether the division hypothesis can account for all the variation seen across the leaf. Figure 3.12 shows the model output for the shortest wall and shortest growth tensor rules. Cells that did not divide were coloured gray as they would have the correct topology and geometry regardless of the division algorithm. I coloured dividing cells if they had the same topology and geometry in the observed cells and the model. The priority was given to correctly predicting the topology as this is easier to asses. A quantitative algorithm would be desirable. However, it is not easy to know what weighting to give to topology verses geometry or how to compare cells that are too different in shape to identify corresponding features. Comparing shapes is a complex process. Based on the qualitative comparison I found that the shortest wall algorithm was able to correctly predict the division of 84%of the cell divisions (160/190) while the shortest growth tensor rule predicted 74% of the divisions (140/190). The incorrectly predicted division walls in the growth tensor model may be due to noise in the data used to calculate the growth tensors as discussed earlier. The incorrectly predicted divisions in the shortest wall algorithm were easier to classify. Figure 3.13 highlights two of the main causes of difference between the observed cells and the model output. Despite being a Speechless mutant some of the cells still divided asymmetrically in a meristemoid mother cell like manner. This maybe due to chance or because there is some redundancy in this pathway and the mutation is being partially rescued (e.g. by the SCRM genes which are thought to act with the three transcription factors mentioned earlier and phenocopy their mutants (Kanaoka et al., 2008)). Whatever the reason for the occurrence of the asymmetric divisions, they can not be predicted by the current model. The difficulty in predicting asymmetric divisions is likely to be a consequence of them not passing through the centre of the cell (Figure 3.9a).

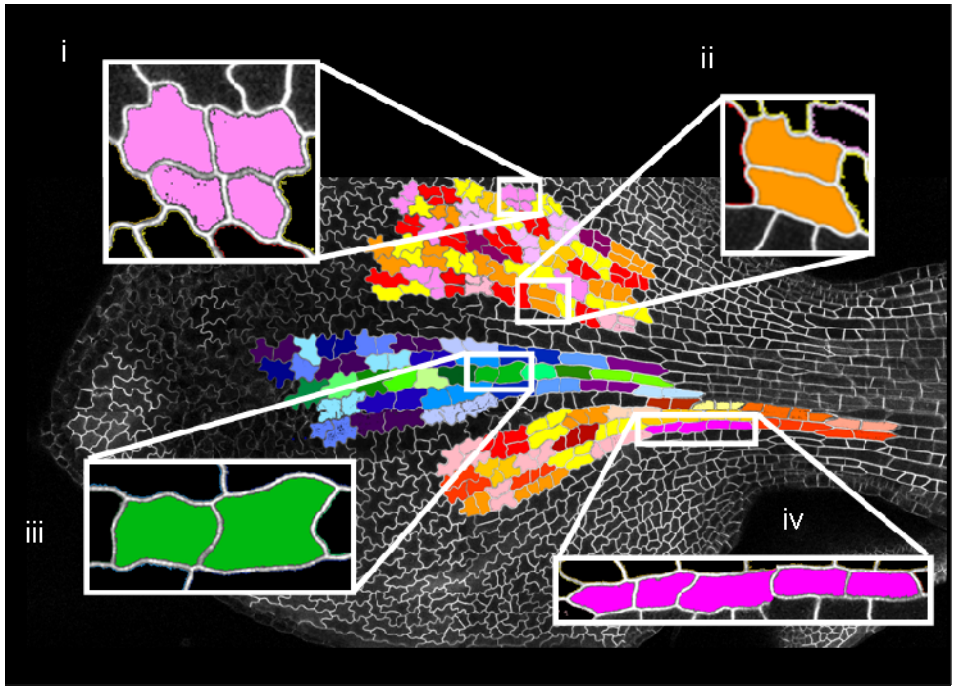

Figure 3. 11 Tracking the division of single cells allows us to generate virtual clones. All cells coloured the same colour came from the same cell. From the clones we can see the orientations of division. Clone i has 3 new division walls in two orientations, clone ii has one new division wall parallel to the orientation of the leaf. clone iii has one new division wall which is perpendicular to the leaf axis, clone iv has 4 division walls which are all perpendicular to the axis of the leaf.

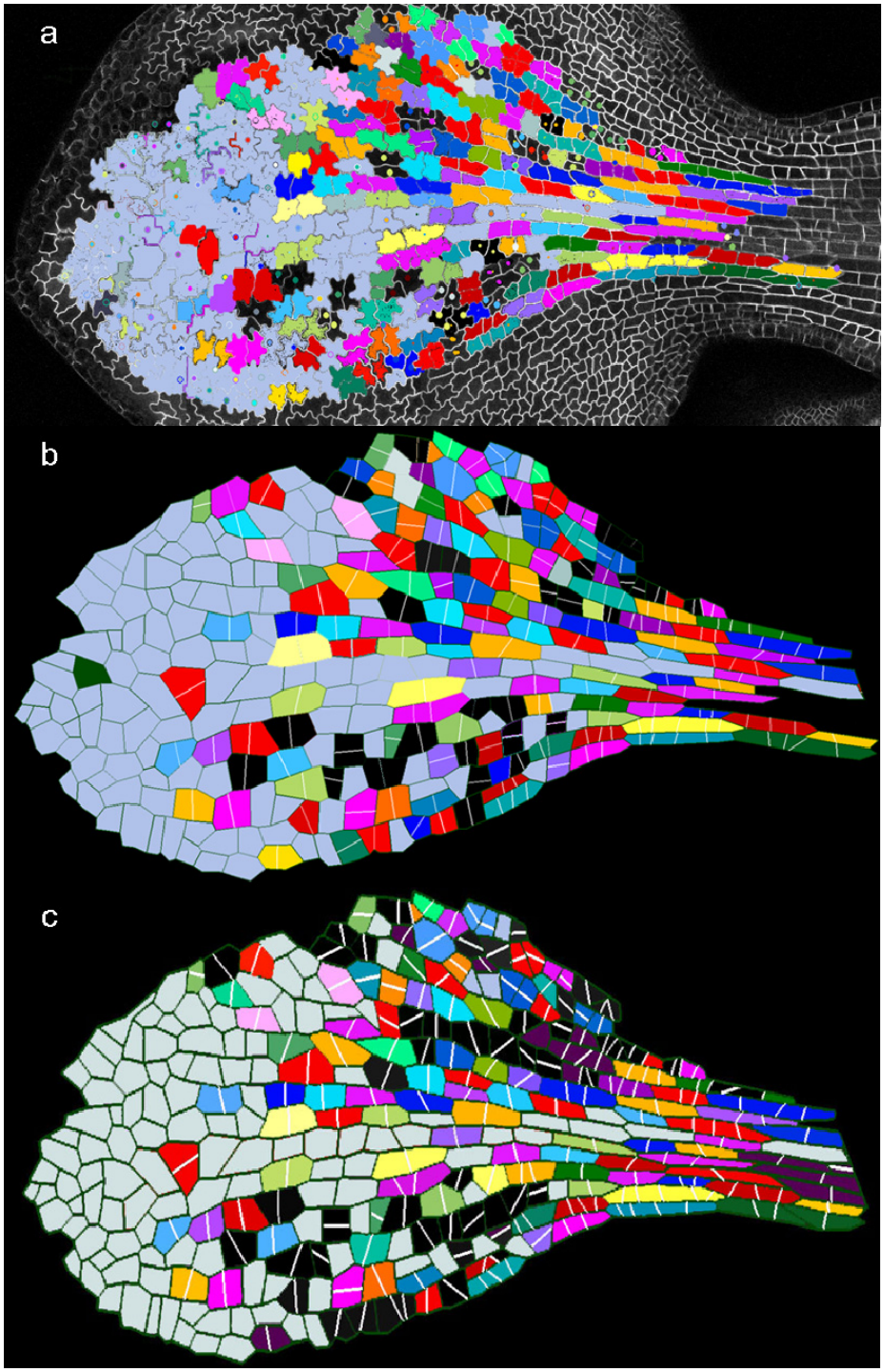

Figure 3. 12 Comparing the division algorithms to the observed cells. The observed cells (a) are coloured to show the clones. The model output of the shortest wall algorithm (b) and the shortest growth tensor (c). Cells are coloured to indicate correspondence to the observed clones where the division is topologically and geometrically similar to the observed division. The new division walls are marked with white lines in the model output. Cells that did not divide are shown in grey. Cells whose divisions were not captured by the model are shown in black.

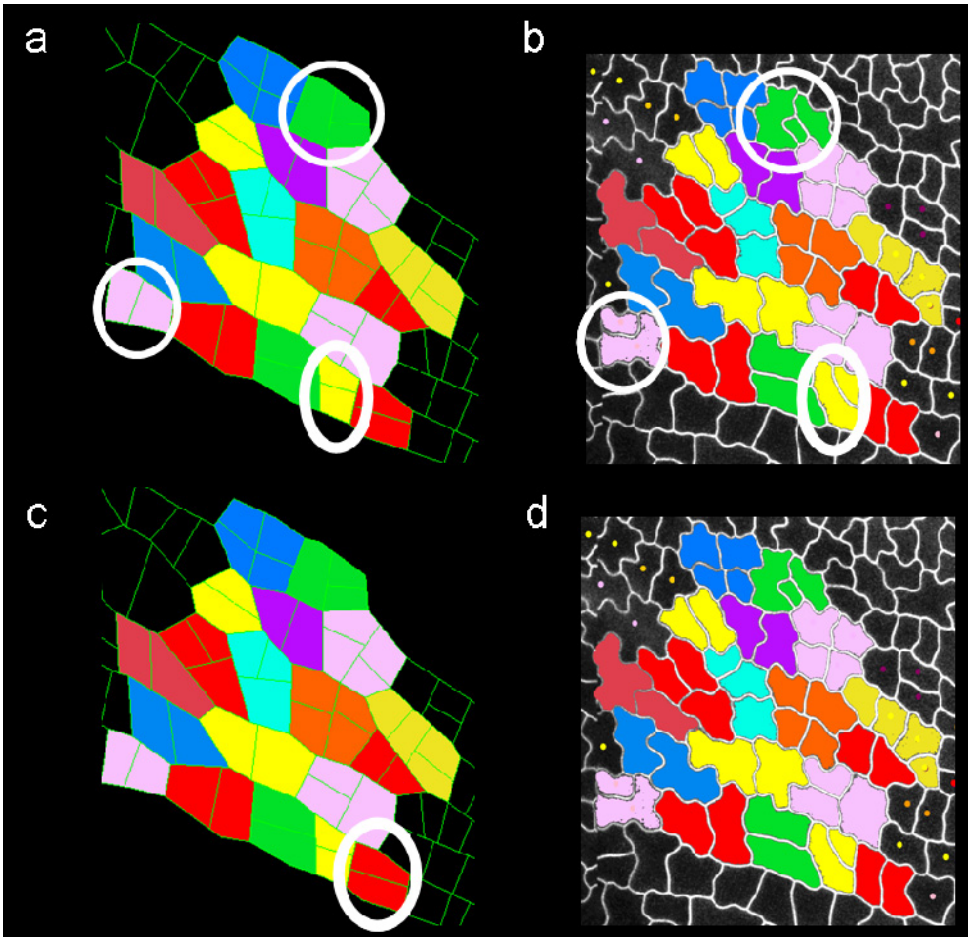

Figure 3. 13 Identifying the incorrectly predicted cells from the model. a and c) model output of the shortest wall algorithm. b and d) the observed cells. All images are from the final time point and the cells are coloured so that they correspond. a-b highlights cells that were observed to divide asymmetrically they could not be recreated by the division algorithm. c-d is a cell that is square so will be divided with an equal probability in either direction. Here it was divided perpendicular to the observed division plane.

This issue will be discussed further in the next chapter when we look at stomata formation. Another type of cell that the model can not re-create is square cells. If a cell is square then the two axes are of equal length so the shortest path will only match the observed division fifty percent of the time. The incorrectly predicted divisions in the shortest wall algorithm could also be due to difference in the time of division and the time the division was recorded. Longitudinal divisions are often observed near the mid-vein of the leaf although sadly none were captured in this data set. Genuinely longitudinal divisions occur if the cell divides along the longest axis of the cell, usually perpendicular to the shortest path. These divisions are rare but also can not be explained by the model, they maybe a result of cell differentiation or mechanical stresses.

Although I did not quantify the shapes of the daughter cells that resulted from the division algorithm, I did quantify other aspects of the division. I produced graphs that plotted features of the division wall against the same feature of the model (see methods on data analysis). Figure 3.14a shows the shortest path across the cells, at the time they divided, plotted against the length of the wall they actually placed. There is a good correlation between the length of the shortest path and the observed path. Not only is there a correlation but the points are quite well distributed around the xy line. This shows that the length of the observed division wall is similar to the shortest possible path. If they were correlated but not clustered around the xy line then this might simply reflect cell size. The data is, however, quite noisy which suggests that the process might be stochastic or imperfect. Accuracy of point placement in the point tracker also provides an additional source of noise. However, the graph highlights another problem with the data. The length of the cell wall formed should never be shorter than the shortest possible path across the cell through the centre. The graph in Figure 3.14a has the xy line marked and there are many points below the line indicating there is a problem with the method. A possible source of discrepancies comes from the limitations of the point tracker. It is only possible to define the cells in terms of straight lines that connect the vertices. As the walls of plant cells are not straight the real walls are often not exactly aligned with the digitised walls. Another source of the discrepancy is if some walls do not pass through the centre. Combined with the qualitative assessment the shortest wall algorithm can give us a good approximation of the division path chosen. This is in agreement with many other studies. However, this graph tells us nothing about the orientation of the division - a square would have two paths of equal

length in opposite directions. To assess this, I plotted the angle between the shortest path and the actual path taken (Figure 3.14b). The majority of cell walls formed between 0° and 20° from the shortest wall. However, some cell walls formed at other angles. Most division walls form close to the shortest path suggesting that many cells have a number of alternate paths that are short but are not in the same orientation. I made the same plot for the growth tensor algorithm and plotted the angle between the major growth axis and the observed division (Figure 3.14c). The results show most divisions happen at 90° to the major growth axis, though the correlation is not as strong and more other angles occur. There is a slight preference to divide at 0° to the major axis although; the result might not be statistically significant. Dividing parallel to the major growth axis would fit with the model of shortest path aligned with one of the growth axes (Nakielski, 2008). The difference in results between the shortest wall and the shortest wall aligned with the growth tensor could be due to the latter division algorithm being less predictive or errors in the growth direction estimation.

This quantitative comparison shows that applying the shortest wall algorithm at the observed times at which cells divide, results in a good match with the observed orientations of division walls. Although the other methods do not perform so badly that we can confidently exclude them.

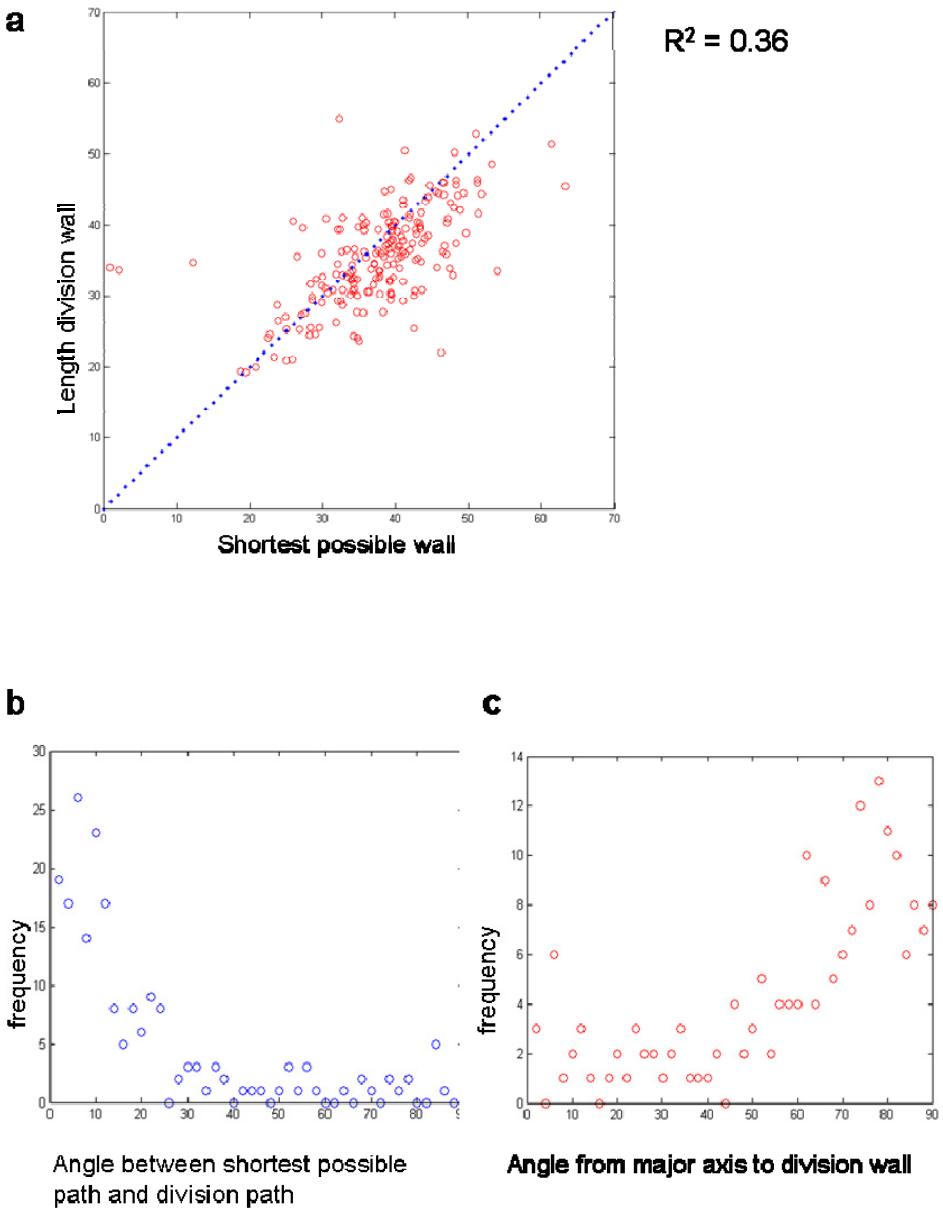

Figure 3. 14 Comparing division walls from the observed data to theoretical division walls based on the model algorithms. a) the length of the division path taken in the observed cell against the shortest possible path across the cell. The y=x line (marked in blue) is where the points would lie if the observed division wall was the same length as the shortest possible path. Note it is not the line of best fit. The r value is 0.6. b) the angle between the division wall in the observed cell and the shortest possible division path for the same geometry. There is a peak at 0°. c) the angle between the observed division wall and the major growth axis of the cell. From the shortest growth tensor division algorithm we would expect a small peak at 0° and a larger one at 90°. There is some indication of this in the data.

3.2.2 The timing of cell division

The timing of cell division has so far been input descriptively into the model i.e. according to the observed time of division. However, we can now test different algorithms using the same framework as we developed for the orientation of cell division. As mentioned earlier when cells divide can be thought of in two different time scales, in the short term it is linked to entry into the mitotic phase of the cell cycle. In this regard it is not known whether cells divide at a threshold area or after fixed cell cycle duration (P.Nurse, 1981). In plants the situation seems to be more complex and many signals feed into the cell cycle components. I aimed to asses whether a threshold area model or a fixed cell cycle model can account for the cell division timing seen in the leaf. In the longer term cells have a limited competence to divide and eventually arrest cell division. Traditionally cell arrest is thought to move from the tip to the base of the leaf in a wave from the tip of the leaf (Donnelly et al., 1999). Recently an alternative model has been proposed whereby a region of division competency is defined at the base of the leaf (Kazama et al., 2010). I will use time-lapse data to evaluate cell division competence. I will consider the interaction between the short and long term regulation of cell division and its affect on tissue patterning.

The timing of cell division in a patch of wild-type cells

Tracking data from the time-lapse studies was used to test whether cells divide at a constant area or after a fixed cell cycle duration. The cell cycle duration is the time between the cell being created by the division of its parent and it dividing again (Mitchison, 1971). I initially assessed the area hypothesis by measuring the areas of the cells at the time of division in the patch of wild-type cells (Figure 3.15).

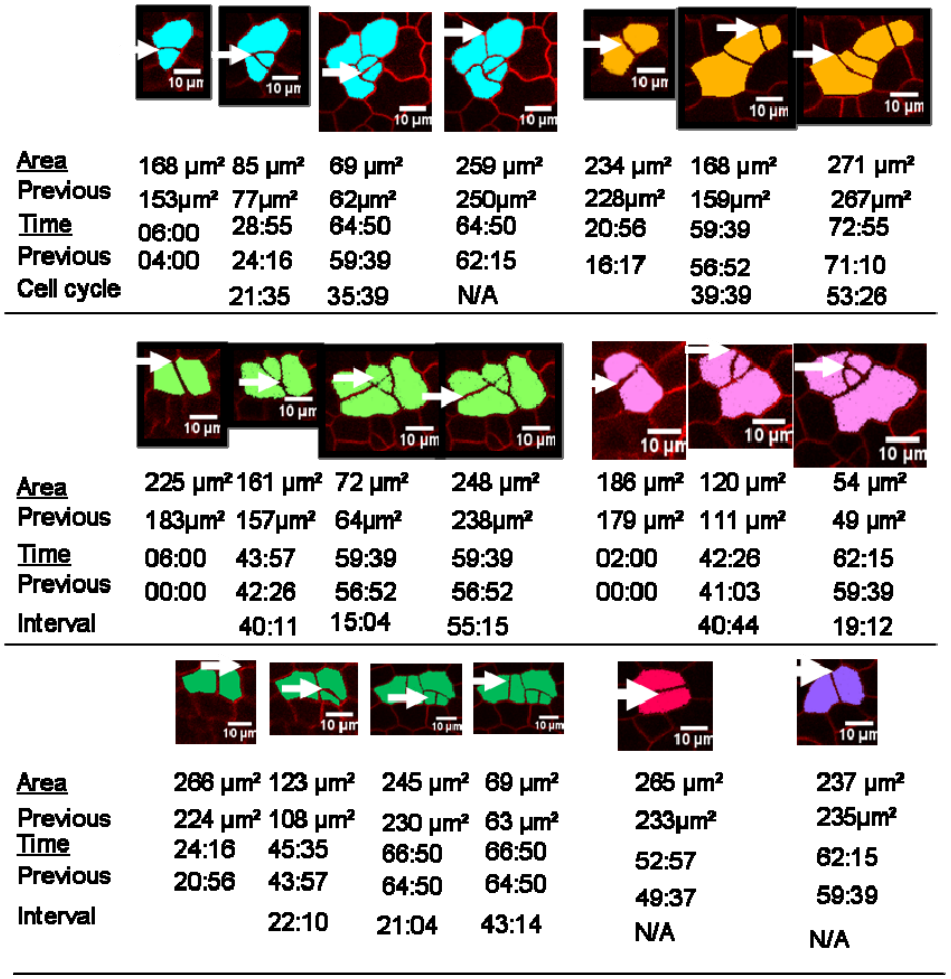

Figure 3. 15 The time interval and cell area of the observed cell when they divided. Row 1) the area of the cell in the first image captured after it has divided. Row 2) the last area observed prior to division. Row 3) The times are when these observations were made in hours and minutes from the start of the experiment. Row 4) The time of the last image of this cell. Row 5) The time interval since that cell last divided i.e. its cell cycle duration. It is calculated from the average of the time before the cell divided and after.

As these measurements maybe sensitive to the frequency of imaging I show the last observed area of the cell prior to the division thus giving an interval in which the division occurred. This analysis shows that even within a single clone there is considerable variation in the area at which cells divide, e.g. the blue clone contains cells that divide at 62-69μm² and 250-259μm². This is strong evidence that they are not dividing at a constant area threshold. I carried out the same assessment for the cell cycle duration and saw a range of timings that cells divide at. The cell cycle duration was calculated using the average of the two times before and after division. The cell cycle durations ranged from 15 hours to 55. This suggests cells are not dividing at a regular time interval.

Although the data is not consistent with cells dividing at a constant threshold area or cell cycle duration, modelling these assumptions can still help to assess the consequences of the cells using such rules to divide, thus providing insight into what might need to be altered to explain the observed division timings.

A constant area threshold model for the timing of wild-type cell division

First let us consider a model where we divide cells at a constant threshold area. To implement this rule, I incorporated an algorithm to measure the area of the cells at each simulation step and compare it to the threshold area which is set as a parameter. If the cell has an area larger than the threshold it is added to the list of cells to be divided. It is not possible to divide the model cells using the description of how the observed cells divided as it is not always possible to know where the wall should go. If the cell was due to divide after 12 hours but reached the threshold area for division at 6 hours the cell might not have a geometry that is comparable enough to identify where the wall should go. Therefore, cells were divided using one of the division algorithms, here I show the results of using the shortest wall. Consequently the output of the model must not be judged on the topology or geometry of the cells. I assessed the division timing algorithms based on the final distribution of cell areas and the frequency of cell divisions. Using criteria in addition to the timing of division allows us to consider

whether there are other ways of generating the same final arrangement of cells, and evaluate whether the precise timing of cell division matters. Figure 3.16b shows the final area of the digitised cells. The area of the digitised cells might vary slightly from the observed cells as the cells are approximated by straight lines so, it is better to compare the model to this. There is a 5 fold difference between the largest and the smallest cells in this patch. For now we will not consider the exact areas as this is sensitive to parameters. Figure 3.16c shows the output of dividing the cells at a constant threshold area. Predictably the output from the model does not produce cells in the range of the observed cells as the area threshold can only produce a range of 2 fold. Dividing cells at a constant area results in all cells having an area between the area threshold and half this area; assuming that the divisions are fairly symmetric. We have already seen that this assumption is not true for all of the observed wild-type cells. I therefore also compared the output of dividing the cells using the shortest wall algorithm at the observed time of division (Figure 3.16d). This model produces cells that have a 3 fold difference in final cell area. Thus, some of the difference is due to the shortest wall algorithm being a bad approximation of the wild-type cells because of asymmetric divisions. We can conclude that the observed distribution of areas seen is a consequence of the cells not dividing at the same area and dividing asymmetrically.

The model can also be assessed based on their ability to re-create the frequency of cell divisions observed. Figure 3.16f shows the frequency of cell divisions using the observed cell timing. Note this measure is not based on the number of rounds of division but is the number of times a particular cell divided. For example if a cell divides and then only one daughter cell divides again this daughter will have a division frequency of two and the other daughter will have a value of one. Some cells in the observed patch divide 3 times while other cells divide only once. The area threshold model output (Figure 3.16e) shows a better match to the observed cells when assessed in this way. The model patch shows a range of division frequencies of 1-3. However, if we compare the model and the observed cells it is not the same cells that are dividing 1, 2 or 3 times.

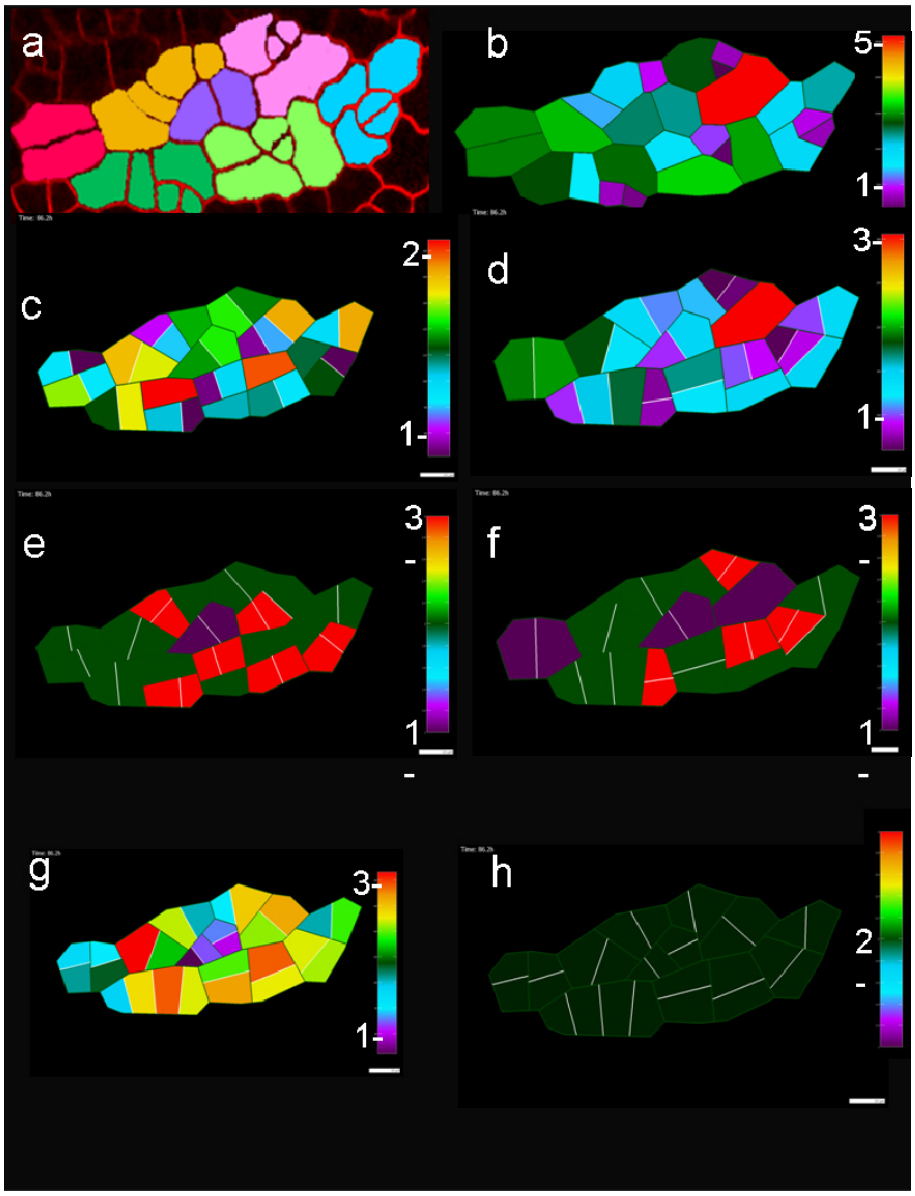

Figure 3. 16 Comparing the constant area threshold and constant cell cycle duration model to the observed wild-type cells. a) the observed clones. b) the area of the cell as they divided in the real leaf. The scale indicates the range of areas seen. The precise area is a matter of parameter fitting so is not shown. Here the range of areas is 5 fold. (c-h) all models use the shortest wall algorithm to divide the cell at different times. the final area of the cells produced with c) the constant area threshold model, d) the observed division time, and g) constant cell cycle duration model. the frequency of cell divisions with e) the constant area model, f) the observed division timing and h) the constant cell cycle duration.

Some care should still be taken in the interpretation of these results as although this method of assessing the model is not sensitive to the division algorithm chosen the algorithm its self is. For example if a cell under goes a physically asymmetric division in the observed leaf then one cell will be larger that the other so only one cell might divide. If the cells in the model divide symmetrically then both cells will be larger than the small cell and both might divide.

A constant cell cycle model for the timing of wild-type cell division

We can assess the consequence of dividing cells at constant cell cycle duration in the same way as we assessed the constant threshold area model. If all cells divide with a constant cell cycle duration there is a 3 fold distribution of cell areas (Figure 3.16g). This is an improvement on the area threshold model as there is a larger range of areas produced, but it still does not match the observed distribution. The cells would have to have very different growth rates in order for this method to produce a greater range of areas. If we assess the model based on the frequency of cell divisions we see that this model can not produce a range of division frequencies and hence does not match the observed frequencies. We could suppose that if there was sufficient noise in the system it might be possible to produce the asynchronous divisions seen in the observed cells and better recreate the division frequencies. However, I am still looking for deterministic rules at this stage.

Neither the constant area threshold nor the constant cell cycle model is capable of producing the 5 fold difference observed for the patch of wild-type cells. Additionally studying the timing of cell division is difficult in the wild-type background because the division orientation can not be predicted. Therefore, I looked at the speechless mutant to determine whether the difficulties in predicting division timing were also due to stomata formation.

The timing of cell division in a small patch of speechless cells

Cells in the speechless clone do not all have the same area at the time of division. However, compared to the wild-type the variation is smaller, ranging from 156µm²-247µm² in the patch studied (Figure 3.17). This suggests that stomata formation affects when cells divide. The number of cell divisions in the speechless mutant is also fewer: only one cell in this patch divides twice, making it impossible to assess whether the cells divide at a regular interval. We therefore need to study a lot more cells.

We can look at the model output for the speechless cells in the same way as the wild-type models to assess the consequences of the different division algorithms. The digitised cells have a 4 fold range of areas (Figure 3.18b). This is slightly smaller than the range for the wild-type cells. Dividing cells at a constant area threshold can still only generate a 2 fold difference in cell area (Figure 3.18c). If the cells are divided at their observed timing using the shortest wall algorithm a range of 3-4 times can be seen (Figure 3.18d). As the range of areas seen is roughly the same for the observed spch cells and the model using the default timings, most of the difference between the area threshold model and the observed cells is due to the timing of cell division. The frequency of cell divisions of the observed cells is 0-2 (Figure 3.18f), which can be re-created in the constant area threshold model (Figure 3.18e). However, the frequencies do not match in corresponding cells. Dividing cells at a constant cell cycle duration instead can generate a 2.5 fold range in areas (Figure 3.18g) but all cells divide only once (Figure 3.18h).

The modelling of cell division in speechless has shown that despite the data analysis suggesting the cells might divide at a constant area putting this into the model does not generate a good match with the observations. We might postulate that reaching the threshold area is required for cell division but is not sufficient to trigger it. We therefore need to explain the presence of cells that are larger than the threshold area but do not divide.

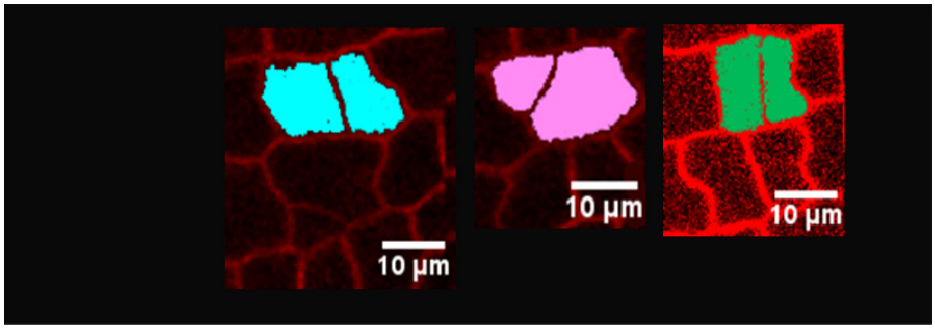

Area	247µm²	225µm²	173µm²
Previous	215µm²	215µm²	173µm²
Time	15h57	16h57	18h02
Previous	13h57	15h57	15h57

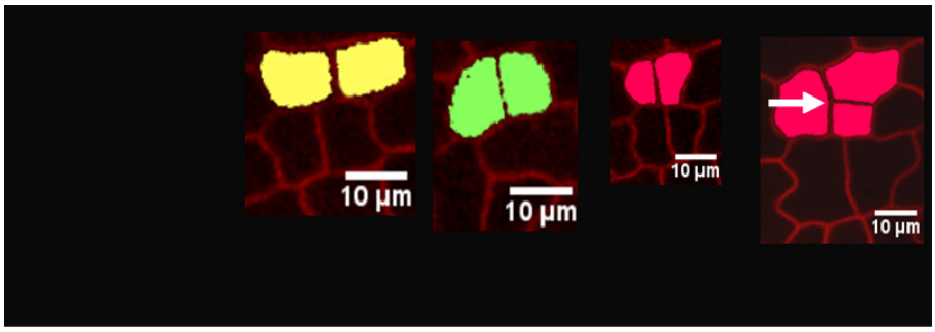

Area	196µm²	163µm²	156µm²	251µm²
Previous	188µm²	157µm²	144µm²	239µm²
Time	1h59	7h57	12h57	42h33
Previous	00h00	6h57	11h57	41h16
Interval			29h19	

Figure 3. 17 The area and times of divisions in the speechless cells. Row 1) the area of the cell in the first image after it has divided. Row 2) the last area observed prior to division. Row 3) The times these observations were made in hours and minutes from the start of the experiment. Row 4) The time the cell was last imaged. Row 5) The time interval shows the time since that cell last divided, as only one cell divided twice only this cell has an interval. It is calculated from the average time of the two times shown.

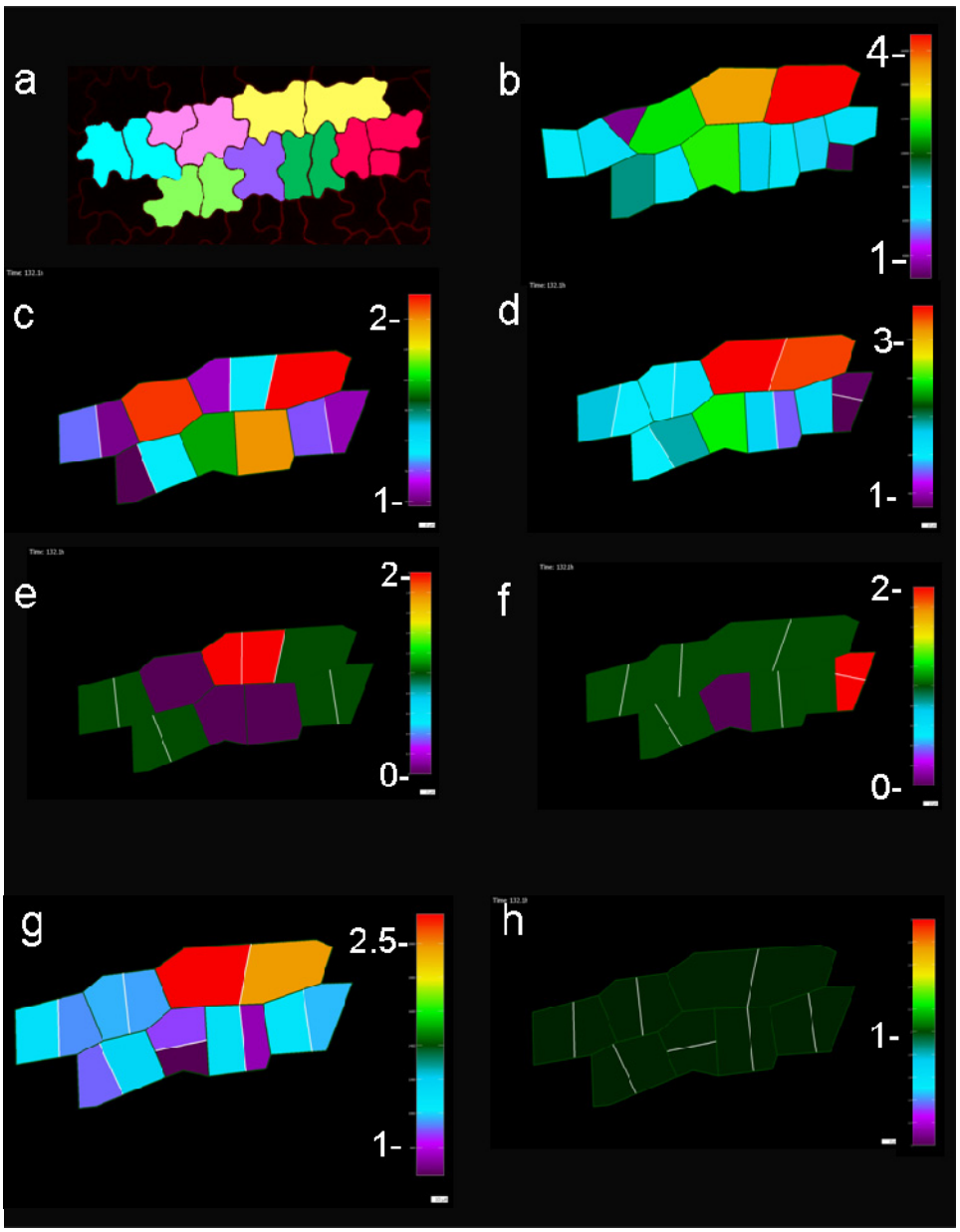

Figure 3. 18 Comparing the constant area threshold and constant cell cycle duration model to the observed *spch* cells. a) the observed clones. b) the area of the cell as they divided in the observed leaf. The scale indicates the range of areas seen. Here the range of areas is 4 fold. (c-h) all models use the shortest wall algorithm to divide the cell at different times. the final area of the cells produced with c) the constant area threshold model, d) the observed division time, and g) constant cell cycle duration model. the frequency of cell divisions with e) the constant area model, f) the observed division timing and h) the constant cell cycle duration.

Cell division timing in a large patch of speechless cells

Cell division timing varies across the leaf

As the clones in the fate map were generated virtually we can be certain that they were all derived from a single cell. By counting the number of cells in the clones I determined the number of rounds of division the cells went through in different parts of the leaf (Figure 3.19). Clones at the tip of the leaf contain only one cell so we know that they did not divide. In comparison clones in the petiole and blade region are made up of many cells. Thus, distal cells did not undergo divisions, while those in more proximal regions underwent 1-3 rounds of division. We also noticed that cells in the mid-vein divided less than cells in the blade region, suggesting a second axis of variation. We can quantify this further by counting the number of rounds of division each cell has gone through. Figure 3.20 shows the number of times each cell divided across the large speechless patch, on a cell by cell basis. This shows a similar distribution to the fate map but with finer detail as it shows division frequency per cell rather than rounds of division for each clone. Cells closest to the base divided more times.

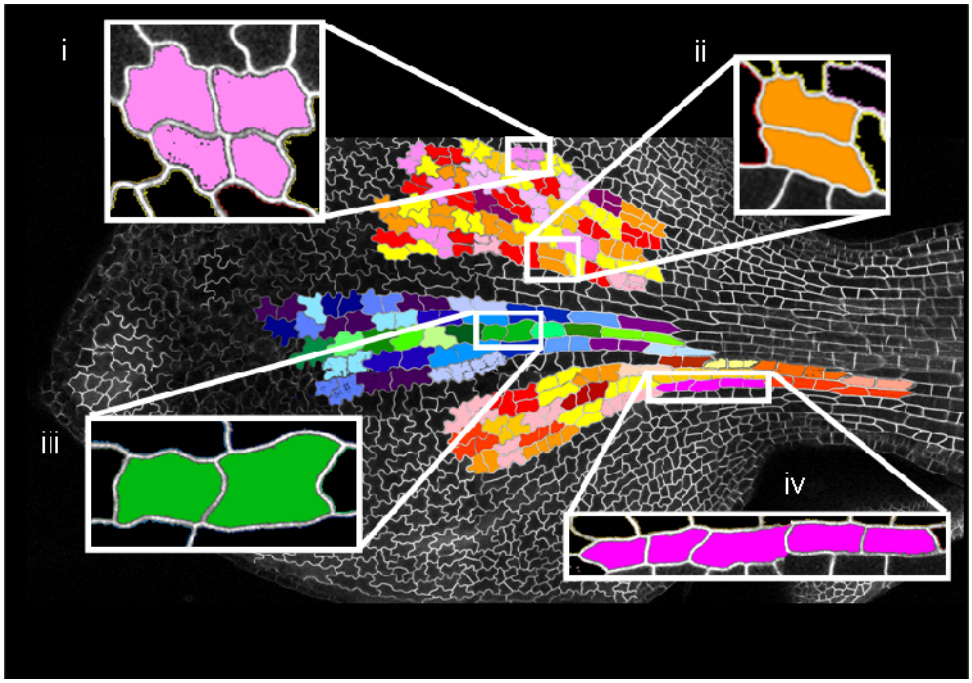

Figure 3. 19 Using the virtual clones to consider division frequency across the leaf. Tracking the division of single cells allows us to generate virtual clones. All cells coloured the same colour came from the same cell. Counting the number of cells in the clones tells us how many rounds of division they went through. i shows a clone that went through 2 rounds of division, ii and iii went through one, and iv went through 3.

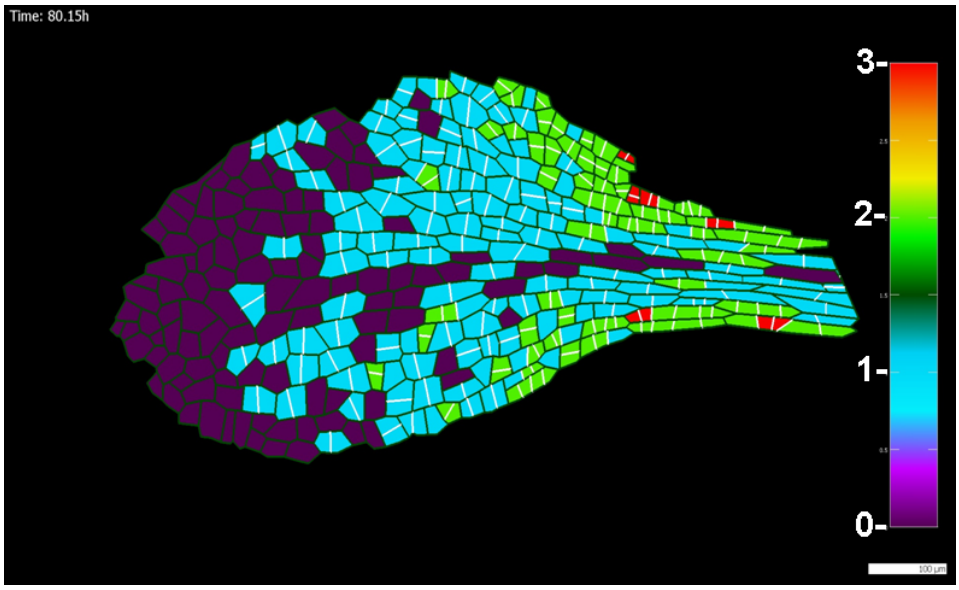

Figure 3. 20 The number of times each cell in the tracked *spch* patch divided as a heat map. During the 82 hours of observation cells marked in red cells divided 3 times, green cells divided twice, blue cells divided once and purple cells did not divide at all. Note: these are the number of times the cells divided not the number of rounds of division the clone underwent as shown in the previous figure.

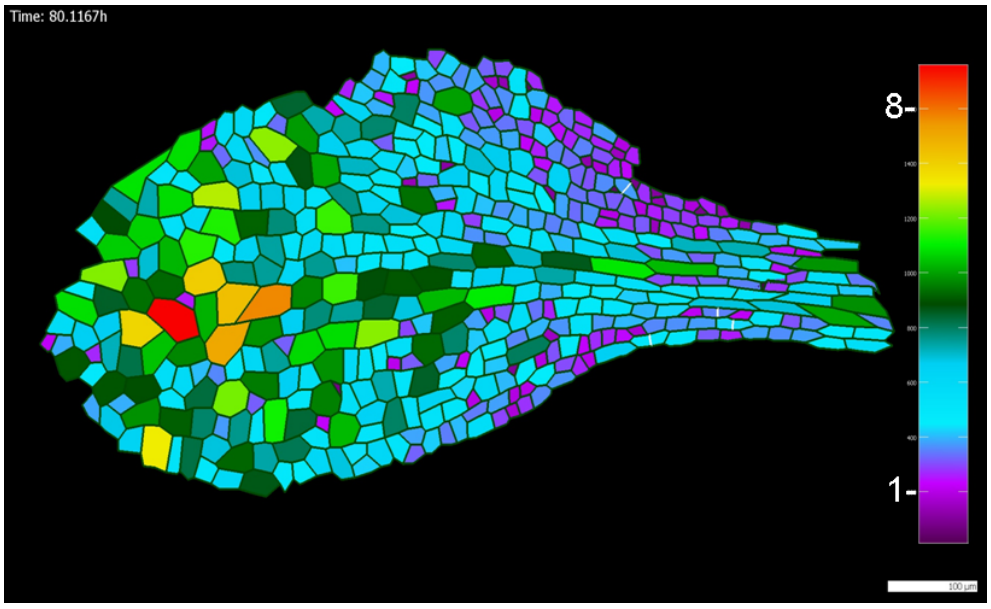

Figure 3. 21 The final area of each cell as a heat map. There is an 8 fold range of areas across the tracked speechless patch. Red cells are 8 times larger than purple cells. The cells in the tip and mid-vein region are larger than cells at the base of the leaf blade.

This indicates that the frequency of divisions a cell under goes might correlate with its position on the leaf. In the small patch the cells had similar division areas and frequencies because they were all from the same part of the leaf.

Division area correlates with distance from mid-vein

In addition to the variation in the number of cell divisions across the leaf there is also variation in area of the cells. There is an 8 fold difference in the area of the smallest and the largest cells in the final image of the large mutant patch (Figure 3.21). The cells in the blade region are much smaller than the cells in the mid-vein and tip regions. This makes a constant area of division unlikely. To investigate this I coloured cells based on the area at which they first divided (Figure 3.22). This plot revealed that the majority of cells divided with a four fold range in division area; cells in the mid-vein divided at up to 400 μm^2 while cells at the edge of the patch divided at less than 100 μm^2. (Two cells divided at even larger sizes) Therefore, cells are not all dividing at the same area threshold. This plot shows only the first division of each cell. To show all of the divisions I used a graph rather than a spatial plot. I identified cells at each end of the mid-vein and used their centres to define a line that represents the mid-vein. I then measured the shortest distance from this line to the centre of the cells at the time of division. I also measured the cells area at the time of division. At all time-points the further cells were from the mid-vein the smaller they were when they divide (Figure 3.23a). Scaling all the leaves to the same patch width shows there is a linear gradient in the area at which cells divide (Figure 3.23b) and the relationship is symmetric around the mid-vein. If the absolute distance from the mid-vein is used so cells from both sides of the mid-vein are compared together the symmetry around the mid-vein is confirmed (Figure 3.23c-d). There is a clear correlation between the distance from the mid-vein and the area at which cells divide. The trend is visible in both the scaled and the un-scaled data set, however, the trend is stronger for the scaled data (r value of -0.55 compared to -0.36).

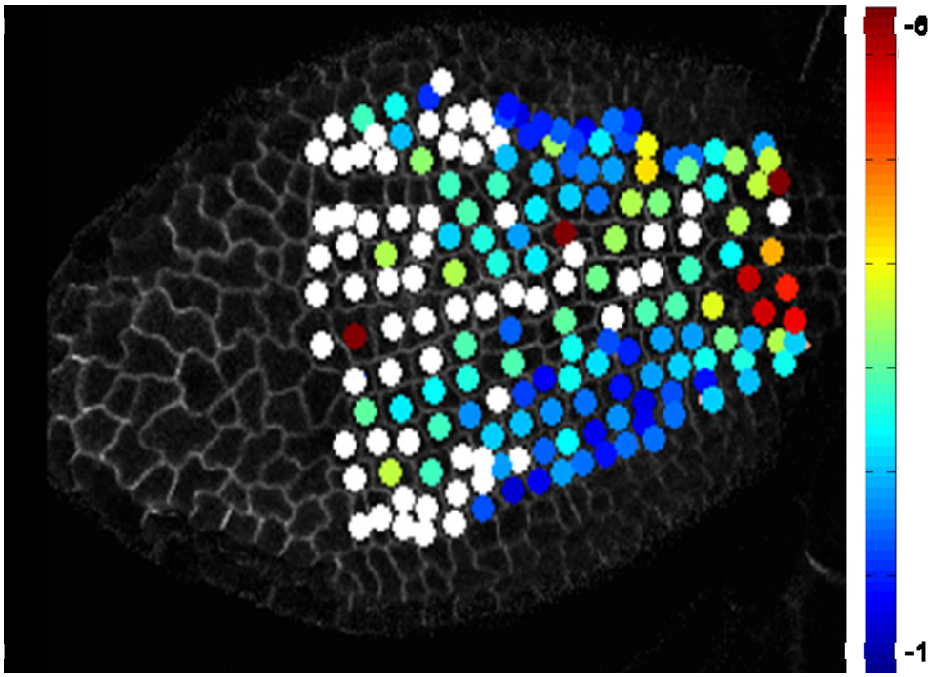

Figure 3. 22 The area each cell was when it first divided. White cells did not divide during the 82hours of tracking. Red cells divide at an area 6 times larger than the blue cells.

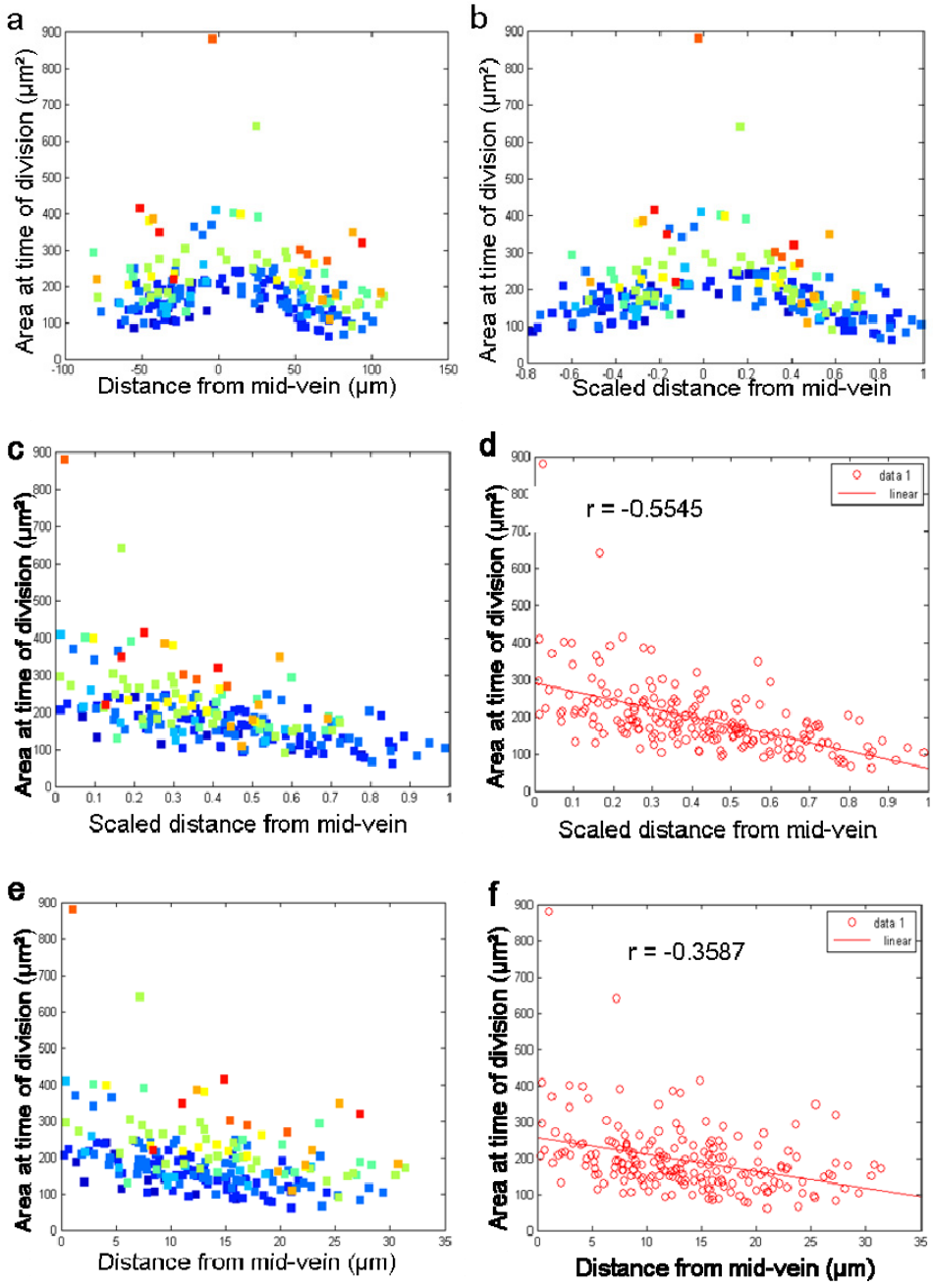

Figure 3. 23 The distribution of cell division areas in the patch of tracked *spch* cells. The area of each cell at the time of division against the distance from the mid-vein (a) Successive time-points are shown as a heat map. The blue points are from cells in the first time-point and red the last. (b) all leaves are scaled to the width of the patch at this time point. c and e are the same plots as b and a but the mid-vein is the origin. (d and f show the same data as c and e but all the time points are combined and a there is a trend line. The r value is the output of the correlation coefficient which gives a value from -1 to 1. The time of the images are 0.00, 6.95, 14.90, 16.94, 33.26, 41.26, 45.54, 53.96, 62.96, 72.11, 80.08.

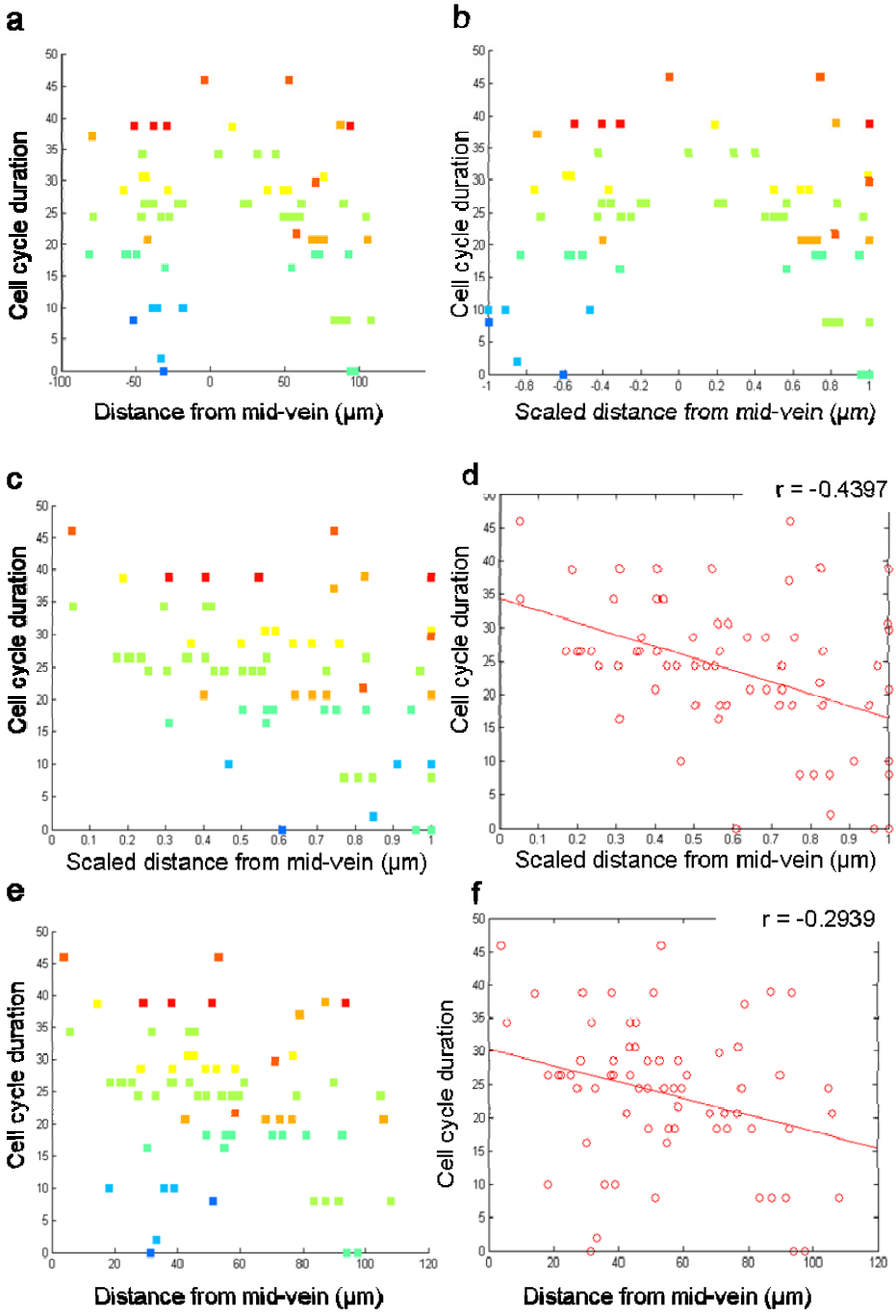

Figure 3. 24 The distribution of cell cycle durations in the patch of tracked speechless cells. The cell cycle duration against the distance from the mid-vein. (a). Successive time-points are shown as a heat map. The blue points are from cells in the first time-point and red the last. (b) all leaves are scaled to the width of the patch at this time point. c and e are the same plots as b and a but the mid-vein is the origin. (d and f show the same data as c and e but all the time points are combined and there is a trend line. The r value is the output of the correlation coefficient which gives a value from -1 to 1.

Cell cycle duration correlates with distance from mid-vein

The variation in cell division frequency across the large mutant patch suggests a spatial correlation with cell cycle duration. The cell cycle duration was plotted against distance from the mid-vein. As the cell cycle duration is the time between a cell being created and it dividing again it can only be calculated for cells that divide twice during the experiment. There is a weak correlation between the distance from the mid-vein and the cell cycle duration (Figure 3.24a). The distribution does not look symmetric and if the mid-vein is positioned at the origin (e-f) there is only a weak correlation (r value of -0.29). Scaling the width of the patch of cells so that it does not change with time improved the correlation (b). The scaled distribution looks symmetric and has a better correlation (c-d) (r value of -0.44). Compared to the cell area plot there are far fewer data points so it is more difficult to reach conclusions. There is a correlation between distance from the mid-vein and cell cycle duration although it seems to be weaker than for the area threshold. There is also a correlation between area threshold and cell cycle duration (Figure 3.25). This makes it more difficult to determine whether one phenomenon is a consequence of the other.

Cell division timing changes with time

In the small speechless mutant patch the area of the cells increased with time. In the large mutant patch this is also true (Figure 3.26), the average cell area increased with time as did the average area of dividing cells. The line representing dividing cells (blue) cross the line representing all cells (red), suggesting that some cells have stopped dividing but are still growing. This is consistent with the findings from the small patch that some cells are larger than the division areas of the other cells. Cells can become larger than the area at which other cells divided but not divide if the area threshold for division increased above their size before they reached it and/or if cells stop dividing before they stop growing. If cells are dividing at a constant area the average area of dividing cells would not increase and cells would divide at twice the size they were created.

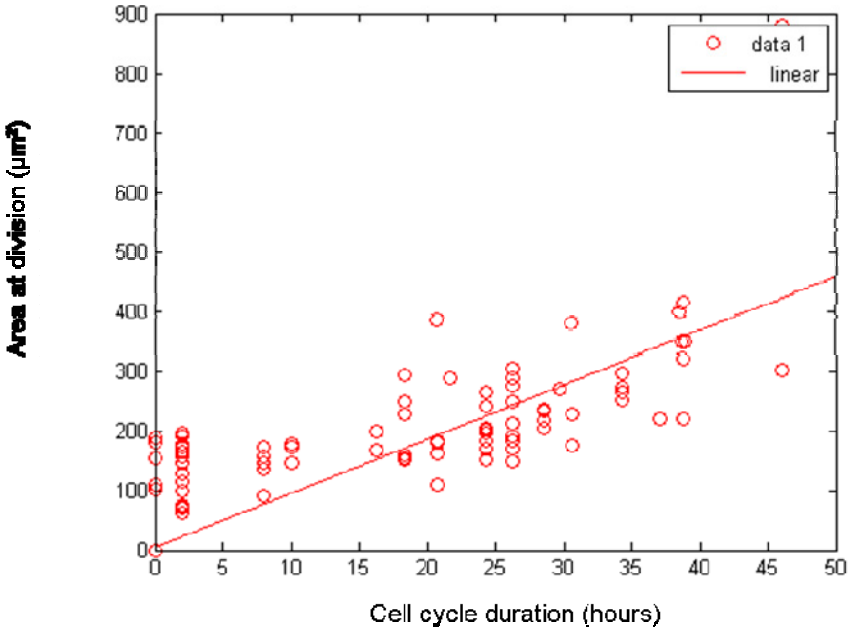

Figure 3. 25 The distribution of cell cycle durations in the patch of tracked speechless cells.. There is a positive correlation between the cell cycle duration of a cell and its area at the time of division**.** A linear trend line was fitted to the data. It has an r value of 0.9003.

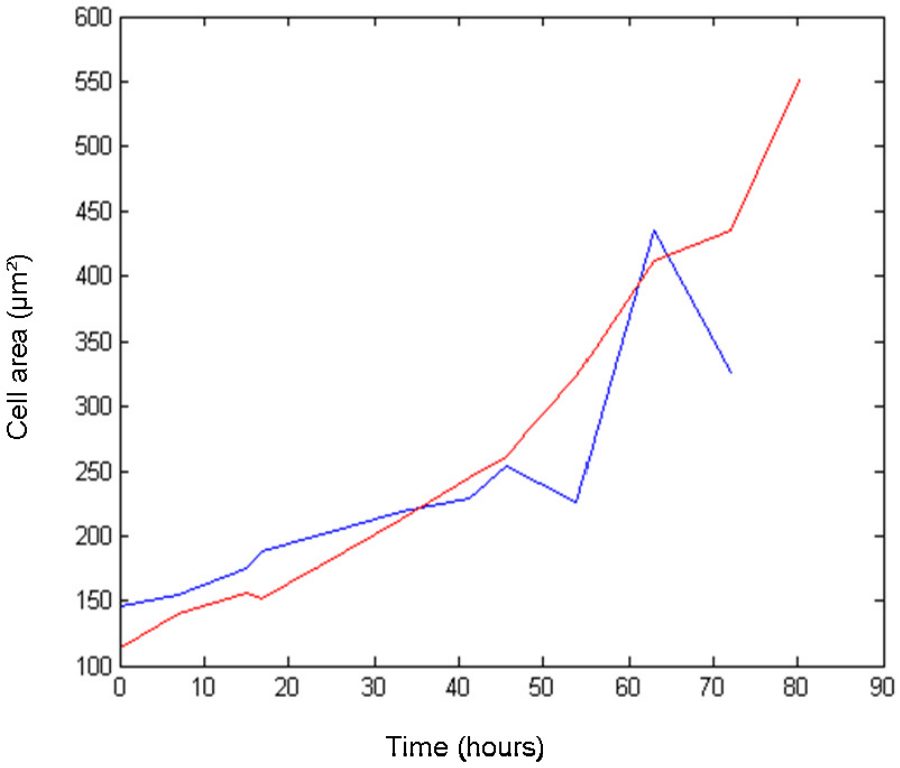

Figure 3. 26 The area of dividing and non-dividing cells changes with time. The average area of cells in the large *spch* patch (red) increases with time. The average area at which cells divide also increases (blue).

We can test this theory by comparing the area of cells when they are created to the area of cells when they divide (Figure 3.27a). The average cell divides at twice the size it is created. However, the average is not representative and most cells lie above or below this line. If we consider how the ratio of birth to division size changes with time we see there is an increasing trend (Figure 3.27b). Initially cells divide at less than twice their birth size, after 30-40 hours many cells are dividing at more than twice their original size. This explains the increase in size seen in Figure 3.27. In the beginning the cells are dividing at less than twice their size. However, the area of cells in Figure 3.26 is not decreasing. This is because all dividing areas can be included in Figure 3.26 however, in Figure 3.27 only cells that divide twice can be used; most divisions in the beginning of the data set are of cells that we did not see created. Generally the area of cells dividing and not dividing increases with time suggesting there is not a constant area threshold in time or space.

I also investigated whether cell cycle duration was constant in time (Figure 3.28). The length of the cell cycle duration appears to increases with time. This again matches what was seen for the area threshold and reinforces that the two are correlated. The data could be biased as the longer the experiment goes on the more chance there is of detecting a division of a cell with a long cell cycle duration. For example only after 70 hours is it possible to detect the presence of a cell with a cell cycle duration of more than 60 hours. However, this bias can not explain the absence of cells with short cell cycles being detected late in the experiment. There are fewer points available for plot considering cell cycle duration very few cells divide twice, so we should be careful not to draw too many conclusions, but it seems that the cell cycle like the area threshold also varies in time and space. This is consistent with the two features being correlated.

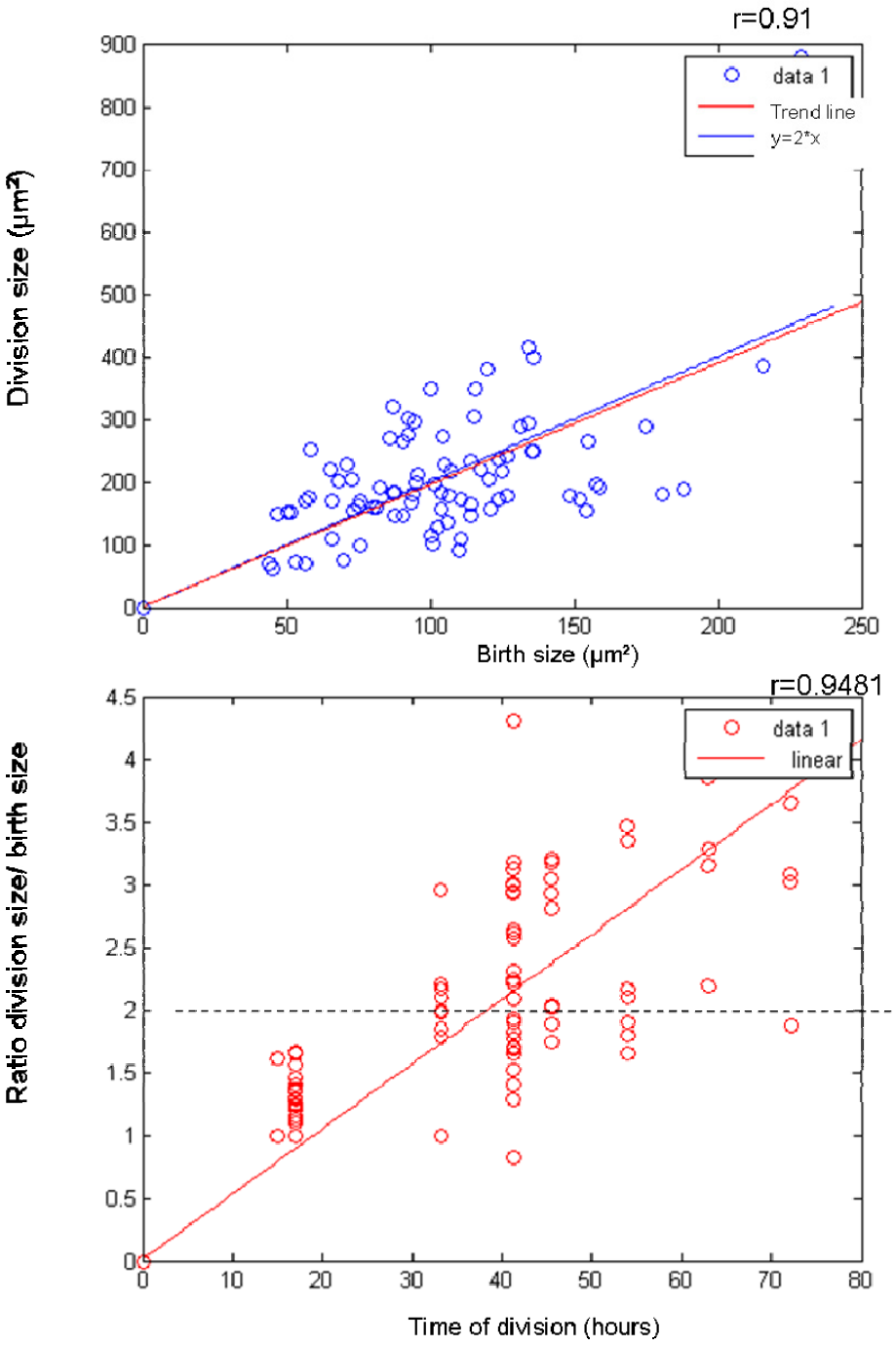

Figure 3. 27 How does division area relate to birth area? (a) Comparing the birth area to the division area of cells. The trend line lies on top of the y=2*x line showing that the average cells divide at twice their birth size. (b) Comparing the ratio of a cells division size to birth size against the time of division. This ratio increases with time. The black line shows the ratio of 2 where cells divide at twice their birth size. Initially cells are dividing at a size below this ratio then after about 40 hours they divide at a ratio above this line.

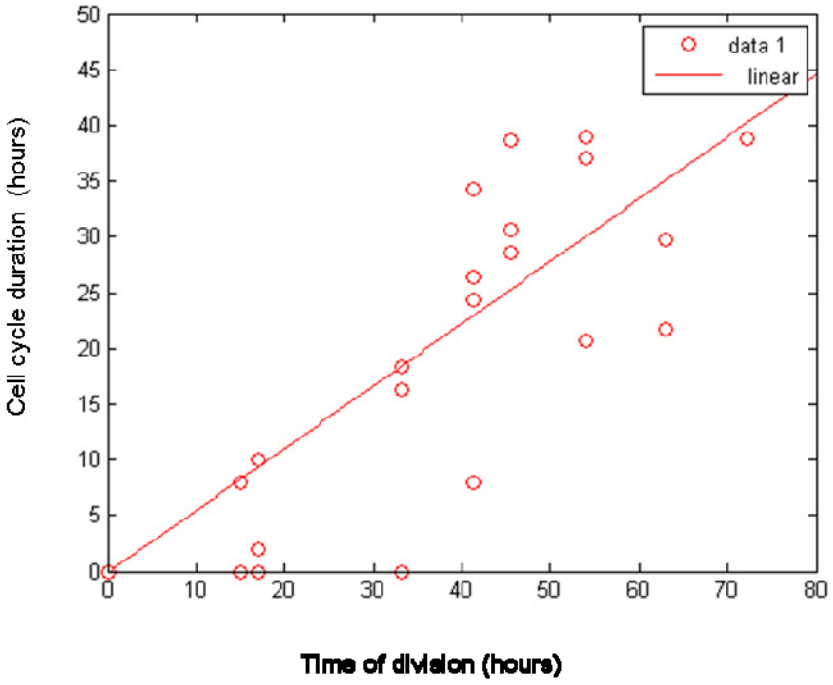

Figure 3. 28 The cell cycle duration of cells increases with time. Cell Cycle duration is plotted against the time at which the cell divided. Only cells that divide twice can be included as their cell cycle duration is know. There is a positive correlation with an r value of 0.95

3.2.3 Cell division arrest

As well as a gradient in division frequency from the mid-vein to the blade there is a gradient from the tip to base of the leaf. The tip to base gradient is consistent with published data on an arrest wave coming from the tip (Donnelly et al., 1999). I therefore evaluated the percentage of cells that had arrested at different distances along the leaf at different time points. From my experiment I do not know exactly when the cells arrest. However, I do know whether they divide again during the experiment, so I used this as an estimate of cell arrest. I estimated the lamina/petiole boundary by defining the cell that I thought was at the base of the mid-vein. This ensures all measurements were made relative to the exact same cell. I measured cells distances from this base cell by projecting their position onto the mid-vein and measuring the distance along it. I then plotted, for each time point, the percentage of cells that will not divide again against this distance. I noticed that if I scaled the leaves so they all had the same length for the defined region it looked as though an arrest wave was moving from the tip of the leaf (Figure 3.29). The percentage of arrested cells is high in the tip of the young leaves and low at the base. As the leaf aged more cells closer to the base arrested. Interestingly there is also a small secondary wave visible coming from the base of the leaf as a higher percentage of cells at the very base are arrested then a little further from the base, shown by a slight upturn in the graph after the 5^{th} time-point. This may suggest a mechanism to arrest cells at the base. My data is not suitable for studying the arrest of the base of the leaf as I do not know whether these cells go onto divide again after I stopped imaging. My analysis artificially arrests the base because I associate cells not dividing again in my experiment to being arrested which is not true. However despite this limitation I can see trends in division patterns that are consistent with other published data (Donnelly et al., 1999; Kazama et al., 2010).

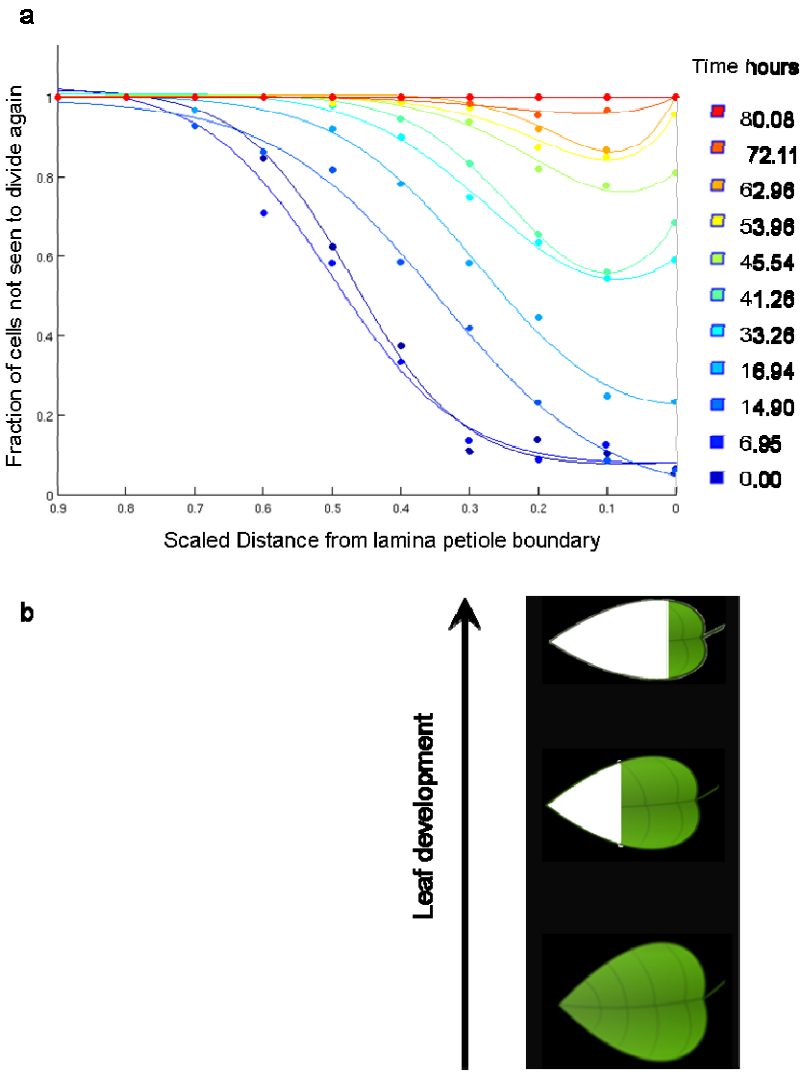

Figure 3. 29 Considering cell arrest along the tracked *spch* patch. (a) The patch of cells in each image was scaled to the same length. The percentage of cells at each distance along the scaled patch that did not divide again was calculated. The first time-step data is shown in blue and the last in red, the time in hours is shown next to the graph. The percentage of cells that did not divide again is plotted against the distance along the leaf. The data is shown as points. The lines show the fitted curve. The fitting was done using a logistic and exponential component (for details see methods). The fitted curves emphasise the shape. (b) a diagram representation of the data. The arrest curve moves along the scaled leaves from the tip to the base.

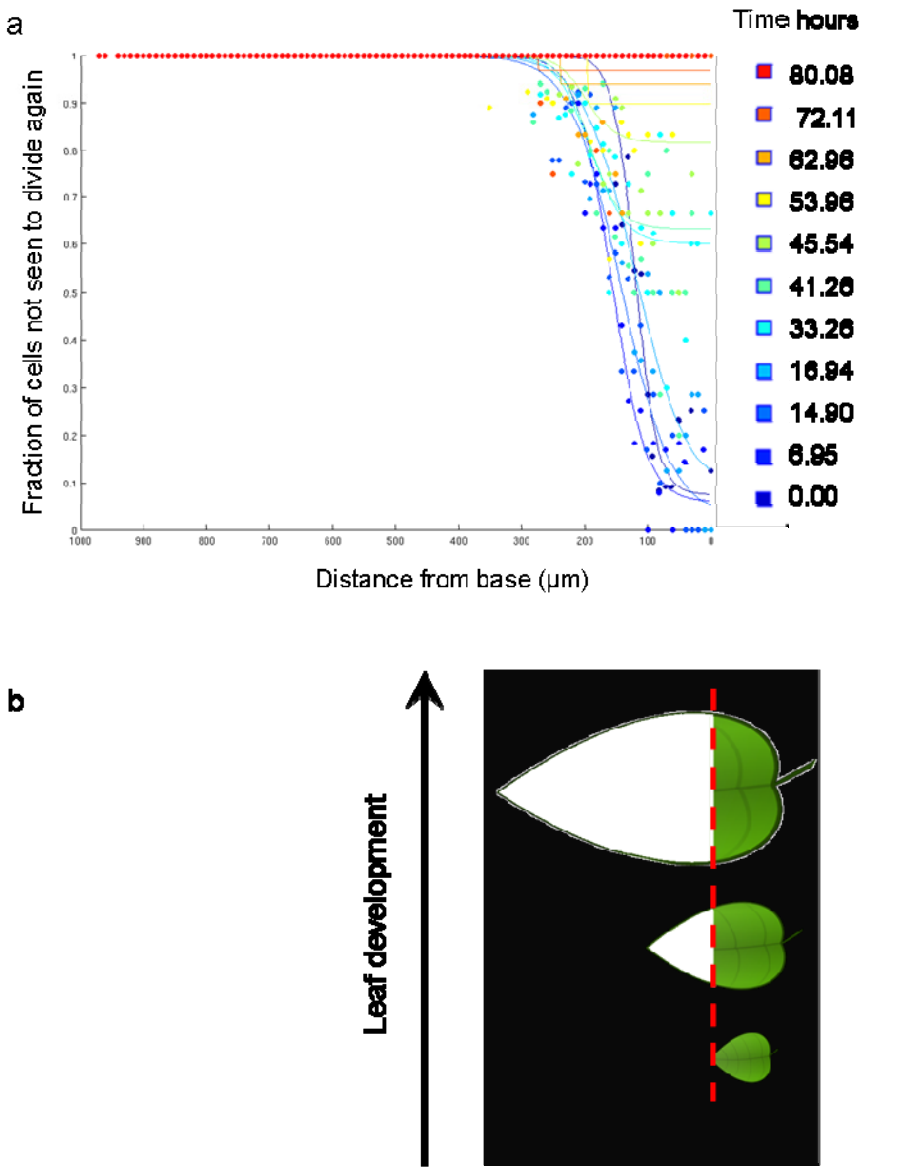

Figure 3. 30 Considering arrest of cell division along the tracked *spch* patch. This figure is like the previous one but the leaves have not been scaled. The leaves were aligned at the laminar/petiole boundary. (a) The percentage of cells at each distance along the patch that did not divide again was calculated. The first time-step data is shown in blue and the last in red, the time in hours is shown next to the graph. The percentage of cells that did not divide again is plotted against the distance along the leaf. The data is shown as points. The lines show the fitted curve. The fitting was done using a logistic. The fitted curves emphasise the shape and the sharp slope of the curve. (b) a diagram representation of the data. There is a defined distance at the base of the leaf where cells divide.

The most interesting result came from aligning the leaves at their base without scaling them. I used the cell that I defined as the lamina/petiole boundary to align them as this is more reliable than using the petiole. Figure 3.30 shows that aligning the leaves in this way results in the distance at which the cells arrest being fixed at about 100- 200 μm from the base of the leaf. Therefore, young leaves are not arrested as their length is less than 200 μm. As they grow distal cells approach the arrest distance and progressively more of the leaf is arrested (b). However, the same distance of cell at the base remains actively dividing. This again raises the question of what eventually arrests the final part of the leaf. These finding are supported by recently published results (Kazama et al., 2010).

In summary the cells in the leaf divided in a way that depends upon their position in the leaf and changes with time.

3.2.4 Modelling cell division timing – a two gradient model

The tracking data of the large patch of speechless cells showed that cells do not all divide at the same area or with the same cell cycle duration. If we model either of the rules (Figure 3.31 b-c) we can see that compared to the observed cells (a) there is little similarity. I tested the models by looking at the distribution of cell areas at the end of the model. Neither of the models was able to generate the large range of cell areas seen in the observed patch or give the right distribution of cell area.

The data showed that there are two axes of variation. A mediolateral gradient in both division area and cell cycle duration, and a 200 μm^2 region in which cells are competent to divide. I therefore built a two gradient model to describe this phenomenon.

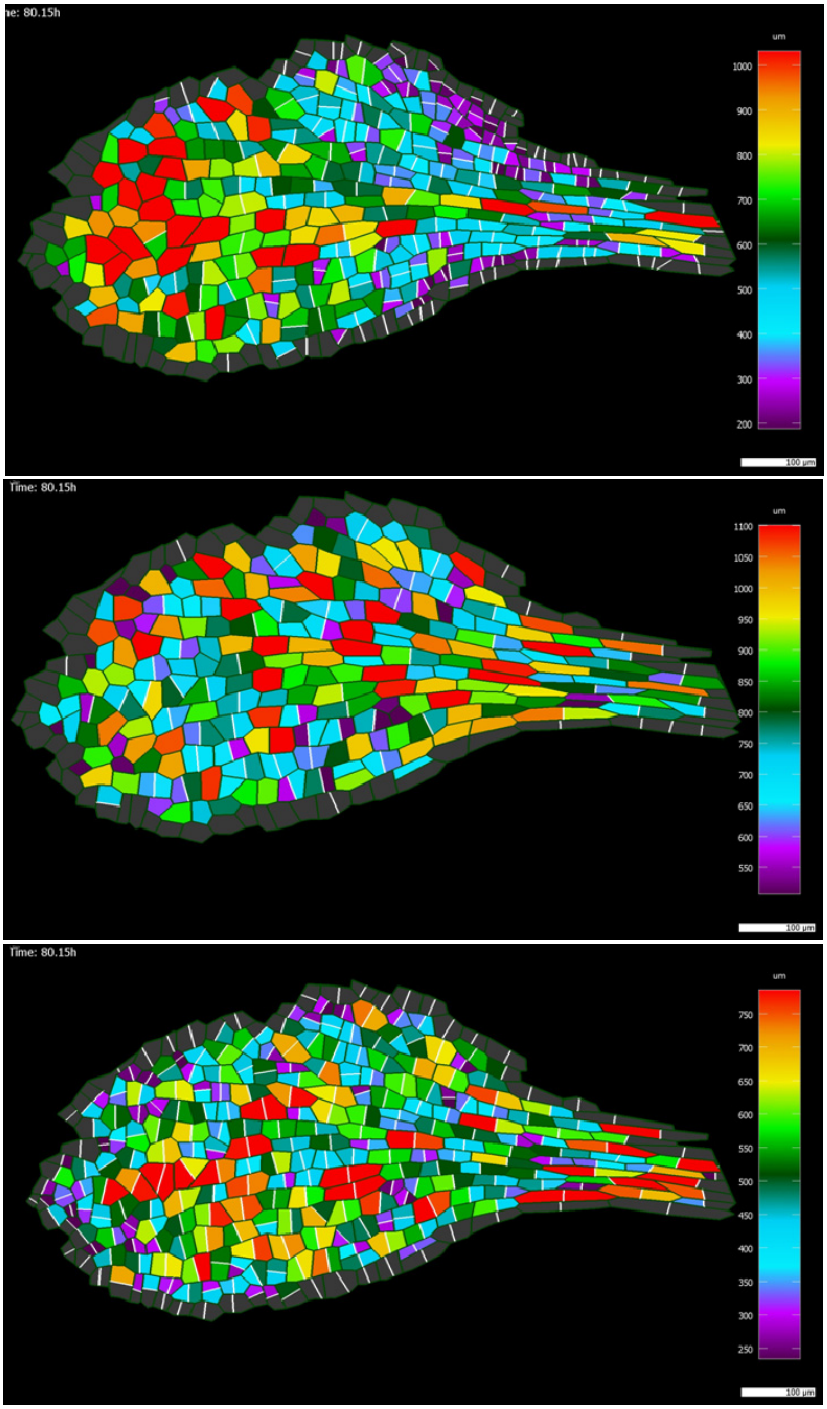

Figure 3. 31 Comparing division timing models to the observed cells. The output of division timing models can be compared by looking at the distribution of cell areas in the final image. The comparison is made to the division the cells using the shortest wall algorithm at the observed timing of division (a) which shows a five fold range in final cell area. The distribution of final cell areas in the constant area threshold model (b) shows a two fold range while the output of the constant cell cycle duration model shows a three fold range in cell area.

Modelling the mediolateral gradient in cell division area

First I will address the observed mediolateral gradient. The data showed that both cell division area and cell cycle duration correlated with distance from the mid-vein, however, as they are also correlated, I chose to use only one to drive cell division in my model. As the strongest correlation was between cell division area and distance from the mid-vein I chose to use my model to recreate this. The correlation showed a linear distribution with cells at the mid-vein dividing at four times the size of the cells at the edge of the patch. I therefore proposed that the mid-vein might produce an inhibitor (h) of cell division that acts by increasing the area cells must reach to divide. I allowed h to diffuse from the mid-vein to influence the division area of the surrounding tissue. In order to re-create the linear decline in cell division area I wanted to establish a linear gradient of h from the mid-vein to the edge of the patch. I therefore made the cells at the edge of the patch sinks for h. As sink cells they had their level of h fixed at a level 4 times lower than the level in the mid-vein. As the patch of cells grows the profile of h remains linear.

Figure 3.32 shows the concentration of h across the patch. My model has discrete cells so the concentration of each cell is calculated at each time step based on the concentration of the neighbours and the diffusion coefficient. The model therefore has a system of ordinary differential equations. I found that solving these equations using the forward Euler method did not reach chemical equilibrium quickly, therefore, I solved using the Adaptive Crank Nicholson method (Flannery 1992). The model is initialised by setting the value of the mid-vein cells to the level of production (4) and all other cells to half this, this ensures the system reaches equilibrium quickly enough to avoid artefacts. The level of h in the edge cells is set to 1 to ensure a 4 fold difference. I assume that growth and diffusion do not occur on the same time-scale. I therefore, allow the chemicals to reach equilibrium before the tissue grows again. This is achieved by updating the concentrations in a loop until the change in concentration is low (less than 4.10^{-8}).

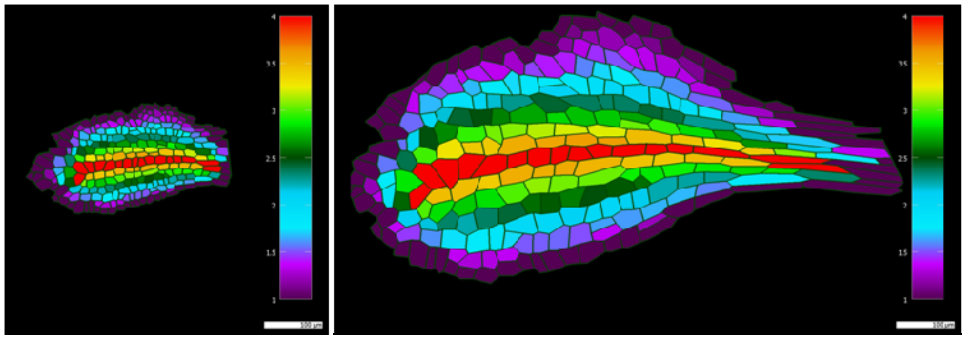

Figure 3. 32 The distribution of cell division inhibitor used in the mediolateral gradient model. Inhibitor of cell division is produced from the mid-vein and has a sink at the cell edges to generate a linear gradient. The source in the mid-vein (red) has a level of 4 while the edge cells are a sink and have a concentration of 1. This level is maintained throughout the model from when the gradient is first established (a) until the final time step (b). The diffusion rate is 0.1, there is no decay, dt is 0.1 and equilibrium is reached before each new growth step.

I use h to regulate the size of cell division by multiplying the area threshold by the concentration of h that each cell has. In this model the basic area threshold for cell division (b) is set equivalent to 252.3µm² (this precision is not necessary but parameters were optimised in pixels). The area threshold of any one cells (A_t) is therefore equal to b*h. If the cells area is larger than A_t then it divides. Cells near the mid-vein therefore divide at a larger area threshold than the cells at the edge. I incorporate the temporal changes in area threshold in to the model by increasing A_t with time by multiplying it by (1+ 0.006dt) where dt is the time interval of the model.

I assessed the mediolateral gradient model by looking at the final area of the cells created. The output of this model is able to capture the mediolateral gradient in cell area (Figure 3.33c). The distribution of cell areas is comparable to the observed cells (Figure 3.33a) and the output of the model which divides the cells at the observed timing of division (Figure 3.33b). Both models use the shortest wall algorithm. I also evaluated the model by comparing the distribution in the frequency of cell divisions (Figure 3.34). Again there is a good match in the mediolateral distribution. However, the difference in the proximal distal distribution is highlighted.

Modelling proximodistal arrest of cell division

The data showed that only cells in the proximal 200 µm² of the leaf lamina are competent to divide. The percentage of arrested cells increased with a very steep slope at this distance from the petiole/lamina boundary. To capture this I used an exponential profile in a factor that promotes division competence. An exponential profile can be generated if the substance produced by the source, diffuses and decays proportional to its concentration. A sink is not necessary. I produced substance r, which promotes competence to divide, in the proximal cells. To simulate production at the base I defined the cells at the base of my patch as producers of substance r.

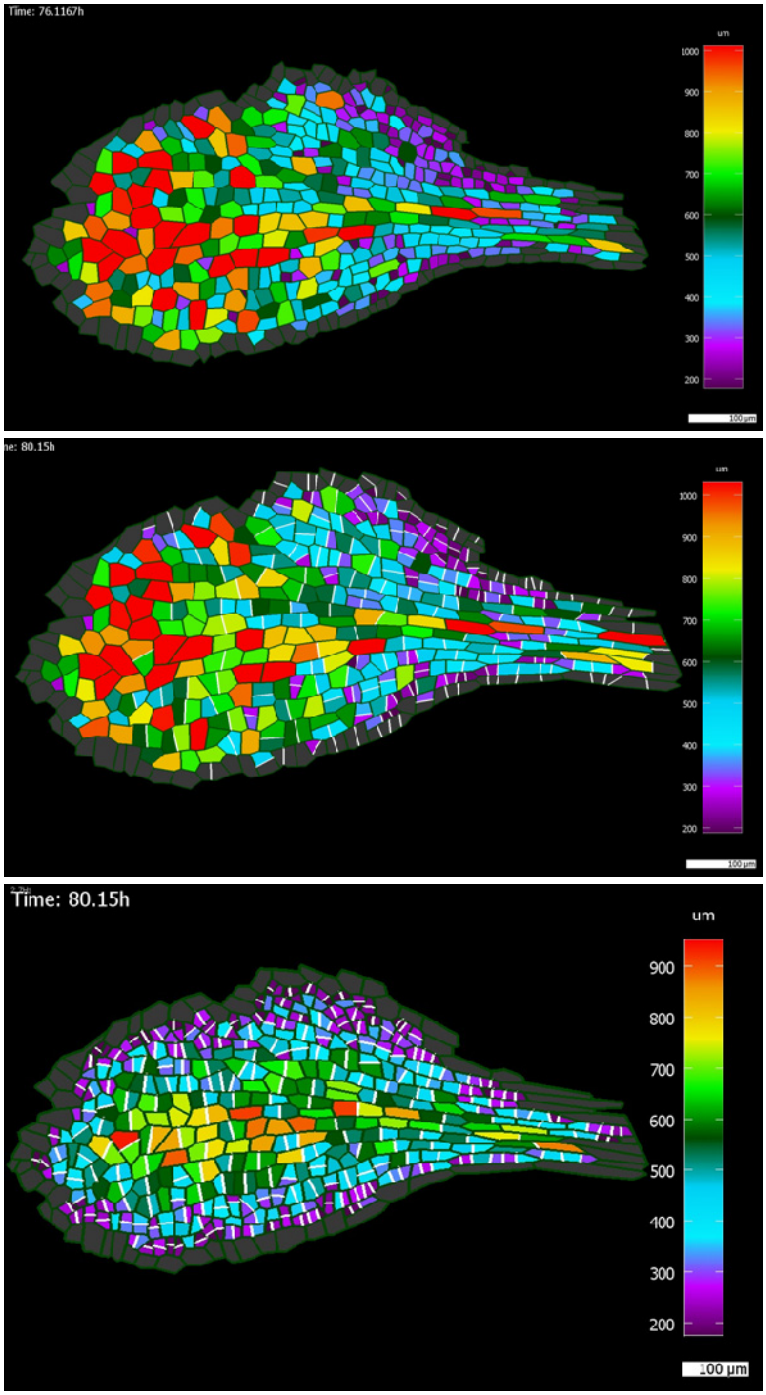

Figure 3. 33 Comparing the mediolateral gradient model to the observed cells. Dividing cells using the mediolateral gradient model generates a range of cell areas across the leaf. The distribution of final cell areas in the model output (c) can be compared to the areas of the digitised cells (a) and the areas of the cell if they are divided at the observed time using the shortest wall rule (b). The parameters are the same as in the previous figure.

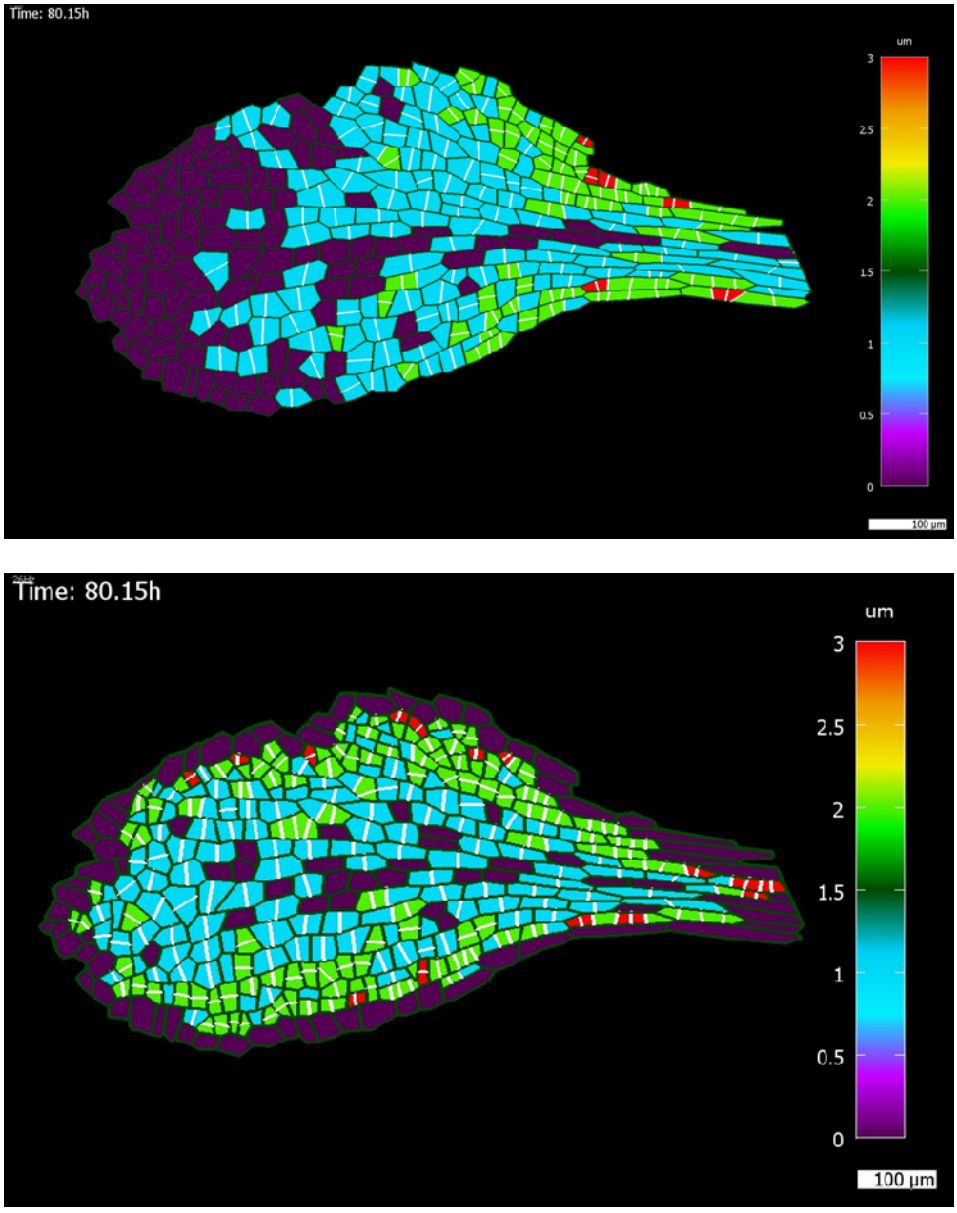

Figure 3. 34 Comparing the mediolateral gradient model to the observed cells. Dividing cells using the mediolateral gradient model generates a range of frequencies of cell division across the leaf. The distribution of cell division frequencies in the model output (b) can be compared to the frequency of divisions of the cells if they are divided at the observed time using the shortest wall rule (a). The parameters are the same as in the previous figure.

They have a constant level of r (200). The arrest substance should have been produced at the mediolateral boundary in line with the data but it is actually produced at the base of the patch a little closer to the petiole as this is easier to define. Substance r diffuses with a rate of (3) and decays with a rate of (0.025) generating an exponential profile along the leaf. As with the linear diffusion the system reaches equilibrium between growth steps. I added this gradient to the mediolateral gradient to create the two-gradient model (Figure 3.35). When cells have a concentration of r that is less than a threshold (0.06) the cells are prevented from dividing. Once cells have been arrested they can not divide again no matter what concentrations they have of the two substances. When the leaf grows the profile does not change. The distance from the base at which cells arrest remains fixed and never reaches the base of the leaf. Changing the parameters changes the number of cell divisions that the leaf can under go. Figure 3.36 shows the cells that are arrested at different times in the model.

Comparing the output of the two-gradient model allows a much better approximation of the final distribution of cell areas (Figure 3.37). There are almost no differences between the model using the observed timings (a) and the two-gradient model (b). In both models cells are dividing using the shortest wall algorithm. The two-gradient model can also be assessed in terms of the distribution of cell division frequency (Figure 3.38). Again the two-gradient model does a good job of matching the observed divisions. The model does not provide a biological mechanism; more work must be done to identify components. The two-gradient model also does not consider the arrest of the base cells; this requires future work and more data so that we can be confident the cells will never divide again. However, the model does show that the timing of divisions in the leaf can be better understood in terms of two gradients rather than a constant area or cell cycle duration.

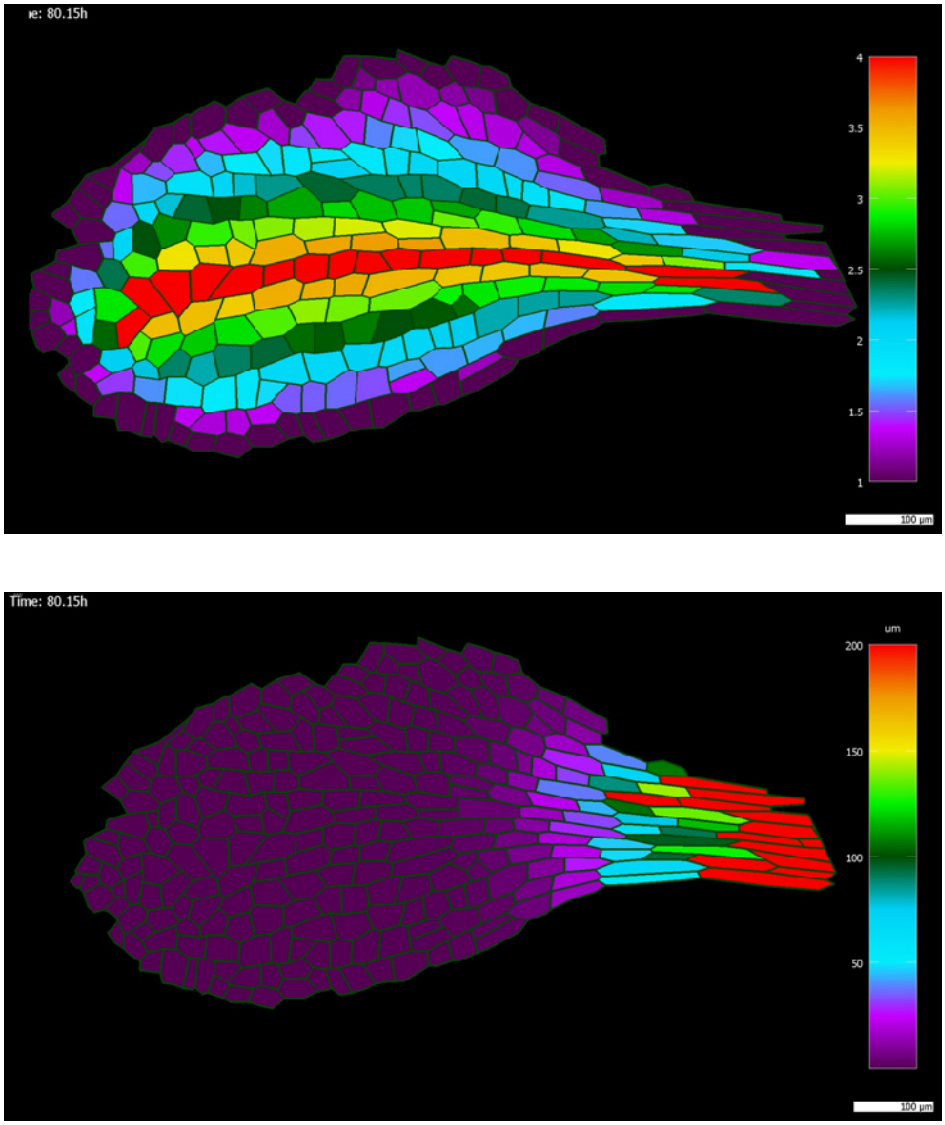

Figure 3. 35 The two gradients of the two gradient model. The two gradient model has a mediolateral gradient which controls cell division size as used in the previous images and a proximat distal gradient that controls cell arrest. The first gradient is linear and has the same parameters as the mediolateral model. The second gradient has an exponential profile. The base cells shown in red are the produces they have a fixed level of 200. The diffusion rate is 3 and the decay rate is 0.025 and the arrest threshold is 0.06. Chemical equilibrium is reached before each growth step.

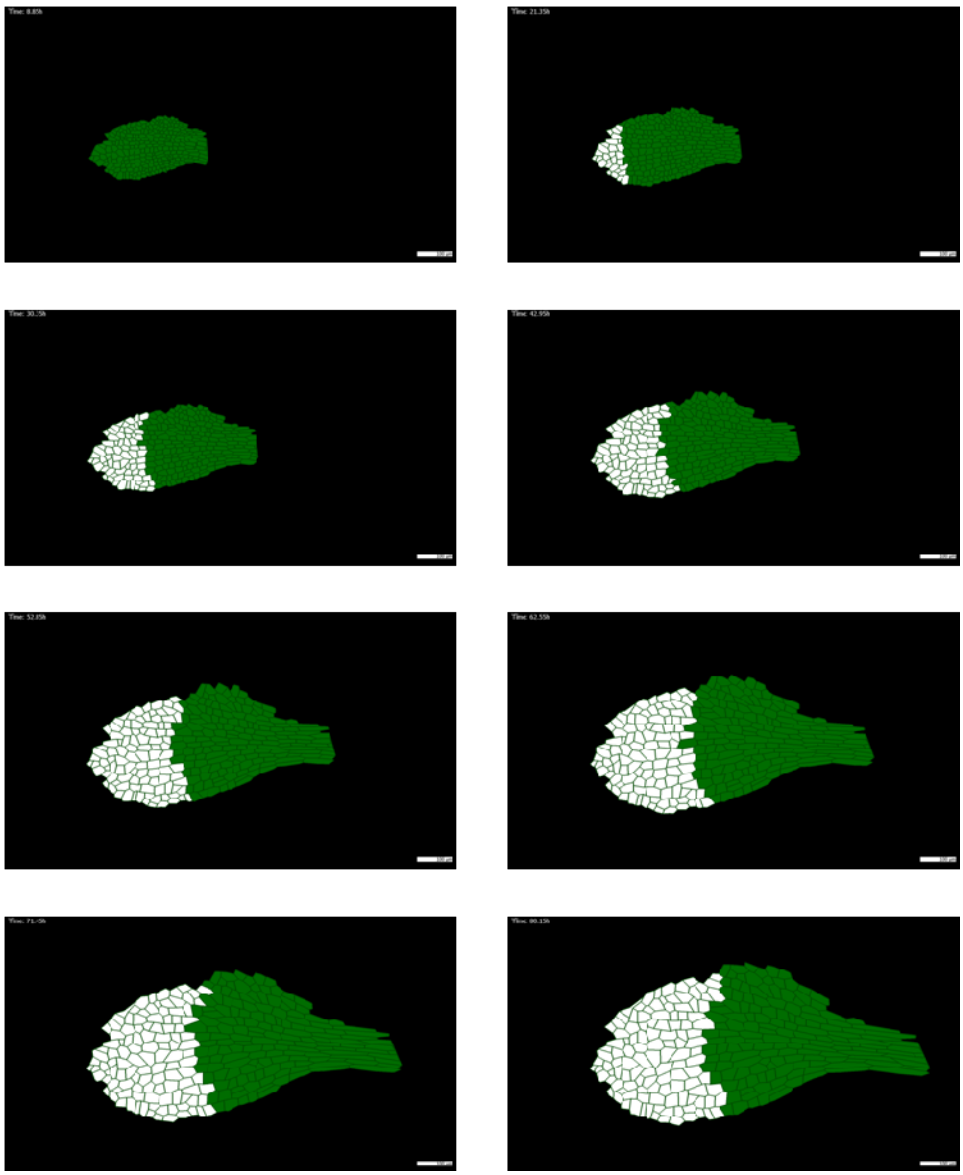

Figure 3. 36 The arrest of the leaf. The proximal distal gradient arrests cells that have less than the threshold amount (0.06) of division promoter. The arrested cells are shown in white. The green cells can divide again if they meet the criteria of the mediolateral gradient.

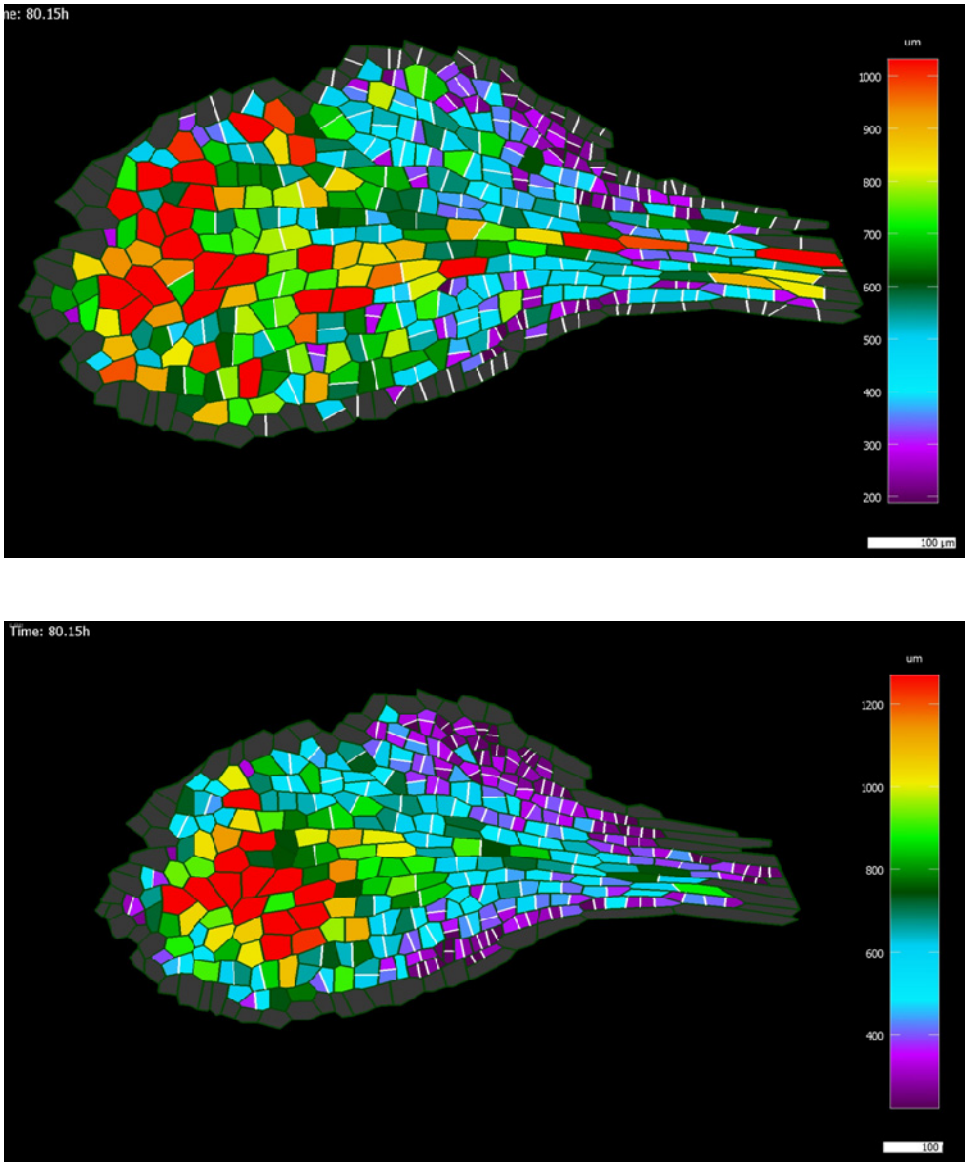

Figure 3. 37 Comparing the two gradient model to the observed cells. The distribution of final cell areas generated by two gradient model (b) can be compared to the areas generated by dividing the cells at the observed time of division (a). Both models divided cells using the shortest wall algorithms. The parameters are the same as in the previous figure. The distribution of cell areas shows a good match between the two gradient model and the descriptive model of when cells divided.

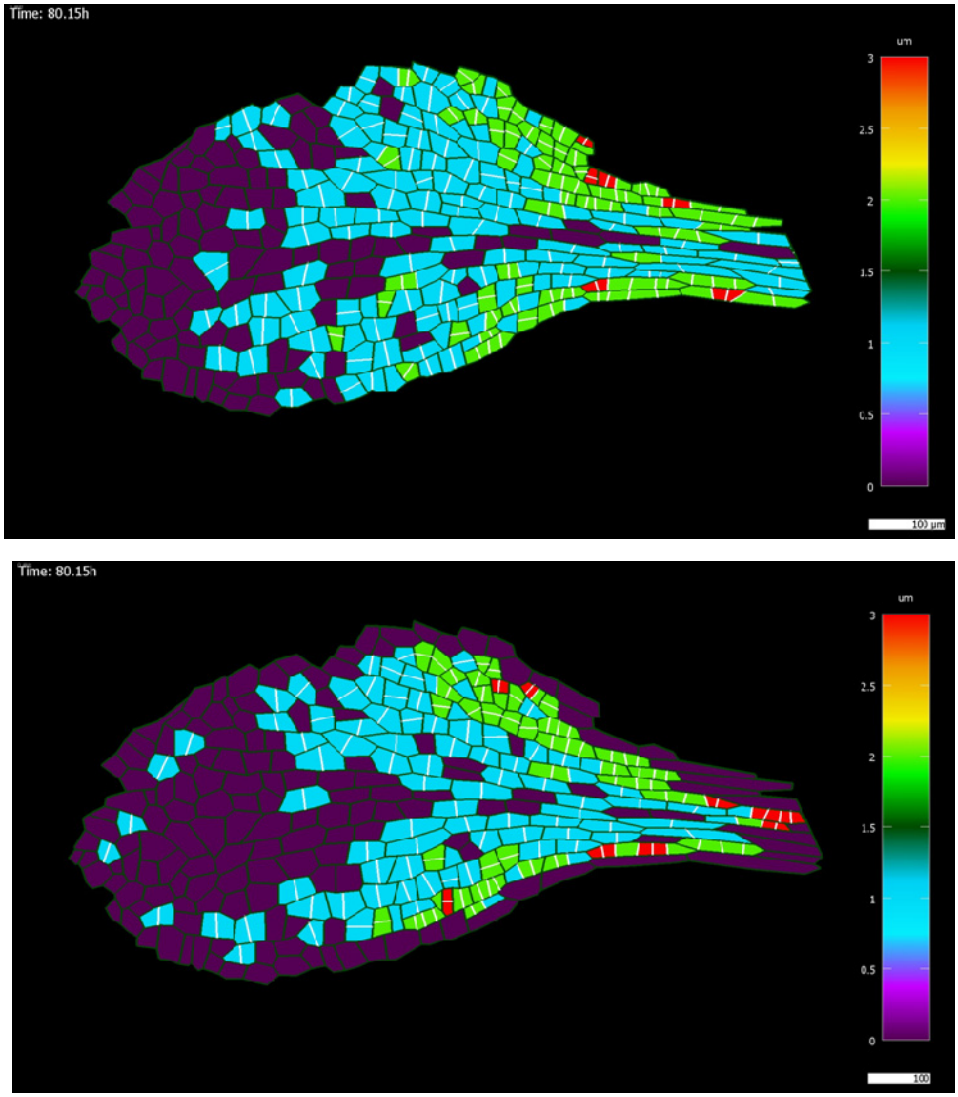

Figure 3. 38 Comparing the two gradient model to the observed cells. The distribution of cell division frequency generated by two gradient model (b) can be compared to the frequencies generated by dividing the cells at the observed time of division (a). Both models divided cells using the shortest wall algorithms. The parameters are the same as in the previous figure. The distribution of cell division frequency shows a good match between the two gradient model and the descriptive model of when cells divided.

3.3 Growth

The frequency and orientation of cell divisions across the leaf is not uniform but how does this relate to the growth of the leaf?

3.3.1 Calculating growth

As plant cells do not slide past each other their vertices can be used as points of correspondence between time-points to calculate growth. The same data which was used to calculate the cell division patterns can, therefore, be used to calculate the growth of the leaf (see methods for details).

To get an overall impression of the relationship between growth and cell division the growth of the large spch patch was computed. To eliminate noise the growth was calculated from the first image to the last image and therefore reflects the amount of growth that occurred in the 80 hour period. The growth rates were computed without considering cell division so reflect the growth parameters for the virtual clones generated from the cells in the first image.

Plotting the areal growth rate of the clones as a heat map shows it is not the same in all parts of the leaf (Figure 3.39). The clones in the tip of the leaf (purple) are growing the slowest. The clones in the mid-vein (blue) grow slowly, while clones in the blade region (red) are growing much faster. The further clones are from the tip and mid-vein the faster they are growing. The heat map gives a good visual impression of the growth rates. However it does not tell us anything about the directions of growth.

To display the directions of growth we need to consider the major and minor axis of growth (Figure 3.40). The major and minor growth directions are orthogonal so can be represented as a cross where their length indicates the relative growth in a particular direction (Hejnowicz and Romberger, 1984).

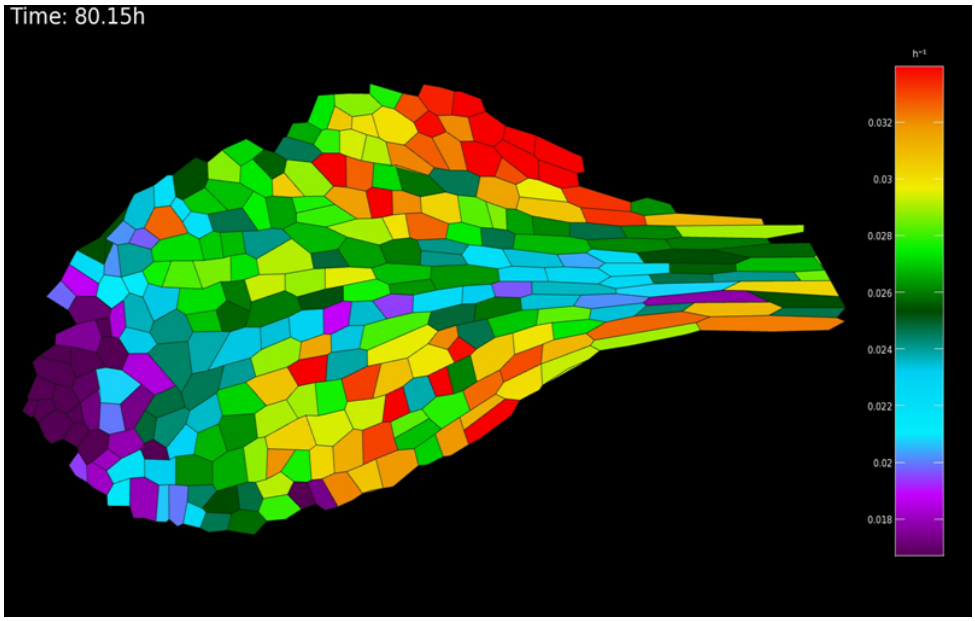

Figure 3. 39 The areal growth rate of the virtual clones of large *spch* patch as a heat map. Clones in the tip (purple) grow the slowest 0.019 % per hour. Clones in the mid-vein and petiole (green - blue) grow a little faster 0.022- 0.026 % per hour. Clones at the edge of the patch (red) grow the fastest at more than 0.032 % per hour.

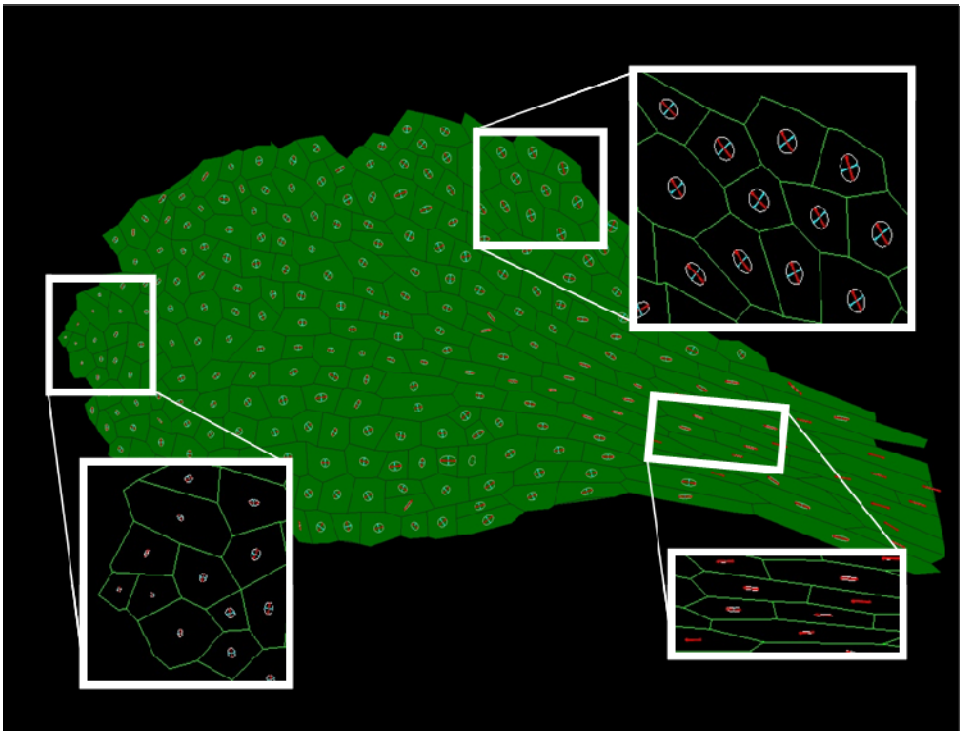

Figure 3. 40 The major and minor directions of growth for the large *spch* patch. The major axis (red) shows the direction of most growth for the clone and its length is the relative amount of growth in this direction. The minor axis (blue) is orthogonal and indicates the relative amount of growth in the minor growth direction. Ellipses emphasises the anisotropy and direction. The clones in the petiole have a major growth direction which is aligned with the main axis of the leaf. The direction of growth in the blade region is diverging away from the main axis outwards. Clones in the tip have no overall direction of growth.

The growth axis can be emphasised by drawing an ellipse around them. Plotting the ellipses shows that the clones do not all have the same major growth direction and the shape of the ellipses shows that the cells do not all have the same isotropy levels. The major axis of growth of the clones in the petiole is aligned with the leaf while the direction of growth of the clones in the lamina diverge from the leaf axis and point outwards. The clones in the tip of the leaf have no major direction of growth. The size of the ellipses represents the relative growth and highlights the slow growth of the tip clones. The shape of the ellipse gives an indication of the isotropy of the growth of the clone indicating that the clones in the petiole are more anisotropic than the clones in the lamina. This method of displaying the growth is not as easy to interpret. We can instead break the information down. Displaying only the major axis gives a better impression of the divergent nature of the growth field (Figure 3.41). Cells in the petiole and mid-vein are growing along the axis of the leaf while, the cells in the blade region are growing out towards the edge of the leaf. Just before the tip the growth directions seem to converge again on to the tip.

We can asses the magnitude of growth in each direction using a heat map. The major growth rate (Figure 3.42a) is lowest at the tip (purple) and gradually increases along the length of the leaf. There is no obvious medio-lateral gradient in the major growth rate. By contrast the minor growth rate (Figure 3.42b) has a gradient from the mid-vein to the blade. The mid-vein has almost no growth in the minor growth rate direction while the rate in the blade is high. The rate is also low in the tip and petiole of the leaf.

Combining the amount of growth in the minor and major axis gives us a measure of how isotropically the cells are growing. I display this as an anisotropy value which I calculate as minor growth rate divided by major growth rate. A value of 1 means the growth is anisotropic while 0 means the growth is isotropic (Figure 3.43). The petiole is growing anisotropically with a value of 1. The mid-vein is growing less isotropically with a ratio of 0.4-0.5. While the blade and tip region are growing isotropically with ratios approaching 1.

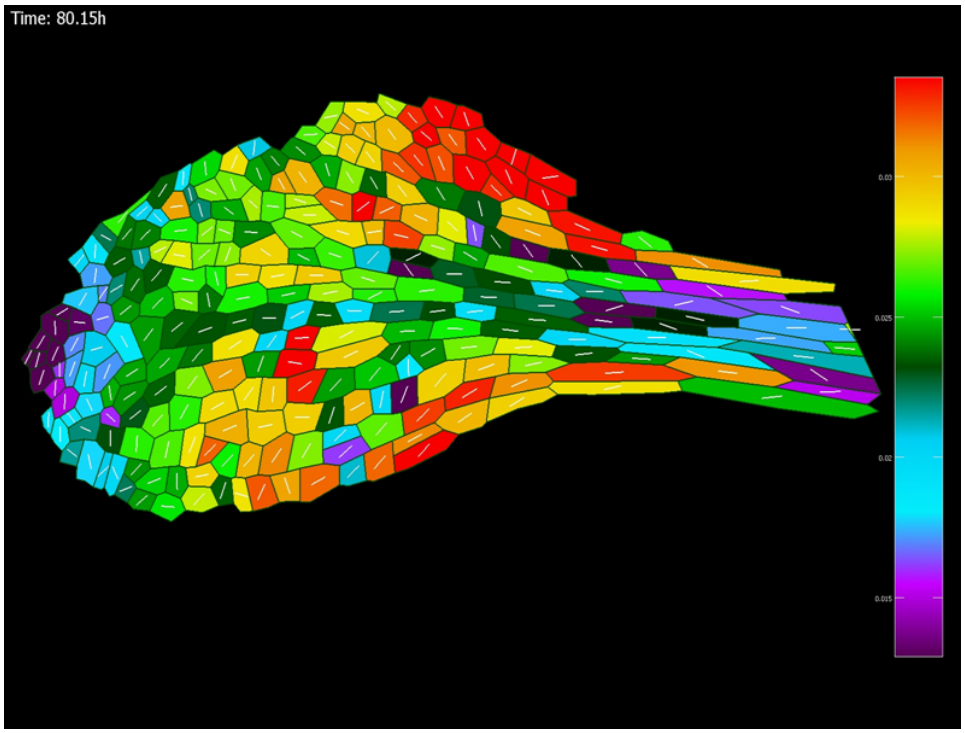

Figure 3. 41 The divergent growth directions of clones in the large *spch* patch. The areal growth of the cells (heat map) with the major axis of growth (white line). The length of the line does represent the amount of growth. The directions of growth are aligned with the leaf in the petiole and mid-vein. In the lamina the major axis of growth is point away from the mid-vein. At the tip there is no clear orientation of growth but just before the tip the growth directions seem to converge again on the tip.

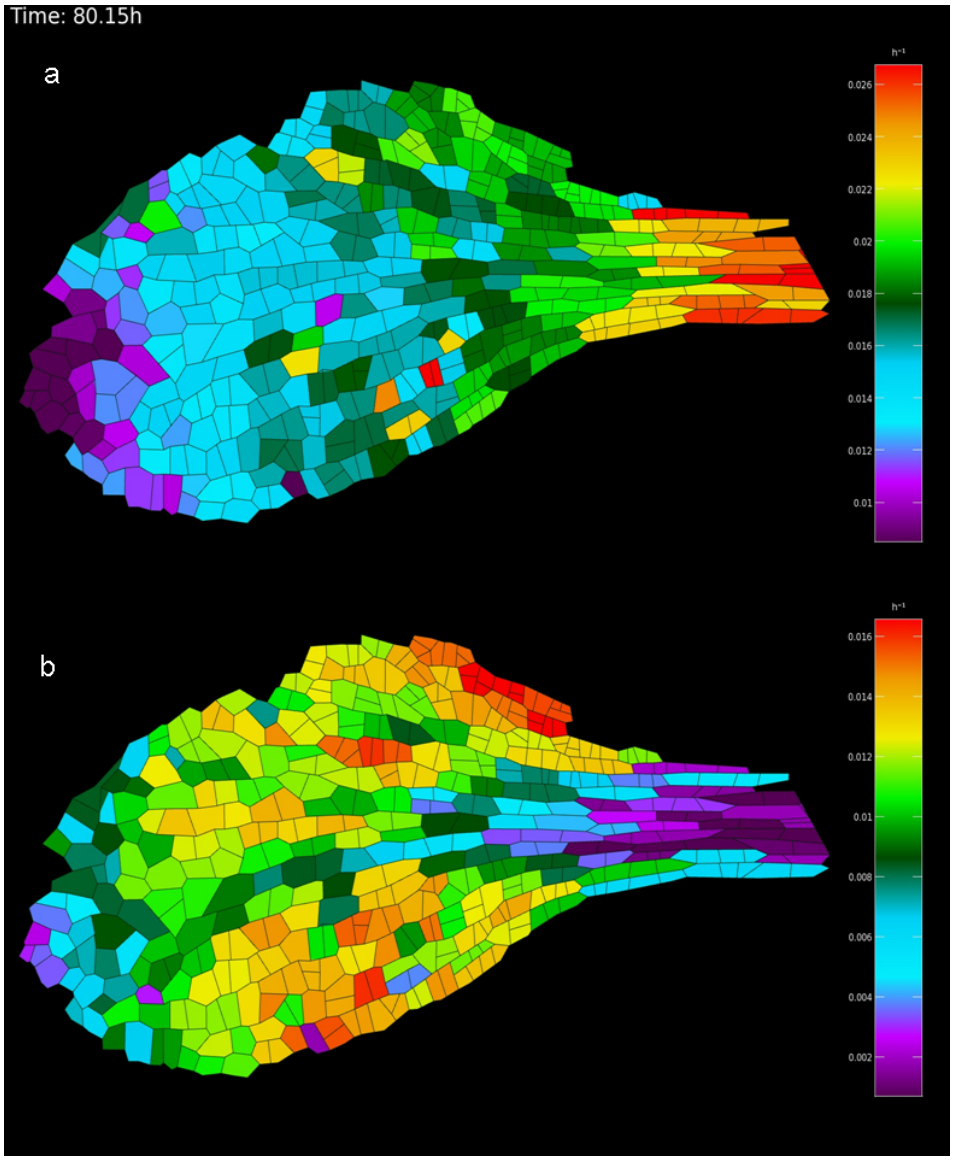

Figure 3. 42 The magnitude of growth in the major and minor directions of growth. (a) Growth in the major growth direction shows a gradient from the tip (purple) with a growth rate of 0.01 percent per hour to the base (red) with a growth rate of more than 0.026 percent per hour. (b) the amount of growth in the minor growth direction is low at the tip, the petiole and the mid-vein (blue-purple) with a growth rate of 0.002 0.006 percent per hour. The growth in the minor direction is higher in the lamina 0.016 percent per hour.

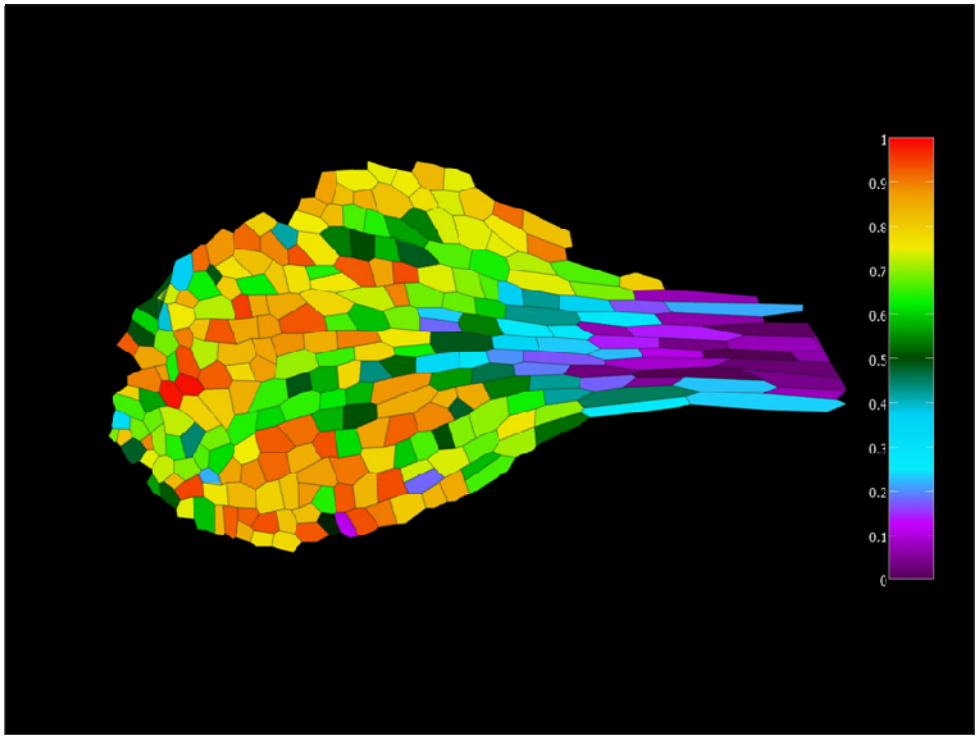

Figure 3. 43 The isotropy value is shown as the growth rate in the minor axis divided by the growth rate in the major growth axis. Clones in the petiole grow anisotropically (purple). Clones in the mid-vein (green - blue) are quite anisotropic with a ratio of 0.4-0.5. Clones in the lamina and tip are isotropic with a ratio that approaches 1.

The different calculations of growth rates show that they are not uniform across the leaf. We can consider four main regions; 1) the tip which grows slowly and isotropically, 2) the mid vein which has a gradient in growth rate from the tip to base in the direction of the leaf but has very little growth orthogonal to this, 3) the petiole which has a high rate of growth, and is anisotropic with a major growth axis oriented in the direction of the leaf axis, 4) the rapidly growing, isotropic blade region.

3.3.2 How does growth relate to the orientation of divisions?

We can look at the cell divisions in the four areas identified as having different growth properties to see if there are any correlations. Comparing the fate map to the growth rates suggests that there are correlations. The petiole grows anistropically and the cells seem to divide perpendicular to the major axis of growth. The cells in the blade divide in both orientations and are growing more isotropically. There are two possible explanations: the growth could determine the orientation either directly or indirectly. This idea of a direct influence of growth on cell division orientation was examined earlier and was not found to be reliable although this could have been due to the growth being noisy. Geometric rules particularly the shortest wall algorithm were more able to match the observed cells, and it is easier to imagine how such mechanisms could exist in the cell. In plant cells, their growth is the main determinant of their shape so will affect the outcome of geometric division algorithms indirectly.

We can study the relationship between growth and the shortest wall algorithm using simple models of a growing rectangle. If we grow a rectangle in one direction, and apply the shortest wall algorithm every time it doubles its size, we can see that all divisions are perpendicular to the direction of growth (Figure 3.44a).

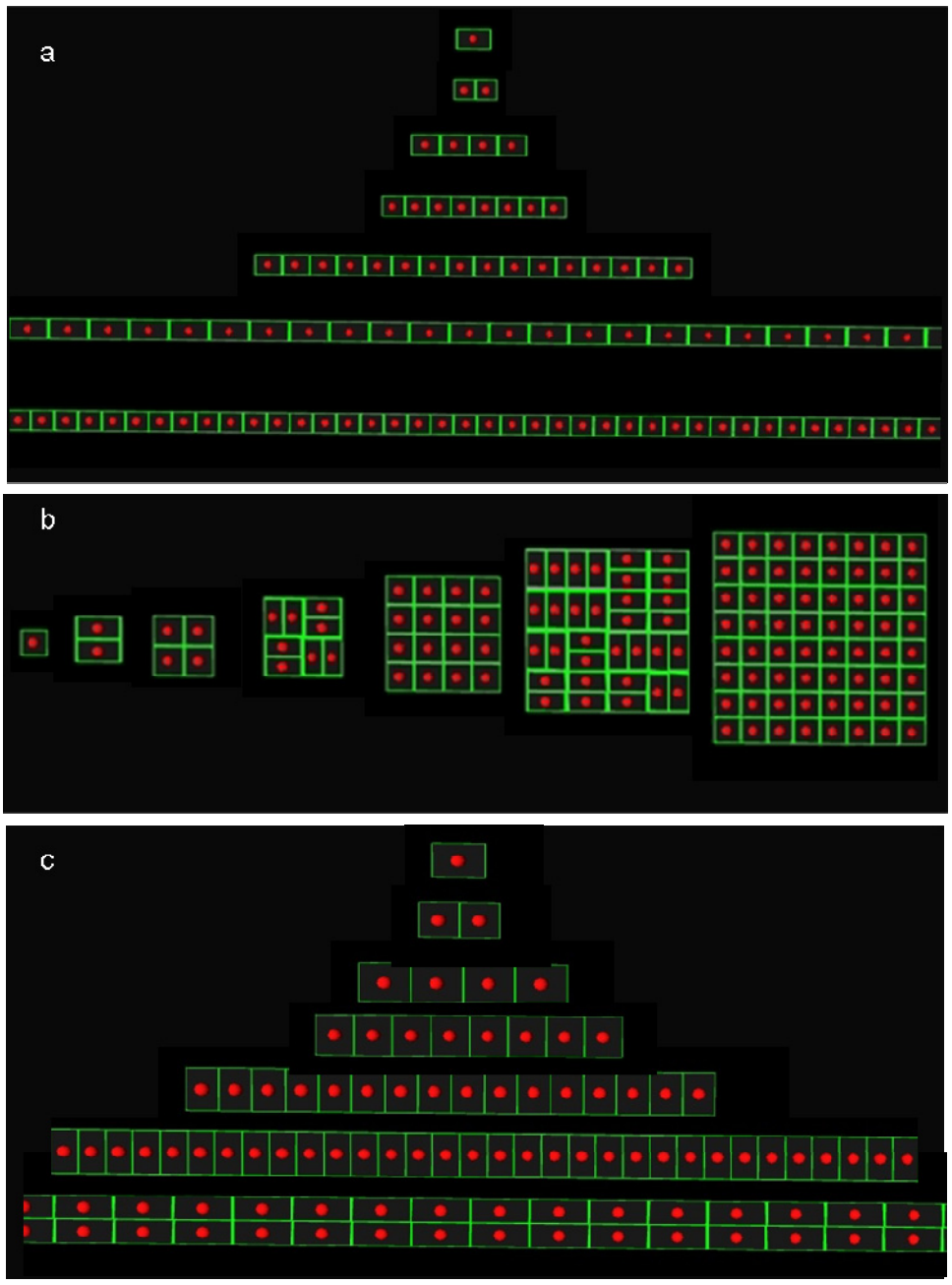

Figure 3. 44 Modelling the relationship between growth and cell division. a) anisotropically growing cells (ratio minor : major growth rate = 0) always divide perpendicular to the growth axis which is aligned with the x axis. b) isotropically growing cells (ratio =1) divide with equal probability in either direction. c) cell growing ten times more in the x axis than the y axis (ratio 0.1) divide mostly perpendicular to the direction of growth but sometimes divide parallel to it. The models are compared having under gone the same number of rounds of division. Growing a and b for longer does not change the outcome of the simulation.

If we grow the rectangle isotropically, there is an equal chance of the first division being in either direction. Subsequent divisions will be in alternating directions (Figure 3.44b). If a cell is growing mostly in one direction the outcome is not so obvious. Even if a cell grows 10 times faster in one direction than the other there will still be divisions parallel to the direction of growth (Figure 3.44c). The shortest wall divides cells in different orientations depending upon their growth. Returning to the fate map, we can see that in the petiole where growth is anisotropic the cells are dividing perpendicular to the axis of growth as predicted from the model. In the lamina there are divisions in both direction and in between there is a gradient in division direction. The correlation in division orientation and growth can, therefore, be explained by the interaction of the shortest wall with the growth. Therefore, although the division orientation looks different across the leaf it is possible that one rule can be responsible for all the divisions and it is not necessary to make it more complex assumptions. It is possible that there might be a feedback between new walls and the growth rates of the cells, if for example they have different mechanical properties. In order to investigate such a feedback a mechanical model would be needed such as mass spring or finite element.

3.3.3 How does growth relate to the frequency of divisions?

A comparison of the growth rate to the frequency of divisions also shows a strong correlation (Figure 3.45). The fastest growing regions are the areas that are dividing the most. As we are assuming cells divide based on their area we could imagine that the cells in the fastest growing areas are simply able to reach their threshold area faster. However, we have shown that the cells in the fastest dividing region are dividing at a rate that is above what could be predicted. They are dividing at a smaller area. There is therefore a correlation between high growth rate and high division frequency. We can not establish a cause or affect, but there seems to be some co-regulation of these two events. It is possible that they are both controlled by another unknown factor that is involved with shaping the leaf.

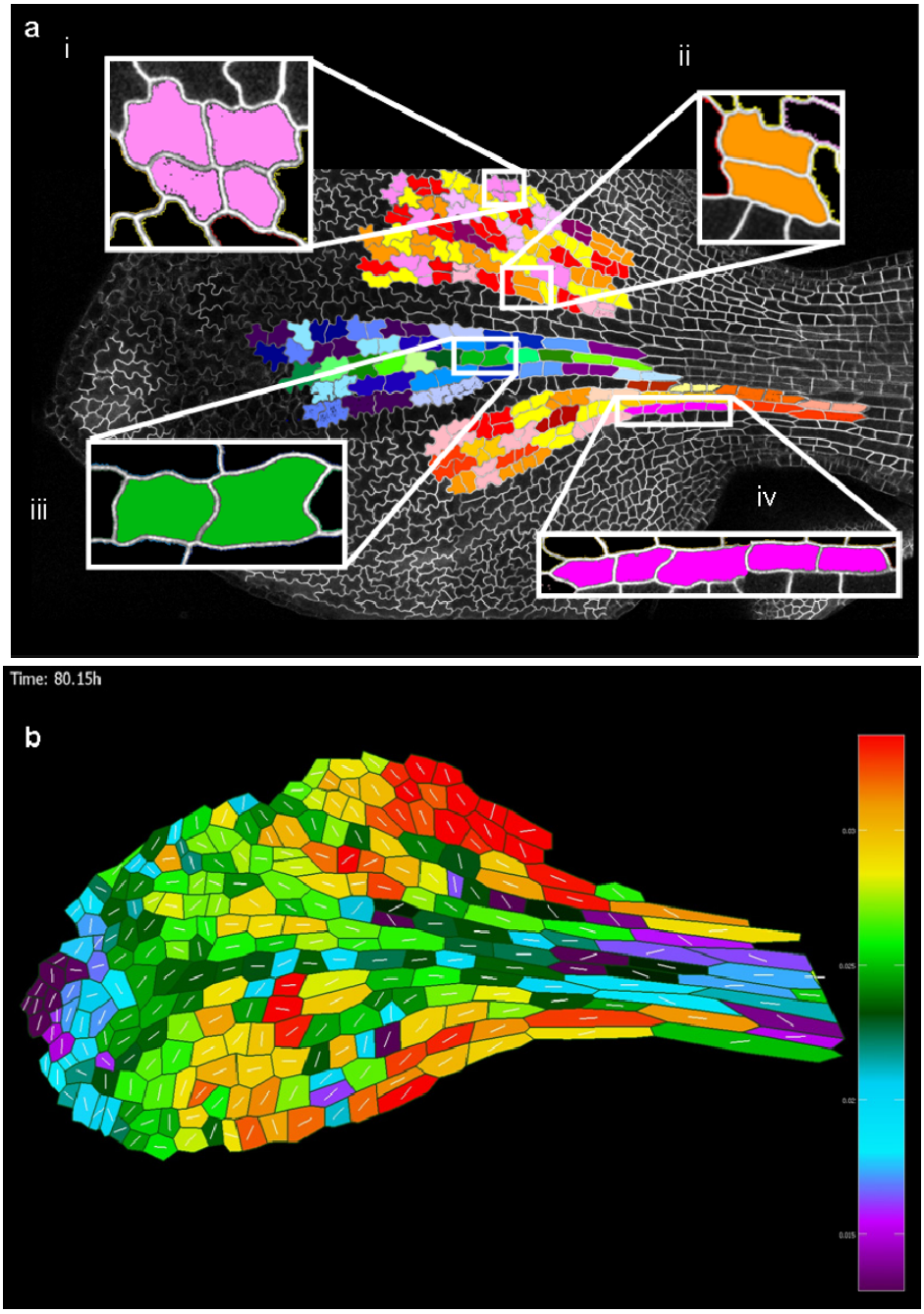

Figure 3. 45 Comparing cell division and growth. a) the fate map of virtual clones shows cell division orientations and number of rounds of division. b) the areal growth rate of the leaf (heat map) with the major directions of growth marked (white). The cells in the petiole produce long clones which divide perpendicular to this, the clones grow anisotropically in line with the leaf axis. The clones in the lamina divide in both directions; they have a high rate of growth and grow isotriopically with a bias away from the axis of the leaf. Clones in the tip do not divide they grow slowly with no predominant direction. Clones in the mid-vein divide perpendicular to the leaf axis and grow in the direction of the leaf axis.

3.4 Summary

In this chapter I looked at the orientation and timing of cell divisions in tracked wild-type and speechless patches. I showed that existing cell division algorithms are not able to predict the placement of new division walls in the wild-type cells. This is because the new walls in the wild-type cells do not always pass through the centre of the cell. This seemed to be due to stomata formation. By following speechless cells I was able to show that the division planes of non-stomata forming cells were easier to predict using existing algorithms. I was able to show that the shortest wall algorithm was better at predicting the observed divisions in my data. However, due to the limited amount of data I am not currently able to exclude the other algorithms so this will be discussed further in the next chapter.

With regard to the timing of cell division I also focussed on the speechless mutant. I saw that cells in the speechless leaves do not divide at constant areas or with a constant cell cycle duration. I showed that the cell divisions varied with respect to both factors in time and space. I was not able to conclusively show that cell area was a better predictor of division time than cell cycle duration although there was a better correlation in my data. I did show that the distribution in division time could be explained in terms of a two gradient model. A mediolateral gradient that dictated the timing of division and an exponential gradient that defined a region of division competence. There is a pattern in the area of cells across the leaf. This pattern can be explained by non-uniform growth, a gradient in division areas, cell division arrest and the interplay between division orientation and changing cell geometry. In the next chapter I will consider the division integration of asymmetric divisions into the developing epidermis.

4 Stomata formation

4.1 Introduction

In the previous chapter the timing and orientation of cell division in the *speechless* mutant was predicted using the two-gradient model and the shortest wall algorithm. However, none of the models tested were able to predict the timing and orientation of the wild-type cells. Wild-type cells can be pavement cells, stomata lineage cells or undifferentiated cells. Stomata start to appear on the abaxial side of the first leaf of *Arabidopsis thaliana* five or six days after germination and continue to do so until the leaf reaches maturity. Stomata are formed by a series of asymmetric cell divisions and the final stomata are spaced apart by at least one cell (Sachs, 1978). Unlike the other cells in the leaf which are thought to be produced and mature in a wave (Donnelly et al., 1999). Stomata are produced in an intercalated pattern (Sachs, 1978). How do the asymmetric divisions that produce stomata differ from the divisions of the *spch* cells and how are they integrated in to the epidermis to create a pattern.

Stomata formation can be classified based on whether they form from isolated MMCs (primary stomata formation) or ones that contact other stomata lineage cells (secondary stomata formation) (Geisler et al., 2000). I will focus on primary stomata formation initially. Primary stomata formation occurs early in development at a time when time-lapse imaging is possible. As primary meristemoids form in isolation there should be less contribution from context rules allowing the contribution of lineage based mechanisms to be considered.

4.2 Retrospective Analysis

Stomata start to appear on the abaxial side of the first leaf of *Arabidopsis thaliana* five or six days after germination and continue to do so until the leaf reaches maturity. To study stomata formation I tracked the cells in leaf one of wild-type seedlings that were five days old for up to six days. The cells were marked with a GFP membrane marker allowing stomata to be identified based on their appearance. Retrospective analysis was used to classify cells that went on to produce stomata in the tracking data. Retrospective analysis can be best described using an example. Figure 4.1 shows a diagram of a fictional data set where two cell types, A and B, can be identified in generation 3. If we look at the earlier generation (Figure 4.1 generation 2) all cells are indistinguishable, but they can be classified based on whether they go on to make A cells or not. Cells that go on to make A cells are marked as P cells, while cells that do not go on to make A cells are marked as Q cells. Generation 2, therefore, has some P cells and some Q cells. We can look backwards again to generation 1 and identify the cells that produced the P cells and mark them as P cells. In generation 1, all cells are P cells as they all include A cells in their descendents. It is possible to follow these lineages back to a single P cell in generation 0. This P cell has two A cells among its descendents while the others have only one A cell, we therefore call this cell P_2 and the others P_1. If we now consider A cells to be in the later stages of stomata development (GMCs) and B cells to be non-stomata cells we can carry out the same analysis on real data and identify real P and Q cells. These classifications are based on lineage and do not indicate cell types. At this stage we do not know when, if ever, the cells have a different type. Meristemoids can be

identified based on their triangular shape. However, I initially wanted to classify cells more generally based only on their eventual fate.

4.2.1 P_1 cells behave as stem cells

I carried out retrospective analysis on real data by identifying stomata and late stomata lineage cells in the final image of the tracking data and working backwards. Initially I based my analysis only on cells that formed stomata. As I become more familiar with the appearance of stomata, I also included data from lineages that only reached the guard mother cell stage. This expanded the number of lineages that I could use. The main focus of this study is not the well characterised division that creates the stomata from the guard mother cell, but the series of divisions that precedes this event.

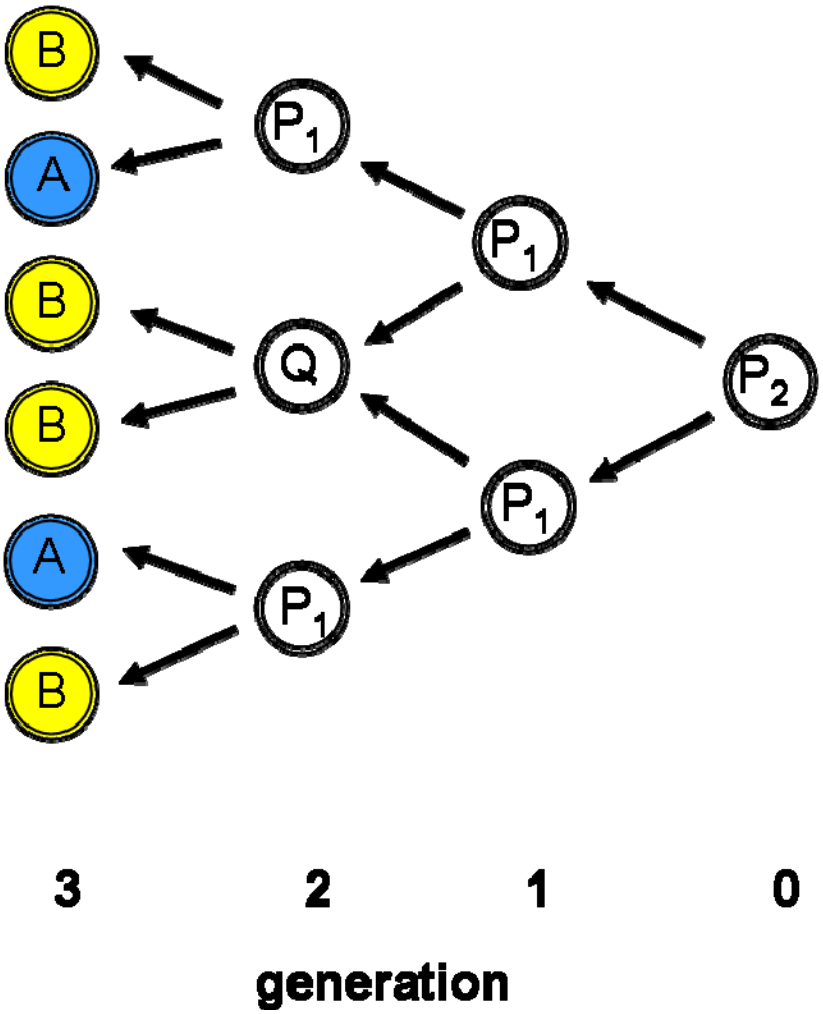

Figure 4. 1 A schematic of retrospective analysis. In generation 3 there are two kinds of cells A cells and B cells. They can be identified based on their colour. In generation 2 all cells are white but they can be identified based on whether they go on to make A cells or not. P_1 cells go on to make A cells while Q cells do not. This can be repeated in generation 1 and all cells that make P_1 cells are marked as P_2 cells, because they make 2 A cells. All cells in generation 1 are P_1 cells. In generation 0 there is only a single cell which is a P_2 cell.

Therefore, GMCs and their two daughter cells will be classified as A cells. Although the retrospective analysis can confirm the identity of a GMC its real strength comes from its ability to classify cells whose fate is otherwise ambiguous and these cells will be our focus.

For simplicity I first consider a single cell lineage. A subset of images where the cells of interest divided are shown in Figure 4.2. In Figure 4.2a generation 4, there is one stoma, both guard cells are coloured blue, and three cells that are not identifiably in the stomata lineage which are coloured yellow. I represent this as a pair of descendents of an A cell (GMC) and four B cells in the scheme in Figure 4.2b. We can then go to the previous image and find the cells that divided to produce these cells. Generation 3 contains the progenitor to the stomata, a GMC classified as an A cell. The other cells have not divided and are still B cells. In generation 2 the cell that divided to produce the A cell can be identified, and classified as a P_1 cell in the scheme. The other two cells are still B cells. In generation 1 there are two cells one P_1 cell and one B cell. Finally there is a single P_1 cell in generation 0. This is a P_1 cell as it leads to the production of a single A cell. Note there are no Q cells, as no cells divided that produced only B cells. Thus, this cell lineage has three cell types: A cells, B cells which do not divide, and P_1 cells which do divide. P_1 cells divide to produce more P_1 cells. P_1 cell division terminates with the production of an A cell. P_1 cells are therefore able to regenerate themselves for a number of rounds of division: three in this case. This suggests that P_1 cells are behaving like stem cells. Stem cells are usually formed by asymmetric divisions, they can renew themselves and produce other cells that usually have a limited ability to divide (Knoblich, 2008) (Figure 4.2c).

Several cells were identified in the final image of the tracking data that had the appearance of stomata or guard mother cells. I was able to identify 12 lineages that were visible for the entire time period of imaging. I followed these lineages backwards and identified the P and Q cells. Figure 4.S1 shows another example that is exactly the same as the one in Figure 4.2 except it does not go through the final division to produce a stoma. Figure 4.3 shows another lineage that is the same but the cells go through one more round of division before producing an A cell, so there are five cells in generation four. Again this lineage does not produce a stoma but seems to form a GMC based on the shape of the cell.

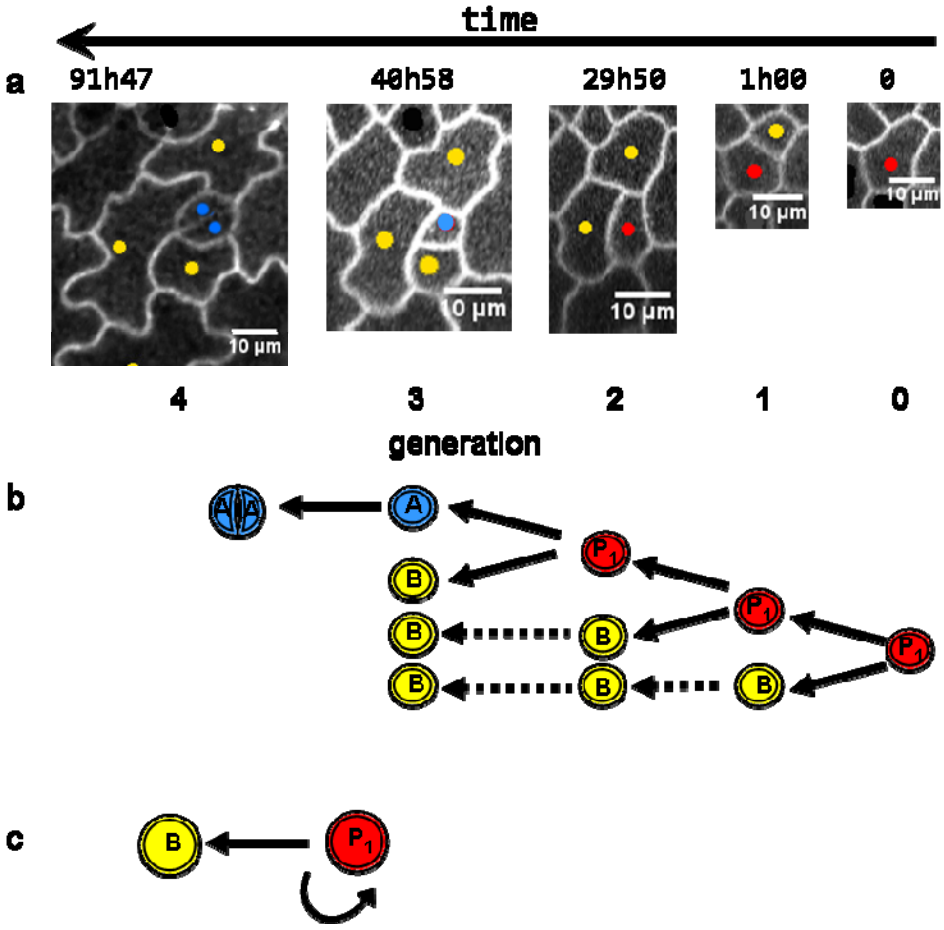

Figure 4. 2 Retrospective analysis of a single stomate lineage. a) the observed cells are highlighted, blue =A cells, yellow = B cells and red = P_1 cells. Sample images where the cells divided are shown. The time shown is in hours and minutes and is relative to when the lineage started being followed. b) the scheme for the observed cells. Cell divisions are marked with a solid arrow while dashed lines represent persistence. The schematic representation is aligned with the corresponding observed cells. Note that only P_1 cells divide. c)P_1 cells behave as stem cells producing a B cell and another cell P_1 when they divide.

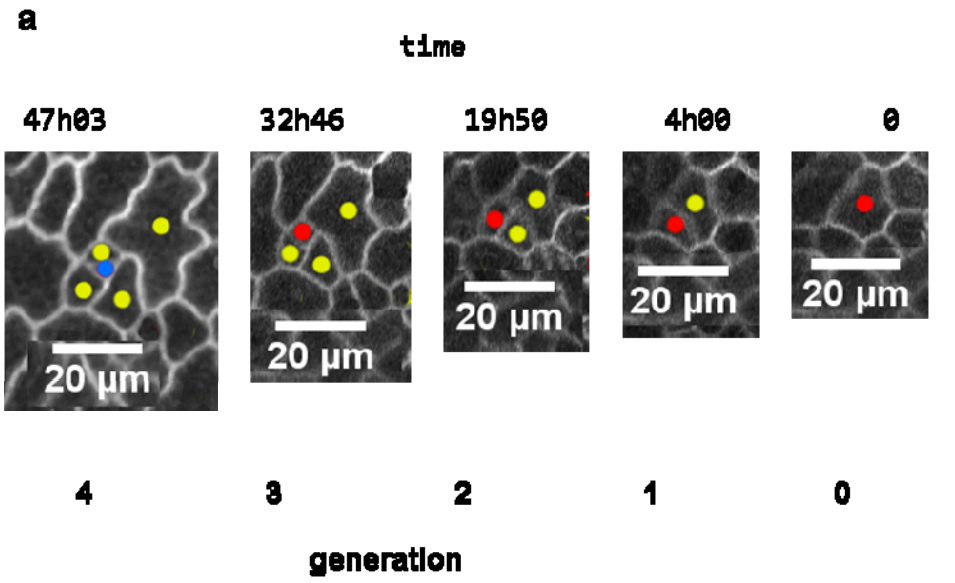

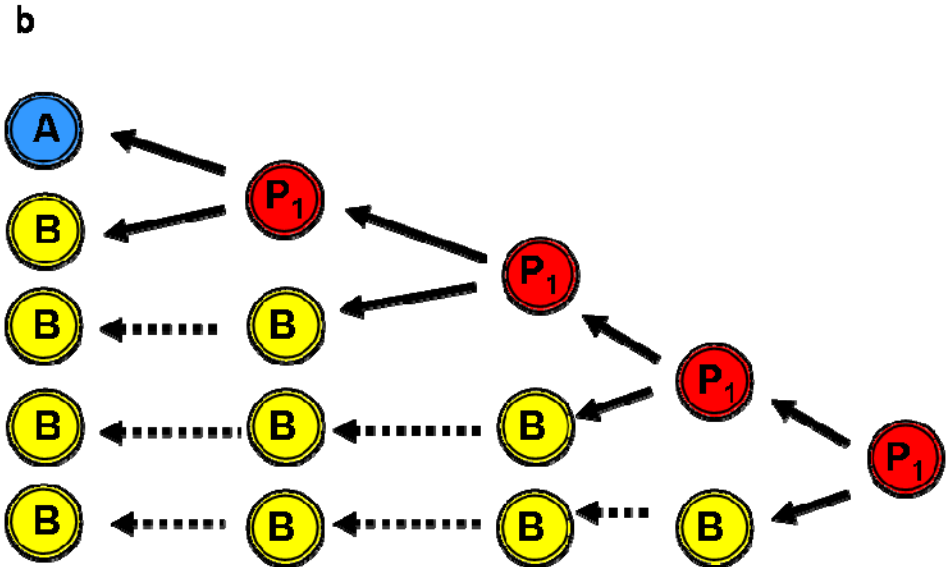

Figure 4. 3 Retrospective analysis of another single stomata lineage. This figure is the same as Figure 4.2 but there is one extra P_1 cell division creating an A cell and 4 B cells.

Another four of the lineages have identical schematics to the one we saw in Figure 4.3 (shown in Figure 4.4). They all had five cells in generation 4, with one cell being a GMC. These lineages were all traced back to one P_1 cell in generation 0. These lineages have the same three cell types and only the P type cells divided. Therefore, five out of the 12 lineages have the same cell classifications and number of divisions. Two of the other lineages are very similar but their P1 cells had one fewer rounds of division (Figure 4.2 and S1). It is possible these two lineages may have divided before I started imaging, or the lineage in Figure 4.S1 could divide again as it has not yet made a stomata, (i.e. it might be a meristemoid rather than a GMC). This would make the lineages identical to the other five. Thus, for seven of the studied lineages, only P_1 cells divided and under went 3-4 rounds of division.

In the remaining five lineages there are Q cells – cells that divide but did not produce stomata within the time that was imaged. All but one of these lineages behaved in the same way. Figure 4.5 shows the first of these lineages. In the final generation there are five cells: one A cell and four B cells. The Q cell was created by the first division of the P cell in generation 0 but the Q cell did not divide until generation 3 (i.e. after the A cell had formed). The Q cell divided only once to create two B cells. Figure 4.S2and S3 show two other lineages that behave in the same way. Figure 4.6 shows a lineage that behaves in a similar way but the Q cell divides twice. In all of these cases the Q cell was produced early in the lineage either generation 1 or 2 and did not divide until after the A cell had been created. The final lineage of the twelve is shown in Figure 4.7. This lineage is the only one where the Q cell divided before the A cell was formed. The Q cell divided three times. The Q cells in the lineages shown in Figure 4.6 and 4.7 both divide more than once and create a Q cell. In these lineages the Q cells are therefore behaving like P_1 cells. The cells created at the end of these lineages by Q cells may include stomata precursor cells, although we can not be absolutely certain. If this is the case it means the cell in generation 0 divided to produce two P cells and is therefore a P_2 cell. We will consider Q cells in more detail later.

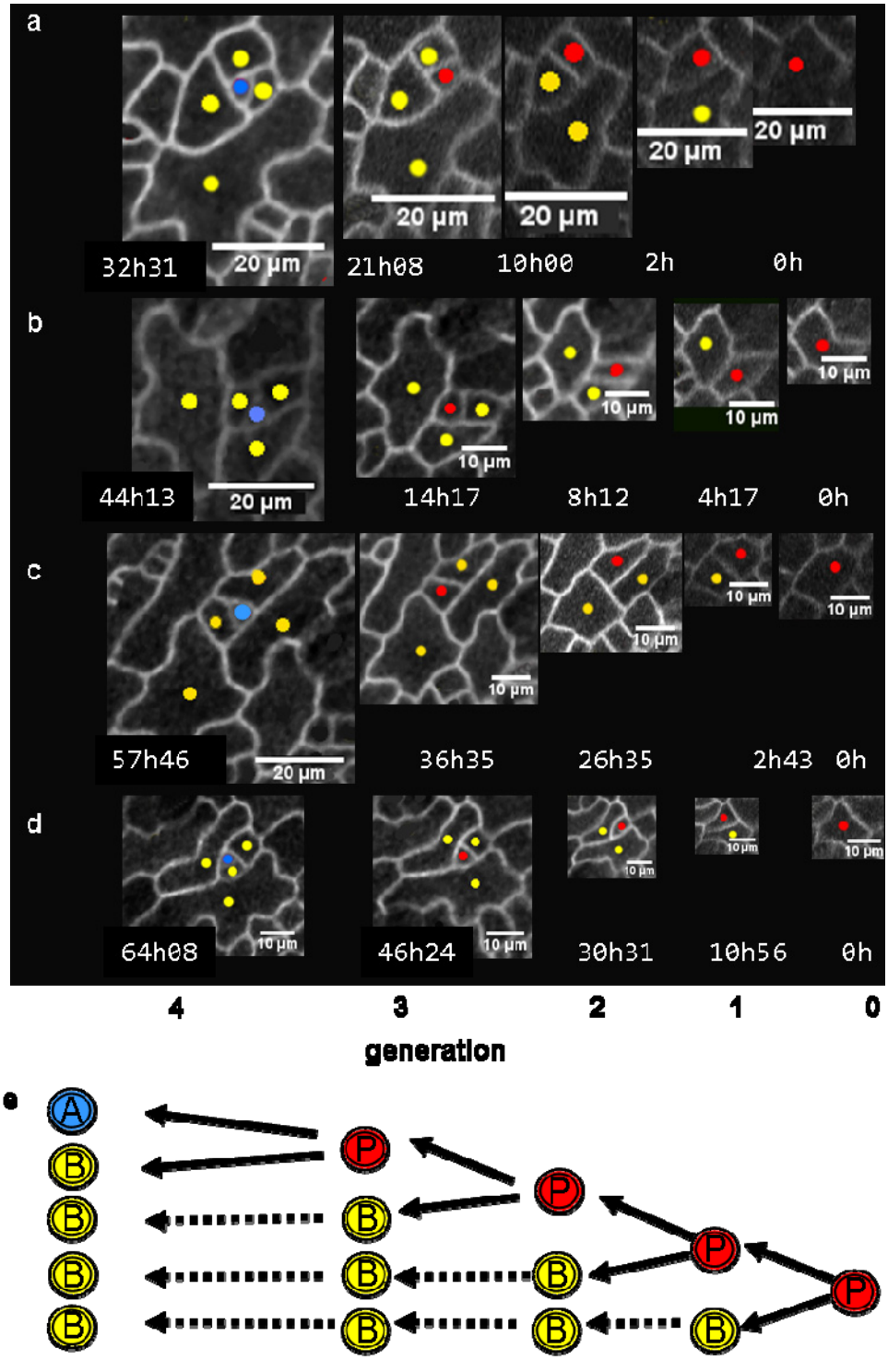

Figure 4. 4 Retrospective analysis shows many lineages have the same pattern of division. These four lineages (a-d) all divide in the same way (e) as the lineage in Figure 4. 3.

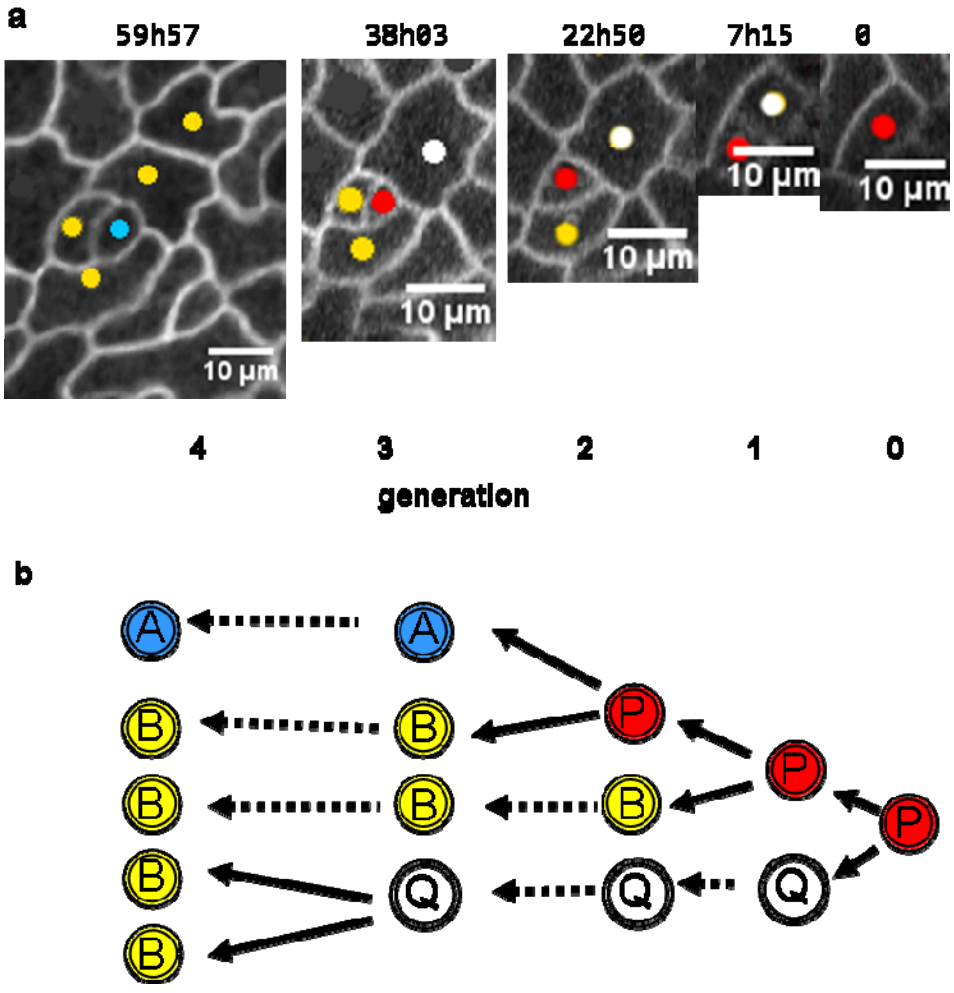

Figure 4. 5 Retrospective analysis of a stomate lineage with a Q cell. a) the observed cells are highlighted with colours as in the previous figures. Additionally Q cells are shown in white. Both P_1 and Q cells divide in this lineage (b). The Q cell is created in generation 1 and divides in generation 3.

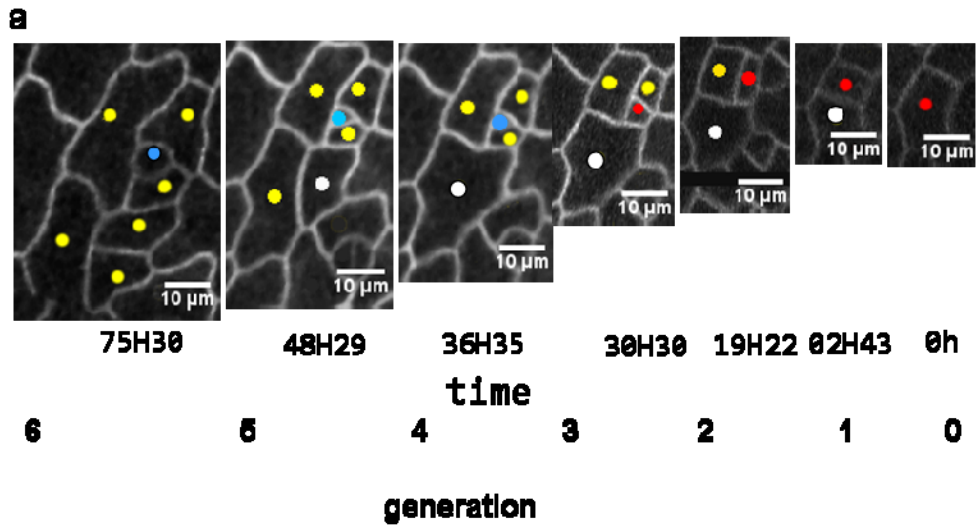

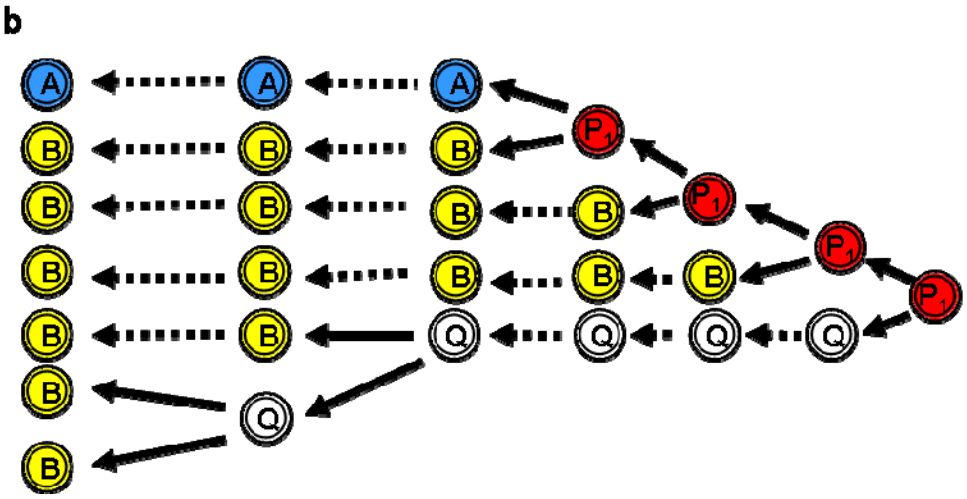

Figure 4. 6 Retrospective analysis of a stomate lineage with a Q cell. This lineage has a similar arrangement to the lineage shown in Figure 4. 4 except the Q cell divides twice, once in generation 4 and once in generation 5.

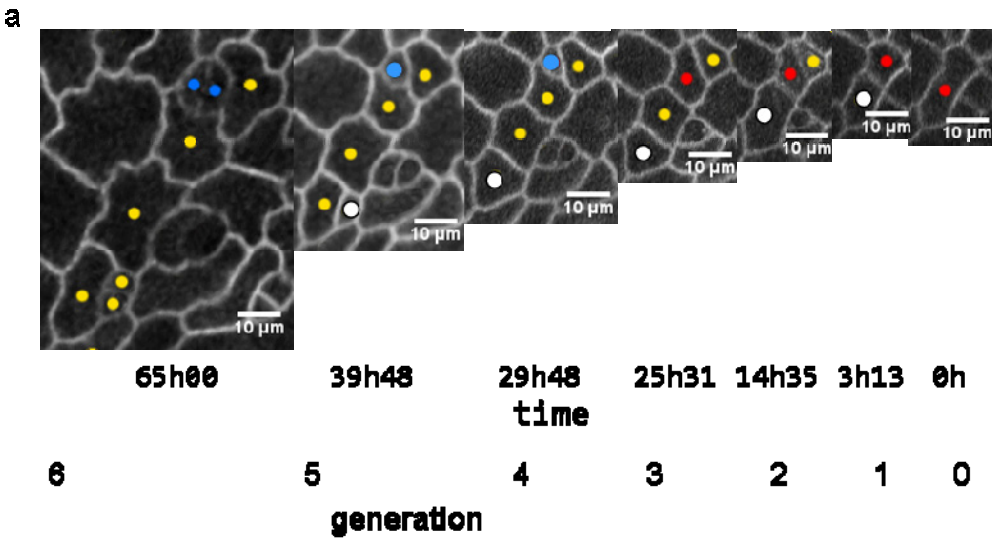

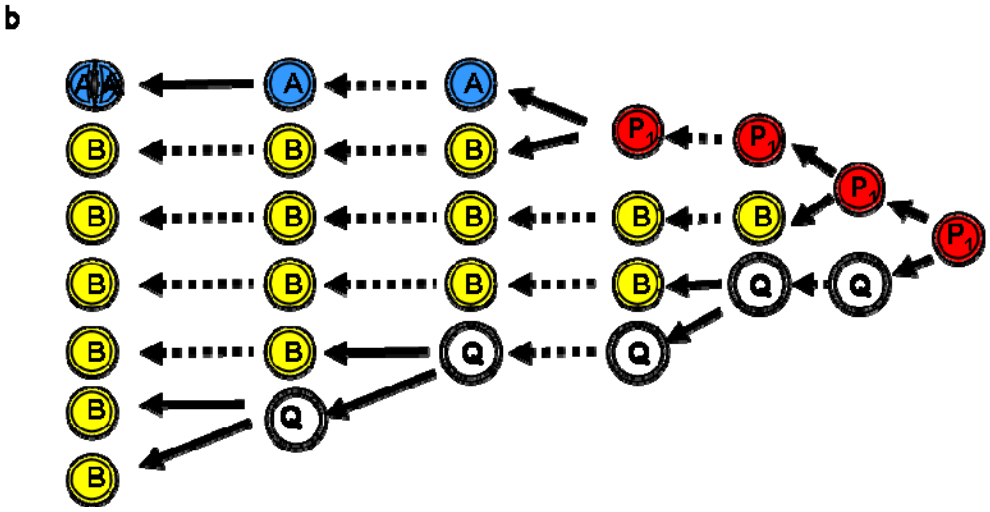

Figure 4. 7 Retrospective analysis of a stomata lineage with a rapidly dividing Q cell. a) the observed cells are highlighted with colours to show the cell types, blue A cells, yellow B cells, red P_1 cells and white Q cells. Only the time-steps where the cells divided are shown. b) the scheme of the observed cells. Cell divisions are marked with a solid arrow while dashed lines represent a cells persistence in its current form. The schematic representation is aligned with the corresponding observed cells. Both P_1 and Q cells divide rapidly in this lineage. The Q cell divides 3 times and resembles a P_1 cell.

4.2.2 P_1 cells divide at a smaller size

In the previous chapter I was unable to explain the timing of cell division of the wild-type cells. I wanted to see if focussing on just the P_1 cells could provide insight into this problem. Just as I did for the *speechless* mutant patch I tried to assess whether the cells were dividing based on a cell cycle timer, e.g. every 6 hours, or upon reaching a threshold area. I looked at the lineages that contained only P_1 cells first. For each division within each lineage I identified the first image where the division was visible. Figure 4.8 shows the divisions for one lineage. The first row of the table gives the time interval between the images. Cell divisions occurred at intervals of 15hours50, 12hours56 and 14hours17. To ensure these observations were not an artefact of the imaging interval I also included the time interval since the cell was last imaged (row 2). All cells had been imaged 6 hours or less prior to division. The cell cycle duration of these cells is quite similar. However, other cells show cell cycle durations ranging from 6 – 16 hours for P_1 cell divisions (Figure 4.11). The P_1 do not all have the same cell cycle duration, however, cell cycle duration control remains a possibility.

To consider the cell division area I measured the cell area in the first frame captured after the division and at the last image before they divided. This means we know the range of areas that the cell could have divided in. Row three of the table in Figure 4.8 shows the area the cells in one lineage divided at, and row four shows the previous area. In this example, the cell divided at 160-163µm² in generation 1, 85-87µm² in generation 2, 44-63µm² in generation 3 and 33-51µm² in generation 4. The area at which P_1 cells are dividing is smaller with successive divisions. The other lineages containing only P_1 cells are shown in S4-S6 and show the same trend. This means the cells in the stomata lineage are getting smaller. This is in contrast to the cells in the *spch* mutant which got larger with time and successive divisions. If cells are getting smaller they must be dividing at less than twice the size they were created or be dividing asymmetrically. The final row of the table in Figure 4.8 shows the size of the cells when they were created. The arrows link the creation to size to the time when the cell was created as a daughter cell. I plotted the size of cells at the time of creation, against the size they divided (using the average size from images before and after division) (Figure 4.9).

a

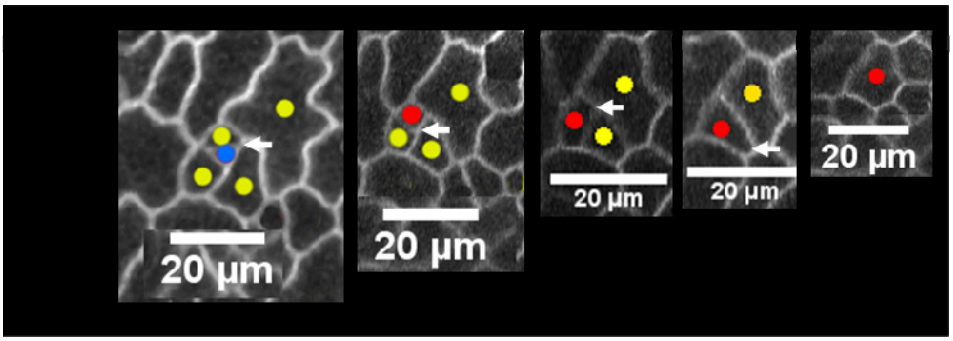

b

Generation	4	3	2	1
Real time interval		14h17	12h56	15h50
Last imaged		6h	3hrs	2hrs
Division area	51µm²	63µm²	87µm²	163µm²
Previous area	33µm²	44µm²	85µm²	160µm²
Daughter areas	19µm²	28µm²	45µm²	59µm²
	33µm²	37µm²	45µm²	108µm²
Creation area	28µm²	45µm²	59µm²	

Figure 4. 8 Timing of cell division. a) an observed cell lineage coloured based on the cells classification. New division walls are marked with solid white arrows**.** The table contains cell cycle duration and area information. Row 1 The interval between two divisions being imaged. Row 2 the time since that cell was last imaged. Row 3 The area of the cell at the time of divisions. Row 4 the area of the cell in the image before it divided. Row5-6 The area of the two daughter cells coloured based on their classification. Row 7 The area the cell that divided was when it was created. The dotted arrows in the table show when the cell was created.

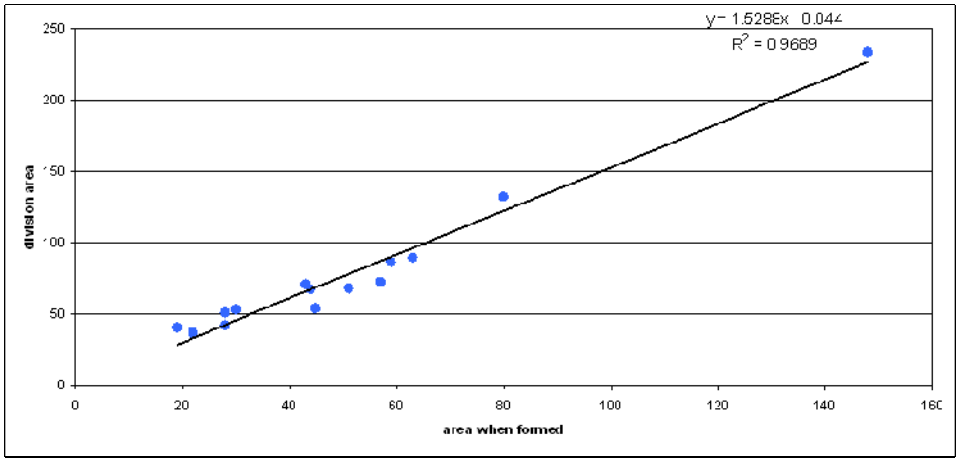

Figure 4. 9. Comparing the size a cell is created to the size it divides. There is a strong correlation between birth size and division size ($r = 0.97$). Cells divide at ≈ 1.53 times their birth size.

There is a good correlation between these values for cells classified as P_1 cells (R^2 of 0.97). The slope is not at y = 2x so cells do not divide at twice their size. Instead they divide at approximately 1.53 times their original size and hence get smaller. Figure 4.10a shows what would happen if a cell of size 100 divided symmetrically to produce two daughters which grow to 1.53 times this size then divide symmetrically, for a few rounds. The cells at the time of division get smaller with an exponential profile. If the division was not symmetric so one daughter was 30 and the other 70 the profile of the curve is changed but it is still exponential (Figure 4.10b). Hence the ratio of division size to original cell size allows the area of cells to be changed.

I looked at lineages with Q cells to see if they are dividing differently. Figure 4.11 shows a lineage that contains a Q cell. Again the time between divisions does not show any pattern. We can see that the P_1 cells are dividing at successively smaller sizes (165-179 µm², 124-140 µm², 64-70 µm² and 25-45 µm²). The Q cell divisions in this lineage occur after the final P_1 cell division at a size of 380-442µm², ten times the size of the last P_1 cell division. The Q cell divides again 27hours later at a size of 192-274µm². Figure 4.S7 –S9 shows other lineages with dividing Q cells. In all cases the Q cells divide at a larger size. I computed the average area of divisions based on the average of the cell's area before and after division. On average P_1 cells divided at 76µm² while Q cells divided at 201µm². Q cells are therefore dividing at an area that is close to the division size of the *spch* mutant cells while the P_1 cells are dividing at about a third of this size. In the two cases where the Q cells divided more than once, the divisions were at successively smaller sizes. I added the Q cell division to the plot of division area against original area (Figure 4.12a). Three of the Q cells (magenta squares) lay above the line and are dividing at 4-6 times the size they were created. Two other divisions are closer to the line, dividing at 2-3 times the creation area. The remaining three divisions lie on the line indistinguishable from the P_1 cells. I wanted to investigate whether the difference in ratios was related to the number of divisions the Q cells had under gone. I therefore indicated the Q cells that had divided previously with yellow triangles (Figure 4.12b). All of these points lay on the line. The first Q cell division occurs at 2-6 times the creation area. However, if the cell divides more than once then the ratio of the subsequent divisions is comparable to that of the P_1 cells. These measurements suggest that Q cells may switch to P_1 cells after their initial division. This would predict that they would go onto make stomata.

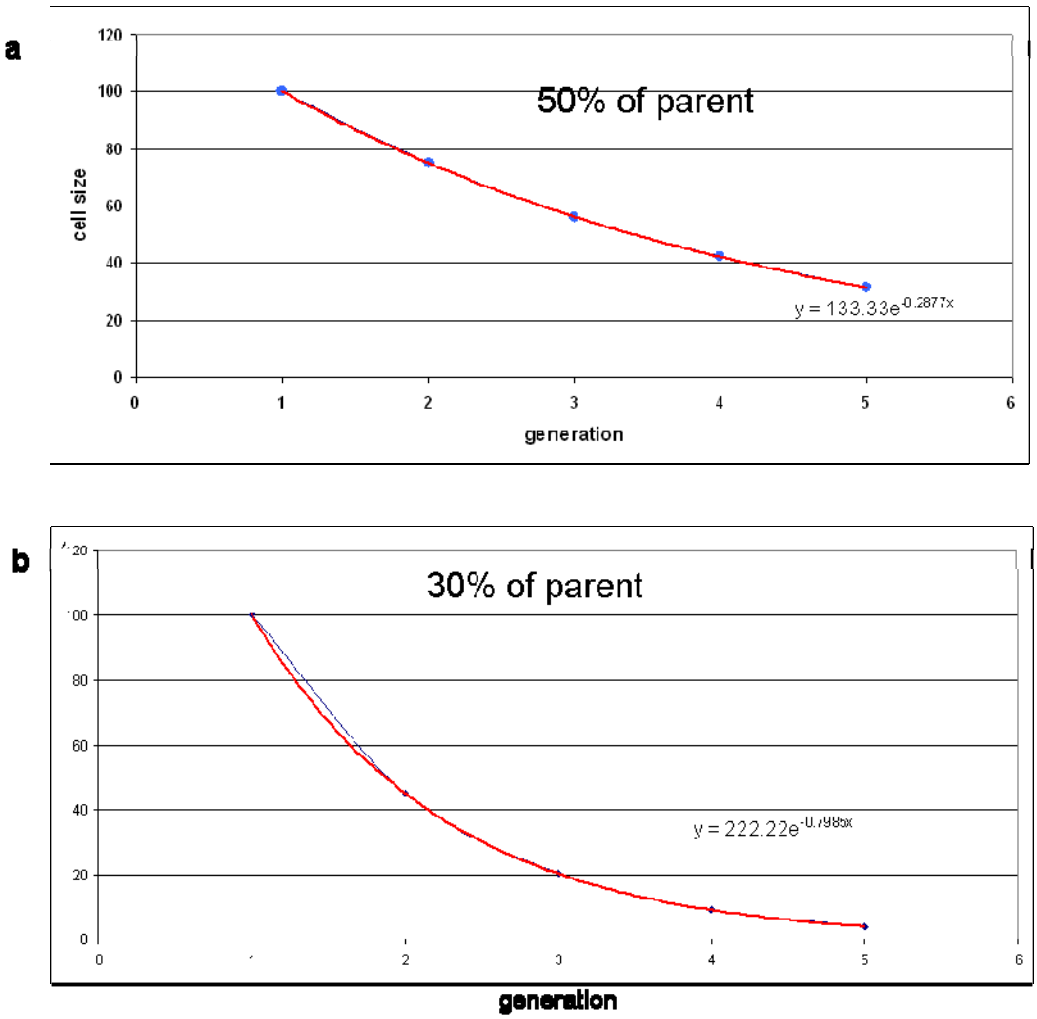

Figure 4. 10. Dividing at less than twice birth size reduces cell size. The theoretical decrease in cell size at the time of division if cells divide at 1.53 times their original size. a) cells dividing symmetrically b) cell divide asymmetrically so the smaller daughter is 30% of the parent cell.

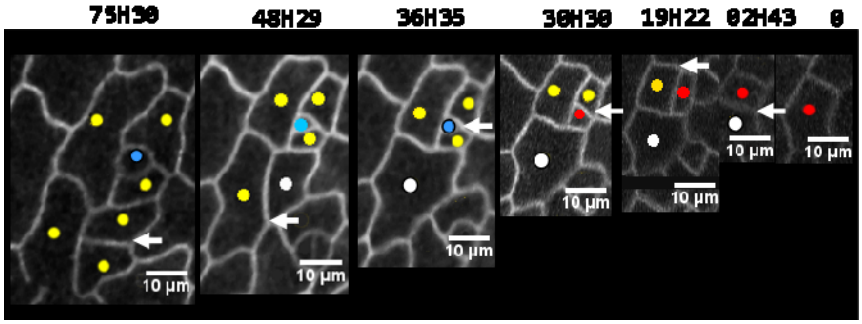

Generation	6	5	4	3	2	1
Real time		27h01 8h59	11h54 6h36	6h05 6h05	11h08 3h55	16h39 4h00
Division area	274µm²	442µm²	45µm²	70µm²	140µm²	179µm²
Previous area	192µm²	380µm²	25µm²	64µm²	124µm²	165µm²
Daughter area	136µm² 142µm²	148µm² 301µm²	13µm² 34µm²	27µm² 44µm²	44µm² 94µm²	80µm² 106µm²
Creation area	148µm²	106µm²	27µm²	44µm²	80µm²	

Figure 4. 11. **Division data for a lineage with a Q cell.** Displays the same information as Figure 4. 8 but for a different lineage that contains a dividing Q cell. Q cells divide at larger areas than P_1 cells.

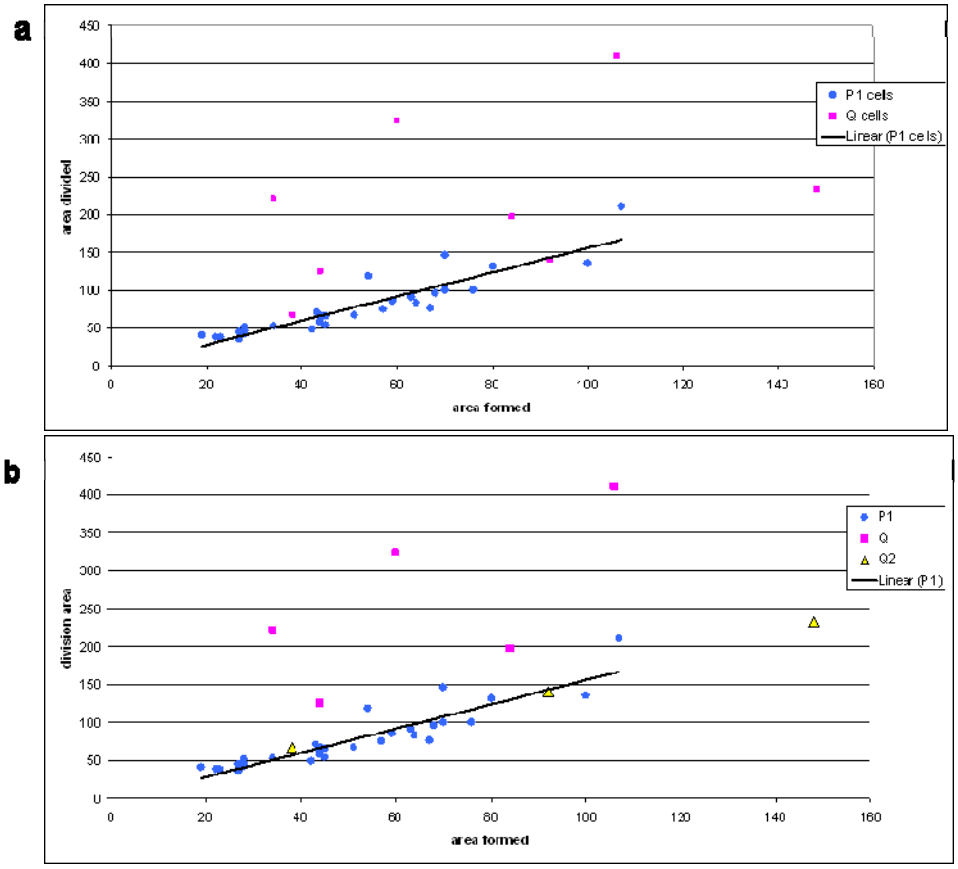

Figure 4. 12. Comparing the size a cell is created to the size it divides at. Plotting the division ratio for P and Q cells. (a) shows Q cells lie above and on the line. b) the Q cells that lie on the line are Q cells that have already divided, referred to in the legend as Q2 cells. P cells are shown as blue circles, Q cells as purple squares and Q cells that have divided previously as yellow triangles.

4.2.3 P_1 cells divide physically asymmetrically

P_1 cell divisions can be further characterised by looking at the relative sizes of the daughter cells produced. The measurements were made in the first frame captured after the division but there could be changes in the area of the daughter cells since they divided. I assume the difference in growth rates between two daughter cells is small enough that changes in the area in the time between them dividing and being measured will be similar. Therefore the measurements from the first image after division are an estimate of the ratio of the areas of the daughters at the time of division. Figure 4.13 shows the sizes of the daughters produced by the division of the P_1 cells in two of the lineages. The percentage of the smaller cell to the total is coloured based on the classification of the smaller cell. In all cases the daughter cell which acquires P_1 cell fate is smaller than its sister cell, except for the division in generation 2 of Figure 4.13a where both daughters have the same size. Figure 4.14 shows two cell lineages with Q cells; these cells also produce daughter cells of different sizes. In all cases where a P_1 cell is produced it is the smallest daughter cell. In Figure 4.14a generation 5 a Q cell divides to produce a Q cell and a B cell, the Q cell (which by definition will go on the divide) is the smallest cell. This is also true for the other lineage where the Q cell divides multiple times (Figure 4.S8). 4.S10-13 shows the same measurements for the other cell lineages. The degree of asymmetry varies for both P_1 and Q cells: the small cell ranges from 26-45% of the progenitor. In this data set the P_1 and Q fate is inherited by the smaller cell. This supports the idea that Q cells might be a form of P_1 cells. It also means that competence to divide is consistently inherited by the smaller daughter cell which is in contradiction to a threshold area for cell division which would see the larger daughter divide first.

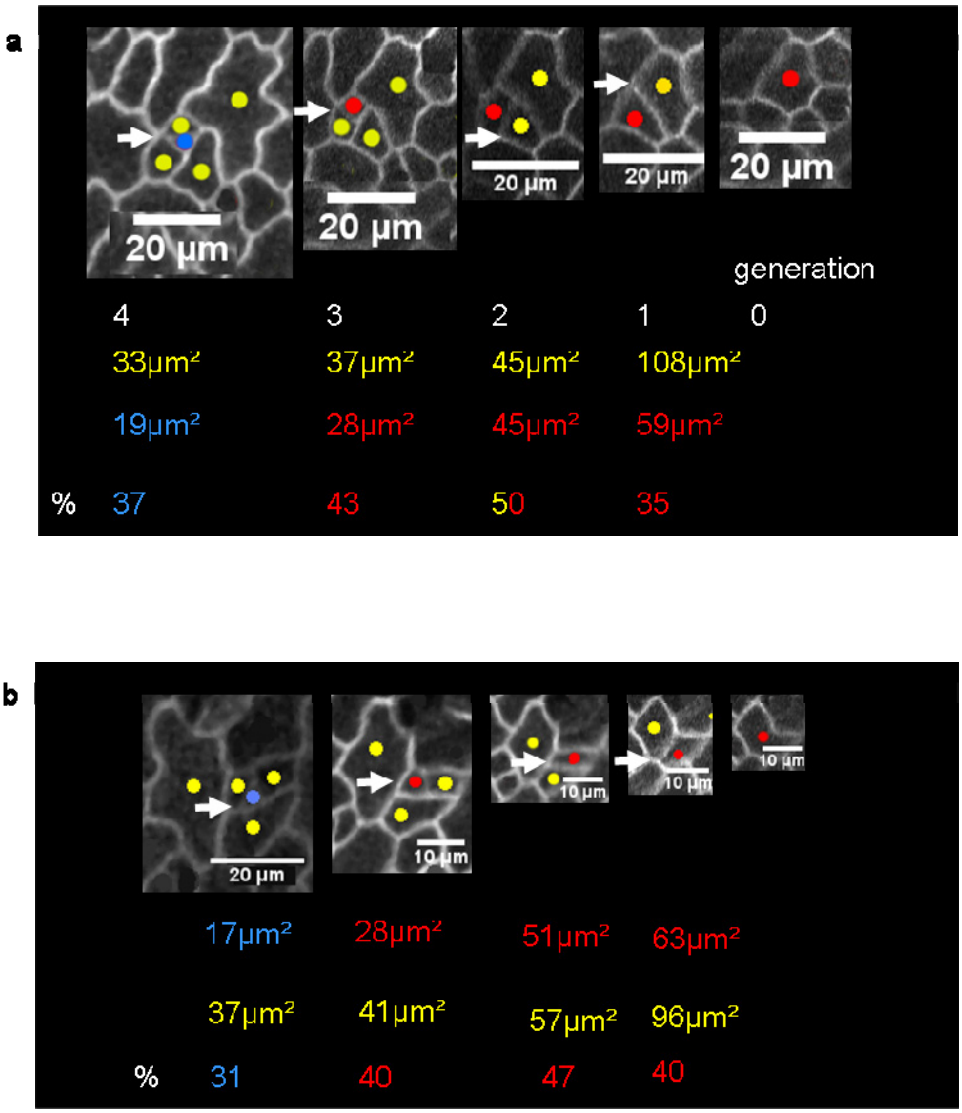

Figure 4. 13 P_1 cells are smaller than B cells when they are produced. Observed cells are coloured based on their classification. New division walls are marked with arrows. The area of the red cell is shown in red and the area of the yellow daughter cell is in yellow. The percentage size of the smallest daughter relative to the whole cell before division is shown. The colour shows which of the cells was the smallest, if the daughters have an equal size then the percentage is shown in both colours as is the case in (a) generation 2.

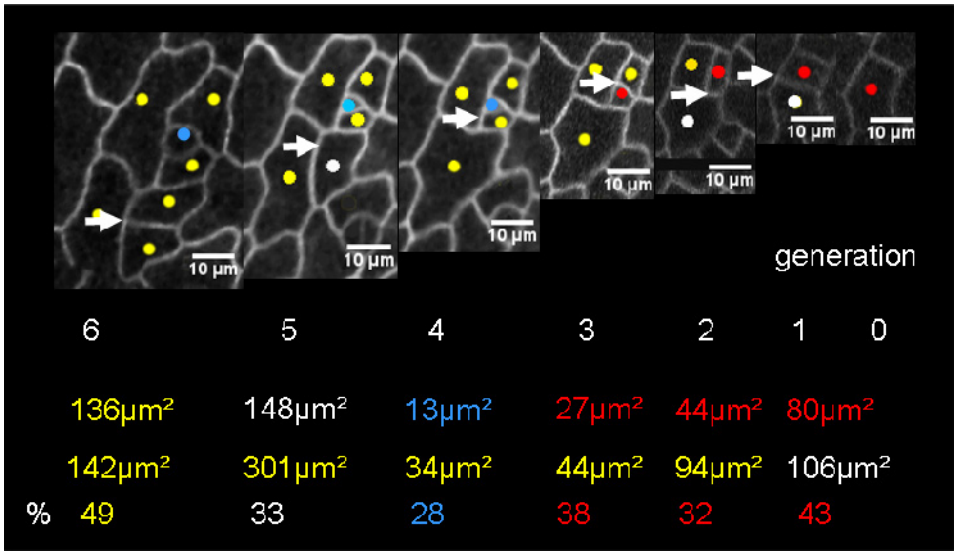

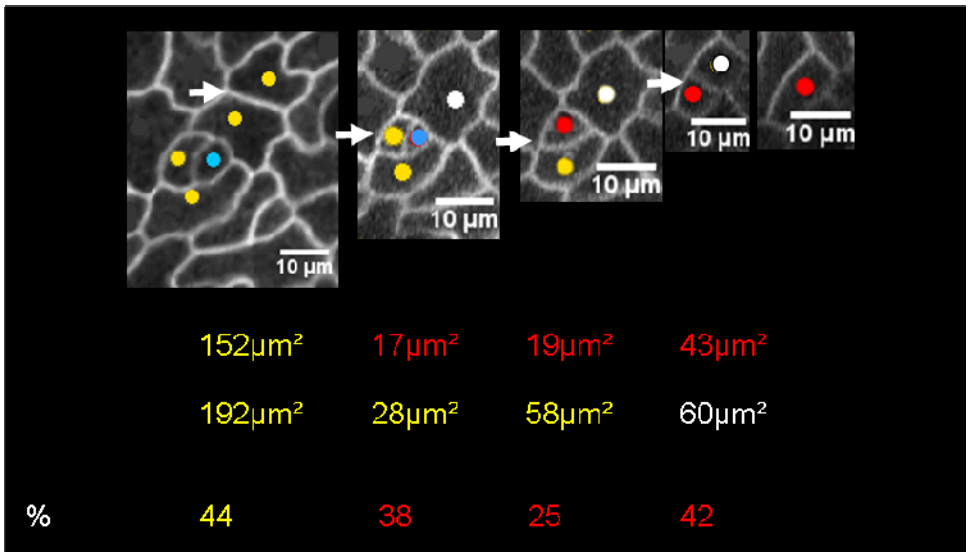

Figure 4. 14 The size of daughter cells of lineages with Q cells. This figure is the same as Figure 4.13 but the lineage has Q cells (white).

P_1 cells do not divide through the cell centre

We saw in the previous chapter that the divisions in the *spch* mutant went through the centre of the cell. However, the division wall of some wild-type cells was not through the centre. It has been shown that prior to the asymmetric division in MMC and meristemoids that the cells nucleus and cytoplasm is displaced from the centre of the cell (Zhao and Sack, 1999). I examined the position of the cell centres in some of the P_1 lineages and found that they were slightly shifted from the centre but only by a small amount (Figure 4.15).

There is another crucial difference between the divisions in the stomata lineage and the non-stomata forming cells. The division walls sometimes join adjacent walls. Eleven of the twelve lineages followed had at least one division that joined two adjacent walls. In all cases this division was the final division seen (Figure 4.16). Therefore the division of P_1 cells differs from the division of the *spch* mutant cells in that the division does not go through the centre, does not join adjacent walls and does not divide the daughter cells equally.

4.2.4 P_1 cells are internalised

So far we have considered the size and lineage of cells, but ignored their spatial arrangement. Stomata are known to be spaced apart by at least one non-stomata cell so their spatial arrangement is likely to be important. We can study the arrangement of cells in the lineages by classifying the possible configurations they could have adopted. First I will focus on the local arrangement of cells and not consider how their orientation relates to neighbouring clones. Figure 4.17 shows a representation of a dividing, P_1 cell. In generation 0 the cell has two planes of symmetry. When it divides the cell on the left or the right could become the P cell and there would be no affect on the final arrangement of cells in terms of local neighbourhood.

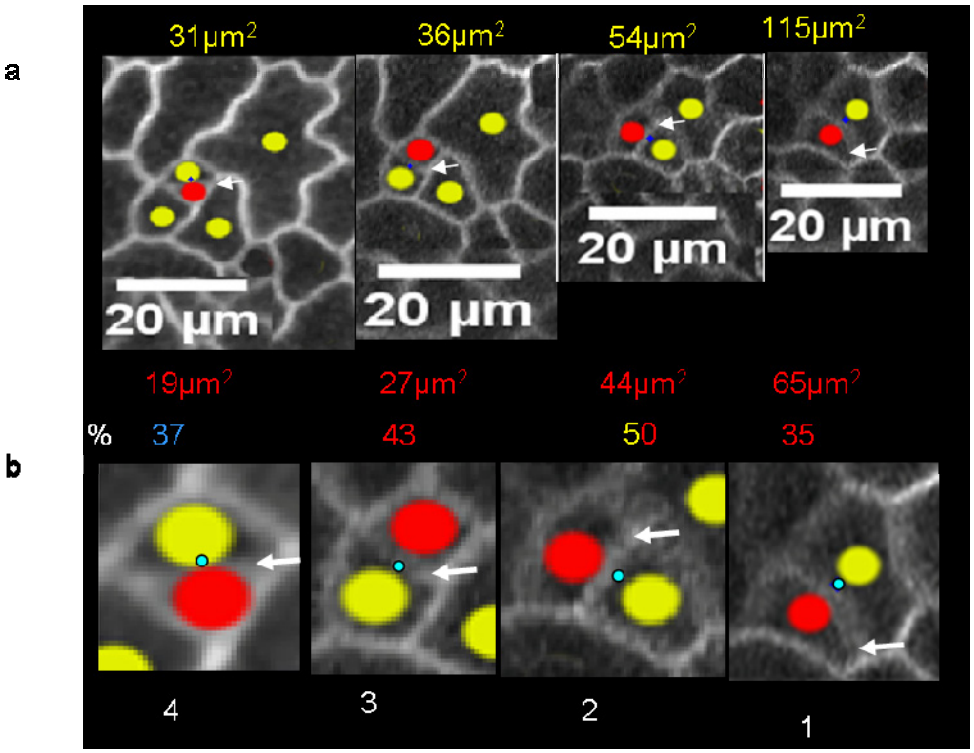

Figure 4. 15 Does the cell division wall pass through the centre of the cell? a) observed cell lineage. The new walls are marked with white arrows. The centre of the cell is marked with a blue circle. The area of the daughters are shown, coloured based on their classification. The percentage of the smaller cell to the parent is coloured based on the classification of the smallest cell. b) is a close up of (a). The new division wall is close to the cell centre but does not bisect it.

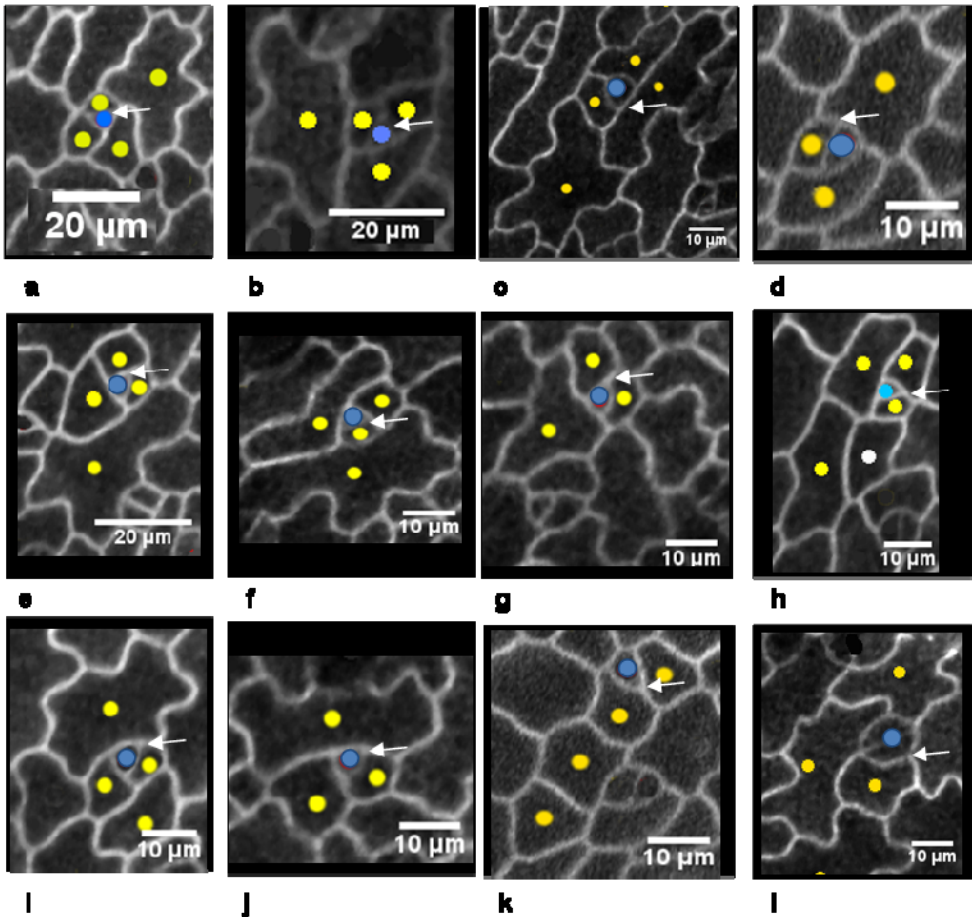

Figure 4. 16 The final division wall often joins adjacent walls. Shown in blue is the A cell of the lineages. In some cases the cell has not become a GMC yet but an earlier image was used to better show the new division wall. The last division wall that created this cell is marked with the white arrow. In all cases a-k this new wall joins adjacent walls in the original cell. In k the division is unusual but it seems that the adjacent walls are also joined. The final cell (l) is an example where adjacent walls are not joined.

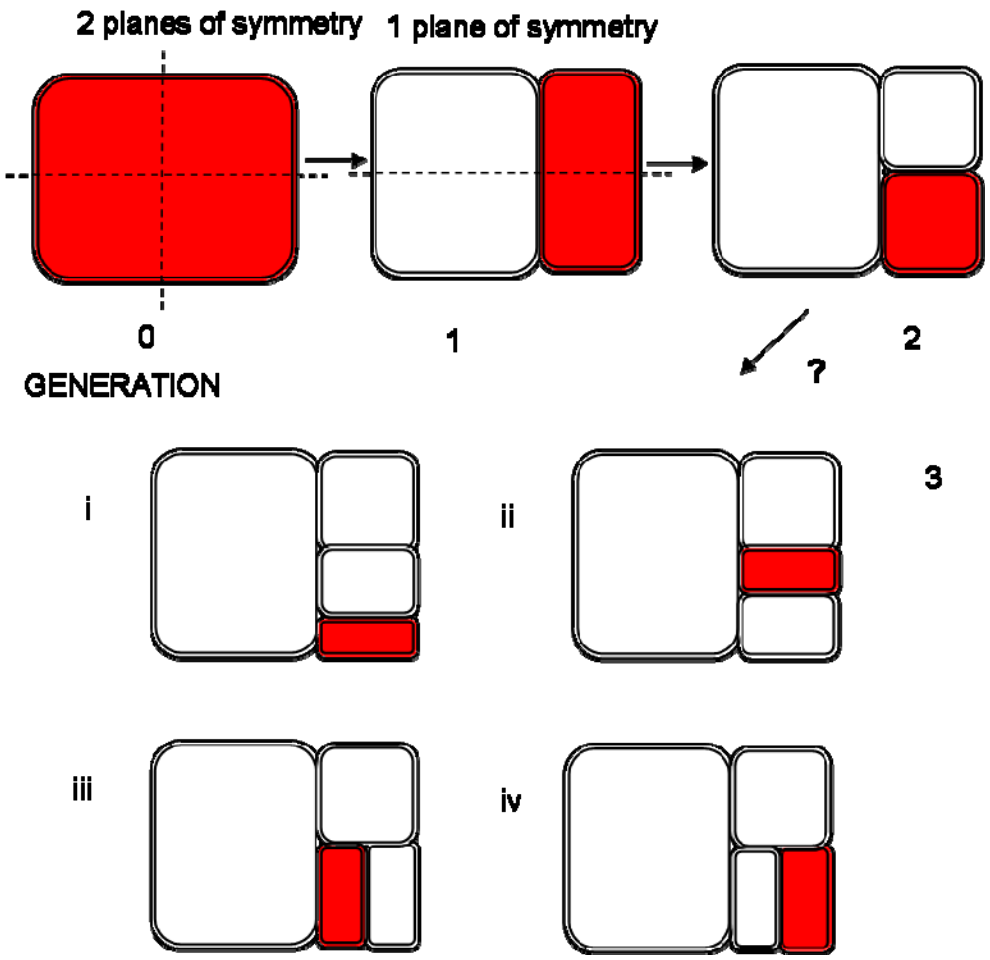

Figure 4. 17 Spatial orientation of the daughter cells. If we consider a cell lineage in isolation we can look at the spatial arrangement of daughter cells. In generation 1 and 2 either daughter can become the smaller P_1 cell (red) as the system is symmetric. However, at the 3rd generation the symmetry is broken. A decision must be made as to which cell becomes the P_1 cell, there are 4 possibilities (i-iv).

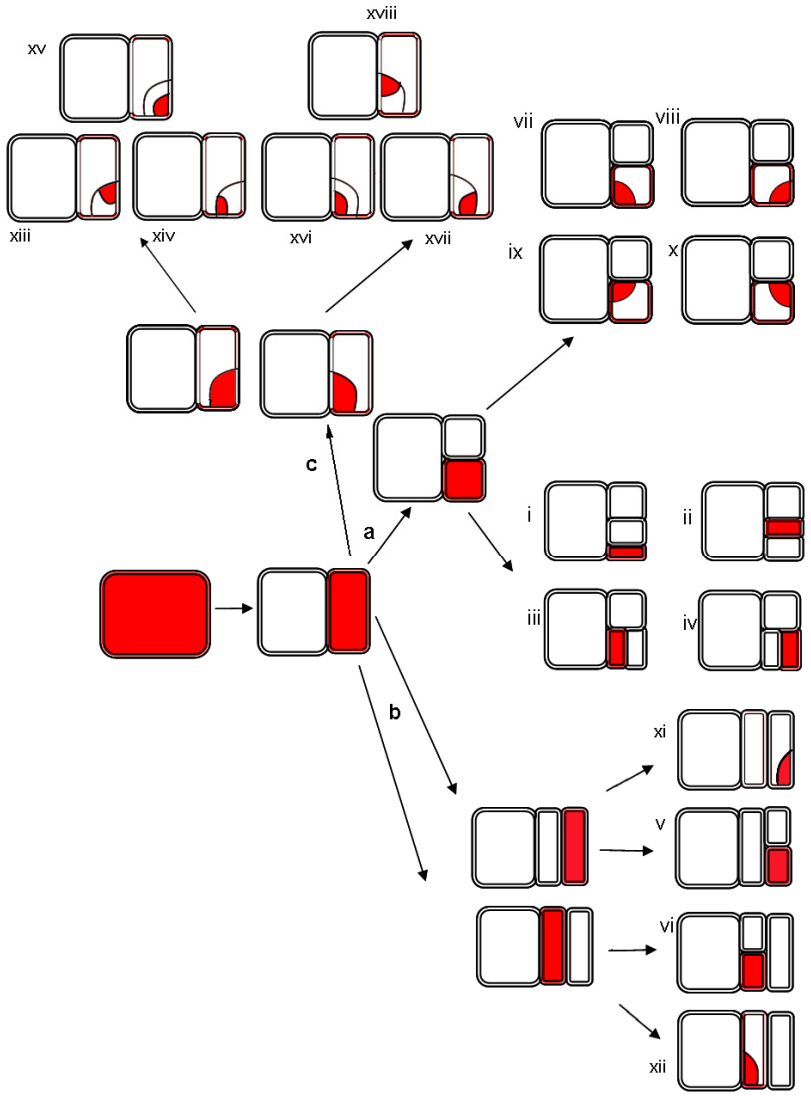

Figure 4. 18 More spatial orientation of the daughter cells. Figure 4. 17 was actually a simplification. If we consider that the cells could divide in three orientations a b or c. Within pathway (a) there are the 4 options (i-iv) previously shown in Figure 4.17. Additionally if the cells divided to join adjacent cells there are four more options (vii-x). In pathway (b) there are four possible arrangements (v, vi, xi and xii). In pathway (c) there are six possible arrangements (xiii-xviii).

The first division reduces the symmetry to one plane, perpendicular to the division orientation. The second division removes any symmetry in the system. So, from the third division onwards different arrangements of cells are created depending on which daughter cells becomes a P_1 cell. The possible configurations that could occur are labelled **i-iv**. It is possible to tell them apart based upon the number of walls the P_1 cell has that are on the exterior of the clone. In option **i** and **iv** the P_1 cell has two external walls and two internal wall. The P_1 cell in option **ii** and **iii** has one external wall and three internal. Options **i** and **iv** differ in terms of the division orientation, as do options **ii** and **iii**. This is actually a simplification, in actual fact there are more variations available (Figure 4.18). If in the second generation the division was in the other orientation (lineage b) then there would be two additional outputs possible (**v** and **vi**). The observation of stomata divisions showed that the new wall can join adjacent walls as well as opposite walls. This opens up more possibilities (**vii-x**). There are ten possible unique configurations from three rounds of division.

I looked at the data to asses which options were more commonly chosen. Figure 4.19a shows an example cell lineage. In this case generation 3 is the point where the 'decision' has to be made. The P_1 cell fate could either be adopted by the upper cell (option **iii**) or the lower cell (option **iv**). The orientation of the division excludes options **i** and **ii**. Option **iii** is the one that is observed. At generation 4, there are more possibilities. The P_1 cell now has two positions **α** and **γ** that have no external walls. They differ only in whether they contact the oldest cell or more closely related cells. This cell lineage places the P_1 cell so that there is no contact with the oldest cell. Figure 4.20 shows another 5 examples of simple cell lineages. All lineages exhibit the same arrangement of cell as the cell in Figure 4.19, i.e. option **iii** and **α** are chosen. They not only positioned the P_1 cell in the same place but they also divided in the same orientation with the new division wall in the alternative plane to the previous one. Figure 4.21 shows another four lineages that went through one less round of divisions. Two of the lineages chose option **ix** while one lineage chose option **iii** and one **xviii**. The lineage (d) shown in Figure 4.21e did not internalise the P_1 cell we can speculate that this lineage may have divided again outside the imaging window. Figure 4.22 shows the remaining two lineages. These two lineages are the only ones to have two successive divisions in the same orientation. We can postulate that this is due to the cells having an elongated shape.

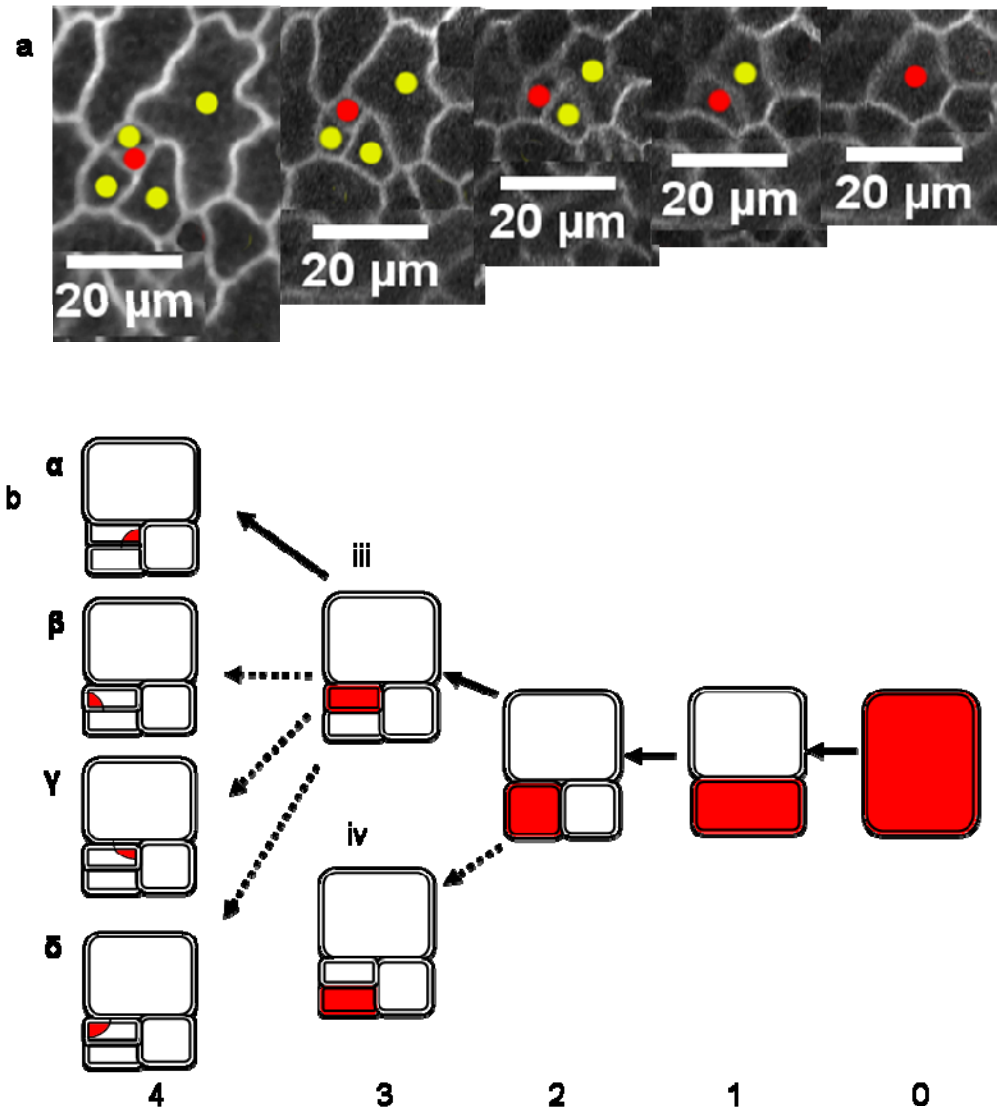

Figure 4. 19 Which arrangement did the observed cells choose? a) a cell lineage. b) the diagram of the decision points. Based on the division orientations there are two options available in generation3. Option (iii) rather than (iv) is taken. (The numbering is kept from Figure 4.18.) Generation 4 sees another decision point; option α is taken

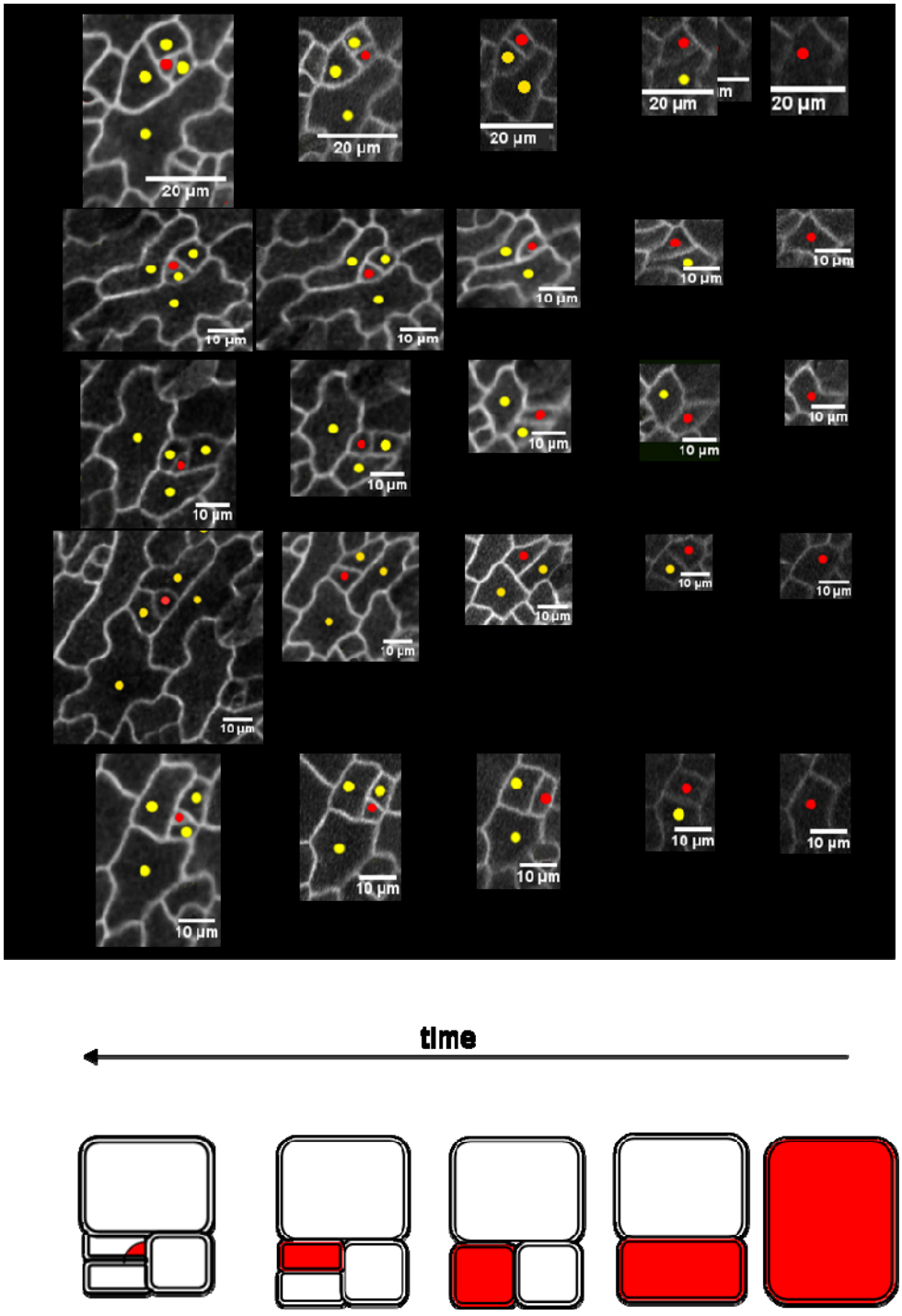

Figure 4. 20 Many lineages have a similar arrangement of cells. These lineage all have a similar arrangement as the cell in figure 19 option (iii) and **α**.

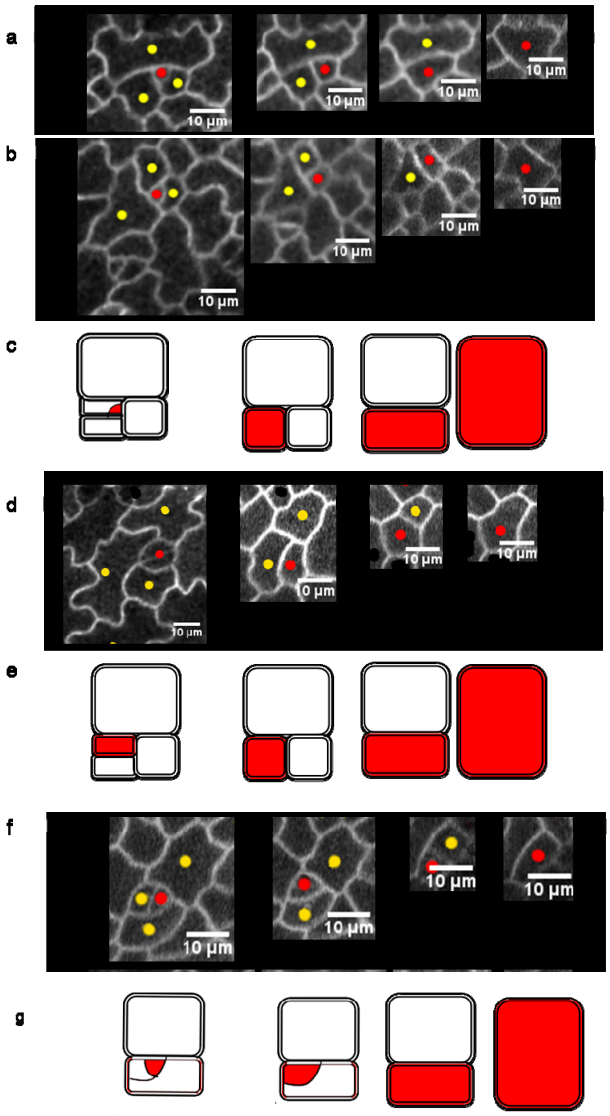

Figure 4. 21 The arrangement of cells in lineages with fewer rounds of division. The lineages a-b have the arrangement (ix) from Figure 4.18 and internalised their P_1 cell in one less division. Lineage (d) has arrangement (iii) but did not divide again before differentiating. (f) has arrangement xviii and can also internalise in one less division.

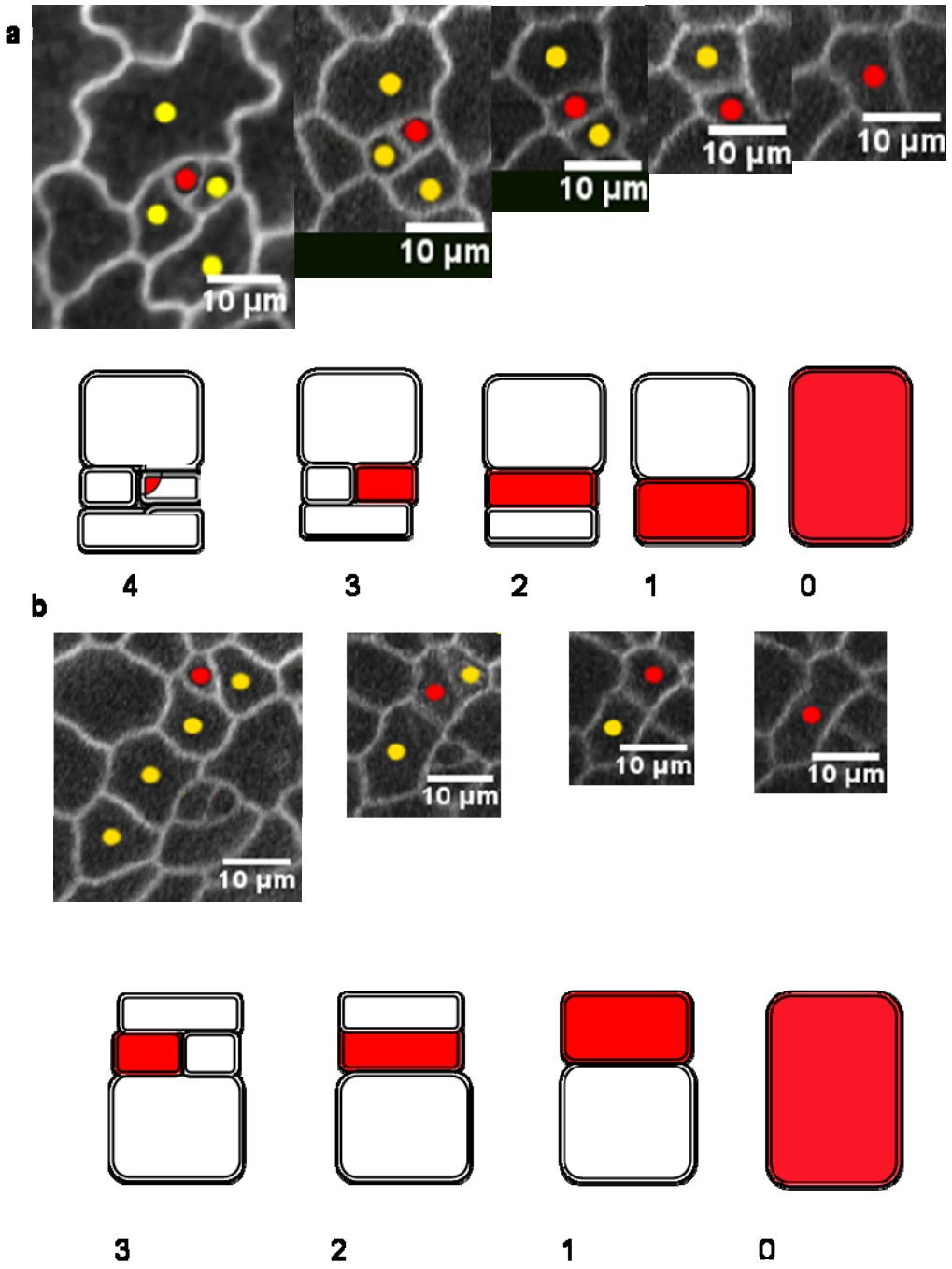

Figure 4. 22 Some lineages divide twice in the same orientation. These lineages took pathway (b) from Figure 4.18 and chose option vi. a) went on to divide again to internalise the cell. Lineage (a) is more clear, (b) divided in an intermediate way and is difficult to classify.

They chose option **vi.** Figure 4.22a is still able to internalise the red cell although it is in contact with the oldest cell of the clone. The orientation of divisions and the final arrangement of cells in the lineage in b is harder to classify but the red cell is not internalised and the division orientation in generation 2 and 3 are neither perpendicular or parallel to the previous ones.

From the eighteen possible options presented for the first three rounds of division only four are chosen, **iii**, **vi**, **ix and xviii**. These options have a commonality in that they all minimise the number of external walls the P_1 cell has. The choice of **vi** over the others seems to be a consequence of the shape of the mother cell. However, if the lineages that chose **iii** had chosen **ix** they would have internalised the cell. Instead they divided again, all choosing the **α** pathway resulting in the P_1 cell being internalised.

Overall 10 of the 12 lineages internalised the red cell entirely in the time they were observed and they achieved this by a limited set of possible arrangements and division orientation.

This analysis ignored Q cell divisions for simplicity. In the cases where the Q cell divides many times the Q cell is the oldest cell in the clone. In the cases where the Q cell does not divide it is the second oldest cell in the clone that divides. However, there are such few cells the significance of this result is unclear.

4.3 Modelling

4.3.1 Building a basic model

Wild-type cells divide differently to cells in the *spch* mutant. I investigated what needed to be added to the *speechless* model to create this behaviour. Just as in the previous chapter I created a model where cells grow exactly as they did in the biological tissue. Figure 4.23a shows a lineage of cells used to drive the growth of the model. The growth occurs by an interpolation of the initial vertices first and final positions (see methods). Initially I specified that all cells divide using the shortest path through their

centre of mass upon reaching the threshold area as before. Here we see that this basic model can produce a clone of cells from one cell (Figure 4.23b). New points are not used in the growth so the clone does not have exactly the same shape at the end. A comparison of the divisions shows that using the threshold area used for the *spch* mutant patch does not produce enough divisions. Lowering the threshold area produces more divisions (Figure 4.23c), however, they do not resemble the real cells. The model cells are too uniform in size. This model provides a starting point to investigate the minimum extensions necessary to account for the wild-type behaviour.

4.3.2 Modelling different cell fates

The basic model has one cell type. However, the retrospective analysis classified cells in the epidermis into many different types. The simplest cell lineage had three cell types, A cells that represent GMCs, B cells that did not divide and P_1 cells that divided to produce a P_1 cell and a B cell.

4.3.3 Modelling P_1 cells stem cell behaviour using the inherited threshold model

The simplest model to consider P_1 cell behaviour would be one with two cell types, B and P_1 cells. I therefore introduced a cell-type to the model cells. This type was specified in the form of a Boolean attribute so a cell is either true or false for the P_1 cell type. B cells are cells that do not have the P_1 cell type. I specified that cells start as P_1 cells as in the retrospective analysis. When we run the model the P_1 cell will divide. In the tracking data the P_1 cell fate was inherited by one daughter.

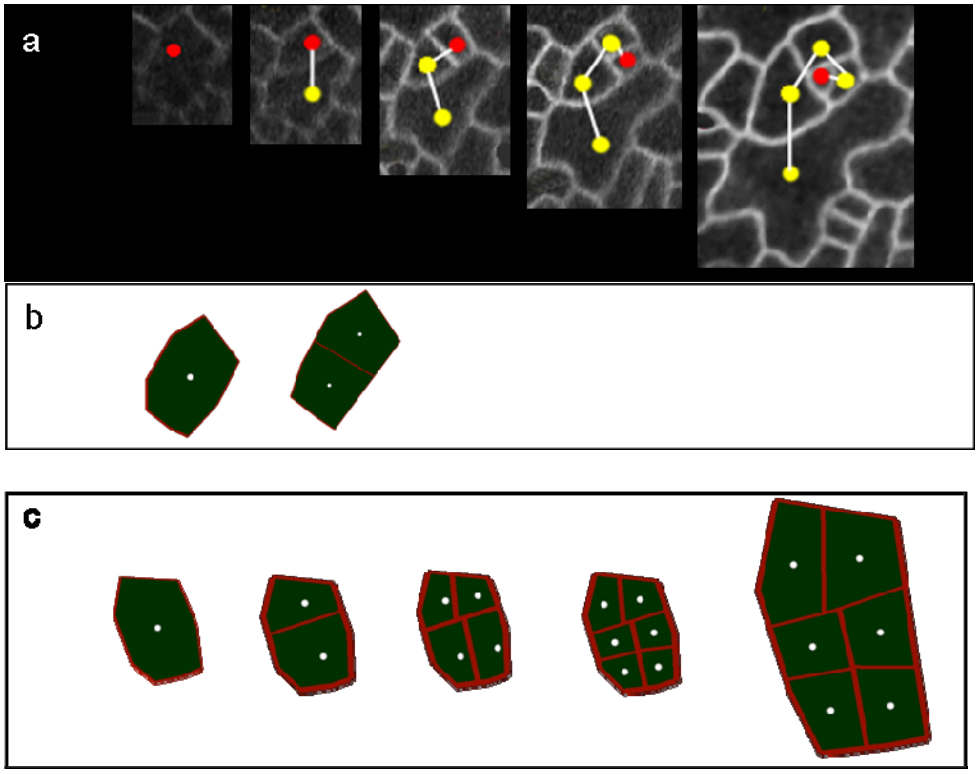

Figure 4. 23 Applying constant area threshold model to wild-type cells. a) The observed cell lineage. b-c) The digitised version of the lineage is used to drive the growth of a model. b) cells are divided when they reach a threshold area of 250μm² (the threshold for the *spch* mutant model). The clone only divides once. c) a lower threshold induces more divisions but the model still does not resemble the observed cells.

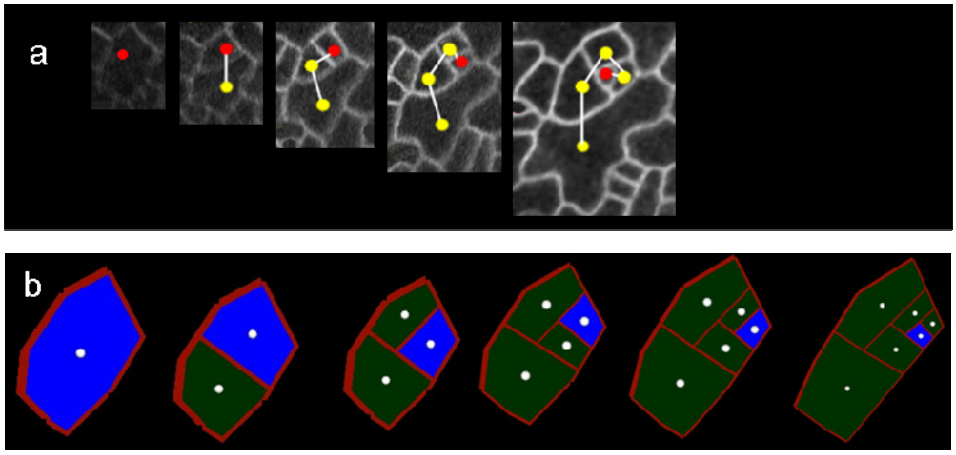

Figure 4. 24 The inherited threshold model The same linage (a) as in Figure 4.23 was used to drive the model. (b) P1 cells (blue) divide at a lower area threshold. Which daughter becomes a P1 cell is determined randomly and the divisions are symmetric. The range of cell sizes is more similar to the observed cells but the arrangement is not.

We therefore need to produce one daughter cell that is positive for the P_1 cell type and one that is negative. Initially I randomly assigned which daughter became a P_1 cell. The data showed it is the P_1 cell that will divide again, so we need to introduce this into the model. Currently both daughter cells have the same area-threshold for division, so assuming the division was symmetric and growth uniform, they will both divide at about the same time. I changed the model by lowering the area-threshold for division of the P_1 cells to a fraction of the size of the other cells. This is the **inherited threshold model**. The lower area-threshold for division is inherited with the P_1 cell fate. Figure 4.24b shows the result of this model. Cells of different sizes are produced as the P_1 cells divide multiple times before the other cells divide again. Comparing this output to the real cells in Figure 4.24a the model output already looks better than in Figure 4.23. However, unlike the real cells the divisions in the model are not physically asymmetric and the P_1 cells are not internalised.

4.3.4 Creating a physically asymmetric division

The P_1 cells divided physically asymmetrically so I wanted to add this to the model. As all cell divisions must go through the nucleus of the cell one hypothesis is that asymmetric divisions can be created by moving the nucleus away from the centre of the cell (Figure 4.25a-b). In meristemoids and MMCs the nucleus and cytoplasm is displaced from the centre (Zhao and Sack, 1999). Moreover, if the nucleus is moved, using optical tweezers, at the right time in yeast the new division wall is also shifted (Tolic-Norrelykke et al., 2005). The tracking data shows that the division wall of the cells is only shifted a little from the cell centre. So I wanted to establish whether the small movement of the division wall away from the centre as observed in the data could create the asymmetry. Figure 4.25c shows the consequence of displacing the nucleus by a small amount in a rectangle that is 10 by 20 units large. A 2 unit shift represents 10% of its length. This movement reduces the area of the smaller cell to 40% of the parent. This change in area can be created without even considering that in many cases the nuclear movement would actually change the orientation of the division plane. As the nucleus moves away from the centre of the cell the shortest path through it will change from joining opposite walls to joining adjacent walls creating, in most cases, an even

smaller cell Figure26a illustrates this. The exact point where this switch will occur or its effect on area is difficult to solve explicitly. However, we can simulate it using a square that grows and has a global vector that moves the nucleus in the diagonal direction. Figure 4.26b shows the plot of the area of the smallest daughter against the distance moved. The graph has a break in it where the switch occurs, but the effect of moving the nucleus is linear either side of the break. We saw previously that 11 or the 12 lines had divisions that joined adjacent rather than opposite walls (Figure 4.16). This result suggests the shape of the cells and their asymmetry could be generated by the same mechanism. This result can also explain the three different arrangements chosen by the cells. Cells that chose option **iii** rather than **ix** may have had a more centrally located nucleus.

It is worth noting that the other division algorithms would not display this phenomenon. If the cells were being divided using the shortest growth tensor algorithm then the cell division could be made asymmetric by moving the nucleus but the division wall would not join adjacent walls unless the cells growth tensor was aligned with the corner. The closest wall algorithm would also never create the diagonal wall as, as it is defined currently the wall must connect the opposite wall. Thus, although I was unable to prove that the shortest wall was the only possible division algorithm to explain cell division in the *spch* mutant, its properties make it an attractive model and it will be the focus of the rest of the chapter.

4.3.5 Modelling physically asymmetric divisions

We have seen how moving the division plane can generate physically asymmetric divisions. But, what happens if we apply this in successive rounds of division? I represented a cell as a rectangle and expanded it with a simple growth tensor matrix aligned to its axis. I specified an inheritance of P_1 cell fate with an associated lower threshold for cell division. If we run the model we see that the cells divide symmetrically through the centre of the cell (Figure 4.27a).

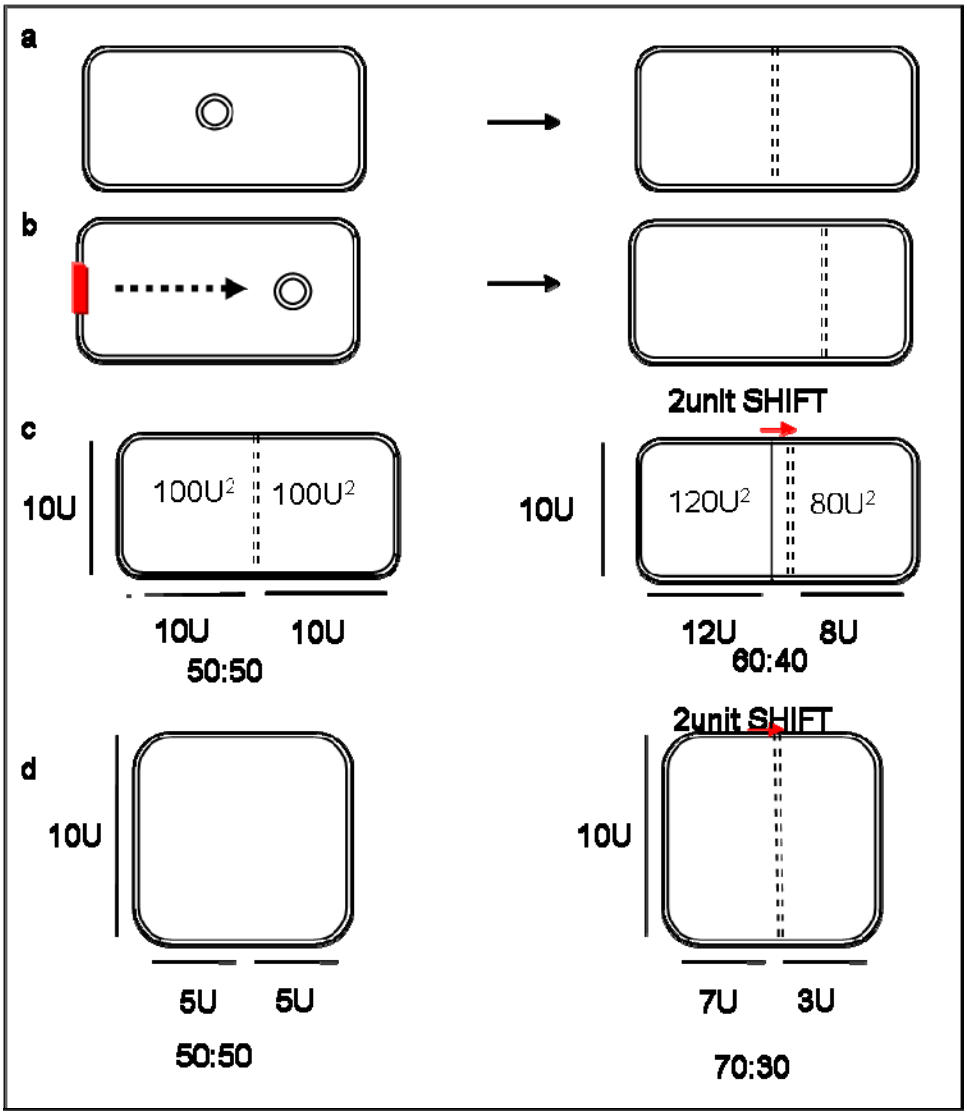

Figure 4. 25 A physically asymmetric division can be created by moving the nucleus away from the centre. If the nucleus remains in place the division will be in the centre and, depending upon cell geometry will create a symmetric division. By contrast if the nucleus is moved by a repelling factor (red) the resultant division will be asymmetric (b). The movement does not need to be very large if the centre is moved 2 units in a cell that is 10 units by 20 units the ratio shifts from 50:50 to 60:40 (c). If the shape is square then the same 2 unit shift moves the areas to 30:70 ratio (d).

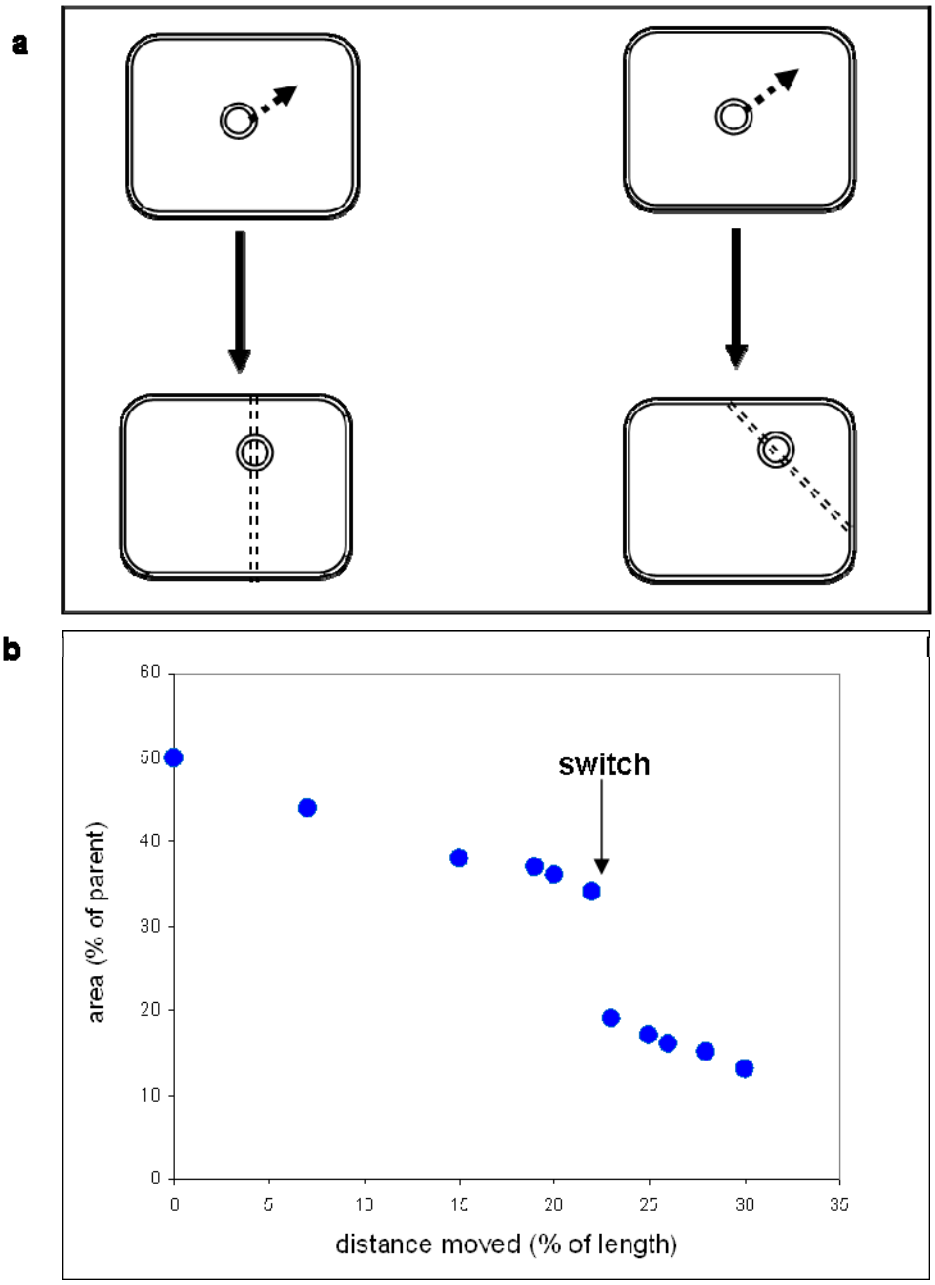

Figure 4. 26 Moving the nucleus can change the division orientation. Moving the nucleus displaces the division wall until the point where a diagonal wall is shorter at which point the wall joins two adjacent walls (a). This switch can be shown by running simulations and plotting the area of the smaller daughter as a percentage of the parent (b). The switch gives a break in the graph.

We can now specify a direction along which we move the nucleus. If this direction is the x-axis, then the nucleus moves along the length of the cell. When the time comes to divide, the nucleus is not in the centre of the cell and therefore the division is asymmetric (Figure 4.27b). In this model the cell is growing twice as much in the x – direction as the y-direction. If the direction of movement of the nucleus was in the y direction it would not alter the symmetry of the division as the division will be perpendicular to the x-axis according to the shortest wall algorithm. Similarly if we ran the model for further divisions we would encounter divisions where the nuclear movement had no effect. Figure 4.27c shows the position of the new division wall in subsequent divisions. The first division is perpendicular to the direction of nuclear movement therefore this division is symmetric. The next division is parallel to the direction of nuclear movement so this division is asymmetric again. This model shows that it is possible to produce an asymmetric division by specifying a global displacement direction. However, it can only produce asymmetric divisions in one direction. Although the degree of asymmetry in the divisions is variable in the observed cell they are not all oriented in one direction, therefore the model needs to be improved to better capture what we observe. One way of doing this would be to have a polarity for each cell that would ensure asymmetric divisions could be created whatever the geometry of the cell and in any direction. How would this local polarity be specified and in what direction should it displace the nucleus?

4.3.6 How to polarise a P_1 cell

A cell polarity can be defined by having something that is localised to a position on the cell membrane. We will call this factor M. We propose that the nucleus moves in a direction away from the location of M. This poses the question of where to position factor M. We have seen that the smaller cell is usually the P_1 cell and that P_1 cells are arranged to minimise their external walls. So the P_1 cells must be polarised in a way that will create the correct spatial arrangement. We can therefore propose that factor is positioned based upon spatial cues. This could work in a number of ways and we can use models to explore their consequence.

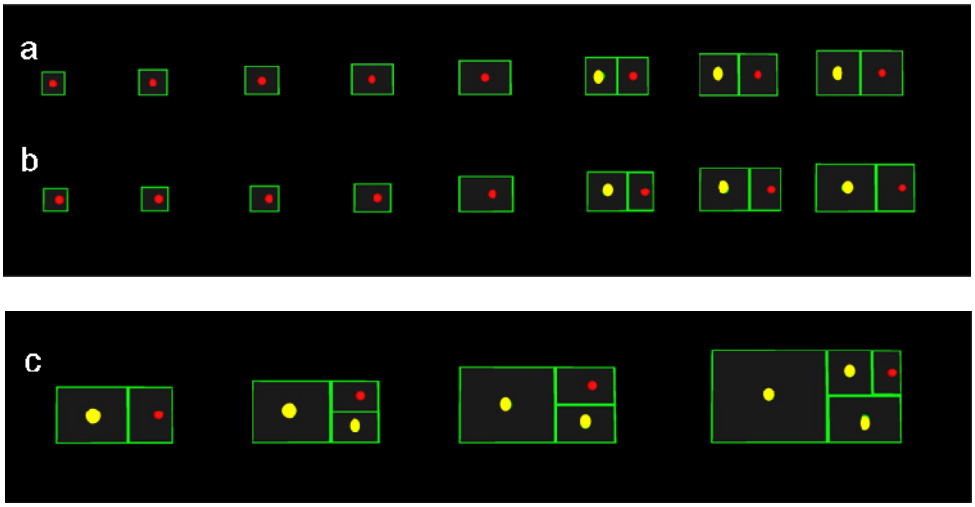

Figure 4. 27 asymmetric division can be generated by pushing the nucleus using a global vector. a) the nucleus is in the centre of the cell, b) the nucleus is displaced in the x direction by percentage of the cell length. c) the output of the model in (b) with more rounds of division. Red circles indicate P cells and yellow circles B cells.

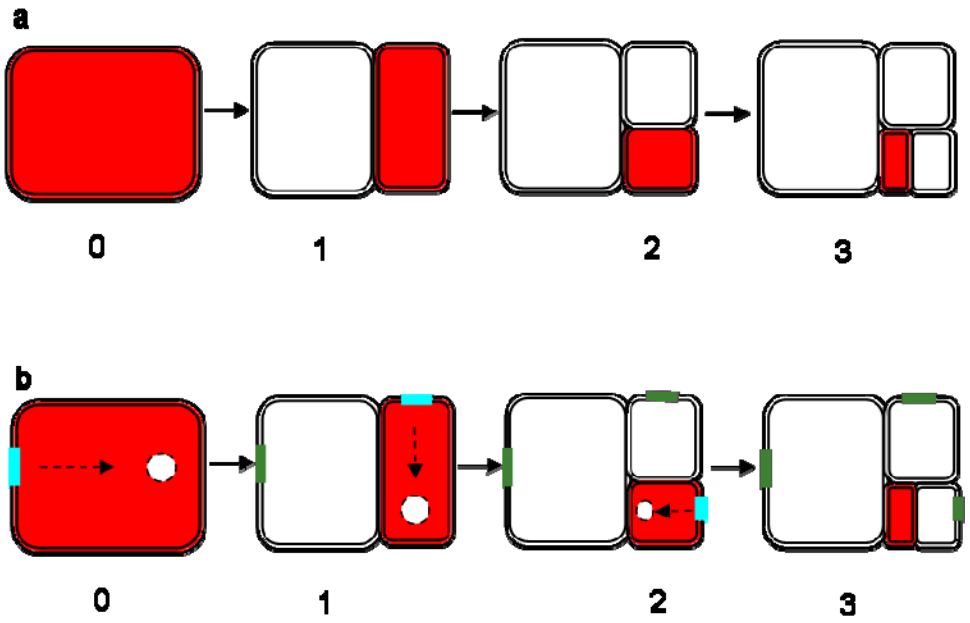

Figure 4. 28 Estimating the position of factor M. a) a typical division sequence (option iii). b) estimated position of M. New M is in blue the old position of M is in green. Dashed arrows show the direction the nucleus was pushed in.

Positioning factor M

The data showed that most lineages divided in a similar way and produced the same arrangement of P_1 cells. Figure 4.28 shows a diagram of this division pathway. Based on this pattern we can guess where M would need to be in order to create these divisions. To do this we need to choose whether we think about M displacing the nucleus away from its location or towards it. I chose to position M as if it was displacing the nucleus away from it. In the diagram (Figure 4.28) the first division is asymmetric so the nucleus must be moved along the axis of the cell (Figure 4.28 b). If M is pushing the nucleus it must, therefore, be placed at the left side of the cell (blue). We will assume that the daughter cells are selected based upon their size (i.e. the smallest cell becomes P_1) but we will examine this assumption further later.

If we look at successive locations of M we can see new locations of M seem to be far from previous ones.

Their arrangement resembles a phylotactic like pattern. This is the arrangement of organs around a meristem so as to maximise their distance from previous organs. Modelling allows us to test whether mechanisms postulated to space organs around a meristem could be acting to position factor M. In models of phylotaxis successive organs are places as far from previous organs as possible but organs move away so the most recently placed are the most influential (Hofmeister, 1868; Snow, 1932). Smith *et al* reviewed different distance functions for placing organs in the meristem to generate robust phylotaxis patterns (Smith et al., 2006b). The simplest of these was to place organs to maximise the distance to the organs (i.e. minimise $\sum \frac{1}{d}$ where d is distance).

Other more complex functions also exist using different functions of distance or including a time element. I initially tested the simplest model by implementing an algorithm that iterates over positions along the walls of the newly formed cell. At each position the algorithm measure the distance to the location of M in the neighbouring

cells and finds $\sum\frac{1}{d}$. The point with the lowest value is selected for the new position of M. I then defined a vector from M to the centre of the cell for the nucleus to move along. If we run this simulation in place of the global direction we can see the output is much better. The cells are more asymmetric and have a better arrangement. However, the locations of M are not exactly what we predicted and the P_1 cells are not reliably placed. The problem seems to come from the placement of M on internal walls thereby pushing P_1 cell fate to the edges of the clone Figure 4.29a. Although this model could work with more complex parameters and functions, and is attractive in that it re-uses an existing patterning mechanism in this case it does not seem to robustly recreate what we see in the data. The difference between this model and the phylotaxis model maybe that the phylotaxis model assumes an active ring where the new primordia can form. This limits their production to the area where they actually appear. It is not possible to define an equivalent of an active ring in my models so I looked for an alternative mechanism.

New wall repulsion model for factor M placement

I therefore explored a mechanism where new cell walls repel M. In this algorithm a new cell places M to minimise $\sum\frac{1}{d}$ but d is now the distance to new walls. I iterate over all of the walls as before and test points along the wall. For each test point I measure the distance to test points all the walls of the neighbouring cells that are new (Figure 4.29c). We can image this occurring by a substance diffusing from the new wall, however, in the model we will just measure the distance. We also need to define new walls, for now we will consider all walls that are not external walls as new walls. This algorithm places M more like we would predict (Figure 4.29b). We can also notice that the new daughters are not only different sizes but one has parental factor M in it and one does not. This means that although we were choosing which cell should inherit P_1 cell fate based on size we could also chose based on the location of M. An alternative model would therefore see M polarising the P_1 cell to create a small cell that already knows it is to become a P_1 cell. This might be a more robust mechanism for determining P_1 cell fate when cells have complex geometries.

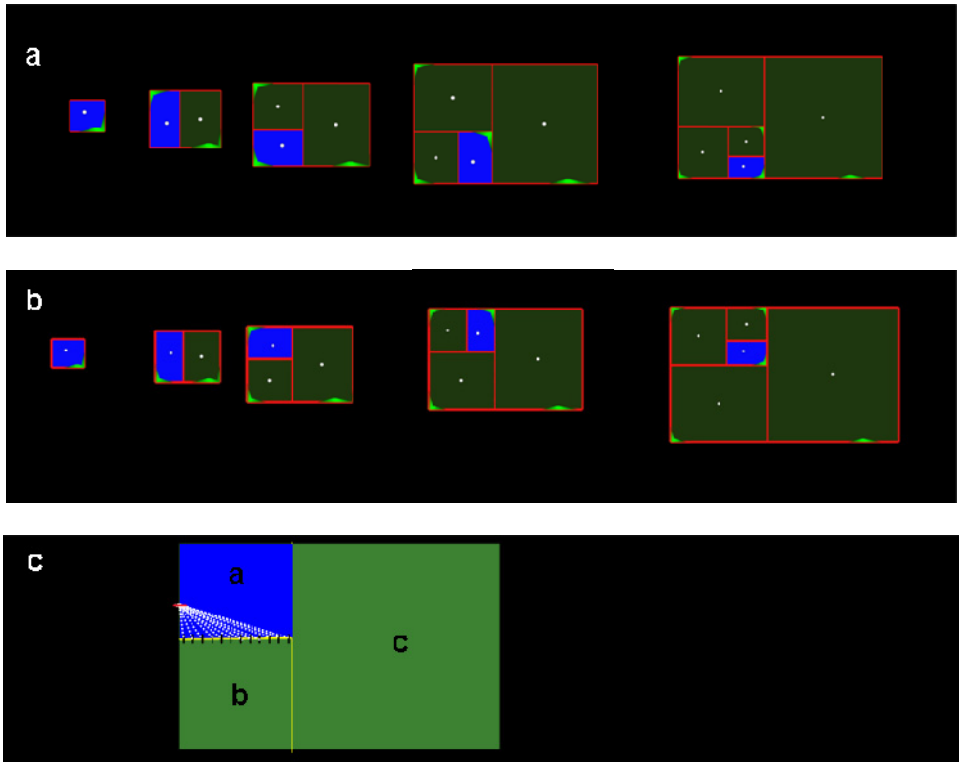

Figure 4. 29 Alternative ways of positioning M. M could be positioned as far from previous locations of M as possible in a phylotaxis like model (a). M can and is placed on internal walls resulting in the P_1 cell (blue) being places on the outside of the clone. A model that works better is to place M a far as possible from the new walls (b) which results in the P_1 cell being internalised. The placement of M by repulsion from new walls works by iterating over the walls of the new P_1 cell (blue). Points along the walls are tested. The distance from one test point (red) to all points (black) along all the new walls (yellow) of the neighbour cells b and c are measured (white lines). The sum is found and the new position of M is the place with the maximum distance from all points along the new walls.

Determining which cell becomes a P_1 cell in this way also solves another problem encountered in building this model. I assumed that after division the P_1 daughter acquires factor M. If the P_1 daughter is the one that does not contain parental factor M then there is no problem but, if the daughters are selected based on size then the P_1 daughter might contain the parental location of factor M. In this case a decision has to be made about whether to remove the existing location or not. The model was, therefore, simplified by using M to determine cell fate as well as nuclear movement. However, more biological data is needed before either hypothesis can be dismissed. Modelling simplicity does not necessarily reflect biological simplicity.

Exploring the new wall repulsion model in different simulated cells

The new wall repulsion method makes it possible to investigate how M would be placed and the resulting arrangement of cells in different conditions. The model allows us to easily change the growth anisotropy value and the amount that M displaces the nucleus. The anisotropy value is $\frac{S\min}{S\max}$ where Smax is the growth rate in the major growth axis direction and Smin is the growth rate in the minimum growth direction. In this model the nucleus is displaced along the vector defined by the position of M and the centre of the cell. The magnitude of the displacement is relative to the distance from the centre of the cell to the closest wall. This method makes it difficult to compare models, however, it ensures that the nucleus never moves outside the cell no matter what shape it has or what direction the nucleus is moving in. Varying these parameters makes it possible to create the all commonly observed arrangements of cells (Figure 4.30). Option **iii** can be created by growing the cells with an anisotropy value of 0.8 and moving the nucleus 30% of the way to the closest wall. If the anisotropy value is increased to 0.9 and the nucleus moved 35% of the distance then the arrangement seen in option **ix** can be seen. At the other extreme lowering the anisotropy to 0.5 so the cell is growing twice as much in one direction and reducing the nuclear movement to 20% can create the arrangement seen in **iv**. There are other ways to create these arrangements (Supp Fig. 4. S19).

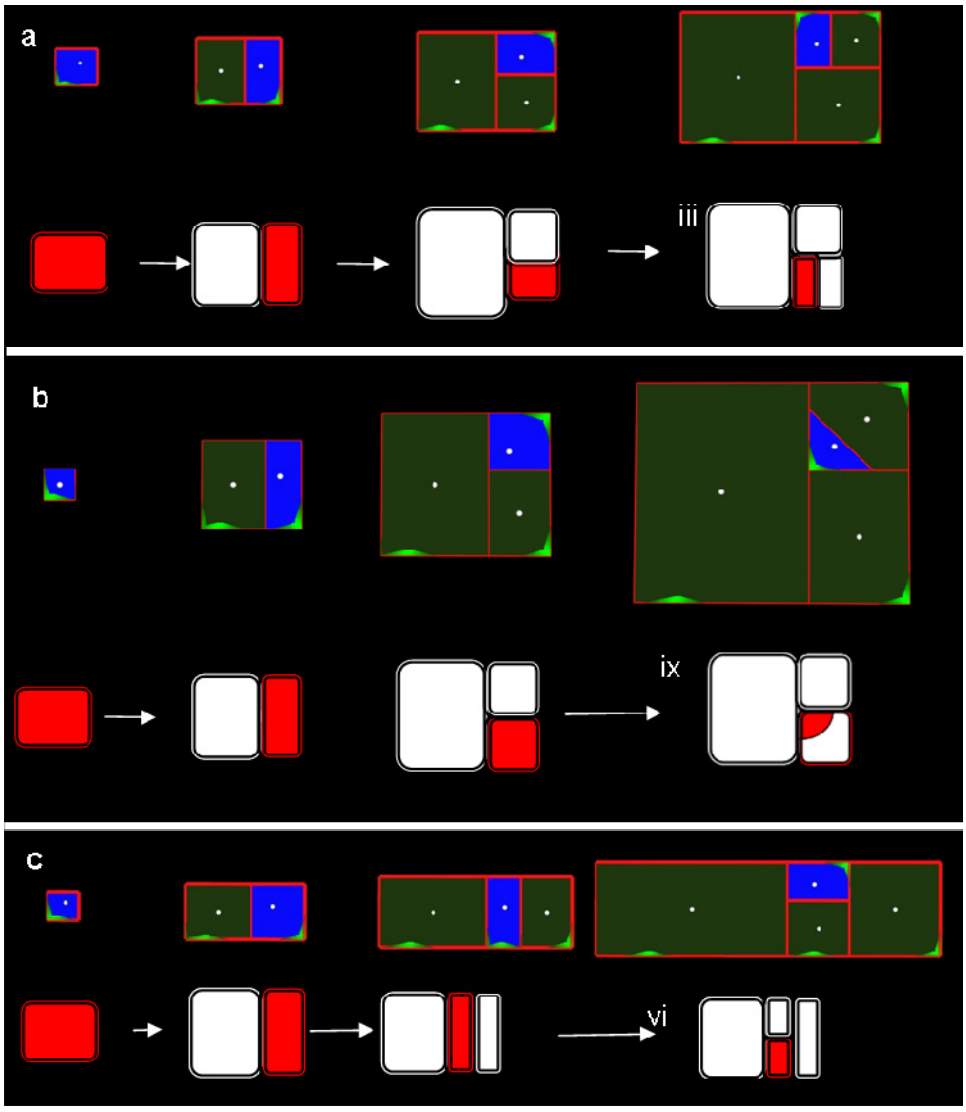

Figure 4. 30 Altering the anisotropy of the growth and the amount the nucleus can move creates different cell arrangements. The three arrangements observed in the data can be created in this simple model. a) creates the arrangement option **iii**. The anisotropy value is 0.8 and the nucleus moves 30% of the distance to the closest wall. b) creates option **ix**, the isotropy is 0.9 and the movement, 35% c) creates option **vi** and the isotropy value is 0.5 and the nuclear movement 20%.

In the previous chapter we saw that the shortest wall algorithm divides cells in different orientation depending upon how isotropically they are growing. In this chapter we saw that displacing the nucleus can cause a switch in the shortest wall algorithm from joining opposite walls to joining adjacent walls. This result suggests that the combination of different growth anisotropies and different amounts of nuclear displacement might be enough to explain the different arrangements of clonally related stomata lineage cells seen in the leaf. Arranging the cells as in option **ix** internalises the P_1 cell in fewer divisions. This may suggest regulating the amount that factor M displaces the nucleus could determine how many divisions a clone needs to internalises its P_1 cell and hence the density of stomata.

Adding factor M to the inherited threshold model

Adding factor M to the inherited threshold model where cells have the observed initial geometry and observed growth allows us to compare its effect on cell behaviour more directly with the data. Just as in the previous models M displaces the nucleus to make the division asymmetric and determines which cell inherits P_1 cell fate. Specifying different start locations for M produces different results. If we place M in certain locations we are able to recreate what we see in the real cell lineage (Figure 4.31e). The new cell walls are in roughly the correct places and the correct cell has P_1 cell fate. Therefore by combing the inherited threshold model and the new wall repulsion model for factor M placement we have specified the factors sufficient to recreate the observed stomata lineage. The other models where the nucleus is not moved or is moved by a global vector are included to show the contribution of the different steps.

The inherited ratio model with new wall repulsion

Although the output of the above inherited threshold and new wall repulsion model created realistic cell geometries the timing of divisions was not similar. As the final area of the P_1 cell is small the threshold area must be very low. However, as the area threshold is constant in this model the low area threshold causes the initial cell to divide many times.

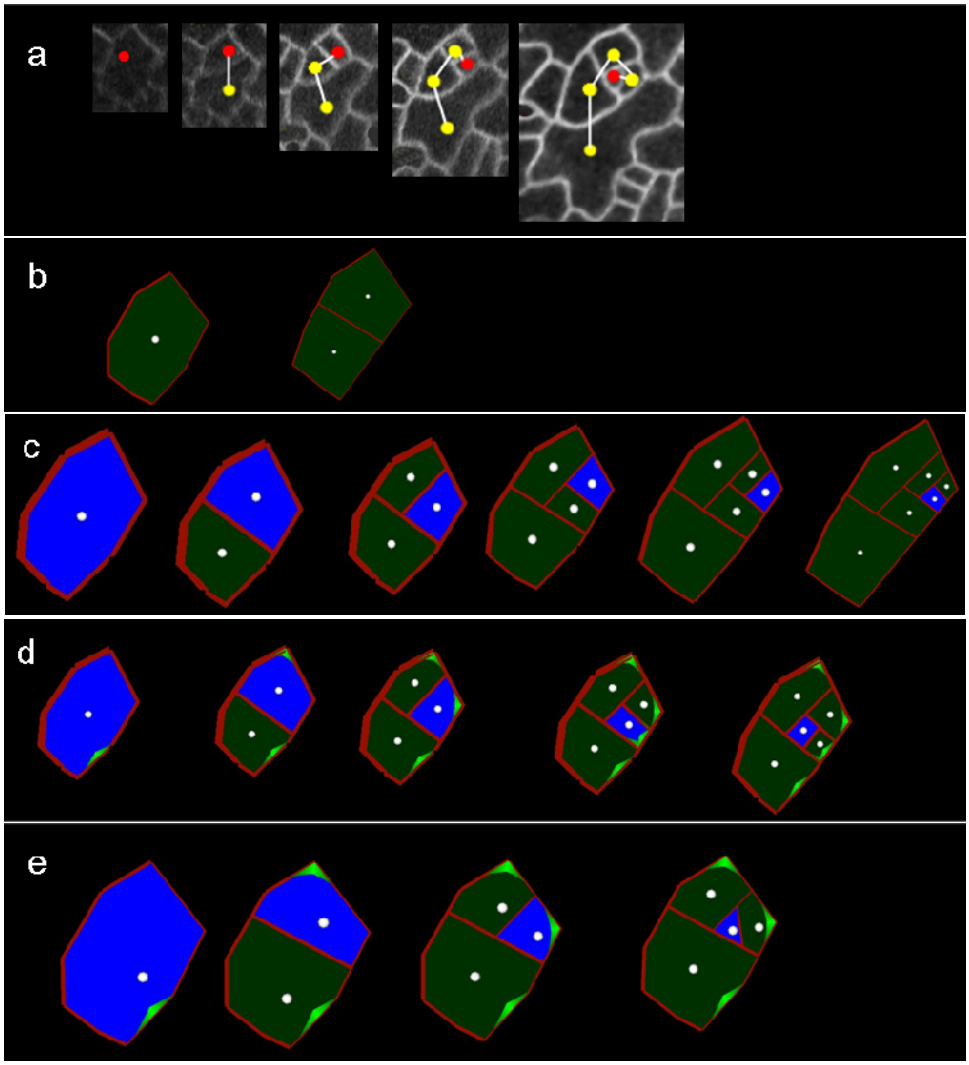

Figure 4. 31 Comparing the inheritance-repulsion model to the other models and the observed cells. a) observed cell lineage used to drive the growth of a model cell. (b) constant area threshold model, c) inherited threshold model, d) inheritance-repulsion model, factor M determines which daughter inherits P_1 cell fate. e) inheritance-repulsion model where factor M also displaces the nucleus to make the division asymmetric. This model shows the best match to the observed cells. Factor M – bright green, P_1 cell (blue).

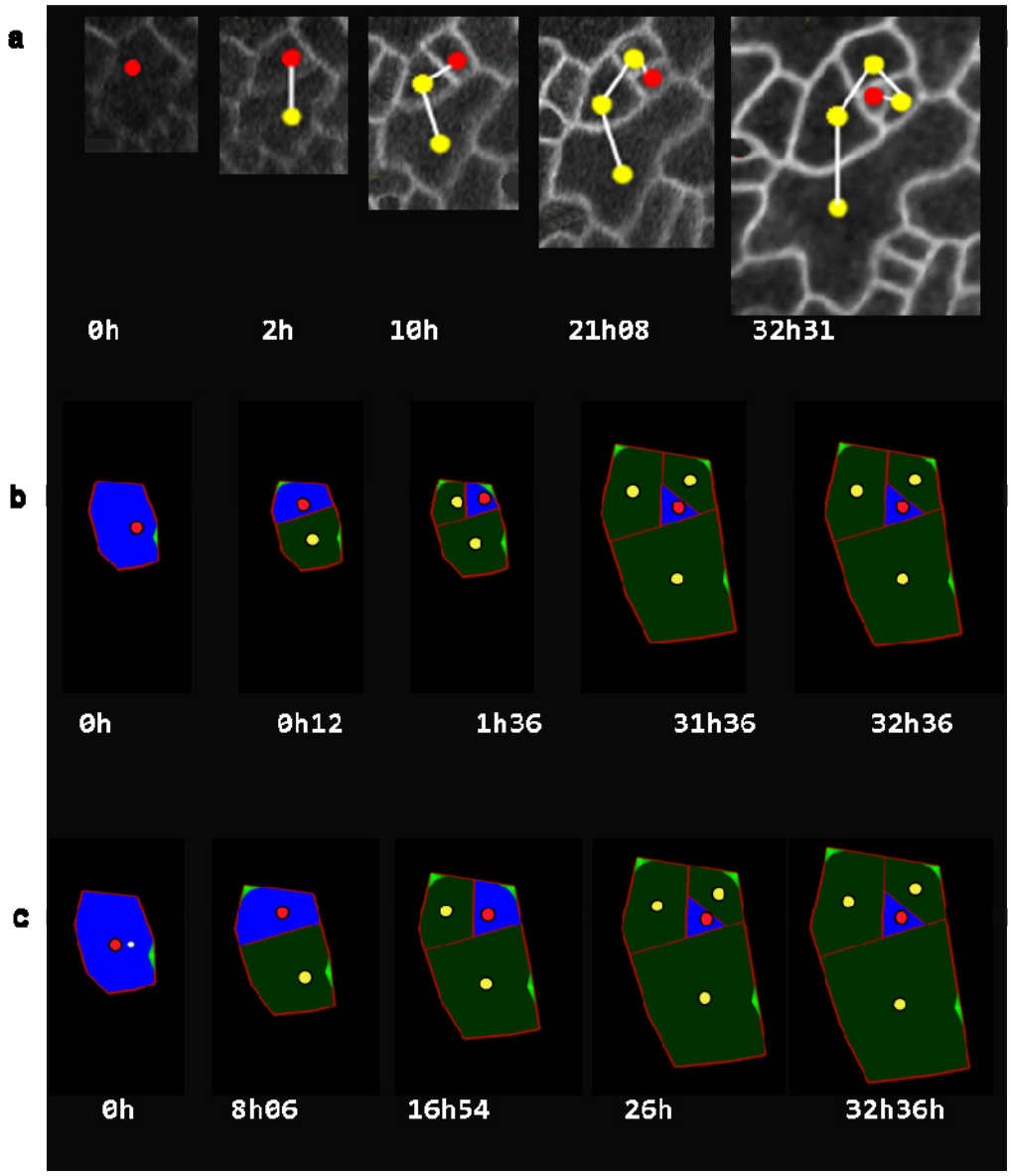

Figure 4. 32 Comparing the area and ratio inheritance-repulsion models. a) the same lineage is used to drive the model, with the division times added. b) Area inheritance-repulsion model with cells dividing at a constant but lower threshold area (the model from figure 31e with the times of the divisions added), c) ratio inheritance-repulsion model the cells are divided when they reach 1.5 times their original size. Although both models (b-c) produce the same arrangement of cells the ratio model shows a better distribution of the division times.

The data showed that contrary to the *spch* mutant model the area of cell division is actually decreasing in the stomata lineage cells. The data suggested the cells were dividing upon reaching approximately 1.5 times their birth size. I therefore replaced the inheritance of a constant lower threshold to an inheritance of a threshold that depended on the birth size of the cell. P_1 cell have a division threshold of 1.5 times their birth size while the other cells have a threshold of 4 times their birth size. This causes the P_1 cells to gradually get smaller over time. Figure 4.32 compares the real data to the inherited threshold model (b) and the inherited ratio model (c). The ratio model produces divisions that are more spaced out in time and better reflect the observed division times. However, the biological mechanism that could for this observation is unclear. These models will be referred to generally as the **threshold** and **ratio inheritance-repulsion** models respectively.

4.4 Validating the basic model through the identification of key factors.

The inheritance-repulsion models are capable of recreating the results from the tracking data. The model identifies two key things: the ability to specify P_1 cells and factor M which moves the nucleus and influence which daughter acquires P_1 cell fate. I aimed to identify genes that could be responsible for determining P_1 cell fate and producing factor M.

4.4.1 Maintenance of SPCH expression is inherited by one daughter cell

The work on the *speechless* mutant in the previous chapter showed that, in comparison to the wild-type, this mutant divided symmetrically and no stomata were produced. *SPEECHLESS* (*SPCH*) is required for the initial asymmetric division of meristemoid

mother cells in stomate formation and the amplifying divisions of meristemoid cells (Lampard). I wanted to see if I could observe SPCH being inherited by the daughter cell that inherits P_1 cell fate and increasing the division rate of these cells. I therefore imaged and tracked SPCH::SPCH:GFP expressing cells (Figure 4.33a). I identified cells that were stomata or guard mother cells and carried out retrospective analysis (Figure 4.33b). In the final image (3) there is a stomate. Non of the cells in the final image have SPCH expression. In generation 2 one cell has SPCH expression in the nucleus. This cell is an A cell as it has been internalised but has not divided to make the guard cells. The cell that divided to produce the A cell is visible in generation 1. It is a P_1 cell and has SPCH expression in its nucleus. The other cells which are B cells do not have SPCH expression. Figure 4.34 shows the same cell with intermediate time points included. Now we can see that after division both of the daughter cells have SPCH expression and it fades in the cell that becomes the B cell. We can also see that the earliest time point has SPCH expression in both daughters. As expression is only seen in both daughters just after division it is likely this cell just divided. This is a very small data set but seems to suggest P_1 fate is correlated with maintenance of SPCH expression. The visibility of SPCH in the A cell before it becomes a stomata supports A cells being matured P_1 cells rather than being produced directly from the division. The fading expression of SPCH correlates with the termination of meristemoid divisions and maturation into a GMC (A cell). We can therefore re-draw the scheme with the P_1 cell gradually becoming an A cell. I investigated more of the lineages (Figure 4.S14 and S15) and saw that in all cases the P_1 cell fate correlated with maintained SPCH expression that was inherited by one daughter cell. The decision of which daughter should keep SPCH seemed to be made after division as both daughters have SPCH just after division. In most cases the lineage went on to make a stomate and this correlated with a fading of SPCH expression. Even in cases where the cells where not imaged long enough for stomata formation to be observed, it is always the cell which will go onto divide that kept SPCH expression (Figure 4.S16).

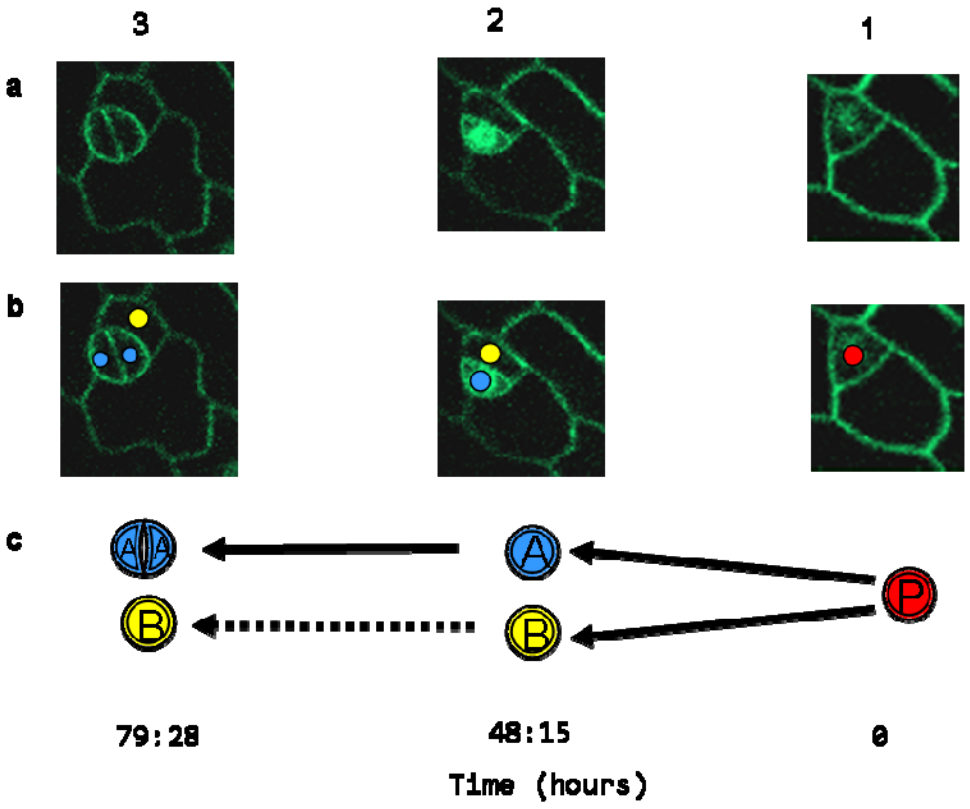

Figure 4. 33 Retrospective analysis of cells with SPCH::SPCH::GFP expression shows a correlation with SPCH expression and P_1 cell fate. a) SPCH::SPCH::GFP expression in a lineage of cells. Expression is in the nucleus of the small cell in generation 1 and 2. (The membrane is labelled with a membrane marker PIN3-GFP.) b) cells are coloured based on their classification. c) retrospective analysis diagram. The time of the divisions is shown relative to when the cells started to be followed.

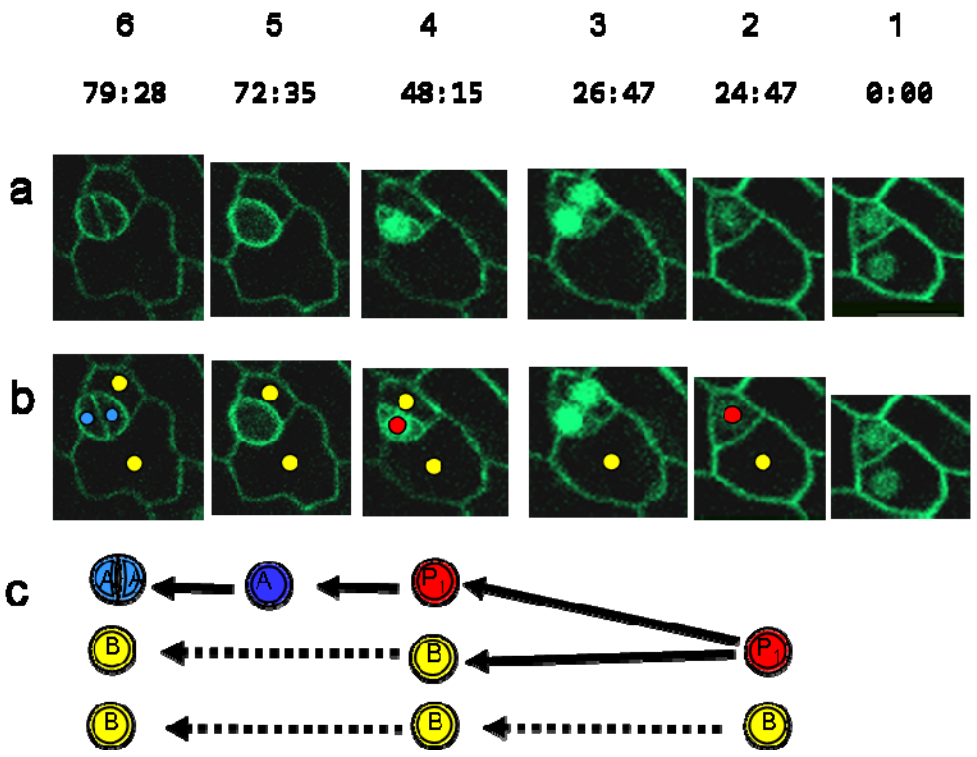

Figure 4. 34 Retrospective analysis of cells with SPCH::SPCH::GFP expression. The same lineage is shown in Figure 4. 33 but here there are intermediate time points to show what happens between divisions. a) SPCH::SPCH::GFP expression. In generation 1-4 expression can be seen in one or two of the daughter cells. After division both daughter show expression, it then fades in one. ((b) the classification of the cells. (c) The scheme for the retrospective analysis. The time shows the time since this clone was first imaged.

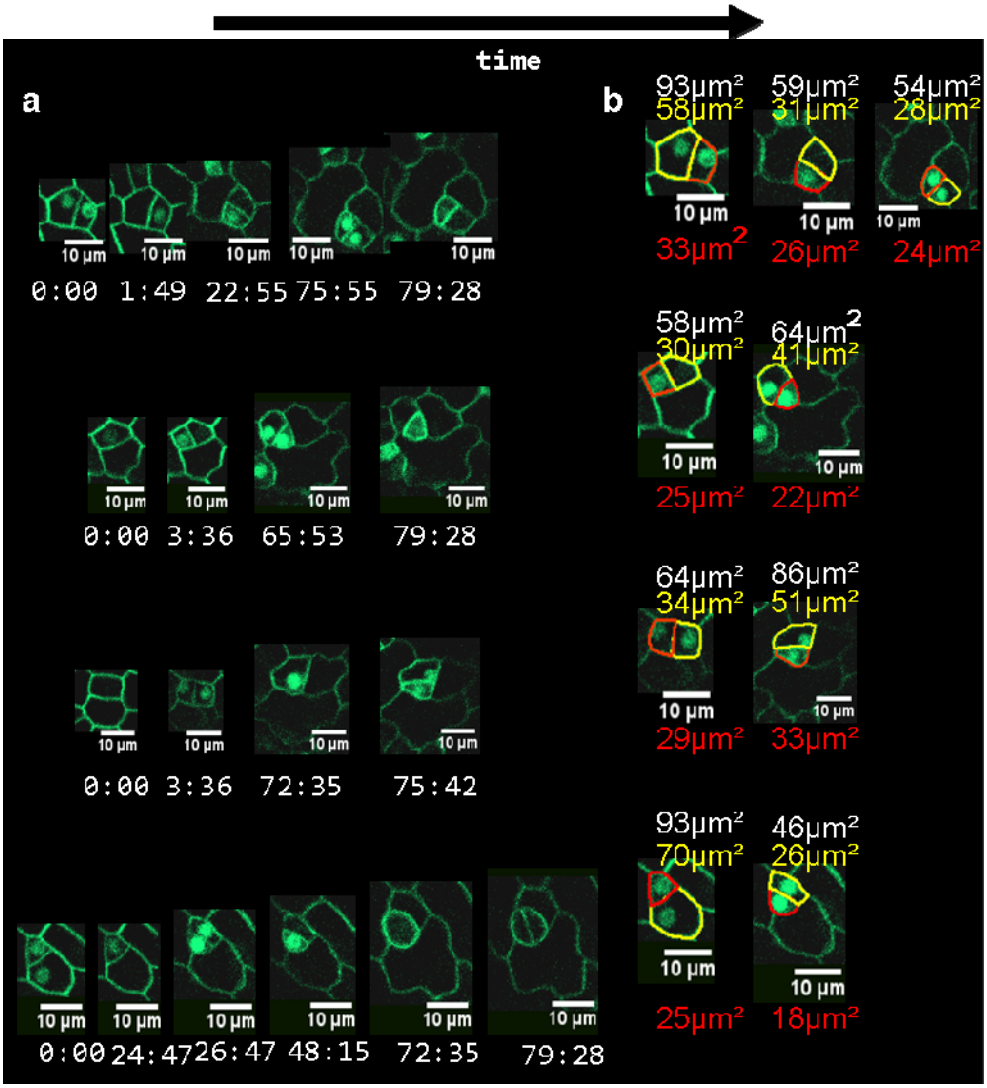

Figure 4. 35 inheritance of SPCH activity. a) Tracking cells expressing SPCH::SPCH-GFP (using PIN3 PM marker) shows that SPCH is active in some cells before division. After division SPCH activity can be seen in both cells however expression quickly fades in one of the daughter cells. The cell that maintains SPCH goes on to divide while the sister cell never divided in these examples. SPCH activity is maintained by the cell which will divide until the lineage terminates with the formation of a GMC. (b) the area of the daughter cells that receives SPCH (red) and the area of the sister cell (yellow). SPCH is always inherited by the smaller cell.

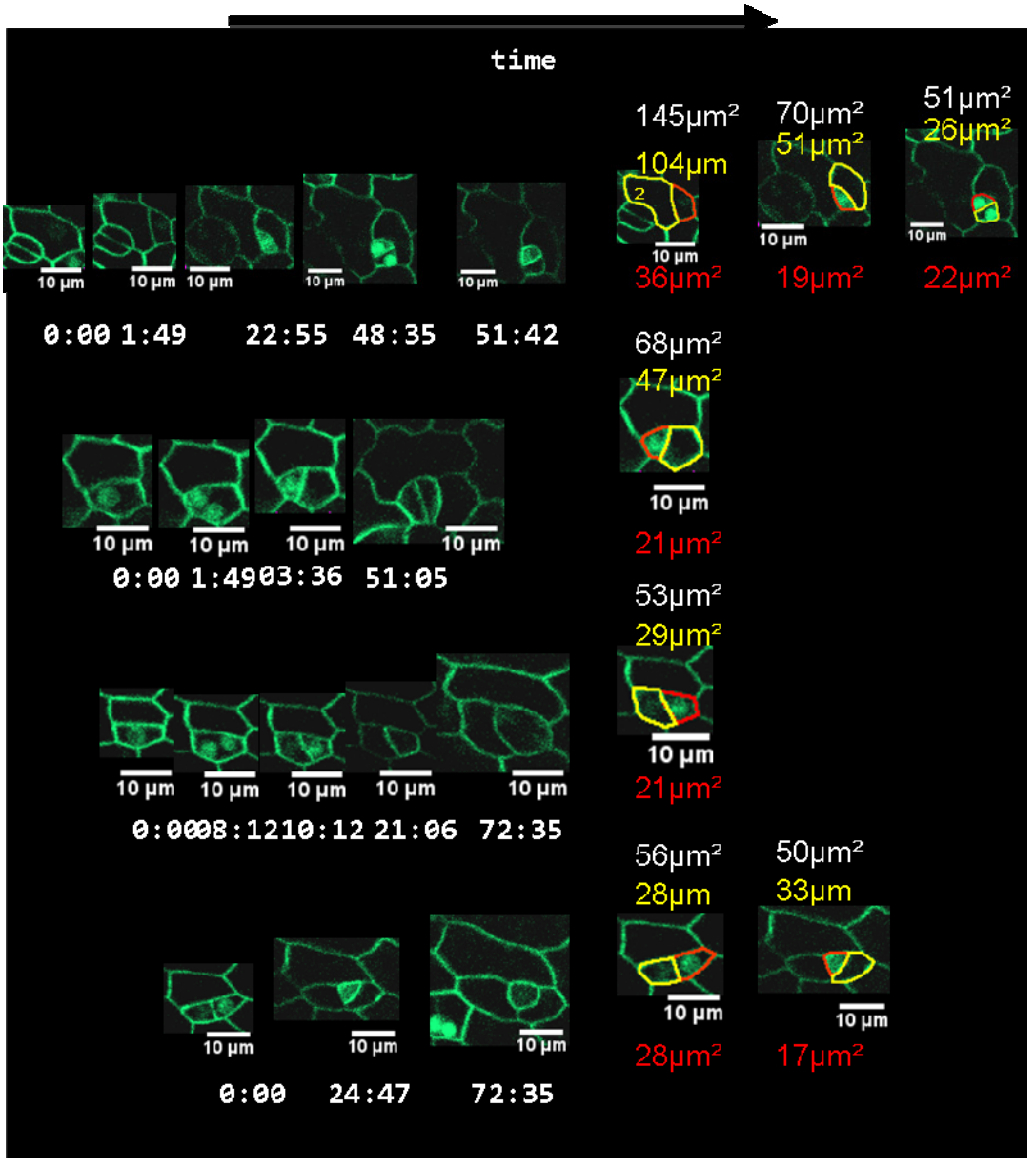

Figure 4. 36 continuation of Figure 4.35

4.4.2 SPCH expression is maintained in the smaller daughter cell

I measured the area of the daughter cells at the time of division to check whether SPCH was maintained by the smallest daughter cell. Figure 4.35 and 36 show lineages of cells with SPCH expression and the sizes of the daughter cells. The daughter cells are coloured based on their classification. All of the divisions are asymmetric and in every case the daughter that maintains SPCH expression is the smaller of the two daughter cells. In most cases the size at which the cells divided is smaller with successive divisions. However, this is not always the case. This might suggest a difference between the initial studies in wild-type where cells always divided at 1.5 times their original size. A possible explanation is that this line was older when it was imaged so in some cases we are looking at secondary stomata formation (Figure 4.36 a) which might form differently (see later section). The timings of the divisions seem to support the division timing not being regulated by cell cycle duration.

The data shows a correlation between SPCH expression and P_1 cell fate. Cells expressing SPCH: divide more, divide asymmetrically and pass on their fate to the smallest daughter cell.

4.4.3 BASL has some of the characteristics of factor M

In addition to being able to define P_1 cells the inheritance-repulsion models require factor M to generate asymmetric divisions and specify fate. *BASL (BREAKING OF ASYMMETRY IN THE STOMATAL LINEAGE)* discovered by Dong *et al* in 2009 is a good candidate for factor M. They reported that the BASL protein is located at the periphery of the cell in a polar way and in the nucleus. They show that peripheral BASL is usually distal to the nuclear position. They propose that if BASL is in the periphery and nucleus of a cell then it will divide asymmetrically.

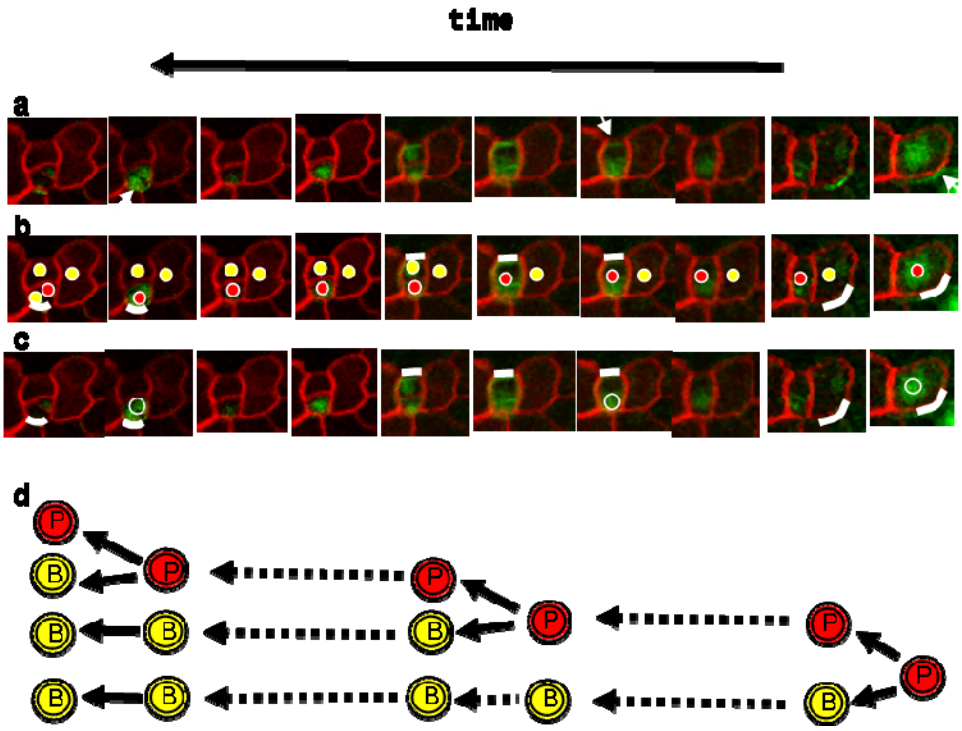

Figure 4. 37 Time-lapse imaging of BASL. a) cell lineage with BASL::BASL-GFP (the plasma membrane is marked with mCherry). BASL is visible in the nucleus and on the cell periphery. The nucleus is brighter so the places on the membrane have been marked with an arrow when they first occur. b) the cells are coloured based on their classification. The location of BASL on the membrane is marked in white. c) the nuclear and peripheral location is marked to highlight it through time. The nuclear position is estimated based on the intensity of the GFP. d) the scheme for the cell divisions. BASL is so bright it is hard to see the membrane and determine exactly when the division occurred but the best estimate has been made. (these images were subject to image processing to remove background noise and sharpen the images they have all been rescaled to emphasis the spatial arrangement of the BASL protein and to improve visibility.)

They also report that BASL will be maintained in the larger daughter cell following division. These findings are all in support of factor M being BASL. I carried out long term time-lapse of BASL::BASL-GFP expressing cells in a plasma membrane marker background and was able to follow the position of BASL in cells undergoing divisions. Figure 4.37a shows one of these lineages (Figure 4.S17 and S18 show more lineages). It is possible to see BASL in the nucleus and on the periphery of some cells. I carried out retrospective analysis to investigate any association between BASL expression and cell classification. The lineage starts with a single P_1 cell which has BASL visible in the nucleus and on the periphery highlighted with an arrow. Figure 4.37b shows the same cells marked with red or yellow depending upon their classification. The location of BASL is also marked in white from the time it first appears until it fades (the arrow only marks the first appearance of BASL). When BASL first appears it is faint and its exact location is hard to see, however, looking forwards and backwards in time allows us to get a consistent picture of where it is expressed. We can see that following the division of the first P_1 cell, BASL remains on the periphery in the same place i.e. in what is now the larger daughter cell. There is also BASL expression visible in the nucleus of both cells. BASL expression fades in the larger daughter cell, the B cell, but remains on in the nucleus of the P_1 cell. Expression appears on the periphery of the P_1 daughter cell (marked with an arrow). Figure 4.37c shows the nuclear position in this cell is distal to the location of BASL. This confirms the published observations and the model hypothesis. This P_1 cell then divides asymmetrically. The nucleus of both daughters again has BASL expression. BASL expression remains in the P_1 daughter and fades in the B cell. It seems that the nuclear expression of BASL in the P_1 cell is not constant: it seems to fade and then get brighter again prior to the next division. However, this is hard to quantify and might be linked to nuclear movements. It is the P_1 daughter cell that will have bright nuclear BASL before the next division and will also acquire membrane localised BASL. This P_1 cell divides asymmetrically producing a P_1 cell and a B cell. The P_1 cell is the smallest cell. Peripheral BASL is only present a small time before division, although, in some cases it is hard to tell whether it occurred before or after the division. This suggests that if BASL is responsible for displacing the nucleus, as the model suggests, it would have to move it just before division. This conclusion is supported by the published data which clearly shows BASL as being distal to the nucleus and the behaviour of the basl mutant. The *basl* mutants have less asymmetric divisions. This supports the hypothesis that BASL is responsible for moving the nucleus

prior to division and that this allows the production of asymmetric divisions. The time-lapse and retrospective analysis allows us to classify cells and see that BASL correlates strongly with cell fate just as the model predicts. BASL expression in the daughter remains on for quite some time after division. The duration is comparable to the time taken for SPCH expression to fade in one of the daughter cells. We do not have any data to conclude a direct interaction between SPCH and BASL. However, the model is supported by the report that *basl* mutants not only lack physical asymmetry but are also defective in their fate with either one, both or neither daughter producing a guard cell (Dong et al., 2009). BASL is unable to explain all of the properties of factor M. If factor M is removed from the model then all cells will divide symmetrically. It is unclear how to assign the daughter fate in such a mutant model, the daughter could randomly acquire P_1 cell fate. The phenotype of the observed *basl* mutant is not severe enough for *BASL* to account entirely for factor M. It is likely that factor M is a complex of BASL and other un-discovered proteins. This would introduce redundancy and make the mutation less severe. Alternatively there may be another mechanism that is unrelated to factor M that acts redundantly to it.

4.4.4 Adding the genes to the model

Identification of real proteins as candidate factors allows us to test and improve the model. Figure 4.38 showed the inherited-repulsion models could produce a spiral arrangement of cells similar to the tracked data. However, the initial position of M was an estimate and we can not asses whether the subsequent M locations are realistic. If we say that BASL is located where factor M is then we can use data from the tracking of BASL expressing cells to seed the model correctly and determine the accuracy with which our model can place the next BASL locations. I input the location of BASL from the data and specified that the cell was a P_1 cell i.e. it had SPCH expression. When the cell divided the daughter cell that did not have BASL in it inherited SPCH expression and the new position of BASL was calculated to place BASL as far as possible from the new division walls. Walls are classified as new when they are formed by the division of SPCH cell. They remain as new walls until the cell loses SPCH and is ready to divide again they could also lose this quality over time.

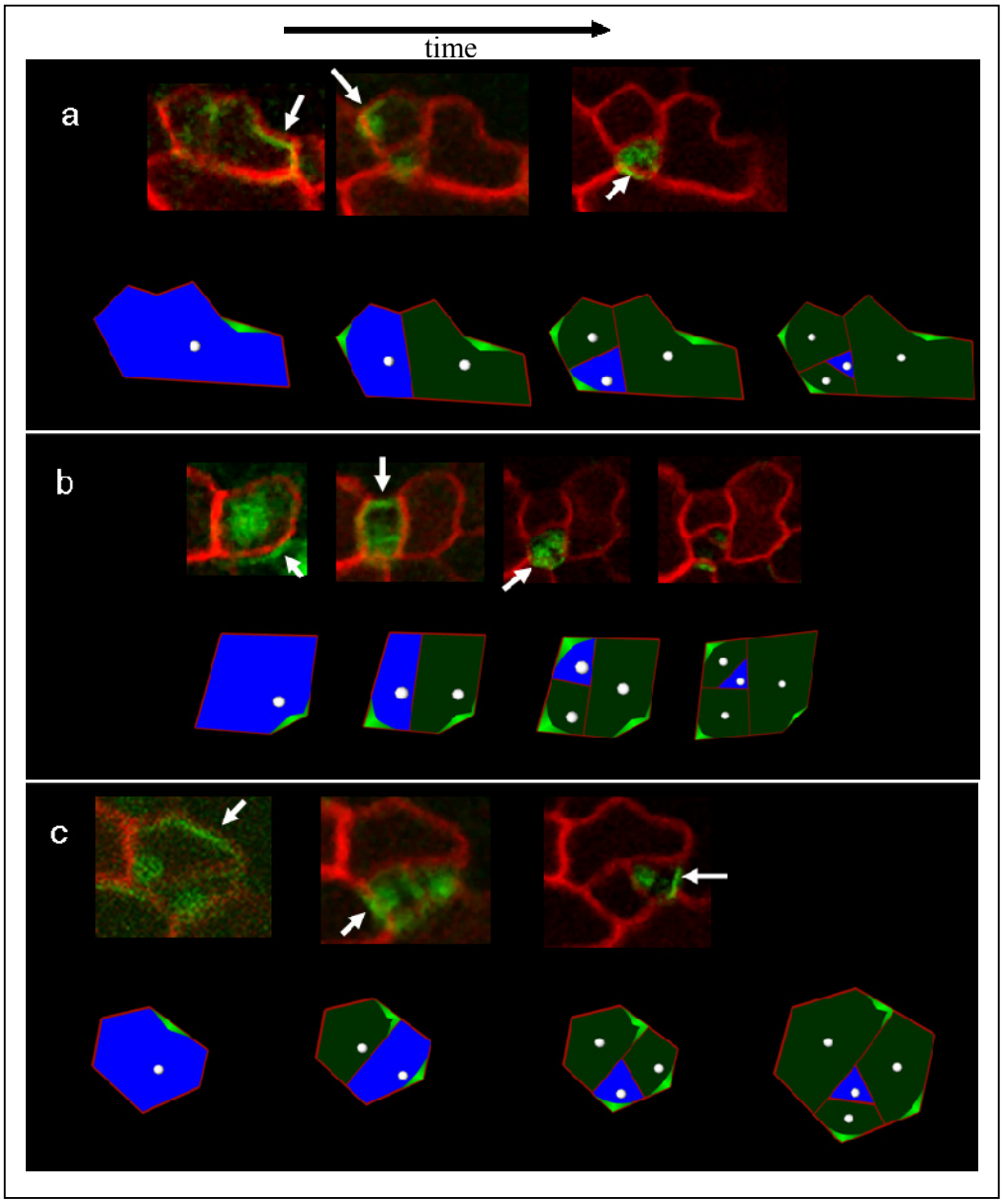

Figure 4. 38 Comparing the new wall repulsion model to observed BASL locations. Tracked BASL expressing cells are shown at key time-points. BASL locations are marked with arrows. Underneath each is the model which was seeded with the initial placement of BASL. P1 cells – blue, BASL - bright green, modelled nuclear position – white. a) subsequent locations of BASL are similar to the observed locations. The cells divided in the same orientation, and produced similar cell shapes and arrangements. There is a good match between the model and the observed cells. b-c) the observed cells and the model are similar in terms of divisions and arrangements but their arrangement is symmetric to the observed cells rather than the same. This shows a limitation of the model to capture the direction of the spiral. BASL locations can be predicted to some extent if the model is seeded with the first one.

This model generates the arrangement of cells seen in the data and placed subsequent BASL in the correct location (Figure 4.38a). However, as many cells are almost symmetric the spiral may form in the opposite direction to that observed (Figure 4.38b and c). The direction of spiralling seems to be a consequence of the cell geometry. The model should be improved so that it can better predict the direction of spiralling. It is possible that including the influence of the previous BASL locations as well as the repulsion from the new walls might generate the observed pattern. For example in Figure 4.38b when BASL is placed in the daughter after the first division it could be placed at the top or the bottom. However, if it was also repelled by the previous BASL location it will be placed at the top of the cell as seen in the data. The contribution of the two factors needs to be investigated thoroughly. However, this type of model would be more like the phylotaxis models which also have an active ring where new primordial form. In this case the old walls define the active ring. This model also suggests the existence of a molecule on the new walls that can repel BASL (anti-BASL).

4.5 Secondary stomata formation

The inheritance-repulsion model is able to arrange the cells in isolated cell lineages. This represents stomata production from primary meristemoids and is relevant for the early events in stomtal patterning. If we consider a patch of cells coloured according to their classification (Figure 4.39) we can see that initially all cells are P_1 cells. As the cells divide the P_1 cells become separated by non-stomatal cells. The number of P_1 cells remains constant. If this was the only method of forming stomata the density would be very low. Some estimates suggest most stomata (75%) are produced from secondary meristemoids. i.e. by the division of meristemoid mother cells (MMCs) which are adjacent to stomata or stomata precursors (Geisler et al., 2000). During the time-lapse imaging of the SPCH and BASL expressing lines I captured some divisions of secondary meristemoids. By considering them in context we can examine the similarities to primary meristemoid formation. Figure 4.40 shows a cell that gives rise to two GMCs. The formation of the first occurs in the same way as the isolated lineages. SPCH is successively maintained by the smallest daughter which divides twice to internalise the GMC.

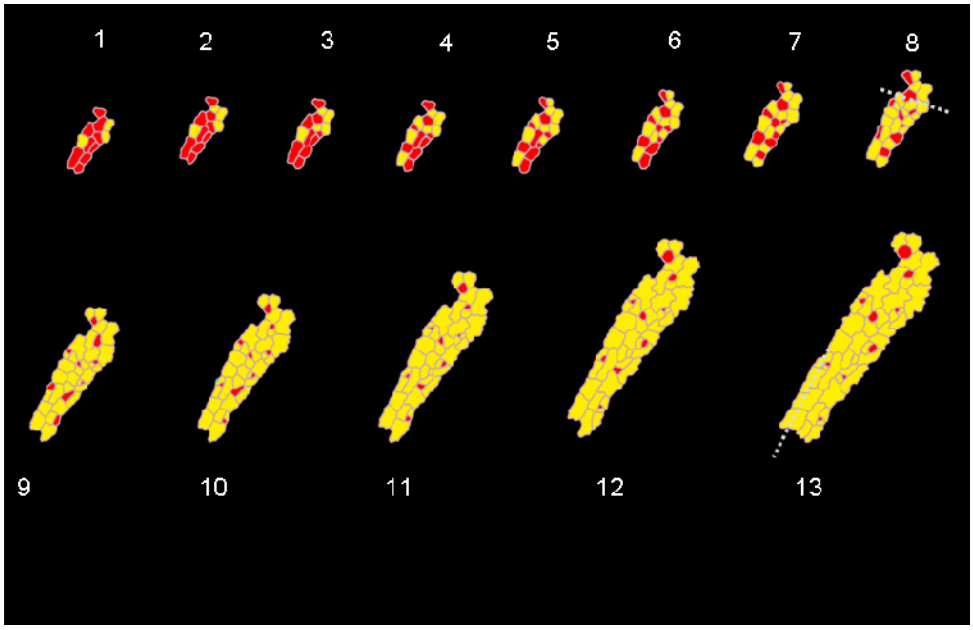

Figure 4. 39 Following inheritance of P_1 cell fate in a patch of cells. A digitised version of a patch of wild-type cells. The cells are coloured based on their classification. As the patch grows the cells divide and the P_1 cells space out. The number of P_1 cells remains constant. Gray lines indicate tiling defects where the images did not fit together perfectly so cell shape and size might be altered.

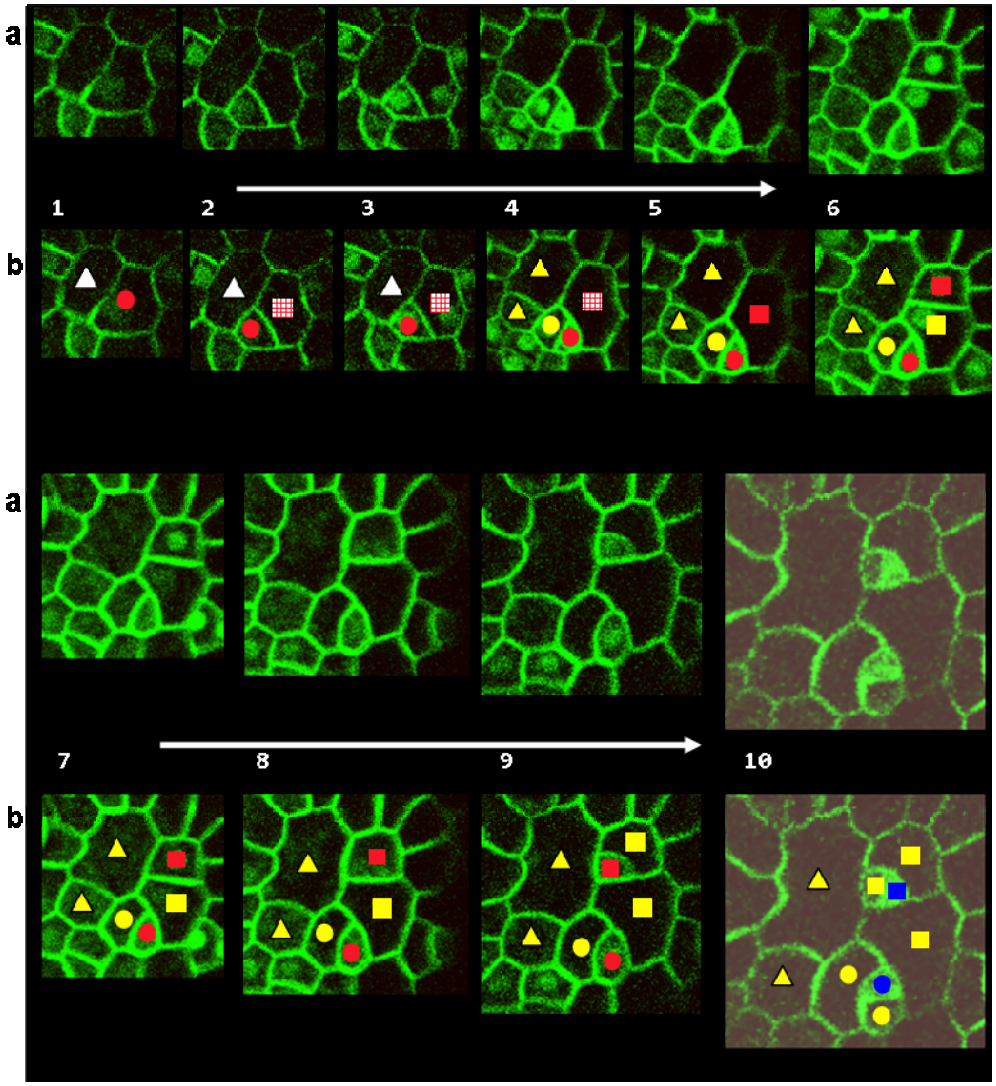

Figure 4. 40 Losing and re-gaining SPCH expression. a) Tracking cells for longer periods of time shows that cells that lose SPCH expression early can re-gain it. b) The cell (red) is a P cell it initially has SPCH expression and passes on its expression to its progeny (circles) that eventually produce a GMC (blue circle) in image 10. However, the sister cell (square (checked red indicates 2° P_1)) initially loses SPCH expression but regains it either before or after division in image 6. This cell then behaves as a P_1 cell and goes on to produce a GMC (image 10). The two P_1 cells spiral away from each other. In contrast the neighbour cell (triangle) never seems to acquire SPCH expression it therefore divides only once and appears to differentiate into a pavement cell. It maybe subject to an alternative developmental signal.

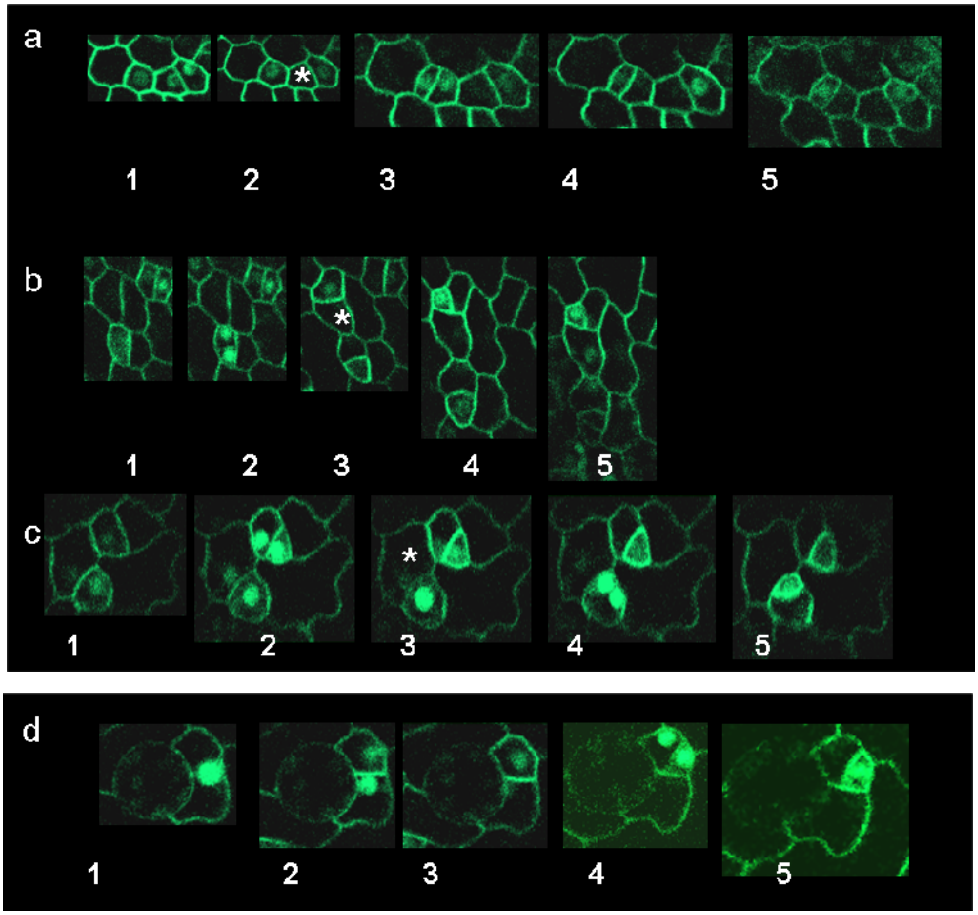

Figure 4. 41 SPCH expression in secondary meristemoids Lineages (a-c) show examples where the decision of which daughter should inherit SPCH expression may have been influenced by neighbouring cells. a) 3 neighbouring cells have SPCH expression. Two of these cells are sisters which have presumably just been created. The smaller cell loses SPCH expression (image 2 *). This ensures a non-SPCH expressing cells separates the two P_1 cells. b) image 2 both daughters have SPCH they are next to a cell that is about to divide. The daughter away from this cell keeps SPCH. When the neighbour divides it also selects the cells which is further away from the SPCH expressing daughters to inherit SPCH. c) another example of neighbours simultaneously expressing SPCH in the daughter cells. Again the SPCH inheriting cells end up spaced apart by non-SPCH expressing cells. d) a cell next to a stomata acquires SPCH expression. It divides twice and inherits SPCH so that it is away from the stomata. This figure shows that cells next to SPCH expressing cells or stomata are not prevented from expressing SPCH. However, after division the inheritance of SPCH seems to be influenced by the neighbours.

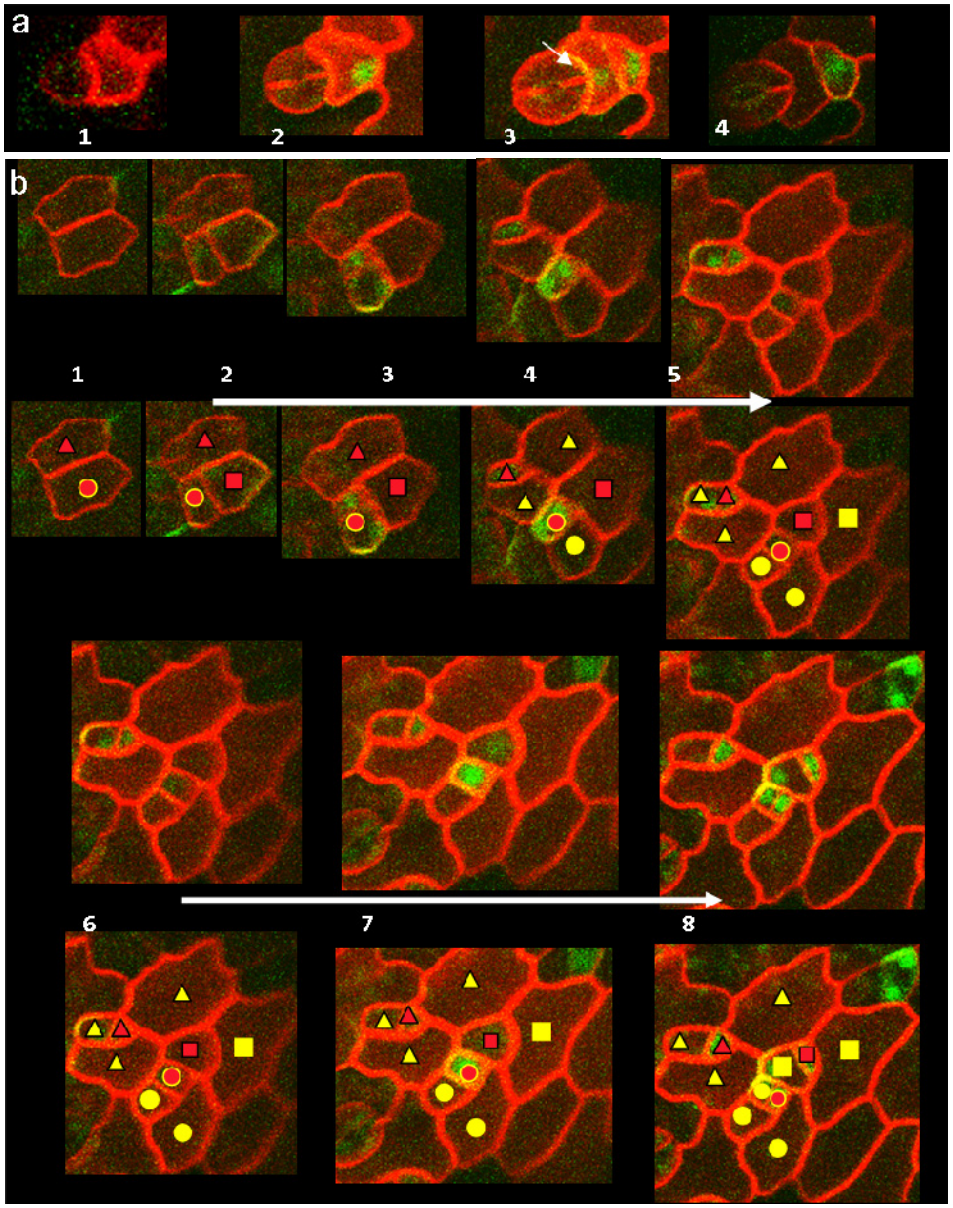

Figure 4. 42. BASL expression in secondary meristemoids. a) BASL expression is visible in the nucleus of a cell next to a stomata (image2). There is also BASL in the periphery of the cell next to the stomata (image 3 arrow). After division BASL is inherited by the smaller cell which is one cell away from the existing stomata (image 4). b) BASL expression in a patch of cells behaves in the same way as in the individual lineages. The three P_1 cells are initially in contact but end up spaced by at least one cell. The BASL expression of the neighbouring (circular and square) P_1 cells (image 8) is in contact and results in the daughters being oriented away from each other. Even though the circular P_1 cell is not fully internalised the BASL location means it is not neighbouring another P_1 cell.

Before this lineage makes the penultimate division to form the GMC the oldest cell in the clone divides and shows SPCH expression in both daughters. SPCH is then maintained by the smaller daughter which divides twice more before forming a GMC. This suggests that secondary meristemoids form by a cell which has lost SPCH expression previously re-gaining it. This idea is similar to the Q cells becoming P_1 cells. The initial division is of a large cell but once SPCH has been acquired it divides rapidly. The two P_1 cells in this lineage spiral away from each other and both fully internalise their GMC. The initial division of the secondary meristemoid is oriented to space stomata (Geisler et al., 2000). The neighbour to the initial P_2 cell, by contrast, only divides once. It does not express SPCH and it does not make a GMC.

There is nothing to prevent SPCH being expressed in neighbouring cells. However, studying more patches of cells suggests that this is not a stable situation. In some lineages a cell divided next to a cell which already had SPCH expression. It produced one daughter that neighboured the SPCH cell and one that did not. In all of these cases the daughter which maintained SPCH was the one that did not neighbour the original SPCH expressing cell (Figure 4.41). In one case SPCH was maintained by the larger daughter cell (a). This may suggest there is an additional layer of specification over which daughter maintains SPCH expression that the inheritance-repulsion model can not account for.

SPCH expression can be seen in secondary meristemoids which form next to mature stomata prior to division. The inheritance of maintained SPCH expression by the daughter cells is again such that the SPCH expressing cell is not in contact with the stomata, although this can take more than one division (Figure 4.41e) depending on the cell geometry. Observations of BASL expressing in cells which neighbour stomata show that its peripheral localisation is proximal to the stomata cell (Figure 4.42a). It is unclear from this data whether BASL is re-located to this position or whether it is still in the same location as it was when it first divided. Previous studies suggest BASL relocates prior to secondary divisions (Dong et al., 2009). Similarly to primary meristemoid formation BASL is also expressed in the nucleus of the small cell after division. This suggests that BASL may also be involved in the process of orienting the division of secondary meristemoids. Considering a patch of BASL expressing cells shows that, BASL expression seems to follow the pattern of inheritance in the

inheritance-repulsion model. The location of BASL in neighbouring cells is very close, resulting in the P_1 cells being spaced apart. This may suggest some communication of the BASL location between neighbours. Further work is needed to determine whether communication of BASL location between cells could play a role in spacing stomata. This may require BASL to be positioned based on the previous locations of BASL rather than just the new walls.

5 Discussion

5.1 Asymmetric cell division

The main focus of this thesis was to understand how asymmetric divisions are linked to patterning within a growing tissue. As described in the introduction, although there have been many studies on asymmetric divisions at the cellular scale, the relationship between this process and patterning of growing tissues has been less well addressed. This is particularly important for plant tissues, where cells are held in fixed relative positions so intrinsic and extrinsic factors are closely coupled. To illustrate this interplay more clearly, I first consider a 1D growing system and the possible ways of patterning it.

5.1.1 Determining which cell inherits stem cell fate in one dimension

Consider a stem cell lineage growing in one dimension (Figure 5.1). There are four ways we may determine which daughter cell inherits the stem cell identity.

1) The stem cell is next to a niche (shown in blue) and during successive divisions an extrinsic signal from the niche ensures that the adjacent cell keeps the stem cell identity. In animals the differentiated cell can move out of the range of the stem cell maintaining signal (e.g. the Drosophila germline stem cells (GSC)) (Figure 5.1a). In plants the cells can not move away they are connected by a cell wall. The differentiated cell can still be away from the niche so long as the division wall is parallel to the niche and the signal range is so short as to require direct contact to act (e.g. in the root meristem) (Figure 5.1b). The cells move further from the niche due to the processes of cell division and growth.

2) If there is no niche then the situation is more complicated; either cell can inherit the stem cell fate. Which cell inherits stem cell fate could be under the control of intrinsic or extrinsic factors. If the tissue has a polarity that is known by all cells then they could use this to ensure that a particular fate is inherited by the daughter cell on one side only (e.g. the Drosophila sensory organ precursor (SOP) cells) (Figure 5.1b).

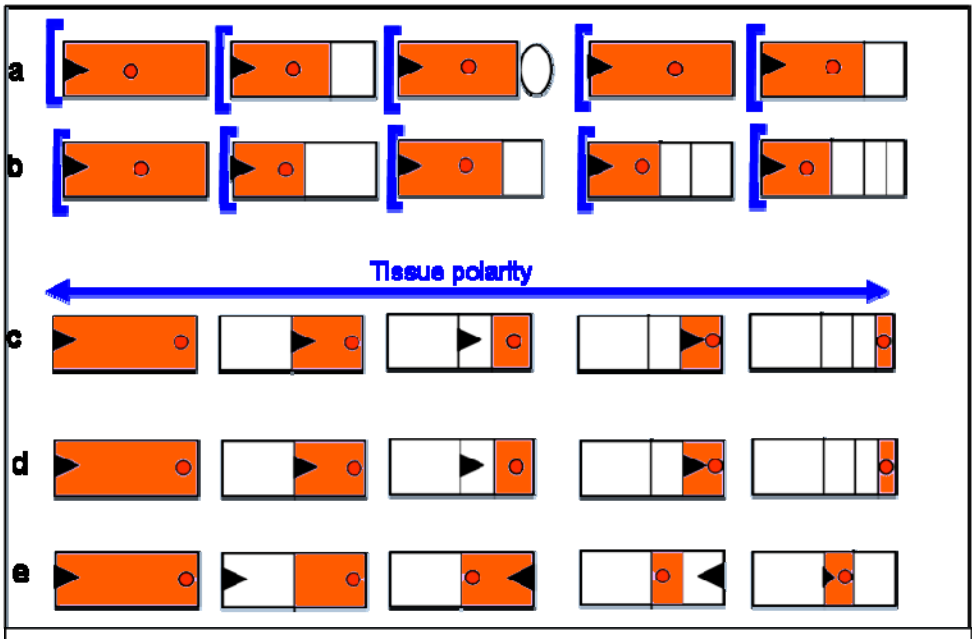

Figure 5.1 Methods of specifying fate segregation in 1D. When stem cells divide one cell maintains stem cell fate (orange). Which daughter inherits stem cell identity can be determined by the polarity of the mother cell (black triangle). a) In NB division the mother cell maintains NB fate and the daughter differentiates. In animals the cells do not have to remain in contact. Here this is represented by the cell becoming round and detaching. The mother NB is polarised by the niche (blue) so that the stem cell fate remains in the mother cell. b) If this type of segregation occurred in a plant where the cells could not move the NB would remain at the end of a line of differentiated cells next to the niche (blue). (c- d) If there is no niche then either daughter can inherit stem cell fate. c) the fate can be aligned with tissue polarity. The stem cell is always inherited by the cell on the same side. (d-e) Use intrinsic factors only. d) The new division wall repels the stem cell identity (black triangle). The stem cell remains on the end of the clone of cells e) the new division wall can attract the stem cell fate resulting in the stem cell remaining in the centre of the line of cells.

3) If there is no niche and no tissue polarity then intrinsic methods must be used. For example when a cell divides it has some imposed polarity from the mother cell. One side of the cell is in contact with the cell's sister while the other side is not. This can be used to polarise the cell and determine the fate of its progeny. If the stem cell fate is inherited by the daughter furthest from the sister then the stem cell will remain at the end of the file of cells (Figure 5.1c). This will be referred to as Type I patterning. It creates the same result as having a tissue polarity.

4) The opposite mechanism to Type I patterning would be if the stem cell fate was acquired by the cell closest to the mother cell's sister. In this case the stem cell would remain in the centre of the file of cells; we will call this Type II (Figure 5.1e). Note that although these mechanisms are classed as intrinsic because it is the polarity of the cell that determines the fate, they are actually also extrinsic because they are polarised by the neighbours. In plant tissues the neighbours of a cell can be its closest relatives. Distinguishing between context and lineage mechanisms can therefore become very difficult.

5.1.2 Generating spacing through stem cell inheritance

What is the impact of these four mechanisms of inheriting stem cell fate on pattern? To see the effect on patterning we must extend the example to consider a line of stem cells.

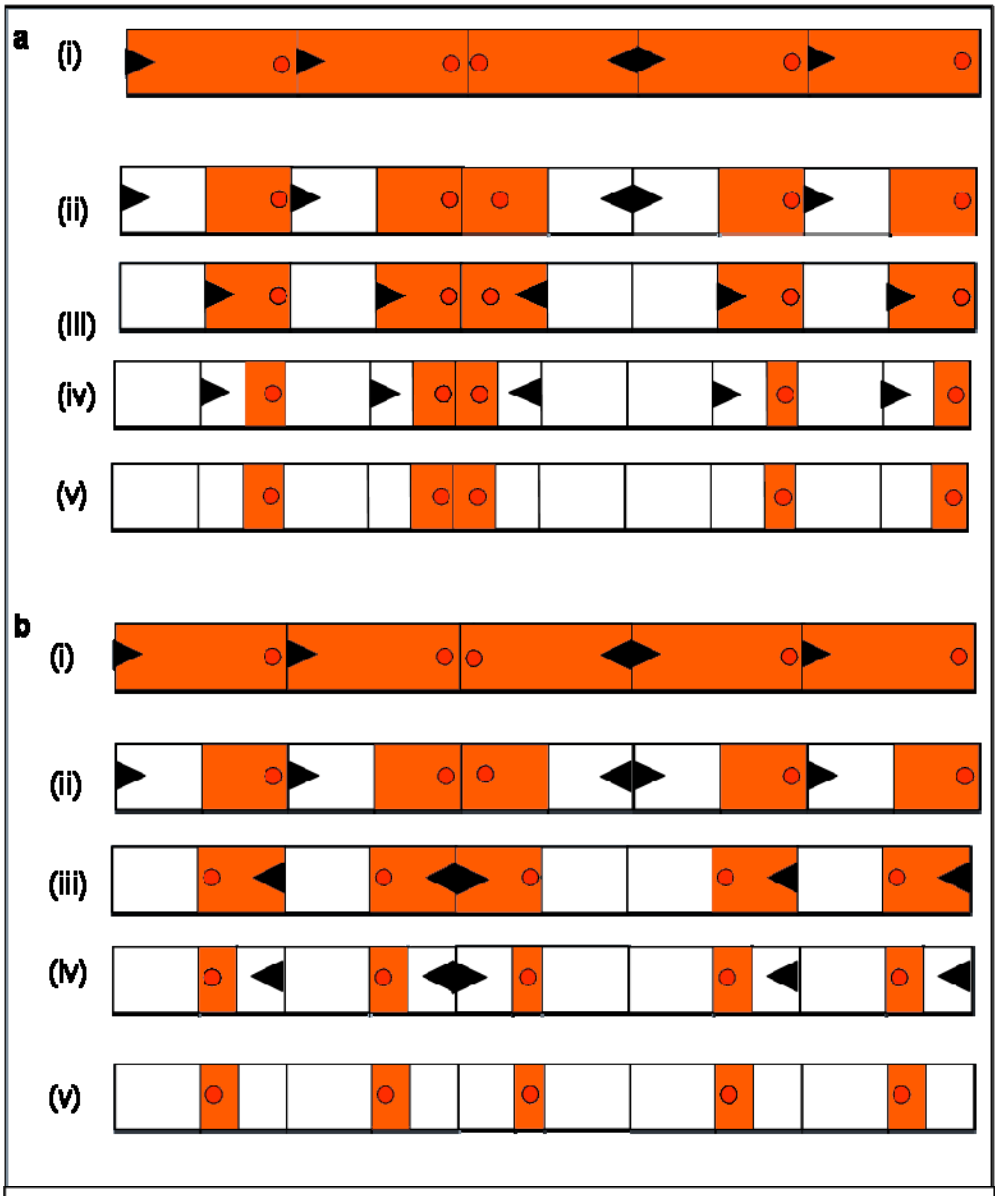

Figure 5.2 Specifying fate segregation in a line of 1D cells. The methods considered in Figure 1 can be considered in the context of multiple stem cells. (i) the cells are all stem cells initially, and have a polarity. (ii) the cells divide and the cell furthest from the polarising factor keeps stem cell identity. (iii) the polarising factor relocates based on the rules of the model and the previous division. (iv) the cells divide again. (v) the cells are shown without their polarity to emphasis the spacing. a) the new wall repels the stem cell fate. Unless all cells have the same polarity this will result in stem cells being in contact. b) if the new wall attracts the stem cell fate the stem cells will quickly become spaced apart regardless of their initial polarity.

1) In 1D only one cell can contact the stem cell niche so the pattern remains the same as it did for a single stem cell. 2) If there is a tissue polarity then the stem cells will be

inherited on one side and will quickly become spaced out. 3) The Type I mechanism produced the same result as having a tissue polarity when there was one cell but if we consider a line of stem cells we see that this is not the case. If the cells have a random initial polarity then they will never space out no matter how many rounds of division they undergo (Figure 5.2a). 4) The Type II mechanism can space out the stem cells without the need for a tissue polarity within 2 rounds of division. In both animals and plants a tissue polarity has been demonstrated (e.g. mouse hair, fly wing, Arabidopsis trichomes and Arabidopsis root hairs). However, Type II is a more favourable mechanism for ensuring one cell spacing mechanism as it is simpler and in the case of stomata the divisions show a spiral arrangement rather than all being oriented in one direction. More details experiments would need to be performed in order to show that a tissue polarity is not playing a role.

5.1.3 Extending to two dimension – the need for a division algorithm

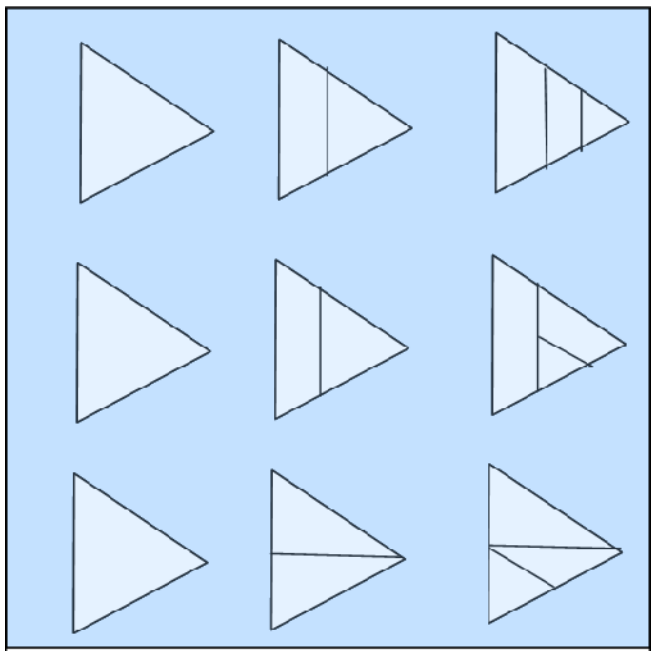

Figure 5.3 How to divide a triangle. In 2D there are many ways to divide a triangle. They result in a different arrangement of the final shapes.

Can we translate the mechanisms of inheriting stem cells from 1D to 2D?

The simplest 2D shape is a triangle. In 1D the orientation of the division was obvious. However, there are many ways to divide a triangle (Figure 5.3a). Unless there is a method of dividing the shape it is not possible to proceed with the analysis.

The shortest wall algorithm gives a good approximation of the observed divisions in the *spch* leaf

The *spch* mutant was used to investigate division algorithms. As the *spch* mutant does not form stomata it provided insight into normal cell divisions.

This analysis showed that even normal divisions are oriented according to a deterministic rule. Comparing the division algorithms in the complex cell shapes of the leaf allowed the algorithms to be distinguished. In agreement with many previous studies the shortest wall algorithm produced the best fit to the observed cells based on geometry and topology. The shortest wall algorithm could account for 160/190 divisions (85%). Studying cell division in the leaf rather than in other tissues with more regular cell shapes (e.g. the root or meristem) allowed the division algorithms to be distinguished.

5.1.4 Aligning the division orientation with the fate determinants

Having established that the shortest wall algorithm provides a reasonable approximation to the observed cell divisions we can return to the 2D example and the problem of inheriting stem cell fate. Applying the shortest wall algorithm to the schematic highlights further problems. 1) The triangle is equilateral and the shortest wall algorithm can still divide the shape in two orientations which results in very different cell arrangements. 2) The new wall can form perpendicular to the cell polarity, bisecting the polarity marker. In this case it is not clear which of the two daughters should inherit the stem cell fate. This problem exists for all of the methods of specifying stem cell fate. If there is a tissue polarity and a cell divides perpendicular to it (Figure 5.4a) then both daughters are equally likely to inherit stem cell fate. The same is true for a stem cell niche. In Type I and Type II the division can be perpendicular to the polarity and thus bisect the polarity marker (Figure 5.4b-c).

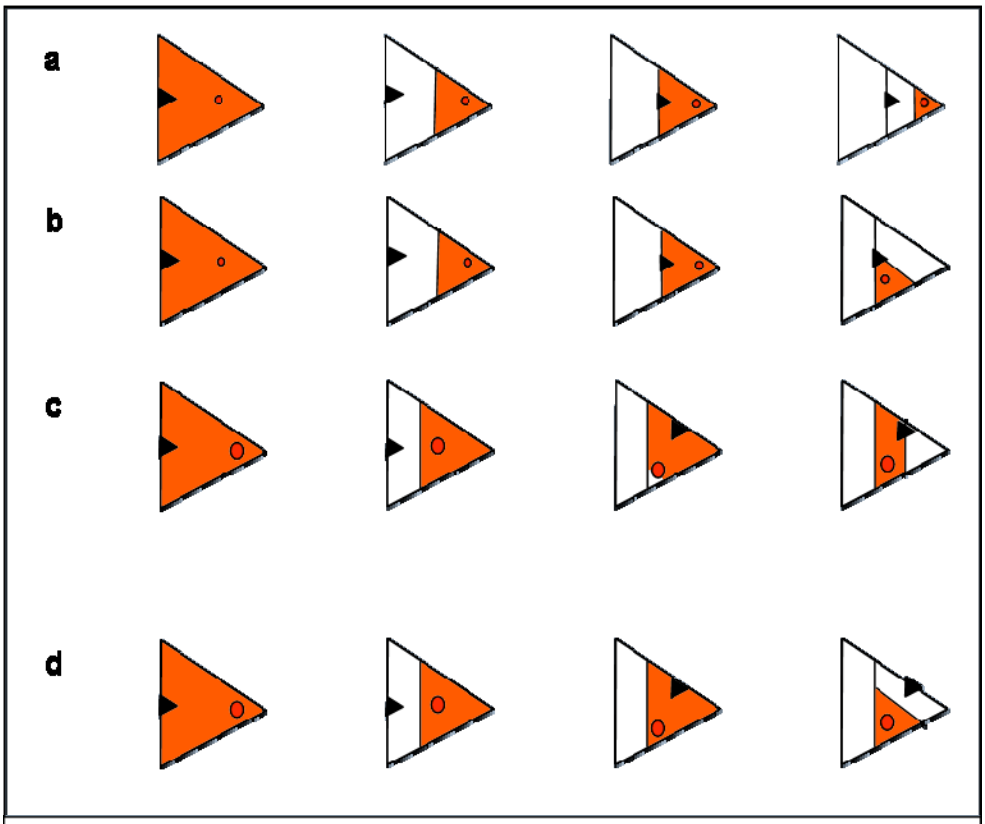

Figure 5.4 aligning division orientation with the fate determinants. The shortest wall algorithm produce more than one solution for an equilateral triangle. a-b) type I inheritance of two divisions that are equally short. a) the inheritance is obvious. b) the shortest wall bisects the polarity marker and the division is perpendicular to the cell polarity. It is not clear which daughter should inherit stem cell fate. c-d) Type II inheritance where the two shortest walls are equally short. c) The polarity and the division orientation are uncoupled and there is ambiguity as to the inheritance of the daughters. d) type II The division orientation and polarity are coupled.

The second issue of aligning the fate determinants and the division is a particular problem for plants. In animals intrinsic fate determinants can be segregated to only one daughter by associating them to one of the spindle poles. However, as we saw in the introduction plants do not divide in the same way as animals. Plants commonly use extrinsic cues to determine the fate of the daughters (e.g. the movement of SHR to confer endodermal cell fate). In stomata there are many signals that could influence the division orientation and the fate of the daughter cells. However, the retrospective analysis and the tracking of SPCH and BASL expression showed that the smaller cell is

usually the one that inherits the stem cell fate, maintains SPCH expression and does not have maternal peripheral BASL (section 4.4.1-4.4.3, Figure 4.34-4.37). This means there must be some intrinsic coupling between the fate determinants and the division machinery. By considering the primary meristemoids this thesis focused on this intrinsic means of determining stem cell fate inheritance.

Displacing the nucleus can change the orientation of the division

The shortest wall algorithm was able to predict the division of the *spch* cells by dividing the cells through the centre. In wild-type cells the division does not always go through the centre. Using the shortest wall algorithm to divide a cell through a point that is displaced from the centre causes a shift in the division wall and a smaller cell to be formed. Displacing the nucleus further showed that the orientation of the division wall can also be changed (Figure 4.26). Modelling the effect of moving the shortest wall algorithm away from the centre showed a switch point at which the wall changed from joining opposite walls to joining adjacent walls. This switch had an associated drop in the percentage size of the smallest cell. Applying the shortest wall algorithm to a cell with a displaced nucleus can therefore generate different physical asymmetries and different division orientations. However, we still have not addressed the question of how to couple division orientation to daughter cell fate.

Orienting nuclear movement

Modelling asymmetric divisions highlights the problem of determining the direction to move the nucleus. For this we can return to our 2D scheme of a dividing triangle. Moving the nucleus of all cells in the same direction is equivalent to having a tissue polarity like FRIZZELED in the SOP cell division. This would result in all cells having a physically asymmetric division oriented in the same direction. If the same tissue polarity moves the nucleus and determines the inheritance of fate then the cell division and the fate are coupled.

Can nuclear movement and fate be coupled in an intrinsic way? We can incorporate nuclear movement into the Type I mechanism by displacing the nucleus away from the polarity factor. The division wall is therefore moved away from the polarity marker and the stem cell fate is inherited by the small cell. Over repeated iterations this continues and like in 1D the stem cell remains at the apex. There are no longer any divisions that are perpendicular to the polarity so the daughter cell fate is clear.

To apply the Type II mechanism we need to clarify how we regard it in the case of a triangle. Rather than thinking about the sister cell attracting the stem cell we have to think about the stem cell fate being repelled by the oldest division wall/ relative. In the triangle it is equivalent to the most recent relatives having a stronger power of attraction. This method is equivalent in the 1D case too. If the polarity marker displaces the nucleus the shortest wall algorithm no longer bisects it. Over a number of rounds of division the Type II mechanism creates a different arrangement of cells to the Type I mechanism. The Type II mechanism can internalise the stem cell in much the same way as it did in 1D. Type II can generate a spacing pattern in 2D without a need for a global tissue polarity and therefore highlights the interplay between asymmetric divisions and patterning. The polarity factor responsible for implementing Type II mechanism is called factor M in the models. It moves the nucleus and determines the inheritance of stem cell fate.

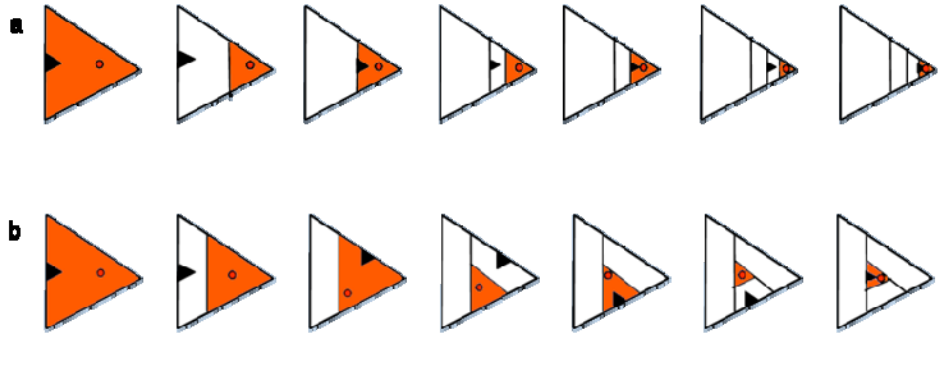

Figure 5.5 Making the division physically asymmetric couples division orientation to fate. If the polarity factor can displace the division wall away from it then the orientation of the division wall is less likely to be perpendicular to it. a) type I keeps the stem cell at the tip while b) type II internalises the stem cell just as in the 1D examples in figure 1.

5.2 Stem cell patterning in a tissue context

Factor M can internalise the stem cell and create a spacing pattern in a triangle by displacing the nucleus and determining cell fate. Factor M was therefore tested on a descriptive model of a real growing cell. Factor M can also internalise stem cells in a descriptive model dividing a realistic cell geometry and growth. The pattern was sensitive to the initial placement of factor M (section 4.3.6, Figure 4.32 & 4.38).

5.2.1 Differential growth accounts for the different cellular arrangements across the leaf

The arrangement of cells created by a stomata lineage varies across the leaf in terms of their overall shape and the orientation of divisions. Applying the factor M model to these cells does not give any insight into what causes the diversity of forms seen. The cells have different initial shapes but they also come from slightly different places on the leaf. In chapter 1 we saw that the growth of the leaf was not uniform, so the cells are likely to be subject to different growth rates. The effect of growth on division orientation was investigated (section 4.3.6, Figure 4.30) and was able to explain the

different clonal arrangements of cells in the *spch* leaf. The effect of different growth rates on the division orientation of stomata lineage cells was investigated by growing a square using different isotropies and applying factor M. Under the different growth conditions the factor M model created different cellular arrangements. By changing the growth and the amount that the nucleus was displaced the models were able to recreate the diverse cellular arrangements observed. This shows the growth of the tissue influences the patterns asymmetric cell divisions can produce and that the patterning mechanisms need to be robust to the different growth conditions.

Factor M includes BASL

In addition to providing information of the cell divisions confocal time-lapse imaging enables protein localisation to be followed. Following the location of BASL showed a good agreement to the predicted location of factor M from the models (Figure 4.38). The location of BASL seen confirmed the published observations (Dong et al., 2009). Following the cells over long time periods enabled specific cell lineages to be modelled descriptively using their shape and growth rates. Initiating the factor M model with the initial location of BASL in the descriptive model enabled the placement of factor M to be tested. Successive locations of factor M matched the observed BASL locations supporting the hypothesis that they are placed in the same way. BASL is also reported to be found distal to the nucleus, consistent with our model and observations. The *basl* mutant has reduced asymmetric divisions in terms of fate and physical asymmetry(Dong et al., 2009). However, although the mutant phenotype of *basl* is consistent with its role as factor M the phenotype is too mild for BASL to be the only protein responsible for the activity of factor M. In the future other components of factor M may be elucidated. There may also be redundant pathways that act by other mechanisms.

5.2.2 Stem cells have increased proliferation

In the 1D and 2D schematic we assumed that only the stem cell was dividing (Figure 5.4). To consider the stem cells in a tissue context we need to consider the division of the other cells. In the leaf there are non-stomata cells that divide, and sisters of stomata

lineage cells which divide to create secondary meristemoids. Studies of the *spch* mutant showed that not all cells divide at the same size. There is a mid-vein to lamina gradient in division area and cell cycle duration. Which is cause and which is effect is not clear, but there is a stronger correlation in the area at the time of division. This gradient was modelled as an inhibitor from the mid-vein (Section 3.2.2, Figure 3.23). The analysis of the tracking also showed that cells are only competent to divide within 200µm² of the petiole laminar boundary (Section 3.2.4, Figure 3.30). Applying a constant production of cell division promoter at the base of the leaf enabled the cell arrest to be re-created. This confirms in 2D a result seen in 1D (Kazama et al., 2010). This result is in contrast to the traditional view of arrest moving from the tip to the base (Donnelly et al., 1999). Combining the two gradients into one model enabled the observed distribution of final cell areas to be re-created (Section 3.2.5, Figure 3.37). Comparing the growth and division of the *spch* leaf shows a correlation between the fastest growing areas and the highest division rate (Section 3.3.3, Figure 3.44). The investigation of cell division area shows that the high division rate is not a consequence of the cells reaching the threshold area faster. The comparison suggests that growth and cell division may be controlled by a common mechanism. The combination of different division frequency and growth rates results in a leaf which has a non-uniform distribution of cell size and cell number. The population of cells available for patterning by asymmetric divisions is, therefore, dependent on the region of the leaf. The identity of the factors in the model is unknown at this stage. These factors would be easier to identify my looking at the phenotype of some mutants in a spch mutant background.

The retrospective analysis allows the division properties of the stomata forming (P_1) cells and the non-stomata forming (Q) cells to be investigated separately (Section 4.2.2). It was found that the P_1 cells divided more than the Q cells consistent with them being stem cells. The P_1 cells had a shortest cell cycle duration (6-16hours) compared to the Q cells (27hours plus) and divided at a smaller average size (P_1 cells = 76µm² , and Q cell = 201µm²). The size of the division of the Q cells was quite close to that of the *spch* cells. The P_1 cells were also dividing at successively smaller sizes while the *spch* mutant cells divided at larger and larger areas. The P_1 cells divided at 1.5 times the area they were created. This suggests there is a mechanism to lower the area at which the P_1 cells divide or shorten the cell cycle time. Adding a lower area threshold to the descriptive

model in place of the observed time of division created realistic division patterns for single cell lineages. Adding a ratio of division area relative to size the cell was created improved the models match to the observed cells.

Mechanisms to regulate proliferation

What kind of mechanism could regulate the size of cell division so that it depends on the size that the cell is created? In the introduction we saw two ideas: production of a fixed amount of inhibitor of division or the gradual build up of a promoter of division through the division cycle (Fantes, 1981a). POM1 regulation of yeast cell division is an example of the former (Moseley et al., 2009). These mechanisms are concerned with maintaining a constant cell size. To create the decreasing size of division seen for the stem cells there could be differential regulation of either: the initial level of the molecule, the decay rate of the molecule or the threshold for triggering cell division. Instead of dividing the cell when the level reached half the original level it could be divided when it reached three quarters of the level or any other level. The alternative could be that a promoter of cell division built up more quickly in the stem cells than the other cells. It is not clear which is more likely to be acting in plants. The identification of stomata specific cell cycle genes might mean the stem cell divisions act through a different cell cycle factor that may have different properties in terms of threshold levels or rates of synthesis. This thesis has shown that studying cell cycle genes in a spch mutant background might help to elucidate mechanisms more easily.

SPCH promotes cell proliferation and stem cell fate in the stomata lineage

How could a higher rate of proliferation be passed on to only one daughter? In animals factors have been identified which are inherited by only one daughter at the time of division and promote proliferation (e.g. aPKC is inherited by the proliferating NB cells). The model highlights the need for a proliferation factor to be inherited by the stem cells. Following SPCH expression in dividing tissue showed that it is likely to be a key factor

in conveying stomata lineage fate and promoting proliferation. SPCH expression correlated with P_1 cell fate and with high division frequency. The *spch* mutant does not form stomata but also divides less (MacAlister et al., 2007). The size of Q cells at the time of division was within the range of cell division sizes seen in the *spch* mutant. Supporting the model that SPCH lowers the division threshold. Over expressing SPCH has previously been shown to increase the number of divisions (MacAlister et al., 2007). Currently the mechanism by which SPCH could lower the division threshold is unclear. We can speculate that if there is a component like POM1 in Arabidopsis that SPCH might act to break it down more quickly. Alternatively SPCH may act to accelerate the cell cycle.

SPCH was not inherited by one cell as the model would predict. Instead immediately after division SPCH was present in both of the daughter cells (Figure 4.34). Expression was then maintained in one cell and extinguished in the other. The cell which maintained SPCH was the one that inherited the stem cell fate. In the model the cell that maintains SPCH expression is determined by the same factor that polarises the cell; factor M. The daughter which loses SPCH expression is the one which has maternal peripheral factor M. The lineages which were followed that expressed the BASL marker showed that the cell which had maternal peripheral BASL was not the one that maintained stem cell fate. Could peripheral BASL or other member of the factor M complex extinguish SPCH expression? Alternatively the decision could be determined based on cell size. This would make the decision extrinsic although the size difference is a result of intrinsic factors. Live imaging of a double BASL SPCH marker would be needed to verify that the cell which maintained SPCH expression was the one without maternal peripheral BASL.

The expression of SPCH in both daughters following division suggests extrinsic factors might play a role in determining which cell maintains SPCH expression. The study of SPCH patches showed an example of SPCH being maintained in the larger cell. In this case the smaller cell was in contact with another SPCH expressing cell. This maybe a coincidence, however, it may suggest a possibility to alter the fate decisions of the daughters after the division as a correction mechanism. The contribution of such an extrinsic mechanism to the primary stomata formation is unclear. Extrinsic signals may

play a more important role in the fate of secondary meristemoids. What could the extrinsic signals be?

5.2.3 Regulating stem cell fate acquisition

Focusing on primary stomata formation simplified the model of stomata formation. It showed that pattern could be created by controlling the division rules. The mechanism was mainly intrinsic although it also involved communication with related neighbours. By focussing on one aspect the model only required two factors. However, many stomata form by secondary meristemoids formation and there are many factors that are not incorporated into the model. Some preliminary observations were made of secondary meristemoids formation and they seemed to fit with the model. In cells that formed secondary meristemoids peripheral BASL was located proximal to the neighbouring stomata and the division was oriented away from it. The live imaging showed examples of cells losing SPCH expression and then re-gaining it some time later. The re-gaining of SPCH expression was associated with a return of the stem cell fate. However, there is insufficient data to exclude the possibility of a different mechanism operating, in part or entirely, for secondary meristemoids. The model was unable to predict when the sister cells regain SPCH or which one of the sisters will be selected. However, regulating the occurrence of new stem cells is vital to maintaining a pattern.

TOO *MANY MOUTHS (TMM)* is thought to regulate stomata density and the orientation of the divisions. In the *tmm* mutant clusters of stomata form. I wanted to see if TMM could be considered within the context of my model and thus establish the role of extrinsic elements and known patterning factors. TMM is thought be a receptor for mobile signals. The *tmm* mutant has been studied in detail including the following of *tmm* mutant followed using dental resin impressions (Geisler et al., 2000). I analysed this data using the retrospective analysis (Figure 5.6). The patch has three cells that are P_1 cells in the first image. One of these (i) behaves in the same way as P_1 cells seen in

wild-type lineage shown below, it divides to produce a B cell and a P_1 cell which makes a stomata. The second (ii) produces a stomata, presumably the GMC phase was not captured. The third (iii) can be classified as a P_3 cell as it produces three P_1 cells. The first division results in a P_1 cell which immediately produces a stomata and a P_2 cell. The P_2 cell produces another two P_1 cells, one of which matures into a stomata while the other divides again to produce another P_1 cell. It is impossible to know whether this P_1 cell divides to produce even more P_1 cells or not. In the *tmm* P_1 cells prematurely produce GMCs and the sister cells maintain P_1 cell fate. According to my model this would mean P_1 cells in the *tmm* mutant lose SPEECHLESS expression too quickly and become GMCs. The sister cells to the P_1 cells seem to have P_1 cell fate. I suggest that they are either not losing SPCH expression as they should or they are re-gaining it almost immediately. In the wild-type lineages there was a significant wait before the sister cells of P_1 cells re-gained SPCH if they ever do. I was unable to suggest a mechanism for the timing of acquisition of SPCH by these cells. A possible role for TMM might be to communicate when a secondary meristemoid can divide and ensure only one of the sister cells divides. This fits with the view that TMM might be similar to CLV2. Structurally the two proteins are similar. (Nadeau, 2003). CLV2 is responsible for regulating the balance between stem cell proliferation and maturation in the shoot apical meristem Jeong (1999). However, it leaves open some questions. Does TMM regulate SPCH expression? If TMM has a role in orienting divisions as is widely suggested does it act through BASL? It would be interesting to look at the distribution of BASL and SPCH markers in the *tmm* mutant background.

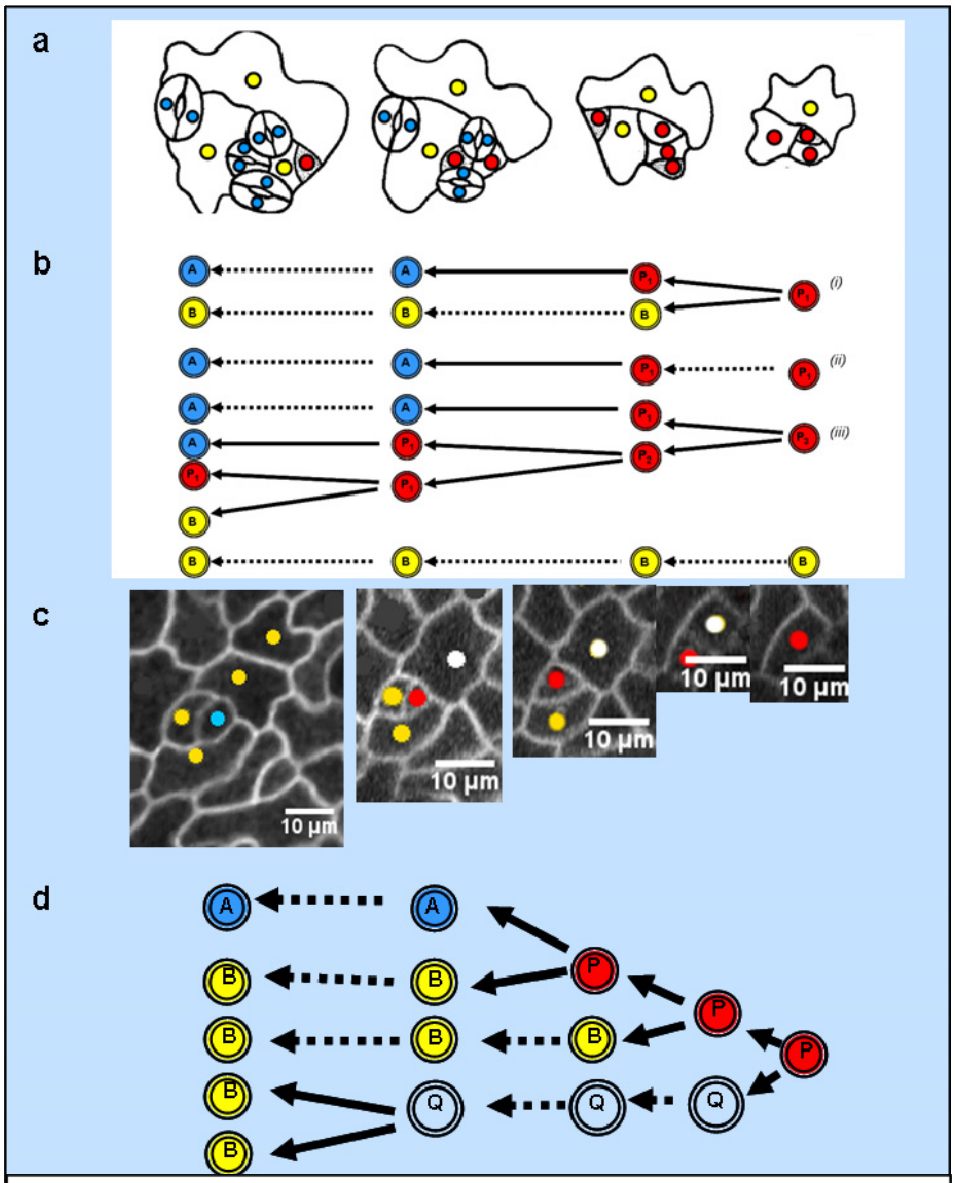

Figure 5.6 Comparing the *tmm* mutant and wild-type using retrospective analysis. a) dental resin impression of *tmm* mutant (Figure 11 part B (Geisler et al., 2000)) classified using the method shown in chapter 3. b) a scheme for the *tmm* lineage. c) a wild-type lineage for comparison with its associated scheme (d).

Other areas for further work are to consider whether all cells have SPCH expression initially and what causes the final arrest of stomata formation.

Conclusion of the thesis

Stomata formation in the Arabidopsis epidermis is a physically accessible system in which to study stem cell divisions in a growing tissue. By focusing on only one specific aspect of stomata formation, the asymmetric cell division of primary stomata, we were able to learn something about how patterns might be generated within a growing tissue. Comparing the development of the wild-type epidermis with that of the *spch* mutant enabled us to distinguish characteristics that are specific to the asymmetric division. Based on these observations, we created a model of the *spch* mutant to capture the properties of the tissue. Using the tissue model as a basis we generated a mechanistic model for patterning stem cell lineages which matched the observed behaviour. Finally further live imaging allowed us to identify known stomata factors that might be responsible for the behaviour of the model and thus suggest a mechanism in which they might function. This work makes some testable predictions about the formation of secondary meristemoids and the function of other known genes.

Abramoff, M.D., Magelhaes, P.J., Ram, S.J. (2004.). "Image Processing with ImageJ". Biophotonics International, *11*, 36-42, .
Abrash, E.B., and Bergmann, D.C. (2009). Asymmetric Cell Divisions: A View from Plant Development. Dev Cell *16*, 783-796.
Avery, G.S. (1932). Structure and development of the tobacco leaf. Am J Bot *20*, 565 - 592.
Barbier de Reuille, P.B., Bohn-Courseau, I., Godin, C., and Traas, J. (2005). A protocol to analyse cellular dynamics during plant development. Plant J *44*, 1045-1053.
Bellaiche, Y., Radovic, A., Woods, D.F., Hough, C.D., Parmentier, M.L., O'Kane, C.J., Bryant, P.J., and Schweisguth, F. (2001). The partner of inscuteable/discs-large complex is required to establish planar polarity during asymmetric cell division in Drosophila. Cell *106*, 355-366.
Benfey, P.N., Linstead, P.J., Roberts, K., Schiefelbein, J.W., Hauser, M.T., and Aeschbacher, R.A. (1993). Root Development in Arabidopsis - 4 Mutants with Dramatically Altered Root Morphogenesis. Development *119*, 57-70.
Berger, D., and Altmann, T. (2000). A subtilisin-like serine protease involved in the regulation of stomatal density and distribution in Arabidopsis thaliana. Gene Dev *14*, 1119-1131.
Boudolf, V., Barroco, R., Engler, J.D., Verkest, A., Beeckman, T., Naudts, M., Inze, D., and De Veylder, L. (2004). B1-type cyclin-dependent kinases are essential for the formation of stomatal complexes in Arabidopsis thaliana. Plant Cell *16*, 945-955.
Bultje, R.S., Castaneda-Castellanos, D.R., Jan, L.Y., Jan, Y.N., Kriegstein, A.R., and Shi, S.H. (2009). Mammalian Par3 Regulates Progenitor Cell Asymmetric Division via Notch Signaling in the Developing Neocortex. Neuron *63*, 189-202.
Cartwright, H.N., Humphries, J.A., and Smith, L.G. (2009). PAN1: A Receptor-Like Protein That Promotes Polarization of an Asymmetric Cell Division in Maize. Science *323*, 649-651.
Chan, J., Calder, G., Fox, S., and Lloyd, C. (2007). Cortical microtubule arrays undergo rotary movements in Arabidopsis hypocotyl epidermal cells. Nat Cell Biol *9*, 171-U157.
Chickarmane, V., Roeder, A.H.K., Tarr, P.T., Cunha, A., Tobin, C., and Meyerowitz, E.M. (2010). Computational Morphodynamics: A Modeling Framework to Understand Plant Growth. Annual Review of Plant Biology, Vol 61 *61*, 65-87.
Claudia Kutter, a.H.S., and Michael Stadler, and Frederick Meins Jr., and Azeddine Si-Ammour (2007). MicroRNA-Mediated Regulation of Stomatal Development in Arabidopsis. The Plant Cell *19*, 2417-2429.
Coen, E., Rolland-Lagan, A.G., Matthews, M., Bangham, J.A., and Prusinkiewicz, P. (2004). The genetics of geometry. P Natl Acad Sci USA *101*, 4728-4735.
Croxdale, J. (2000). Stomatal Patterning in Angiosperms. Am J Bot *87*, 1069-1080.
Cui, H.C., Levesque, M.P., Vernoux, T., Jung, J.W., Paquette, A.J., Gallagher, K.L., Wang, J.Y., Blilou, I., Scheres, B., and Benfey, P.N. (2007). An evolutionarily conserved mechanism delimiting SHR movement defines a single layer of endodermis in plants. Science *316*, 421-425.
De Veylder, L., Beeckman, T., Beemster, G.T.S., Engler, J.D., Ormenese, S., Maes, S., Naudts, M., Van der Schueren, E., Jacqmard, A., Engler, G., and Inze, D. (2002). Control of proliferation, endoreduplication and differentiation by the Arabidopsis E2Fa-DPa transcription factor. Embo J *21*, 1360-1368.

De Veylder, L., Van Montagu, M. and Inze, D. (1998). Cell cycle control in Arabidopsis. In Plant cell division, D.D.a.D.I. D. Francis, ed. (Portland Press), pp. 1-20.
Dewitte, W., and Murray, J.A.H. (2003). The plant cell cycle. Annu Rev Plant Biol *54*, 235-264.
DiLaurenzio, L., WysockaDiller, J., Malamy, J.E., Pysh, L., Helariutta, Y., Freshour, G., Hahn, M.G., Feldmann, K.A., and Benfey, P.N. (1996). The SCARECROW gene regulates an asymmetric cell division that is essential for generating the radial organization of the Arabidopsis root. Cell *86*, 423-433.
Dolan, L., and Poethig, R.S. (1998). Clonal analysis of leaf development in cotton. Am J Bot *85*, 315-321.
Dong, J., MacAlister, C.A., and Bergmann, D.C. (2009). BASL Controls Asymmetric Cell Division in Arabidopsis. Cell *137*, 1320-1330.
Donnelly, P.M., Bonetta, D., Tsukaya, H., Dengler, R.E., and Dengler, N.G. (1999). Cell cycling and cell enlargement in developing leaves of Arabidopsis. Dev Biol *215*, 407-419.
Dumais, J., and Kwiatkowska, D. (2002). Analysis of surface growth in shoot apices. Plant J *31*, 229-241.
Errera, L. (1888). Uber zellformen und seifenblasen. . Bot Centralbl *34*, 395-398.
Fantes, P.A.a.N., P. (1981a). Division timing: controls, models and mechanisms. In The cell cycle, P.C.L. John, ed. (Cambridge University Press), pp. 11-35.
Fantes, P.N.a.P.A. (1981b). Cell cycle controls in fission yeast: a genetic analysis. In The cell cycle, P.C.L. John, ed. (Cambridge University Press), pp. 85-99.
Fernandez, R., Das, P., Mirabet, V., Moscardi, E., Traas, J., Verdeil, J.L., Malandain, G., and Godin, C. (2010). Imaging plant growth in 4D: robust tissue reconstruction and lineaging at cell resolution. Nat Methods *7*, 547-U594.
Fuller, M.T., and Spradling, A.C. (2007). Male and female Drosophila germline stem cells: Two versions of immortality. Science *316*, 402-404.
Gallagher, K., and Smith, L.G. (2000). Roles for polarity and nuclear determinants in specifying daughter cell fates after an asymmetric cell division in the maize leaf. Curr Biol *10*, 1229-1232.
Geisler, M., Nadeau, J., and Sack, F.D. (2000). Oriented asymmetric divisions that generate the stomatal spacing pattern in Arabidopsis are disrupted by the too many mouths mutation. Plant Cell *12*, 2075-2086.
Geisler, M.J., Deppong, D.O., Nadeau, J.A., and Sack, F.D. (2003). Stomatal neighbor cell polarity and division in Arabidopsis. Planta *216*, 571-579.
Gho, M., and Schweisguth, F. (1998). Frizzled signalling controls orientation of asymmetric sense organ precursor cell divisions in Drosophila. Nature *393*, 178-181.
Grandjean, O., Vernoux, T., Laufs, P., Belcram, K., Mizukami, Y., and Traas, J. (2004). In vivo analysis of cell division, cell growth, and differentiation at the shoot apical meristem in arabidopsis. Plant Cell *16*, 74-87.
Grieneisen, V.A., Xu, J., Maree, A.F.M., Hogeweg, P., and Scheres, B. (2007). Auxin transport is sufficient to generate a maximum and gradient guiding root growth. Nature *449*, 1008-1013.
Guo, M., Jan, L.Y., and Jan, Y.N. (1996). Control of daughter cell fates during asymmetric division: Interaction of numb and notch. Neuron *17*, 27-41.
Hamant, O., Heisler, M.G., Jonsson, H., Krupinski, P., Uyttewaal, M., Bokov, P., Corson, F., Sahlin, P., Boudaoud, A., Meyerowitz, E.M.*, et al.* (2008). Developmental Patterning by Mechanical Signals in Arabidopsis. Science *322*, 1650-1655.

Hara, K., Kajita, R., Torii, K.U., Bergmann, D.C., and Kakimoto, T. (2007). The secretory peptide gene EPF1 enforces the stomatal one-cell-spacing rule. Gene Dev *21*, 1720-1725.
Hara, K., Yokoo, T., Kajita, R., Onishi, T., Yahata, S., Peterson, K.M., Torii, K.U., and Kakimoto, T. (2009). Epidermal Cell Density is Autoregulated via a Secretory Peptide, EPIDERMAL PATTERNING FACTOR 2 in Arabidopsis Leaves. Plant Cell Physiol *50*, 1019-1031.
Hejnowicz, Z., and Romberger, J.A. (1984). Growth Tensor of Plant Organs. J Theor Biol *110*, 93-114.
Helariutta, Y., Fukaki, H., Wysocka-Diller, J., Nakajima, K., Jung, J., Sena, G., Hauser, M.T., and Benfey, P.N. (2000). The SHORT-ROOT gene controls radial patterning of the Arabidopsis root through radial signaling. Cell *101*, 555-567.
Hofmeister, W. (1863). Zusätze und berichtigungen zu den 1851 veröffentlichen untersuchungengen der entwicklung höherer krytogamen. . Jahrb Wiss Bot *3*, 259-293.
Hofmeister, W. (1868). In in Handbuch der Physiologischen Botanik, A.d. Bary, Irmisch, T. H. & Sachs, J., ed. (Engelmann, Leipzig, Germany), pp. 405–664.
Horvitz, H.R., and Herskowitz, I. (1992). Mechanisms of Asymmetric Cell-Division - 2 Bs or Not 2 Bs, That Is the Question. Cell *68*, 237-255.
Hunt, L., and Gray, J.E. (2009). The Signaling Peptide EPF2 Controls Asymmetric Cell Divisions during Stomatal Development. Curr Biol *19*, 864-869.
Hunt, L., Gray, J. (2010). BASL and EPF2 act independently to regulate asymmetric divisions during stomatal development. Plant Signaling and Behaviour *5*, 278-280.
Ivanov, V.B., Dobrochaev, A.E., and Baskin, T.I. (2002). What the distribution of cell lengths in the root meristem does and does not reveal about cell division. J Plant Growth Regul *21*, 60-67.
J-L. Giavitto, C.G., O. Michel & P. Prusinkiewicz (2002). Computational Models for Integrative and Developmental Biology. In proceedings
of the workshop "Mod´elisation et simulation de processus biologiques dans le contexte de la gnomique".
Jan, Y.N., and Jan, L.Y. (1998). Asymmetric cell division. Nature *392*, 775-778.
Kanaoka, M.M., Pillitteri, L.J., Fujii, H., Yoshida, Y., Bogenschutz, N.L., Takabayashi, J., Zhu, J.K., and Torii, K.U. (2008). SCREAM/ICE1 and SCREAM2 specify three cell-state transitional steps leading to Arabidopsis stomatal differentiation. Plant Cell *20*, 1775-1785.
Kazama, T., Ichihashi, Y., Murata, S., and Tsukaya, H. (2010). The Mechanism of Cell Cycle Arrest Front Progression Explained by a KLUH/CYP78A5-dependent Mobile Growth Factor in Developing Leaves of Arabidopsis thaliana. Plant Cell Physiol *51*, 1046-1054.
Knoblich, J.A. (2001). Asymmetric cell division during animal development. Nat Rev Mol Cell Bio *2*, 11-20.
Knoblich, J.A. (2008). Mechanisms of asymmetric stem cell division. Cell *132*, 583-597.
Kono, A., Umeda-Hara, C., Adachi, S., Nagata, N., Konomi, M., Nakagawa, T., Uchimiya, H., and Umeda, M. (2007). The Arabidopsis D-type cyclin CYCD4 controls cell division in the stomatal lineage of the hypocotyl epidermis. Plant Cell *19*, 1265-1277.
Korn, R.W. (1993). Heterogeneous growth of plant tissues. Bot J Linn Soc *112*, 351-371.
Kwiatkowska, D. (2006). Flower primordium formation at the Arabidopsis shoot apex: quantitative analysis of surface geometry and growth. J Exp Bot *57*, 571-580.

L. De Veylder, M.V.M.a.D.I. (1998). Cell cycle control in Arabidopsis. In Plant cell division, D.D.a.D.I. D. Francis, ed. (Portland Press), pp. 1-20.
Lampard, G.R., Lukowitz, W., Ellis, B.E., and Bergmann, D.C. (2009). Novel and Expanded Roles for MAPK Signaling in Arabidopsis Stomatal Cell Fate Revealed by Cell Type-Specific Manipulations. Plant Cell *21*, 3506-3517.
Lampard, G.R., MacAlister, C.A., and Bergmann, D.C. (2008). Arabidopsis Stomatal Initiation Is Controlled by MAPK-Mediated Regulation of the bHLH SPEECHLESS. Science *322*, 1113-1116.
Larkin, J.C., Marks, M.D., Nadeau, J., and Sack, F. (1997). Epidermal cell fate and patterning in leaves. Plant Cell *9*, 1109-1120.
Levesque, M.P., Vernoux, T., Busch, W., Cui, H.C., Wang, J.Y., Blilou, I., Hassan, H., Nakajima, K., Matsumoto, N., Lohmann, J.U*., et al.* (2006). Whole-genome analysis of the SHORT-ROOT developmental pathway in Arabidopsis. Plos Biol *4*, 739-752.
Lynch, T.M., and Lintilhac, P.M. (1997). Mechanical signals in plant development: A new method for single cell studies. Dev Biol *181*, 246-256.
MacAlister, C.A., Ohashi-Ito, K., and Bergmann, D.C. (2007). Transcription factor control of asymmetric cell divisions that establish the stomatal lineage. Nature *445*, 537-540.
Martin, S.G., and Berthelot-Grosjean, M. (2009). Polar gradients of the DYRK-family kinase Pom1 couple cell length with the cell cycle. Nature *459*, 852-U857.
McCarthy, E.K., and Goldstein, B. (2006). Asymmetric spindle positioning. Curr Opin Cell Biol *18*, 79-85.
Melaragno, J.E., Mehrotra, B., and Coleman, A.W. (1993). Relationship between Endopolyploidy and Cell-Size in Epidermal Tissue of Arabidopsis. Plant Cell *5*, 1661-1668.
Mineyuki, Y., Marc, J., and Palevitz, B.A. (1991). Relationship between the Preprophase Band, Nucleus and Spindle in Dividing Allium Cotyledon Cells. J Plant Physiol *138*, 640-649.
Mitchison, J.M. (1971). The biology of the cell cycle (Cambridge University Press).
Mitchison, J.M. (1981). Changing perspectives in the cell cycle. In The cell cycle, P.C.L. John, ed. (Cambridge University Press), pp. 1-11.
Moseley, J.B., Mayeux, A., Paoletti, A., and Nurse, P. (2009). A spatial gradient coordinates cell size and mitotic entry in fission yeast. Nature *459*, 857-U858.
Mundermann, L., Erasmus, Y., Lane, B., Coen, E., and Prusinkiewicz, P. (2005). Quantitative modeling of Arabidopsis development. Plant Physiol *139*, 960-968.
Murata, T., and Wada, M. (1991). Effects of Centrifugation on Preprophase-Band Formation in Adiantum Protonemata. Planta *183*, 391-398.
Nadeau, J.A.a.S., F.D (2002). Control of stomatal distribution on the Arabidopsis leaf surface. . Science *296*, 1697-1700

Nadeau, J.A.a.S., F.D (2003). Stomatal development: cross talk puts mouths in place. . trends in Plant Sciences *6*, 294-299.
Nakajima, K., Sena, G., Nawy, T., and Benfey, P.N. (2001). Intercellular movement of the putative transcription factor SHR in root patterning. Nature *413*, 307-311.
Nakielski, J. (2008). The tensor-based model for growth and cell divisions of the root apex. I. The significance of principal directions. Planta *228*, 179-189.
Ohashi-Ito, K., and Bergmann, D.C. (2006). Arabidopsis FAMA controls the final proliferation/differentiation switch during stomatal development. Plant Cell *18*, 2493-2505.

Olivier, N., Luengo-Oroz, M.A., Duloquin, L., Faure, E., Savy, T., Veilleux, I., Solinas, X., Debarre, D., Bourgine, P., Santos, A.*, et al.* (2010). Cell Lineage Reconstruction of Early Zebrafish Embryos Using Label-Free Nonlinear Microscopy. Science *329*, 967-971.
P.Nurse, P.A.F.a. (1981). Division timing: controls, models and mechanisms. In The cell cycle, P.C.L. John, ed. (Cambridge University Press), pp. 11-35.
Palubicki, W., Horel, K., Longay, S., Runions, A., Lane, B., Mech, R., and Prusinkiewicz, P. (2009). Self-organizing tree models for image synthesis. Acm T Graphic *28*, -.
Pickett-Heaps.Jd, and Northcot.Dh (1966). Organization of Microtubules and Endoplasmic Reticulum during Mitosis and Cytokinesis in Wheat Meristems. J Cell Sci *1*, 109-&.
Pillitteri, L.J., Bogenschutz, N.L., and Torii, K.U. (2008). The bHLH protein, MUTE, controls differentiation of stomata and the hydathode pore in Arabidopsis. Plant Cell Physiol *49*, 934-943.
Priestley, J.H. (1930). Studies in the physiology of cambial activity.I.The concept of sliding growth. New Physiol *29*, 96-140.
Reddy, G.V., Heisler, M.G., Ehrhardt, D.W., and Meyerowitz, E.M. (2004). Real-time lineage analysis reveals oriented cell divisions associated with morphogenesis at the shoot apex of Arabidopsis thaliana. Development *131*, 4225-4237.
Roeder, A.H.K., Chickarmane, V., Cunha, A., Obara, B., Manjunath, B.S., and Meyerowitz, E.M. (2010). Variability in the Control of Cell Division Underlies Sepal Epidermal Patterning in Arabidopsis thaliana. Plos Biol *8*, -.
Sachs, J. (1878). Üeber die Anordnung der zellen in jüngsten pflanzentheilen. Arb Bot Inst Wurzburg *2*, 46–104.
Sachs, T. (1978). The development of spacing patterns in the leaf epidermis. In The Clonal Basis of Development S.S.a.I.M. Sussex, ed. (New York Academic Press), pp. 161-183.
Sachs, T. (1991). Pattern formation in plant tissues, Vol chapter 1

Sachs, T. (1994). BOTH CELL LINEAGES AND CELL-INTERACTIONS CONTRIBUTE TO STOMATAL PATTERNING International Journal of Plant Sciences *155*, 245-247.
Sack, F.D., and Chen, J.G. (2009). Plant Science Pores in Place. Science *323*, 592-593.
Sahlin, P.a.H.J. (2010). A modeling study on how cell division affects properties of epithelial tissues under isotropic growth. PLOS one *5*, 1-9.
Scheres, B. (2001). Plant cell identity. The role of position and lineage. Plant Physiol *125*, 112-114.
Scheres, B., and Benfey, P.N. (1999). Asymmetric cell division in plants. Annu Rev Plant Phys *50*, 505-537.
Scheres, B., Dilaurenzio, L., Willemsen, V., Hauser, M.T., Janmaat, K., Weisbeek, P., and Benfey, P.N. (1995). Mutations Affecting the Radial Organization of the Arabidopsis Root Display Specific Defects Throughout the Embryonic Axis. Development *121*, 53-62.
Serna, L. (2009). Cell fate transitions during stomatal development. Bioessays *31*, 865-873.
Serna, L., and Fenoll, C. (1997). Tracing the ontogeny of stomatal clusters in Arabidopsis with molecular markers. Plant J *12*, 747-755.
Serna, L., Torres-Contreras, J., and Fenoll, C. (2002). Clonal analysis of stomatal development and patterning in Arabidopsis leaves. Dev Biol *241*, 24-33.

Serna, L.a.F.C. (2002). Reinforcing the idea of signalling in the stomatal pathway. . Trends in Genetics.
Shaw, S.L. (2006). Imaging the live plant cell. Plant J *45*, 573-598.
Shpak, E.D., McAbee, J.M., Pillitteri, L.J., and Torii, K.U. (2005). Stomatal patterning and differentiation by synergistic interactions of receptor kinases. Science *309*, 290-293.
Siegrist, S.E., and Doe, C.Q. (2005). Microtubule-induced Pins/G alpha i cortical polarity in Drosophila neuroblasts. Cell *123*, 1323-1335.
Siegrist, S.E., and Doe, C.Q. (2006). Extrinsic cues orient the cell division axis in Drosophila embryonic neuroblasts. Development *133*, 529-536.
Sinnott, E.W. (1936). Growth and differentiation in living plant meristems. PNAS *25*, 55-58.
Smith, C., Prusinkiewicz, P., and Samavati, F. (2003). Local specification of surface subdivision
algorithms (Applications of
Graph Transformations with Industrial Relevance (AGTIVE 2003)). Lecture Notes in Computer Science *3062*, 313-327.
Smith, L.G. (2001). Plant cell division: Building walls in the right places. Nat Rev Mol Cell Bio *2*, 33-39.
Smith, R.S., and Bayer, E.M. (2009). Auxin transport-feedback models of patterning in plants. Plant Cell Environ *32*, 1258-1271.
Smith, R.S., Guyomarc'h, S., Mandel, T., Reinhardt, D., Kuhlemeier, C., and Prusinkiewicz, P. (2006a). A plausible model of phyllotaxis. P Natl Acad Sci USA *103*, 1301-1306.
Smith, R.S., Kuhlemeier, C., and Prusinkiewicz, P. (2006b). Inhibition fields for phyllotactic pattern formation: a simulation study. Can J Bot *84*, 1635-1649.
Snow, M.S., R. (1932). Experiments on Phyllotaxis. I. The effect of isolating a primordium. Philosophical transactions of the royal society London B *221*, 1-43.
Sugano, S.S., Shimada, T., Imai, Y., Okawa, K., Tamai, A., Mori, M., and Hara-Nishimura, I. (2010). Stomagen positively regulates stomatal density in Arabidopsis. Nature *463*, 241-U130.
Sylvester, A.W., Smith, L., and Freeling, M. (1996). Acquisition of identity in the developing leaf. Annu Rev Cell Dev Bi *12*, 257-304.
ten Hove, C.A., and Heidstra, R. (2008). Who begets whom? Plant cell fate determination by asymmetric cell division. Curr Opin Plant Biol *11*, 34-41.
Toledano, H.a.J., D.L. (2009). Mechanisms regulating stem cell polarity and the specification of asymmetric divisions. In StemBook, T.S.C.R. Community, ed. (StemBook).
Tolic-Norrelykke, I.M., Sacconi, L., Stringari, C., Raabe, I., and Pavone, F.S. (2005). Nuclear and division-plane positioning revealed by optical micromanipulation. Curr Biol *15*, 1212-1216.
Vandenberg, C., Willemsen, V., Hage, W., Weisbeek, P., and Scheres, B. (1995). Cell Fate in the Arabidopsis Root-Meristem Determined by Directional Signaling. Nature *378*, 62-65.
von Groll, U., Berger, D., and Altmann, T. (2002). The subtilisin-like serine protease SDD1 mediates cell-to-cell signaling during arabidopsis stomatal development. Plant Cell *14*, 1527-1539.
White, D.W.R. (2006). PEAPOD regulates lamina size and curvature in Arabidopsis. P Natl Acad Sci USA *103*, 13238-13243.
Willemsen, V., Bauch, M., Bennett, T., Campilho, A., Wolkenfelt, H., Xu, J., Haseloff, J., and Scheres, B. (2008). The NAC Domain Transcription Factors FEZ and

SOMBRERO Control the Orientation of Cell Division Plane in Arabidopsis Root Stem Cells. Dev Cell *15*, 913-922.
Wu, P.S., Egger, B., and Brand, A.H. (2008). Asymmetric stem cell division: Lessons from Drosophila. Semin Cell Dev Biol *19*, 283-293.
Yang, M., and Sack, F.D. (1995). The too many mouths and four lips mutations affect stomatal production in arabidopsis. Plant Cell *7*, 2227-2239.
Yu, F.W., Kuo, C.T., and Jan, Y.N. (2006). Drosophila neuroblast asymmetric cell division: Recent advances and implications for stem cell biology. Neuron *51*, 13-20.
Zadnikova, P., Petrasek, J., Marhavy, P., Raz, V., Vandenbussche, F., Ding, Z.J., Schwarzerova, K., Morita, M.T., Tasaka, M., Hejatko, J.*, et al.* (2010). Role of PIN-mediated auxin efflux in apical hook development of Arabidopsis thaliana. Development *137*, 607-617.
Zhang, L.G., Hu, G.Z., Cheng, Y.X., and Huang, J.R. (2008). Heterotrimeric G protein alpha, and beta subunits antagonistically modulate stomatal density in Arabidopsis thaliana. Dev Biol *324*, 68-75.
Zhao, L.M., and Sack, F.D. (1999). Ultrastructure of stomatal development in Arabidopsis (Brassicaceae) leaves. Am J Bot *86*, 929-939.

Supplementary Figures

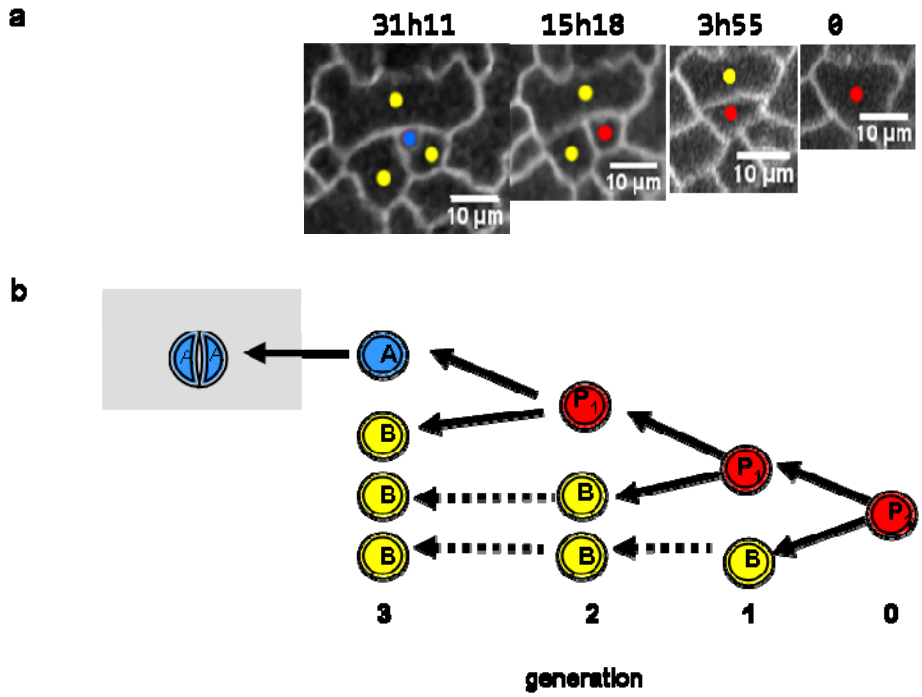

Figure 4. S1 Retrospective analysis of another single stomata lineage. Another example of the same lineage as shown in Figure 4. 2. The greyed out box represent an event that is probable but was not captured.

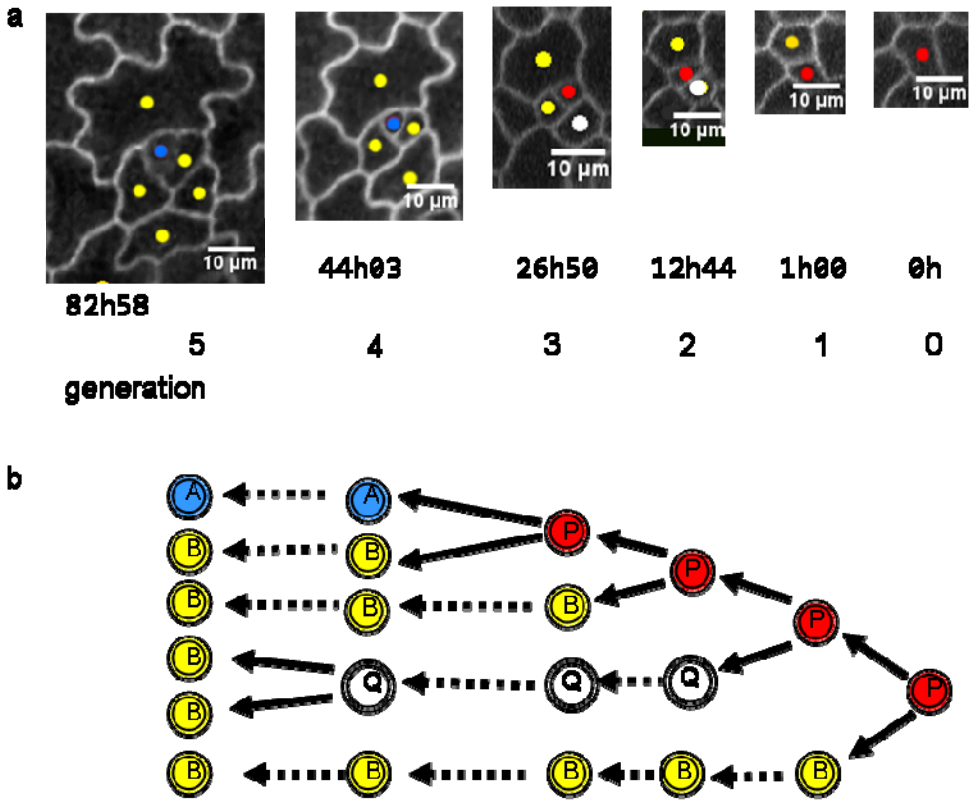

Figure 4. S2 Retrospective analysis of a stomata lineage with dividing Q cells. This lineage has a similar arrangement to the lineage shown in Figure 4. 5.

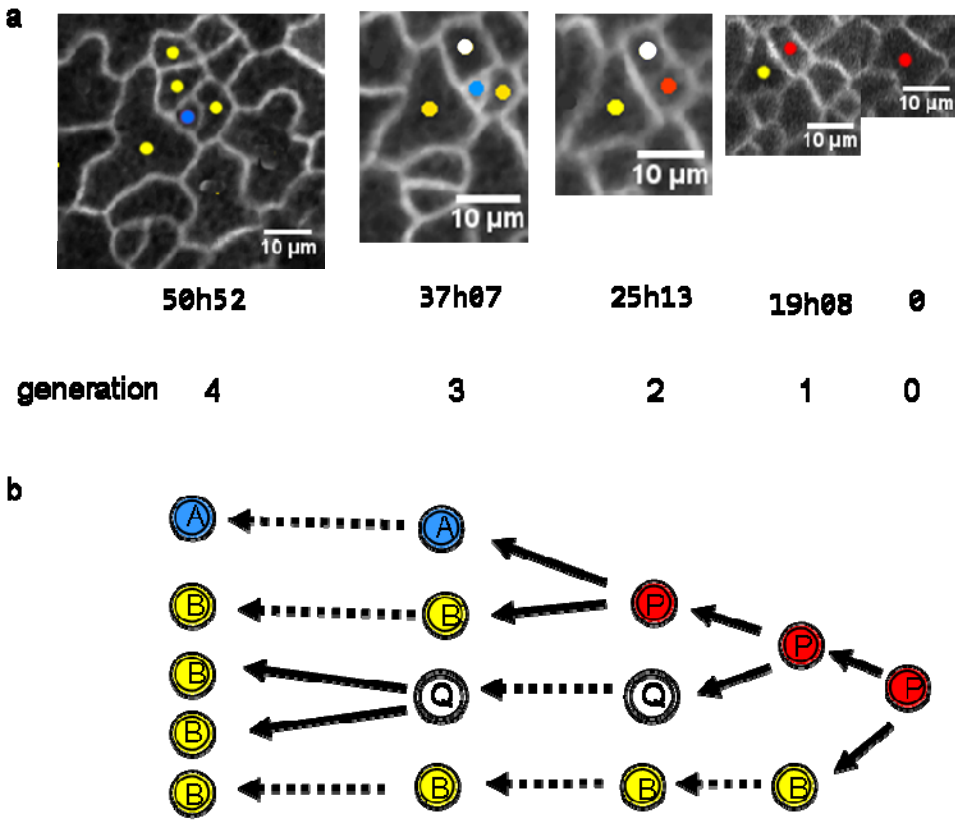

Figure 4. S3 Retrospective analysis of a stomata lineage with dividing Q cells. This lineage has a similar arrangement to the lineage shown in Figure 4. 5.

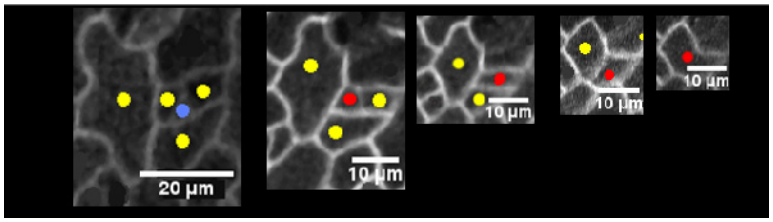

Generation	4	3	2	1
Division area	55µm²	70µm²	105µm²	159µm²
Previous area	47µm²	65µm²	77µm²	131µm²
Daughter areas	17µm²	28µm²	51µm²	63µm²
	37µm²	41µm²	57µm²	96µm²
Creation area	28µm²	51µm²	63µm²	
Real time		18h02	11h54	10h00
		4h44	6h36	6h05

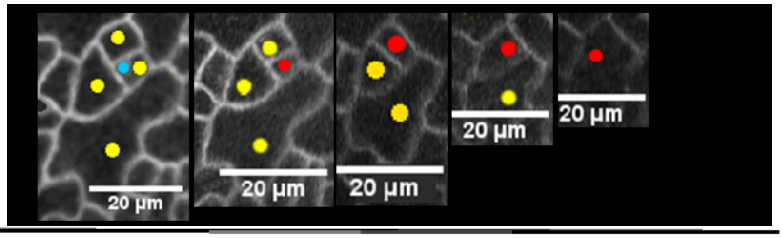

Generation	4	3	2	1
Division area	43µm²	57µm²	81µm²	196µm²
Previous area	33µm²	49µm²	69µm²	156µm²
Daughter areas	13µm²	22µm²	34µm²	57µm²
	31µm²	36µm²	47µm²	134µm²
Creation area	22µm²	34µm²	57µm²	
Real time		11h23	11h08	8h00
		5h18	3h55	4hrs

Figure 4. S4 Division data for more lineages.

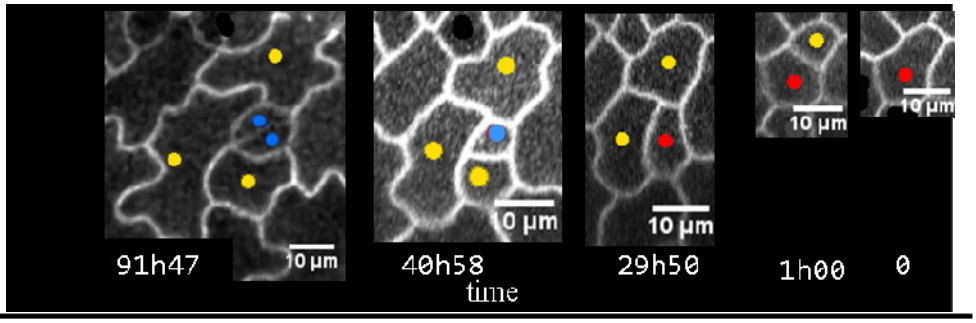

Generation	4	3	2	1
Division area		107µm²	221µm²	168µm²
Previous area		93µm²	200µm²	164µm²
Daughter areas		37µm² 71µm²	76µm² 145µm²	107µm² 62µm²
Creation area		76µm²	107µm²	

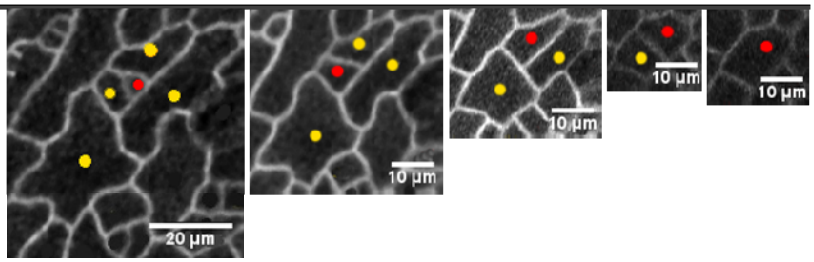

Generation	4	3	2	1
Division area	93µm²	165µm²	225µm²	186µm²
Previous area	73µm²	105µm²	165µm²	163µm²
Daughter areas	65µm²	104µm²	125µm²	85µm²
Creation area	27µm² 64µm²	64µm² 100µm²	100µm²	98µm²

Figure 4. S5 Division data for more lineages.

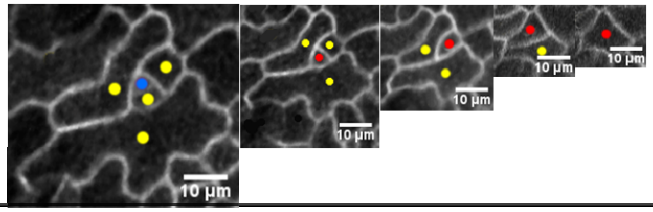

Generation	4	3	2	1
Division area	49µm²	65µm²	161µm²	182µm²
Previous area	40µm²	51µm²	130µm²	158µm²
Daughter areas	33µm² 17µm²	39µm² 27µm²	120µm² 44µm²	107µm² 70µm²
Creation area	27µm²	44µm²	70µm²	

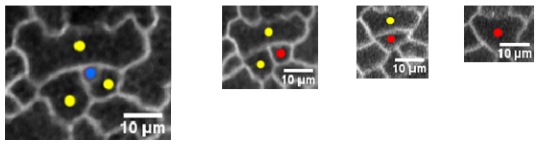

Generation	3	2	1
Division area	74µm²	126µm²	202µm²
Previous area	57µm²	110µm²	179µm²
Daughter areas	54µm² 21µm²	84µm² 45µm²	145µm² 54µm²
Area created	45µm²	54µm²	

Figure 4. S6 Division data for more lineages.

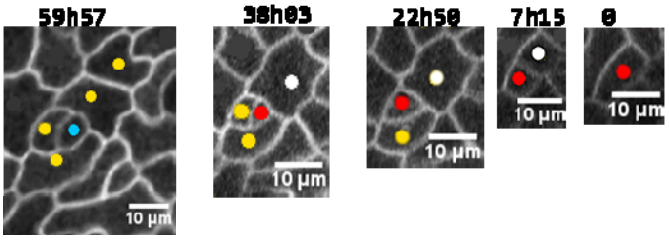

Generation	4	3	2	1
Division area	341µm²	44µm²	80µm²	104µm²
Previous area	307µm²	37µm²	62µm²	
Daughter areas	152µm² 192µm²	17µm² 26µm²	19µm² 58µm	43µm²
Creation area	60µm²	19µm²	43µm²	60µm²

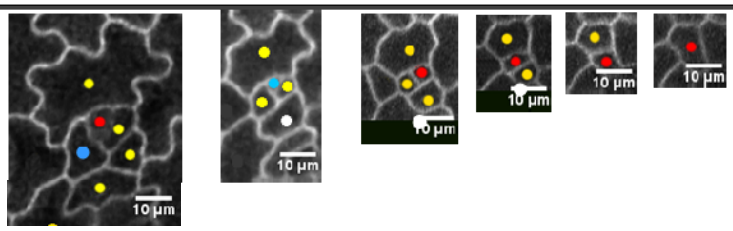

Generation	5	4	3	2	1
Division area	237µm²	42µm²	49µm²	63µm²	110µm²
Previous area	204µm²	35µm²	42µm²	56µm²	104µm²
Daughter areas	83µm² 155µm²	29µm² 16µm²	27µm² 23µm²	34µm² 28µm²	66µm² 44µm²
Creation area	34µm²	23µm²	28µm²	44µm²	

Figure 4. S7 Division data for more lineages.

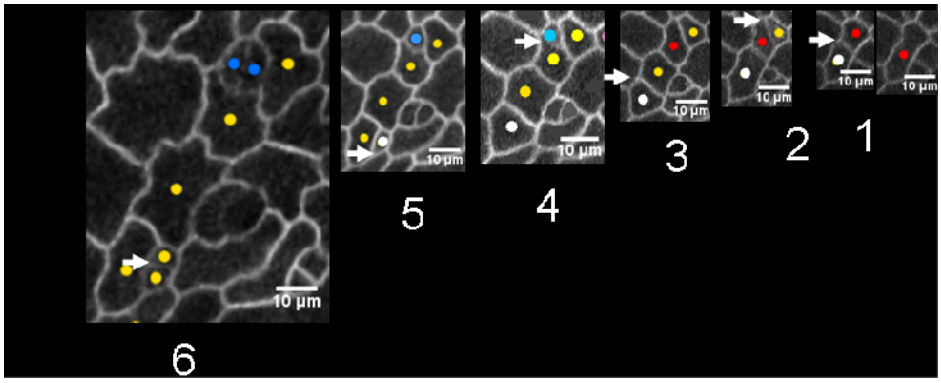

Generation	6	5	4	3	2	1
Division area	72µm²	153µm²	109µm²	206µm²	111µm²	153µm²
Previous area	63µm²	128µm²	91µm²	190µm²	82µm²	150µm²
Daughter areas	38µm²	122µm²	81µm²	117µm²	44µm²	84µm²
	32µm²	38µm²	25µm²	92µm²	70µm²	68µm²
Creation area	38µm²	92µm²	70µm²	84µm²	68µm²	

Figure 4. S8 Division data for more lineages.

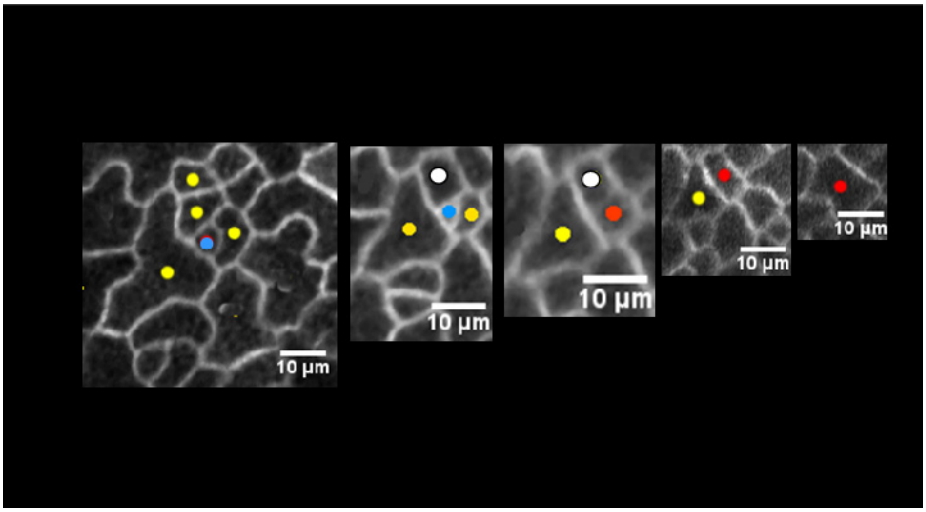

Generation	4	3	2	1
Division area	136µm²	53µm²	86µm²	163µm²
Previous area	113µm²	44µm²	67µm²	142µm²
Daughter areas	77µm²	38µm²	44µm²	92µm²
	60µm²	13µm²	42µm²	67µm²
Creation area	44µm²	42µm²	67µm²	

Figure 4. S9 Division data for more lineages.

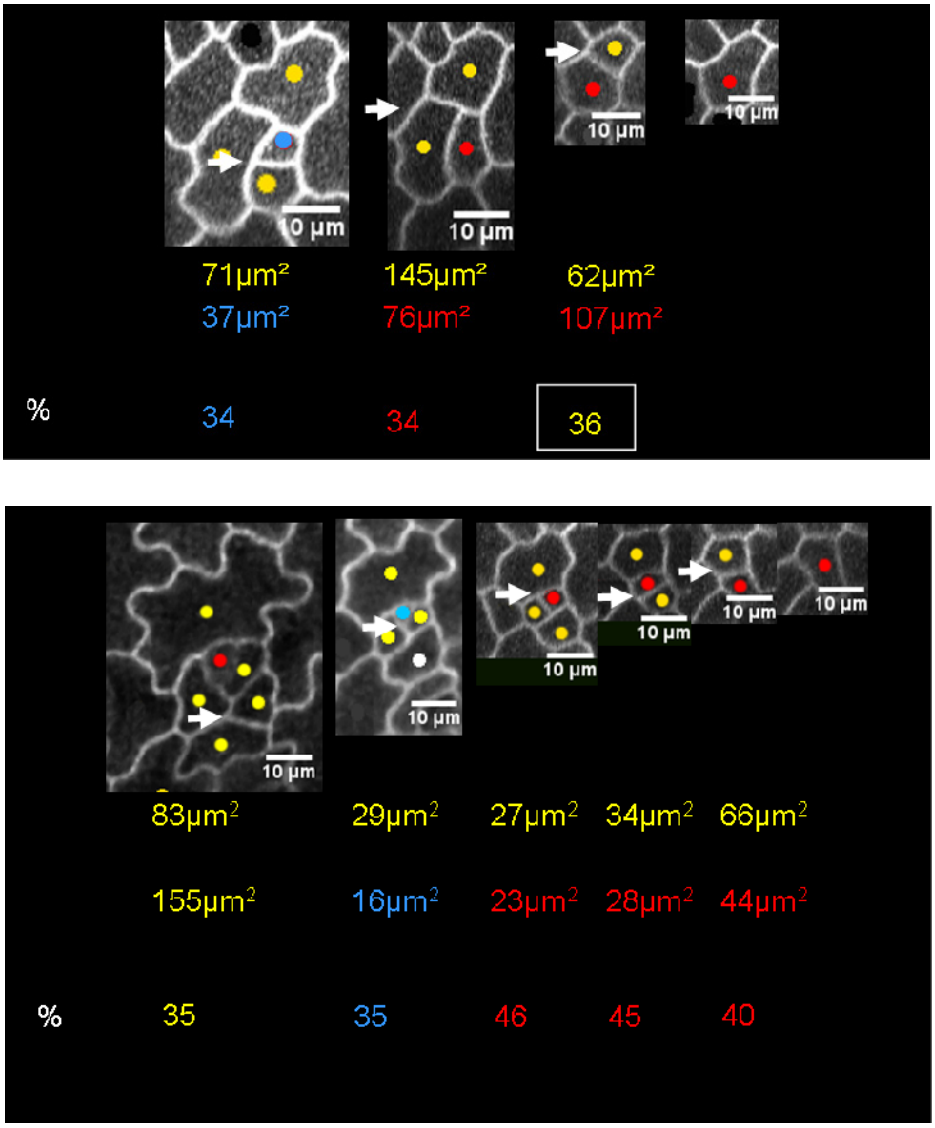

Figure 4. S10 Percentage areas of daughter cells at the time of division. The colour of the percentage is the classification of the smaller daughter cell.

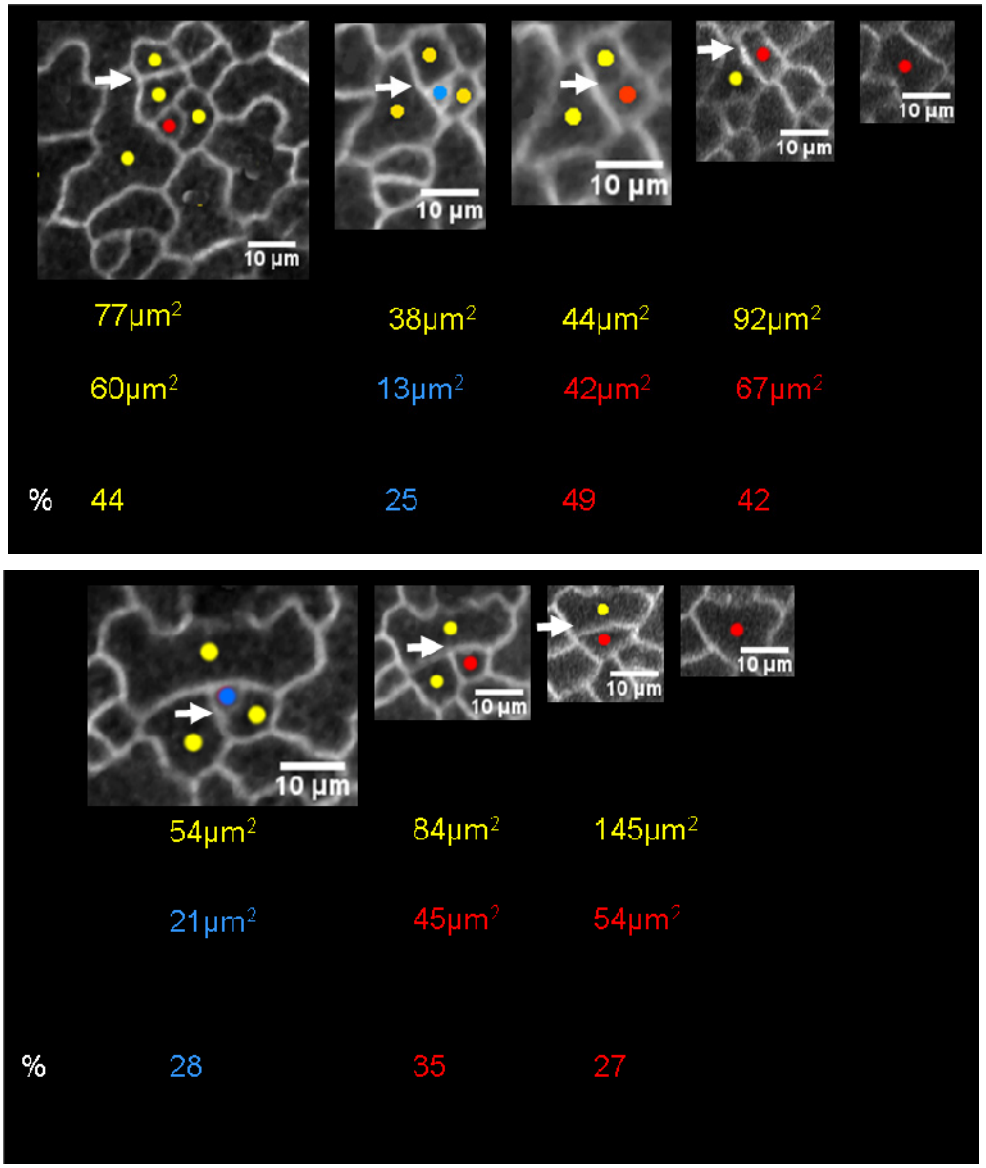

Figure 4. S11 Percentage areas of daughter cells at the time of division. The colour of the percentage is the classification of the smaller daughter cell.

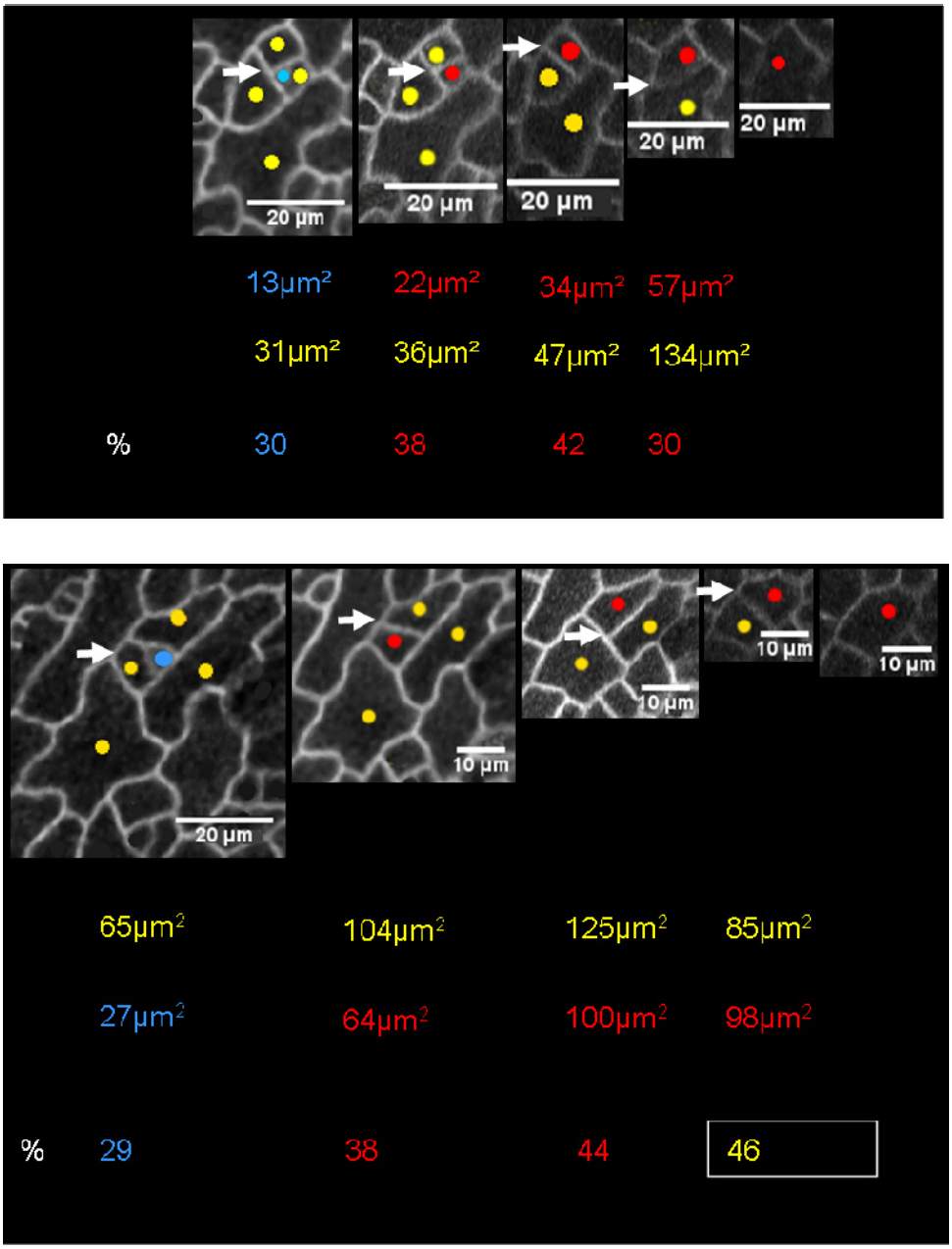

Figure 4. S12 Percentage areas of daughter cells at the time of division. The colour of the percentage is the classification of the smaller daughter cell.

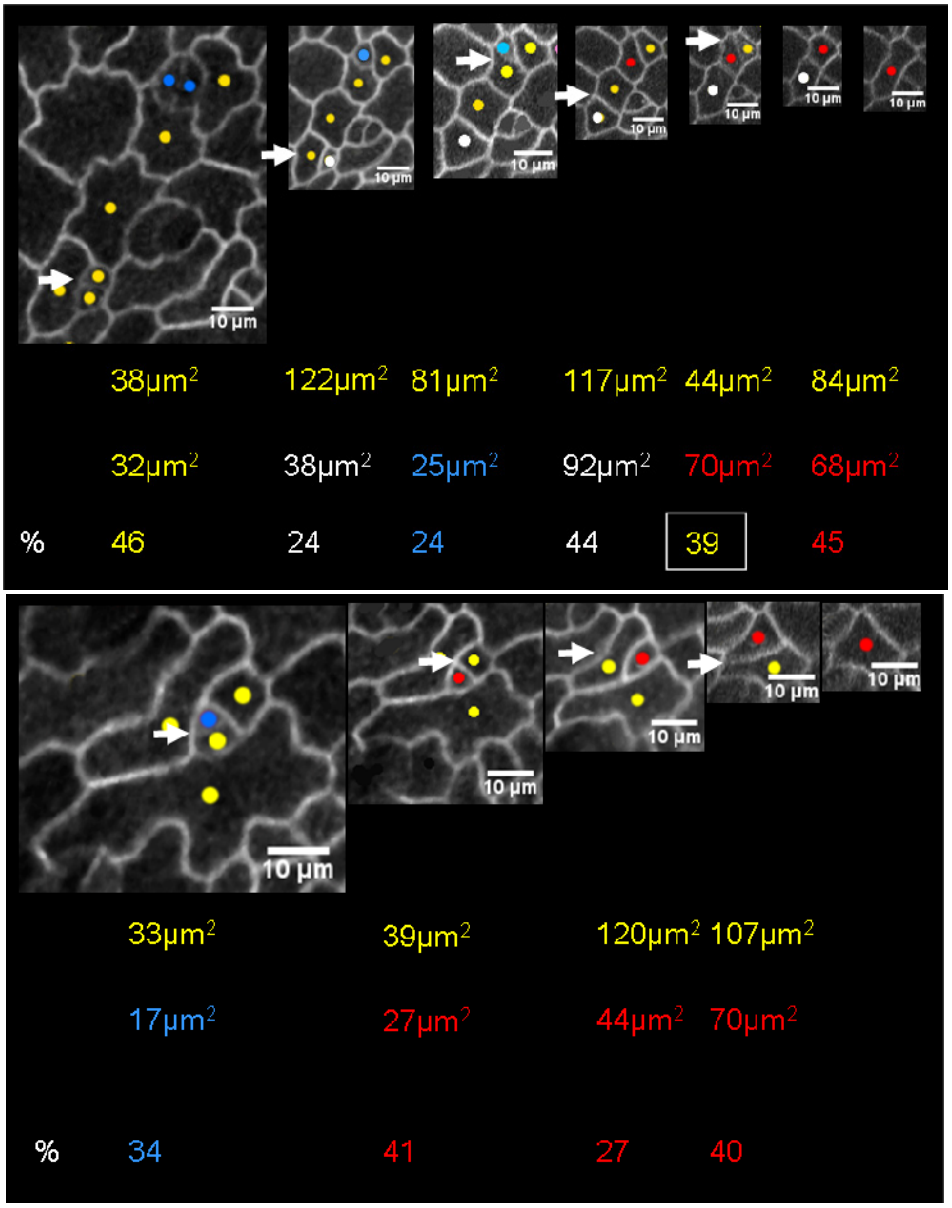

Figure 4. S13 Percentage areas of daughter cells at the time of division. The colour of the percentage is the classification of the smaller daughter cell.

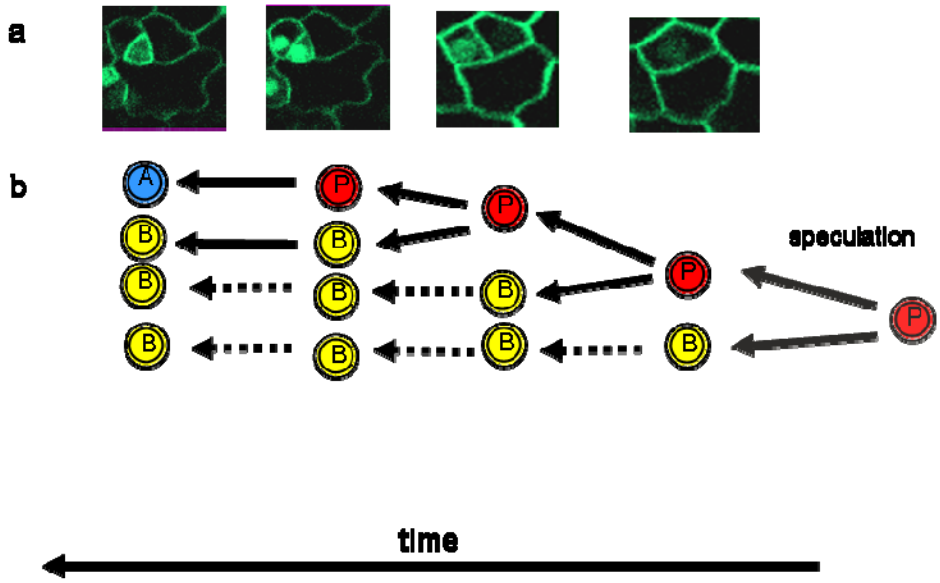

Figure 4. S14 Scheme for SPCH expressing cells. a) observed SPCH expressing cells. b) schematic of the divisions. SPCH expression correlates with P_1 expression.

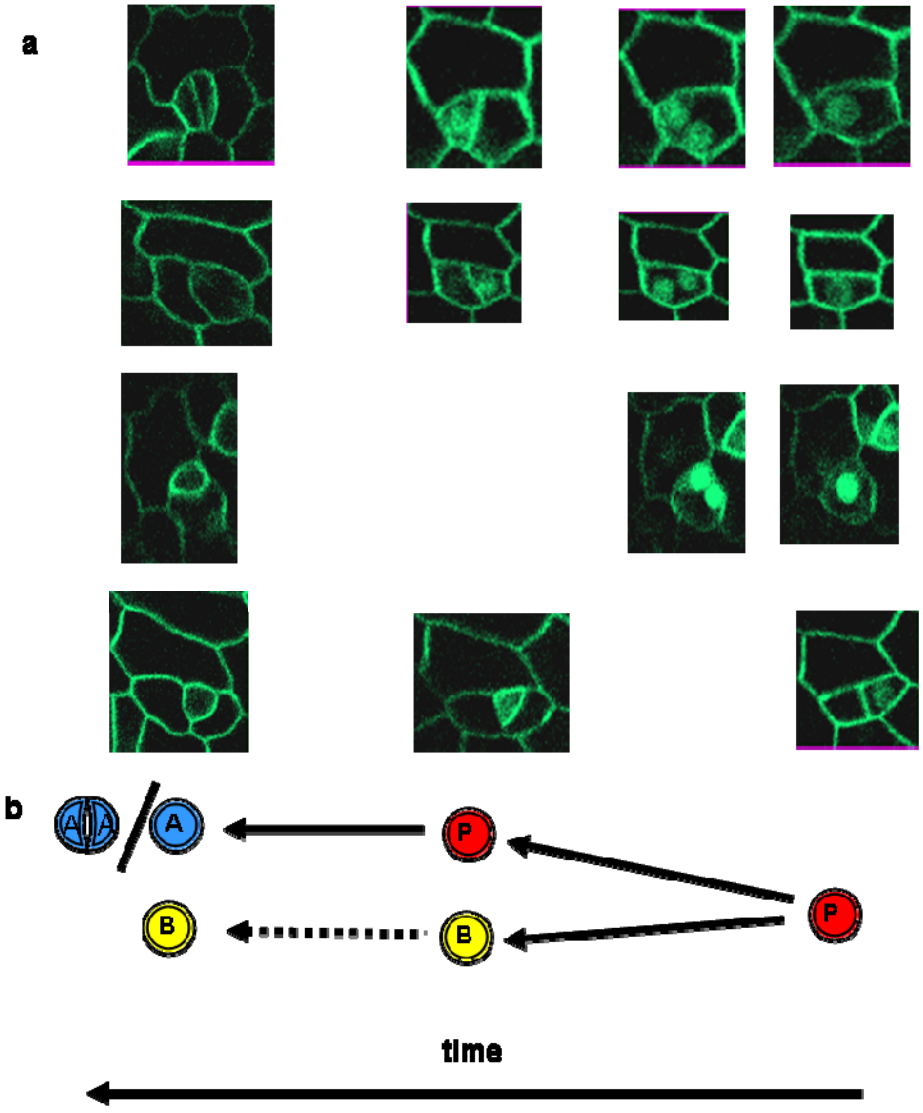

Figure 4. S15 Scheme for SPCH expressing cells. a) multiple lineages of SPCH expressing cells. b) schematic of the divisions. In all cases SPCH expression correlates with P1 expression.

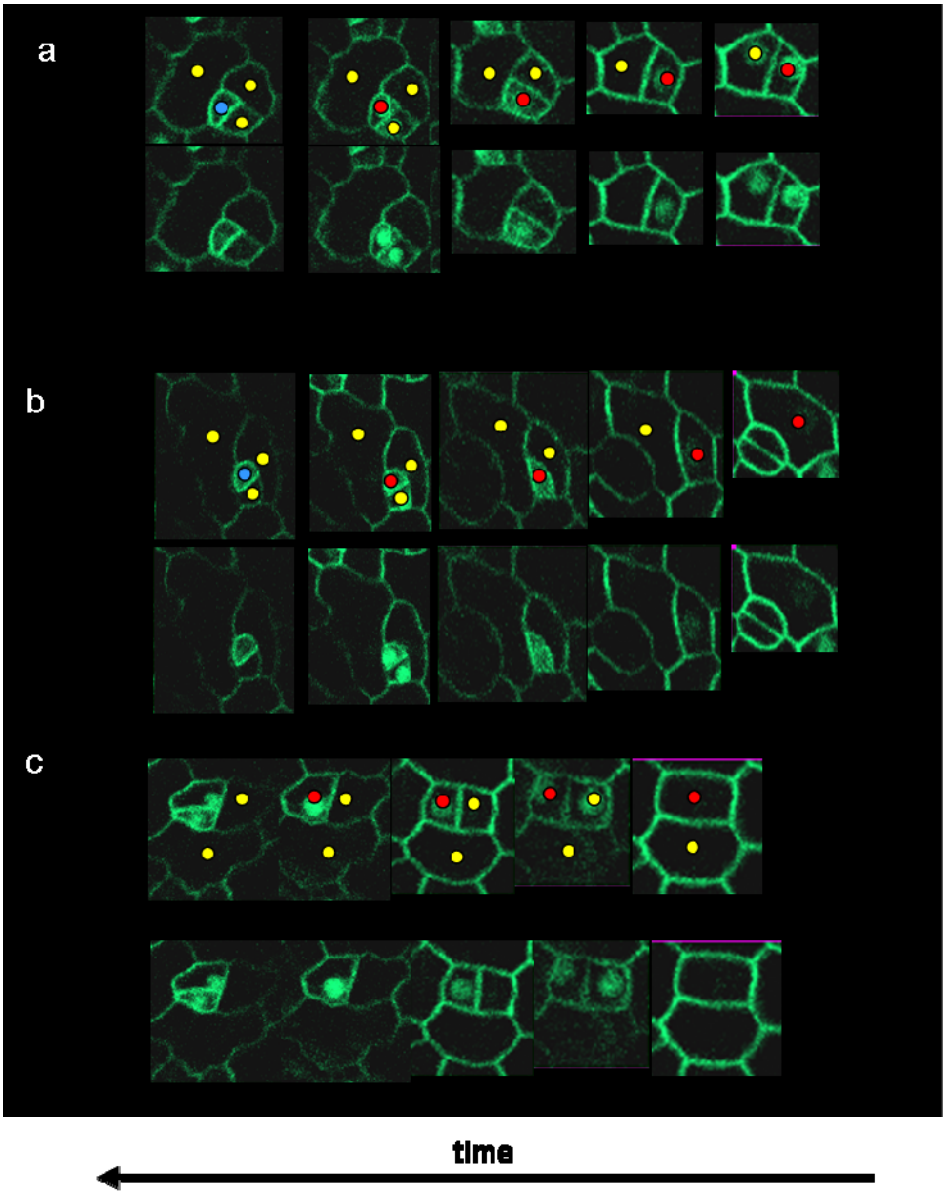

Figure 4. S16 SPCH expression in more lineages. Even in lineages that do not definitely form GMCs SPCH expression can be seen in stomata lineage cells. SPCH expression correlates with P_1 cell fate

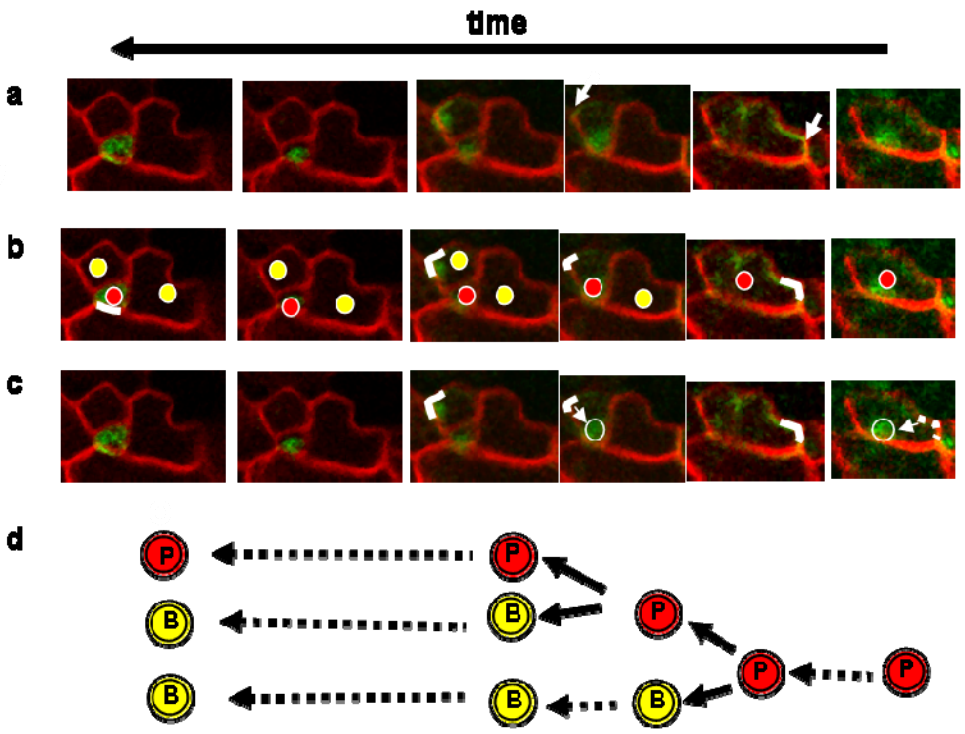

Figure 4. S17 BASL expression in another cell lineage. a) BASL expression in observed cells. b) BASL expression correlates with P_1 cell fate. c) the position of BASL in the nucleus is marked. The nucleus is BASL to peripheral BASL (the arrows indicate a direction of movement). d) schematic of the cell divisions.

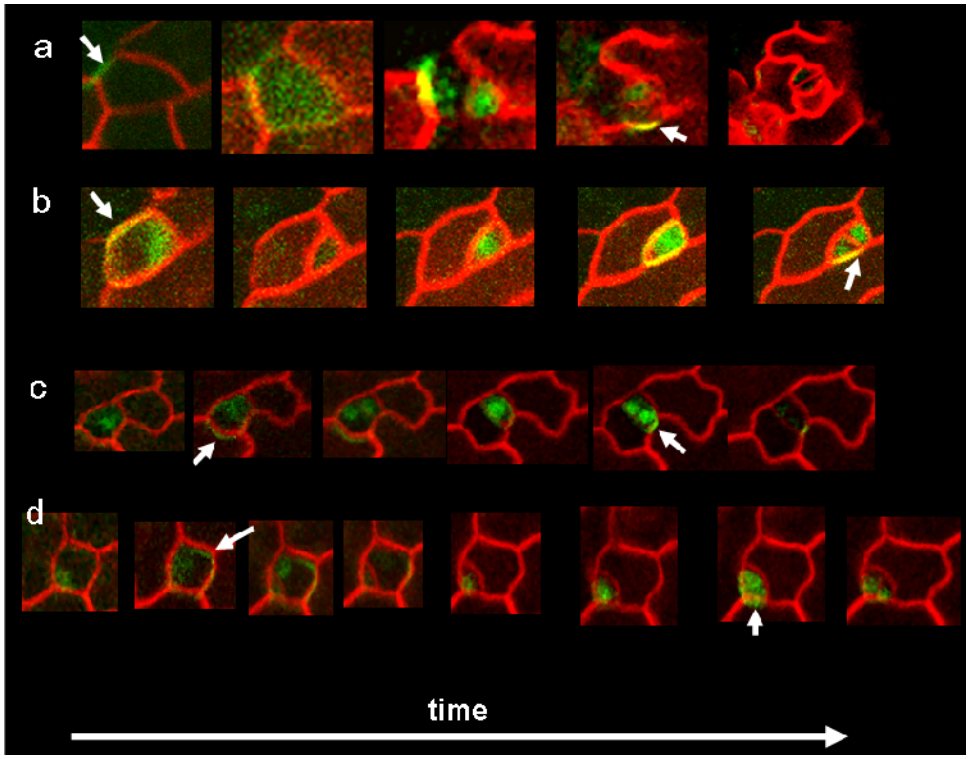

Figure 4. S18 More examples of inheritance of BASL expression. BASL is inherited by the small cell. This cell is the cell that goes on to divide. a) makes a stomata after 3 divisions.

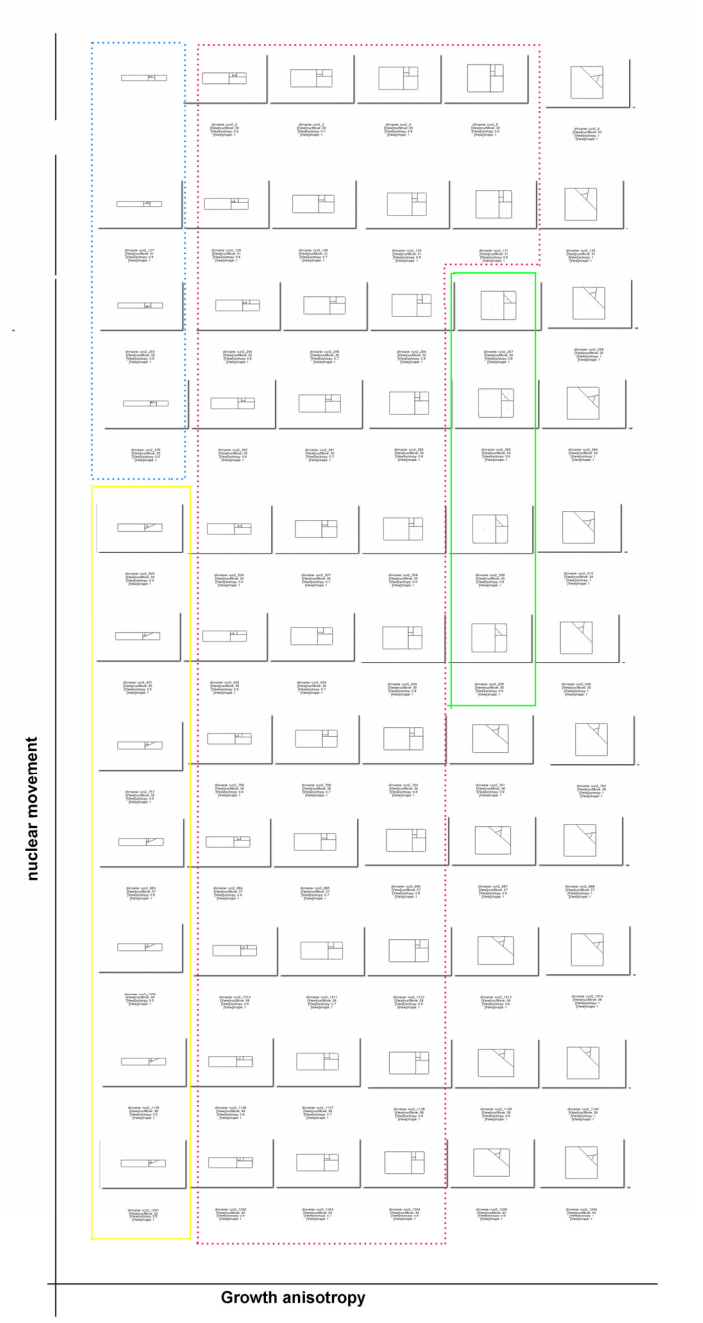
nuclear movement
Growth anisotropy

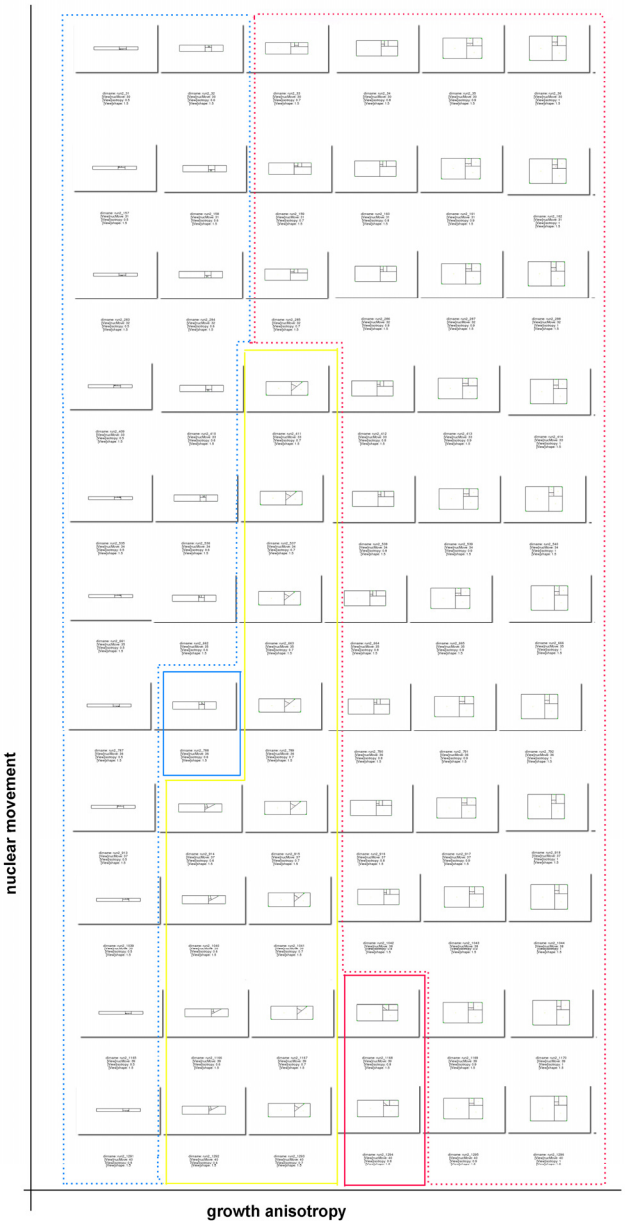
nuclear movement
growth anisotropy

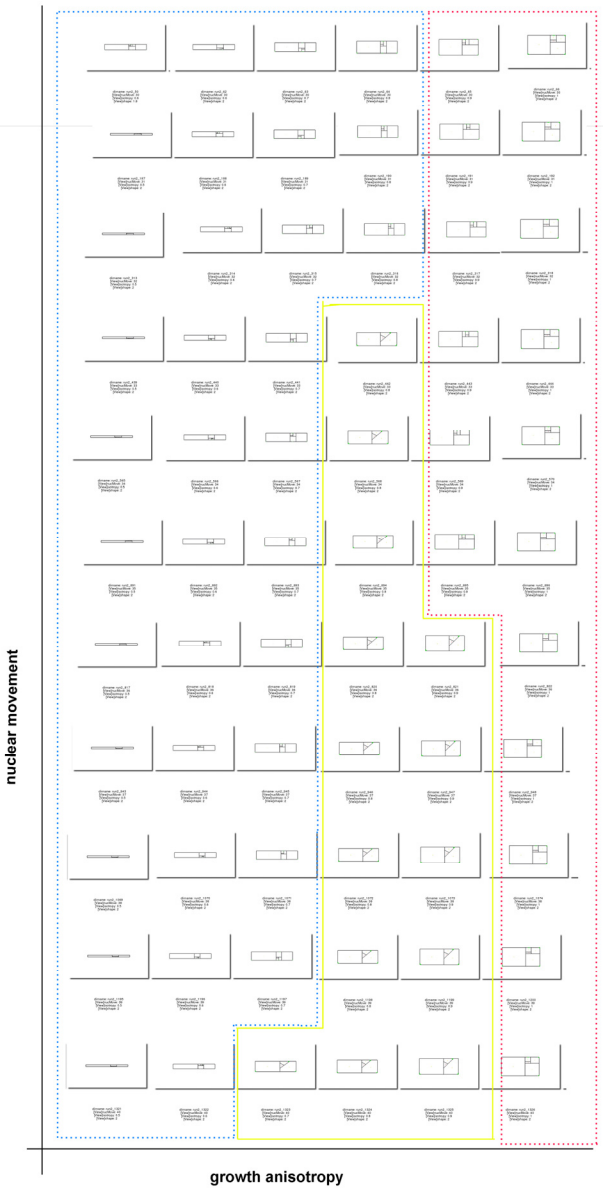

Figure 4. S19 Parameter space exploration of the stomata model. The outcome of varying the growth anisotropy from 90.5 to 1 and varying nuclear displacement from 30% to 40% of the longest distance from the centre. These rules are applied to a rectangle who's length is a) 1 times the width, b) 1.5 times the width or c) 2 times the width. The shapes are highlighted to show the shapes that they have: red type iii, blue type vi, yellow type xviii and green type ix. The solid lines indicate that the pattern went on to make a final division joining adjacent walls the pattern usually seen. All simulations were run until the P cell was internalised. The very anisotropic shapes do not generate realistic looking arrangements.